Title
Reinforced Concrete Structural Walls: Test Database and Modeling Parameters

Author
Abdullah, Saman Ali

Publication Date
2019

Peer reviewed|Thesis/dissertation

UNIVERSITY OF CALIFORNIA

Los Angeles

Reinforced Concrete Structural Walls: Test Database and Modeling Parameters

A dissertation submitted in partial satisfaction of the

requirements for the degree Doctor of Philosophy

in Civil Engineering

by

Saman Ali Abdullah

2019

ABSTRACT OF THE DISSERTATION

Reinforced Concrete Structural Walls: Test Database and Modeling Parameters

by

Saman Ali Abdullah

Doctor of Philosophy in Civil Engineering

University of California, Los Angeles, 2019

Professor John Wright Wallace, Chair

Reinforced concrete (RC) structural walls (also known as shear walls) have commonly been used as lateral force-resisting elements in buildings in regions of moderate-to-high seismic hazard because they provide substantial lateral strength and stiffness to buildings when subjected to strong ground shaking. Although relatively few wall tests were reported in the literature prior to 1990, a substantial number of tests have since been reported, primarily to assess the role of various parameters on wall deformation capacity, failure mode, strength, and stiffness. However, a comprehensive database that summarizes information and results from these tests does not exist. To address this issue, a comprehensive experimental wall database, referred to as the UCLA-RCWalls database, was created. The database currently contains detailed and parameterized information on more than 1100 wall tests surveyed from more than 260 programs reported in literature, and enables assessment of a spectrum of issues related to the behavior and performance of structural walls. The database was developed using software that enabled use of an engineering database structure with a user-friendly interface to manipulate data, i.e., filter, import, export, and review, and a secure background to store the data.

The underlying premise of the ASCE 7-10 and ACI 318-14 provisions is that special structural walls satisfying the provisions of ACI 318-14 §18.10.6.2 through §18.10.6.4 possess adequate deformation capacity to exceed the expected deformation demand determined using ASCE 7-10 analysis procedures. However, observations from recent laboratory tests and reconnaissance efforts following strong earthquakes, where significant damage occurred at boundary regions of thin walls due to concrete crushing, rebar buckling, and lateral instability, have raised concerns that current design provisions are inadequate. To address this concern, the database was filtered to identify and analyze a dataset of 164 tests on well-detailed walls generally satisfying ACI 318-14 provisions for special structural walls. The study revealed that wall lateral deformation capacity is primarily a function of the ratio of wall neutral axis depth-to-width of flexural compression zone (c/b), the ratio of wall length-to- width of flexural compression zone (l_w/b), wall shear stress, and the configuration of boundary transverse reinforcement (e.g., use of overlapping hoops versus a single perimeter hoop with intermediate crossties), and that, in some cases, the provisions of ACI 318-14 may not result in buildings that meet the stated performance objectives. Based on these observations, an expression is developed to predict wall drift capacity associated with 20% lateral strength loss with low coefficient of variation, and a new reliability-based design methodology for structural walls is proposed. The approach has been adopted for ACI 318-19, where a drift demand-to-capacity ratio check is performed to provide a low probability that roof drift demands exceed roof drift capacity at strength loss for Design Earthquake hazard level.

A large number of RC buildings constructed prior to the mid-1970s in earthquake-prone regions rely on lightly reinforced or perforated, perimeter structural walls to resist earthquake-induced lateral loads. These walls are susceptible to damage when subjected to moderate-to-strong shaking; a number of such cases were observed in 1999 Chi-Chi and Kocaeli Earthquakes, and more

recently in 2010 Maule and 2011 Christchurch earthquakes. Despite these observations, limited studies have been reported in the literature to investigate the loss of axial (gravity) load carrying capacity of damaged walls and wall piers, primarily due to the lack of experimental data. To study axial failure of structural walls, the database was filtered to identify and analyze datasets of tests on shear- and flexure-controlled walls. Based on the results, expressions were derived to predict lateral drift capacity at axial failure of RC walls and piers.

Furthermore, the ASCE/SEI 41 standard (and other similar standards or guidelines, e.g., ACI 369) represents a major advance in structural and earthquake engineering to address the seismic hazards posed by existing buildings and mitigate those hazards through retrofit. For nonlinear seismic evaluation of existing buildings, these standards provide modeling parameters (e.g., effective stiffness values, deformation capacities, and strengths) to construct backbone relations, as well as acceptance criteria to determine adequacy for a given hazard level. The modeling parameters and acceptance criteria for structural walls were developed based on limited experimental data and knowledge available in the late 1990s (FEMA 273/274-1997), with minor revisions since, especially for flexure-controlled walls. As a result, the wall provisions tend to be, in many cases, inaccurate and conservative, and can result in uneconomical retrofit schemes. Therefore, one of the objectives of this study involved utilizing the available experimental data in the UCLA-RCWalls database and new information on performance of structural walls to develop updated modeling parameters and acceptance criteria for flexure-controlled walls. The updated provisions include a new approach to identify expected wall dominant behavior (failure mode), cracked and uncracked flexural and shear stiffness values of flexure-controlled walls, and updated modeling parameters (backbone relations) and acceptance criteria for flexure-controlled walls. The updates

are expected to be significant contributions to the practice of seismic evaluation and retrofit of wall buildings.

The dissertation of Saman Ali Abdullah is approved.

Henry J. Burton

Kristijan Kolozvari

Scott Joseph Brandenberg

John Wright Wallace, Committee Chair

University of California, Los Angeles

2019

This dissertation is dedicated to the soul of Dr. Abdul Hakim Ahmed Alrawi, who, although no longer with us, continues to inspire me by his example and dedication to the students he served over the course of his career.

TABLE OF CONTENTS

LIST OF FIGURES

LIST OF TABLES

ACKNOWLEDGEMENTS

I am profoundly thankful for the unconditional love my wonderful wife and best friend, Shayda, has given me while I worked on completing my doctoral studies and conducted other research efforts. Without her patience, support, and devotion, this dissertation would have not been completed. I am also incredibly grateful for my beautiful daughter, Saveen, who has brought a tremendous joy into my life, and whose existence has made me a better person. It is not possible for me to express in words how grateful I am for having Shayda and Saveen in my life. It is truly a blessing to share my life with you both. I would also like to express my sincere love and gratitude towards my parents and siblings for their boundless love and consistent prayers and motivations. They are instrumental in all aspects of my life. If it were not for the support of my mother, I would have had left school even before high school. For that, I thank her from the bottom of my heart.

I would like to extend my profound gratitude to my advisor Professor John Wallace for his supervision, guidance, and constant support during this research and other graduate studies. I want to sincerely thank him for entrusting me with and giving me the opportunity to work on few exciting and impactful projects, for always challenging me, and encouraging me to think more independently. He has also provided numerous opportunities for me to get involved with different ACI committees and work with other academics and practitioners in the field. I am incredibly grateful to have the opportunity to work with him and learn from his extensive expertise and knowledge.

My special thanks go to Professors Scott Brandenburg, Henry Burton, and Kristijan Kolozvari, who served on my Doctoral Committee, for offering their insight, input, and helpful suggestions on this research.

I wish to extend my gratitude to my colleagues Negin Tauberg, Elham Moore, Amin Safdari, Han Sun, Chris Segura, Sofia Gavridou, Sunai Kim for their feedback, friendship, and support. It was very rewarding that I had the opportunity to do research, be co-teaching assistant, and share an office space with them.

My sincere appreciation goes to the University of Sulaimani, Kurdistan-Iraq, where I had a truly rewarding experience as an undergraduate student. I want to thank all faculties in the Civil Engineering department, especially Assistant Professor Paiman Mohammed and Dr. Sirwan Al-Zahawi, for their constant guidance and encouragement throughout my undergraduate and graduate studies.

Of course, I am genuinely thankful to Endreson's family for letting me be a part of their wonderful family, especially Dan and Barbara. Knowing them is one of the best privileges my journey to the United States offered me. Therefore, thank you very much.

VITA

Education and Work Experience

2008	B.S., Building Construction Engineering, University of Sulaimani, Kurdistan-Iraq
2008-2010	Engineer, Consultant Engineering Bureau at University of Sulaimani, Iraq
2008-2010	Teaching Assistance, University of Sulaimani, Kurdistan-Iraq
2013	M.S., Structural Engineering, California State University, Fullerton
2014-2019	Graduate Student Researcher, Civil and Environmental Engineering, UCLA
2014-2018	Teaching Assistant, Civil and Environmental Engineering, UCLA

Publications and Presentations

Journal Papers

Abdullah, S., Naish, D., and Abo-Shadi, N., 2016, "Experimental study of out-of-plane wall-to-beam connections under cyclic loading," ACI Structural Journal, Vol. 113, No. 4, pp. 355–664.

Motter, J. C., Abdullah, S., and Wallace, J. W., 2018, "Reinforced concrete structural walls without special boundary elements," ACI Structural Journal, V. 115, No. 3, pp. 723–733.

Abdullah, S. and Wallace, J. W., 2019 "Drift capacity of reinforced concrete structural walls with special boundary elements," ACI Structural Journal, V. 116, No. 1, pp. 183–194.

Abdullah, S. and Wallace, J. W., "New design methodology for RC structural walls with special boundary elements," ACI Structural Journal, submitted for review and publication, 33 pp.

Abdullah, S. and Wallace, J. W., 2019, "UCLA database for reinforced concrete structural walls: UCLA-RCWalls," Earthquake Spectra, submitted for review and publication, 23 pp.

Abdullah, S., Aswegan, K., Jaberansari, S., Klemencic, R., and Wallace, W., 2019, "Performance of RC coupling beams subjected to simulated wind loading," ACI S.J., submitted for review & publication, 33 pp.

Abdullah, S. and Wallace, J. W., 2019, "Drift capacity at axial failure of RC structural walls and wall piers," Journal of Structural Engineering, submitted for review and publication, 36 pp.

Abdullah, S. and Wallace, J. W., "Evaluation of flexural Stiffness and Strength of Reinforced Concrete Walls," ACI Structural Journal, (has been drafted).

Abdullah, S. and Wallace, J. W., "Nonlinear modeling parameters for reinforced concrete structural walls," ACI Structural Journal, (has been drafted).

Conference Papers

Abdullah, S., Naish, D., and Abo-Shadi, N. "Experimental evaluation of out-of-plane wall-to-beam connections under cyclic loading-preliminary," *Proceedings of the 10th International Conference on Urban Earthquake Engineering,* March 1-2, 2013, Tokyo Institute of Technology, Tokyo, Japan: 1-7 pp.

Abdullah, S. and Naish, D. "Experimental evaluation of non-planar wall-to-beam connections under cyclic loading," *Proceedings of Structures Congress,* April 23-25, 2015, Portland, Oregon: 2078-2088 pp.

Abdullah, S. and Wallace, J. W. "Parameters impacting drift capacity of reinforced concrete structural walls with special boundary elements" *11th US National Conference on Earthquake Engineering, 11NCEE 2018,* Los Angeles, CA, June 25-29, 2018.

Abdullah, S. and Wallace, J. W. "UCLA robust database for reinforced concrete structural walls: UCLA-RCWalls" *11th US National Conference on Earthquake Engineering, 11NCEE 2018,* Los Angeles, CA, June 25-29, 2018.

Abdullah, S. and Wallace, J. W. "A reliability-based design approach for RC walls in ACI 318 code," 2018 Structural Engineers Association of Southern California (SEAOC) Annual Convention, Palm Desert, CA, September 11-15, 2018.

Abdullah, S., Aswegan, K., Jaberansari, S., Klemencic, R., and Wallace, W., "Performance of RC coupling beams subjected to simulated wind and seismic loading," 2019 Conference of Los Angeles Tall Building Seismic Design Council.

Abdullah, S. and Wallace, J. W., "Drift capacity at axial failure of RC structural walls and wall piers," International Conference in Commemoration of 20th Anniversary of the 1999 Chi-Chi Earthquake Taipei, Taiwan, September 15-19, 2019.

Selected Poster Presentations

Abdullah, S. and Naish, D. "Experimental Evaluation of Out-of-Plane Wall-to-Beam Connections under Cyclic Loading" *Structures Congress,* April 23-25, 2015, Portland, Oregon.

Abdullah, S. and Wallace, J. W. "UCLA-RCWalls Database" 11th National Conference on Earthquake Engineering Los Angeles, June 25-29, 2018.

Abdullah, S. and Wallace, J. W. "New Wall Modeling Parameters" 2019 Annual EERI Meeting, Vancouver, Canada, March 5-8, 2019.

Selected Presentations

Abdullah, S. and Wallace, J. W. "UCLA Database for Experimental RC Structural Walls (UCLA-RCWalls)" ACI Convention: Fall 2016, Philadelphia, PA, October 23-27, 2016.

Abdullah, S. and Wallace, J. W. "UCLA-RCWalls Database, Wall Modeling Parameters and Flexural Stiffness" ACI Convention: Fall 2017, Committees 369D and 374, Anaheim, CA, October 15-19, 2017.

Abdullah, S. and Wallace, J. W. "Wall Modeling Parameters" ACI Convention: Spring 2018, Committee 369D, Salt Lake City, UT, March 23-28, 2018.

Abdullah, S. and Wallace, J. W. "Drift Capacity of RC Structural Walls with Special Boundary Elements" 11th National Conference on Earthquake Engineering, Los Angeles, June 25-29, 2018.

Abdullah, S. and Wallace, J. W. "UCLA-RCWalls Database" 11th National Conference on Earthquake Engineering, Los Angeles, June 25-29, 2018.

Abdullah, S. and Wallace, J. W. "New Design Approach for RC Structural Walls" SEAOC Convention 2018, Palm Desert, CA, September 12-15, 2018.

Abdullah, S. and Wallace, J. W. "ATC 140 Project Update" ACI Convention: Fall 2018, Committees 369D and 374, Las Vegas, NV, Oct. 13-18, 2018.

Abdullah, S. and Wallace, J. W. "Performance of RC Coupling Beams Subjected to Simulated Wind Loading" ACI Convention: Fall 2018, Committee 375, Las Vegas, NV, Oct. 13-18, 2018.

Abdullah, S. and Wallace, J. W. "New Modeling Parameters for Seismic Evaluation and Retrofit" ACI Convention: Spring 2019, Committees 369D and 374, Quebec City, Canada, March 24, 2019.

Abdullah, S. and Wallace, J. W. "Update on Performance of RC Coupling Beams Subjected to Simulated Wind Loading" ACI Convention: Spring 2019, Committees 375 and 374, Quebec City, Canada, March 24.

Abdullah, S., Aswegan, K., Jaberansari, S., Klemencic, R., and Wallace, W., "Performance of RC coupling beams subjected to simulated wind and seismic loading," 2019 LATBSDC Conference, LA, CA, May 3.

CHAPTER 1. Introduction

1.1. Background and Motivation

RC structural walls are commonly used as lateral force-resisting systems in tall and moderately tall buildings because they provide substantial lateral strength and stiffness against wind and earthquake loads and are designed and detailed in accordance with ACI 318 code. Major updates to the wall provisions of ACI 318 code occurred in 1983, 1999, and 2014. Even with these updates, the underlying premise of ACI 318-14 approach to design and detailing of walls is that walls satisfying the provisions of the code for Special Structural Walls possess adequate displacement capacity to exceed the expected displacement demands (i.e., collapse prevention). However, observations from recent earthquakes and experimental studies have demonstrated that this underlying premise is not always correct and is in fact a significant deficiency.

Furthermore, the ASCE 41 standard (and other similar documents, e.g., ATC-78) represents a major advance in earthquake engineering to address the seismic hazards posed by existing buildings and mitigate those hazards through retrofit. The wall provisions in the ASCE 41 standard were developed based on limited experimental data available in the late 1990s, with minor revisions since; therefore, the existing provisions tend to be in many cases very uncertain and conservative. However, over the last two decades, a substantial number of experimental studies have been conducted, and several attempts have been made to assemble wall databases to assist in the development of code provisions and to validate analytical models for RC structural walls; however, these databases do not contain sufficient and well-detailed information to allow detailed and robust assessment of the above issues. Therefore, in this work, a comprehensive and very detailed database called UCLA-RCWalls was developed. The database has been extensively used to accomplish a fairly broad set of research objectives, as outlined below, which focus primarily

on developing reliable provisions for design codes and standards to improve safety concerns for both new and existing buildings.

1.2. Objectives

The specific and detailed objectives of this dissertation are outlined in each chapter, starting with Chapter 2; however, the key objectives are:

1. to develop a comprehensive and detailed relational database of RC wall tests reported in the literature.
2. to develop an accurate, yet simple, drift capacity and curvature capacity models for flexure-controlled walls with special boundary elements (SBEs) satisfying the detailing requirements of ACI 318-14 §18.10.6.4.
3. to highlight the deficiencies in the current design approach of ACI 318-14 and ASCE 7-16 for RC structural walls that led to inadequate performance of walls in recent earthquakes and laboratory tests and to develop a new reliability-based design approach to address the deficiencies.
4. to develop a quantitative approach to identify the dominant behavior of structural walls (i.e., whether a wall is shear- or flexure-controlled).
5. to develop models to evaluate the loss of axial load carrying capacity of both flexure- and shear-controlled structural walls.
6. to propose updated modeling parameters (backbone relations that includes shear and flexural stiffness values, lateral strengths, and deformations-based modeling parameters) and other provisions for seismic evaluation and retrofit of existing flexure-controlled walls.

1.3. Dissertation Outline

This dissertation is comprised of nine chapters and one appendix. It starts with an Introduction in Chapter 1 and ends with the Conclusions and Recommendations in Chapter 9. The main body consists of seven distinct yet closely related chapters. Chapters 2 through 5 are adopted from four research journal papers that have either been published or submitted for review and publication. Chapters 6 through 8 contain results that have been drafted into two additional journal papers.

Chapter 2 presents details of a comprehensive and large database of RC walls known as UCLA-RCWalls that currently contains detailed and parameterized information and test results of over 1100 wall tests from more than 260 experimental programs reported in the literature around the world.

Chapter 3 presents a study of parameters that primarily impact lateral drift capacity (associated with 20% lateral strength loss) of structural walls with special boundary elements that results in a drift capacity model.

Chapter 4, based on the results of Chapter 3, highlights the deficiencies existing in the design approach of structural walls using current codes (ACI 318 and ASCE 7). To address these deficiencies, Chapter 4 also presents a new reliability-based design methodology where a drift demand-capacity ratio (DDCR) check is performed to provide a low probability (i.e., 10% or lower) that roof drift demands exceed roof drift capacity at strength loss for the Design Earthquake shaking.

Chapter 5 describes drift capacity models for axial collapse (loss of axial load-carrying capacity) of both flexure- and shear-controlled walls.

Chapter 6 provides an approach to quantitatively distinguish between shear- and flexure-controlled walls and between diagonal-shear- and sliding-shear-controlled walls. The approach uses a shear-flexure strength ratio as the criteria, as opposed to aspect ratio or shear span ratio.

Chapter 7 presents uncracked and cracked flexural and shear stiffness values for flexure-controlled structural walls.

Chapter 8 presents updated modeling parameters to construct backbone relations of flexure-controlled walls and wall segments with conforming and non-conforming detailing.

Chapter 9 summarizes the key findings of the previous chapters.

Appendix A presents all the references where information on the wall tests in UCLA-RCWalls database are reported and that were available to the author

CHAPTER 2. UCLA-RCWalls: A Database for RC Structural Wall Tests

2.1. Abstract

Reinforced concrete (RC) structural walls have been commonly used as lateral force-resisting elements in buildings subjected to strong earthquake shaking. Although relatively limited number of wall tests were reported in the literature prior to 1990, a substantial number of tests have since been reported since 1990, primarily to assess the role of various parameters on wall deformation capacity, failure mode, strength, and stiffness. However, there is a lack of a robust and detailed database that summarizes the results of these tests. Therefore, a robust database called UCLA-RCWalls, which contains detailed and parameterized information on more than 1000 wall tests reported in the literature, was assembled to serve as a resource for both researchers and practitioners. The database was developed using software that enabled use of an engineering database structure with a user-friendly interface to manipulate data, i.e., filter, import, export, and review, and a secure background to store the data.

2.2. Background

Structural RC walls have been commonly used as lateral force-resisting elements in low- to high-rise buildings because they efficiently provide large lateral strength and stiffness to resist strong ground shaking. Test programs on squat walls were initiated in the 1950s at Stanford University and Massachusetts Institute of Technology. The main objectives of these tests were to evaluate peak lateral shear strength of barbell-shaped walls under monotonic loading (Benjamin and Williams 1953, Benjamin and Williams 1954, Benjamin and Williams 1956, Galletly 1952). Following these tests, seismic provisions for design of structural walls first appeared in the 1971

version of ACI 318. Tests on squat walls under quasi-static, cyclic lateral loading began with the work performed by Barda (1972) in the United States (US), Hirosawa (1975) in Japan, and Beekhuis (1971) and Synge (1980) in New Zealand. Results from these tests led to the introduction of significant changes to wall shear strength provisions in ACI 318-83.

Experimental studies on slender (i.e., flexure-dominated) walls under quasi-static, cyclic loading initiated in mid-1970s in the US with the Portland Cement Association's (PCA) extensive, three-phase experimental program (Oesterle et al. 1976, Oesterle et al. 1979, Oesterle 1984). The PCA wall testing programs, which consisted of testing 19 walls (excluding repaired walls) between 1974 to 1983, were designed to mainly address existing knowledge gaps related to the influence of boundary element detailing and wall shear stress on the load versus deformation behavior and failure modes of slender walls with various cross sections (i.e., rectangular, barbell, and flanged), and to develop design criteria for walls in earthquake resistant buildings. These tests, along with tests by Paulay and Goodsir (1985) in New Zealand, were primarily responsible for the introduction of design and detailing provisions for wall boundary elements in ACI 318-83. Another prominent wall testing program was conducted at University of California, Berkeley to study the impact of different forms of confinement (i.e., spiral or hoop reinforcement), wall cross-sectional shapes (i.e., rectangular or barbell), loading protocols, shear span ratios, and repair procedures (Wang et al. 1975, Vallenas et al. 1979, Iliya and Bertero 1980). Following these initial studies conducted at PCA and Berkeley, relatively few additional experimental studies on slender walls were conducted in the US in the 1980s and early 1990s. The limited testing was generally focused on assessing the behavior of coupled walls (Shiu et al. 1981a,) and isolated walls pierced with openings (Shiu et al. 1981b, Ali and Wight 1991). However, a large number of tests, mostly on barbell-shaped walls, were conducted in Japan throughout the 1980s and into the 1990s.

Thomsen and Wallace (1995) reported on testing of slender walls with rectangular and T-shaped cross-sections to assess boundary element detailing using a displacement-based design approach, which was introduced into ACI 318-99. Introduction of displacement-based design approach (Wallace and Orakcal 2002), observations from major earthquakes in the US and Japan in the mid-1990s, and the expansion of experimental testing facilities around the world have since led to a significant increase in the available wall test results reported in the literature.

This paper presents a robust, well-detailed, and organized database of RC wall tests (hereafter referred to as UCLA-RCWalls) developed at University of California, Los Angeles, that currently contains detailed and parameterized data on more than 1000 isolated solid RC wall tests collected from more than 200 test programs reported in the literature around the world. Currently, the database does not include tests of repaired, retrofitted, perforated (pierced), coupled, and precast walls, as well as walls tested under dynamic loading referring to the use of earthquake simulators (shake tables) or blast loading.

2.3. Motivations

Several factors motivated the development of UCLA-RCWalls database. First, there have been attempts by researchers and institutions to gather the available experimental data of RC walls and utilize them to assess behavior of walls and validate analytical studies. However, those efforts have not been comprehensive in a sense that they only include tests conducted at particular geographic regions (e.g., wall databases in Japan and China, which tend to be difficult to obtain by other researchers) or pertinent to tests of a specific type of walls (e.g., squat walls). Furthermore, existing databases (e.g., NEEShub Shear Wall Database (Lu et al. 2010) and SERIES Database 2013) do not contain sufficiently detailed and parameterized information about reinforcement details, test

setups, experimental results, and analytical results (e.g., moment-curvature response and depth of neutral axis). In addition, a significant number of wall tests, mostly code-compliant, have been conducted since the 2010 Chile and 2011 New Zealand earthquakes, and data from these more recent tests are typically not included in these databases. Therefore, there was a lack of a robust wall database with a uniform approach to assembling data from the available tests and to identify gaps in the available test results to guide future experimental programs on RC walls (some of these gaps are summarized later).

Second, following observations of poor performance and severe damage of walls during recent earthquakes and laboratory tests (e.g., Wallace 2011, Elwood et al. 2011, Wallace et al. 2012, Birely 2012, Arteta et al. 2014, Nagae et al. 2011), researchers have raised concerns about potential deficiencies in the current building code provisions and have suggested more studies be conducted to address these issues (Wallace 2012). Furthermore, there are uncertainties related to the effectiveness of some boundary element details and configurations that are not specifically addressed in the current ACI 318-14 provisions, e.g., the type of hooks used on crossties, the effectiveness of overlapping hoops relative to a perimeter hoop with intermediate crossties, and the need to support all boundary longitudinal bars versus every other bar. To enable investigation of these concerns, and, ultimately, provide guidance that could lead to better performance of walls, a robust wall database that contains very detailed (parameterized) information is required. As part of the effort to address the above issues, Abdullah and Wallace (2019a, 2019b) utilized this database to assess the impact of various design parameters on lateral drift capacity (defined at 20% strength degradation from peak) of walls with special boundary elements (SBE). The database enabled the authors to answer some important questions related to potential for brittle compression failure of walls and deficiencies in the current ACI 318-14 code provisions, develop an empirical

model to estimate drift capacity of walls with SBE details, and propose a drift demand-capacity ratio (DDCR) check for ACI 318-19.

Lastly, documents such as ASCE 41-17 and ACI 369-17, which provide wall modeling parameters for plastic deformation capacity and sectional stiffness, have been developed based on review of limited number of experimental results (FEMA 273-1997, FEMA 365-2000). Research (e.g., Tran 2012, Birely et al. 2014, Segura and Wallace 2018, Motter et al., 2018) has demonstrated that the existing provisions are, in many cases, generally conservative, and there have been limited studies to improve those provisions due to lack of a robust and detailed wall database. Therefore, the authors are currently using the database to develop updated modeling parameters that reflect the current state of knowledge of performance of RC walls.

2.4. Database Structure

Important features of any engineering database should include the ability to efficiently manipulate data (i.e., filter, modify, import, export, and preview), ensure that data are secure and unauthorized changes cannot be performed, be widely available to enable use by researchers and practitioners, and be easily updated to include new data. To address these needs, a sophisticated database management software (Microsoft SQL Server, 2014) and a web application framework (ASP.NET MVC4) were utilized to develop the background (data repository) and foreground (interface) of the database, respectively. Fig. 2-1 shows the database interface, where data manipulations can be performed.

Fig. 2-1– Interface of UCLA-RCWalls database.

Since the number of experimental programs on RC walls is rapidly rising and new data becomes available every year, it was deemed necessary to ensure the database is capable of accepting further data in an efficient manner by inputting data into a pre-formatted Microsoft Excel spreadsheet and then simply importing the spreadsheet to the database. An important feature of the database is that the stored data can be conveniently filtered based on as many criteria as the user wishes to apply, e.g., see Fig. 2-2. The filtered data can then be downloaded to an Excel spreadsheet (Fig. 2-3). This filtering capability is essential because, in addition to accuracy, it saves researchers/practitioners time and effort that would otherwise be needed to manually refine datasets to satisfy specified criteria.

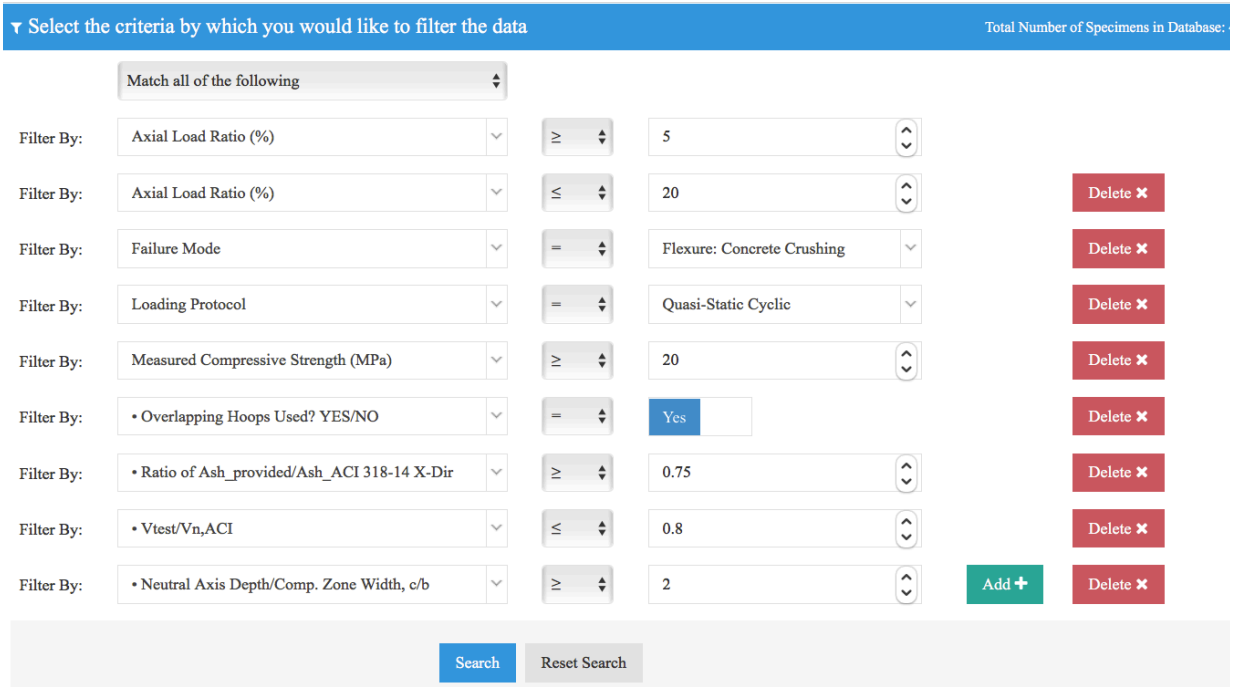

Fig. 2-2–An example of how filters can be used to screen data.

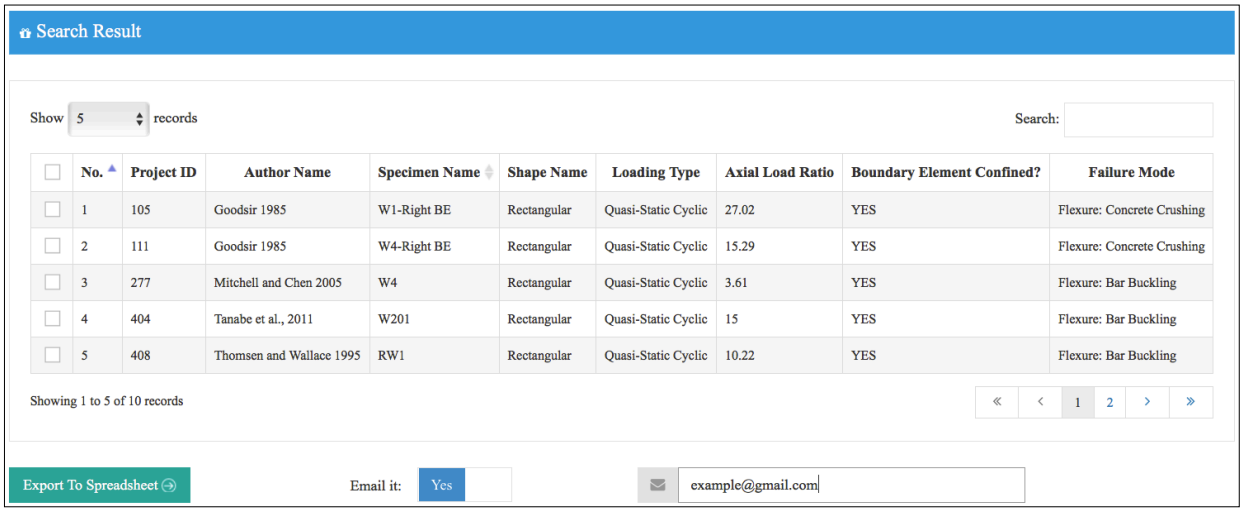

No.	Project ID	Author Name	Specimen Name	Shape Name	Loading Type	Axial Load Ratio	Boundary Element Confined?	Failure Mode
1	105	Goodsir 1985	W1-Right BE	Rectangular	Quasi-Static Cyclic	27.02	YES	Flexure: Concrete Crushing
2	111	Goodsir 1985	W4-Right BE	Rectangular	Quasi-Static Cyclic	15.29	YES	Flexure: Concrete Crushing
3	277	Mitchell and Chen 2005	W4	Rectangular	Quasi-Static Cyclic	3.61	YES	Flexure: Bar Buckling
4	404	Tanabe et al., 2011	W201	Rectangular	Quasi-Static Cyclic	15	YES	Flexure: Bar Buckling
5	408	Thomsen and Wallace 1995	RW1	Rectangular	Quasi-Static Cyclic	10.22	YES	Flexure: Bar Buckling

Fig. 2-3–Partial view of filtered data that can be exported in a spreadsheet.

2.5. Database Organization and Content

Organization of data in a database can be challenging, particularly for RC wall tests, which include a substantial amount of detail and data. Throughout the development of the database, attempts were made to ensure the data are neatly organized, and navigation through the database is straightforward. Although UCLA-RCWalls contains three major clusters of data, namely, specimen and test setup data, experimental data, and analytical/computed data, it is organized into nine main sections: *general information, test setup and loading, geometry, concrete material properties, web details, boundary element details, experimental results, flexural strength parameters*, and *shear strength parameters*. Some of these sections are further divided into sub-sections to further organize the database and, more importantly, to allow recording more detailed and parameterized information.

Currently, UCLA-RCWalls database contains over 1000 isolated solid RC wall tests collected from more than 200 experimental programs reported in the literature around the world, making it by far the largest database of RC wall tests. It is noted that UCLA-RCWalls does not currently include tests of repaired, retrofitted, perforated (pierced), coupled, and precast walls, as well as walls tested under dynamic loading referring to the use of earthquake simulators (shake tables) or blast loading. If a wall is asymmetric about the cross-section centerline in terms of geometry, longitudinal reinforcement, detailing, and/or loading, the database contains details on either side of the wall centerline and test results of both directions of loading. However, to avoid increasing the number of rows of data needed for each wall test, those asymmetric walls are treated as two separate tests. For example, TW1, a T-shaped wall specimen tested by Thomsen and Wallace (1995), is registered twice: once as “TW1-web BE” to record details of the web boundary element with backbone curve of the direction of web in compression, and again as “TW1-flange BE” to

record details of the flange with backbone curve of the direction of flange in compression, with BE referring to boundary element. In case of symmetric walls, only the test results of the positive direction of response are included. A brief description of some of the details of UCLA-RCWalls database are presented in the following sections. Appendix A presents all the references where information on the wall tests in UCLA-RCWalls database are reported and that were available to the author

2.5.1. General Information

This section contains information such as name of the program (i.e., Thomsen and Wallace, 1996), specimen name, year when the test results were first published, and country where the tests were performed. Fig. 2-4(*a*) indicates that more than half of the walls in the database have been tested in China, Japan, and the US. Reporting of wall test results increased drastically starting in 1990s and especially after 2010 (Fig. 2-4(*b*)), due to observations following major earthquakes in the US and Japan in the mid-1990s and in Chile and New Zealand in the early-2010s and the expansion of experimental testing facilities around the world.

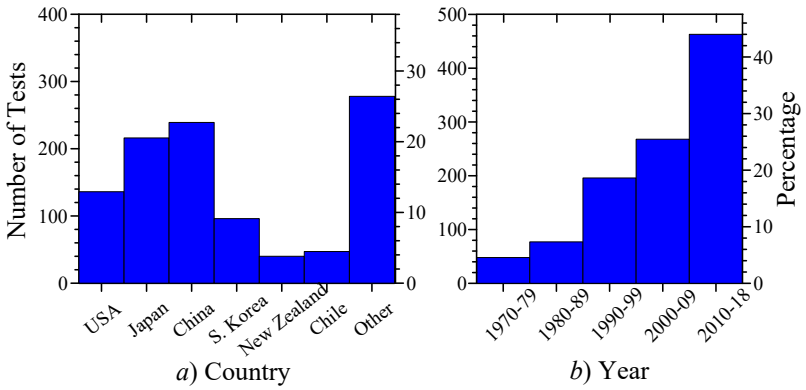

a) Country *b*) Year

Fig. 2-4–Distribution of wall tests: (*a*) country and (*b*) year.

2.5.2. Test Setup and Loading

The walls included in UCLA-RCWalls database are tested under either uni-directional monotonic, uni-directional or bi-directional quasi-static, cyclic loading protocols, using test setup configurations shown in Fig. 2-5. Other details such as heights at which global measurements are taken, type of cyclic histories (Fig. 2-6), total number of cycles, number of repeated cycles at each displacement/load level, shear span ratio (*M/Vlw*), and level of axial load are also included.

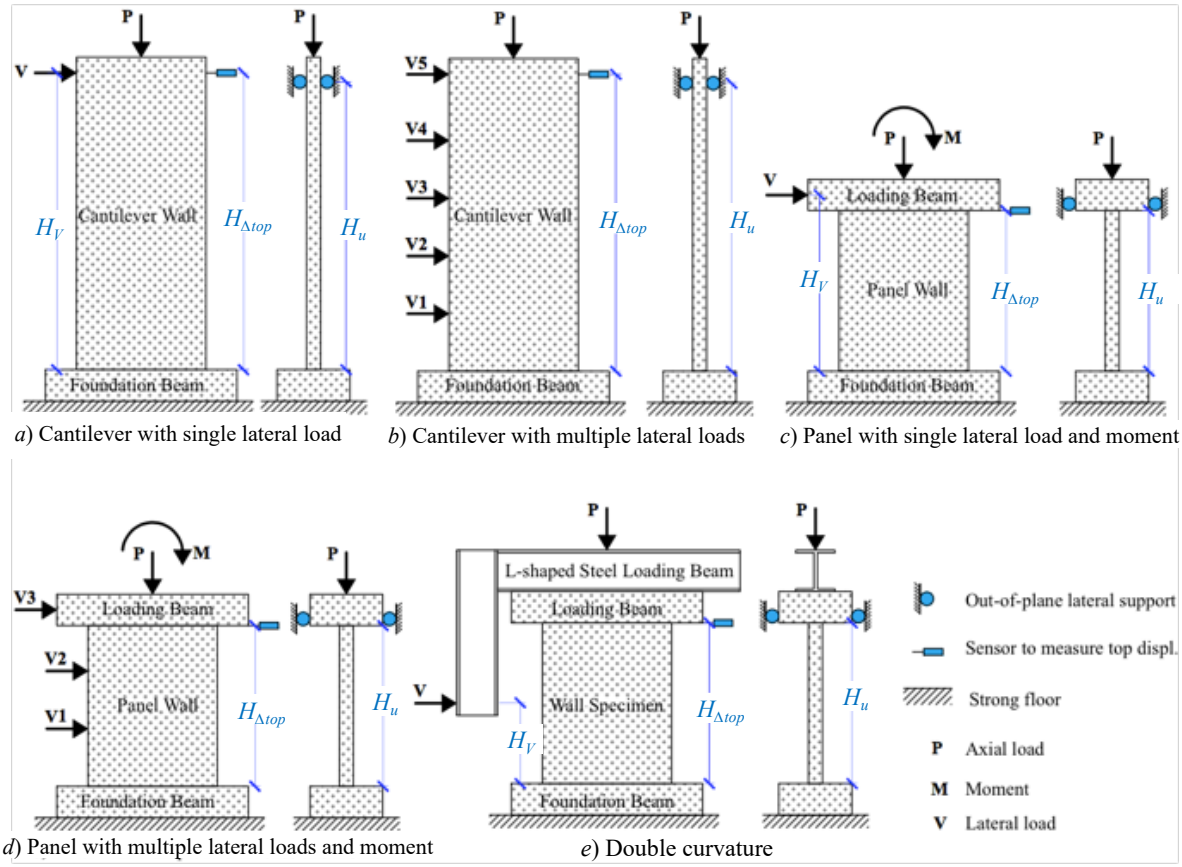

a) Cantilever with single lateral load *b*) Cantilever with multiple lateral loads *c*) Panel with single lateral load and moment

d) Panel with multiple lateral loads and moment *e*) Double curvature

Fig. 2-5– Wall test setup configurations.

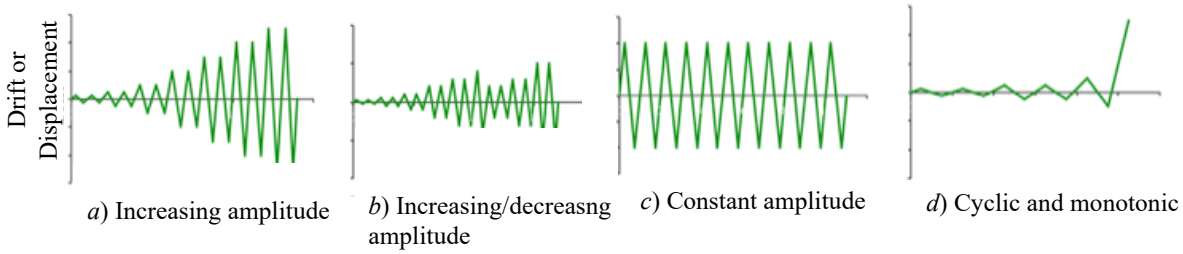

Fig. 2-6–Types of cyclic loading histories.

Fig. 2-7(*a*) indicates that about 90% of the walls in the database have been tested under uni-directional quasi-static, cyclic loading and only 7% and 2% being tested under monotonic and bi-directional quasi-static, cyclic loading, respectively. Sparseness of wall tests under bi-directional loading is partly due to limitations of laboratory capabilities to perform more complicated loading schemes. Fig. 2-7(*b*) shows that the vast majority of the tests in the database are conducted on cantilever walls with a single lateral load applied at the top of the wall (i.e., approximate effective height, h_{eff}) with or without axial load (e.g., Thomsen and Wallace 1995) due to the simplicity of cantilever wall test setups (Fig. 2-5(*a*)). Tests of cantilever walls with multiple lateral loads (Fig. 2-5(*b*)) have rarely been conducted (e.g., Wang et al. 1975, Vallenas et al. 1979, Iliya and Bertero 1980) due to the complexity associated with stability and application of multiple actuators simultaneously and the fact that multiple actuators can be replaced with application of a single actuator acting at h_{eff} of the wall. One important limitation of cantilever wall tests is that it does not allow testing of walls at larger scale or walls subjected to larger shear span ratios and axial loading, i.e., very slender walls, due to height limitations. As a result, walls tested under high axial load ratios $\left(P / A_g f'_c > 0.3\right)$ and large shear span ratio (M/Vl_w > 4.0) are rare, as seen from Fig. 2-7(*c*) and Fig. 2-7(*d*). However, researchers have recently overcome this issue by testing panel or partial height walls, in which the lower one or two stories of a high-rise wall is tested under a

combined effects of lateral load(s), axial load, and bending moment at the top of the panel (Fig. 2-5(*c*) and Fig. 2-5(*d*)), which allows testing of walls at a larger scale and walls subjected to larger shear span ratios (e.g., Segura and Wallace 2018, Birely 2012, Furukawa et al. 2003, Kabeyasawa et al. 2012, Tabata et al. 2003, Lu et al. 2017, Shegay et al. 2018). An important aspect of creating the database involved providing a unified approach to convert drift capacity of panel walls to that of cantilever walls at h_{eff} to allow a more meaningful comparison of wall tests. That is, for panel and partial wall height tests, the UCLA-RCWalls database includes drift capacity at h_{eff}, determined as sum of the measured displacement at the top of the panel (experimental) and an estimated contribution of elastic bending deformations between the top of the panel and h_{eff}. To estimate the latter, the wall panel is converted to an equivalent cantilever wall based on the M/Vl_w used in the test. Then, the contribution of the upper part of the wall to the top displacement is computed analytically using the wall effective stiffness (EI_{eff}) obtained from analytical moment-curvature response. This approach has been shown to be reasonable (Massone and Wallace 2004).

Double-curvature test setups (Fig. 2-5(*e*)) have been used to test shear-controlled walls and piers (e.g., Lopes and Elnashi 1992, Orakcal et al. 2009) to address conditions for pierced (or punched) walls.

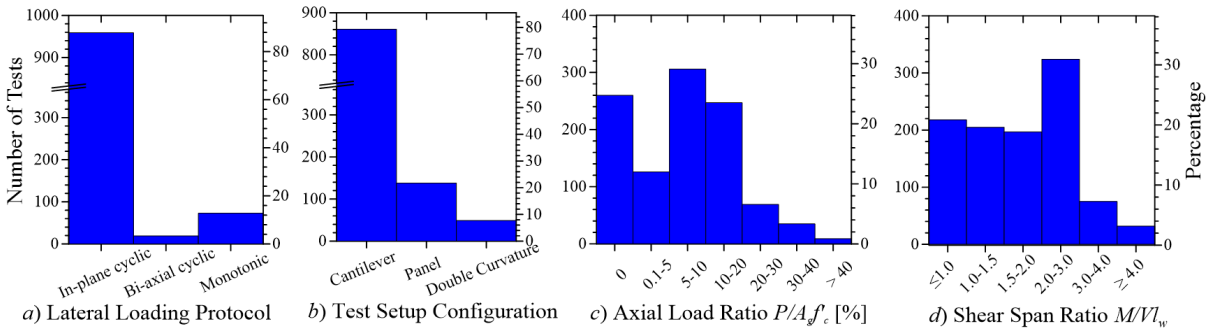

a) Lateral Loading Protocol *b*) Test Setup Configuration *c*) Axial Load Ratio $P/A_g f'_c$ [%] *d*) Shear Span Ratio M/Vl_w

Fig. 2-7–Histograms of test setup and loading.

2.5.3. Geometry

The wall tests included in UCLA-RCWalls have either rectangular, barbell, flanged, T-shaped, L-shaped, or half-barbell cross-section (Fig. 2-8). Walls that have C-shaped cross-sections are not currently included. Fig. 2-8(*a*) shows that the majority of the wall tests have rectangular cross-sections. This is mainly due to the transition in the use of barbell-shaped to rectangular walls that began in the late 1980s, at least in the US and New Zealand, to simplify formwork. This transition has recently been taking place in Japanese practice after the Architectural Institute of Japan (AIJ 2010) relaxed mandatory requirements of enlarged boundary columns to permit use of rectangular walls with confined end regions. The majority of the walls have web thickness, t_w, ranging from 3 to 8 in., with only 18 walls with $t_w > 8$ in (Fig. 2-9(*b*)). Fig. 2-9(*c*) indicates that about 92% of the walls have ratio of wall length normalized by width of compression zone, l_w/b, ≥ 15, with relatively few tests with $15 < l_w/b < 20$ and even fewer tests with very slender cross-sections (i.e., $l_w/b > 20$).

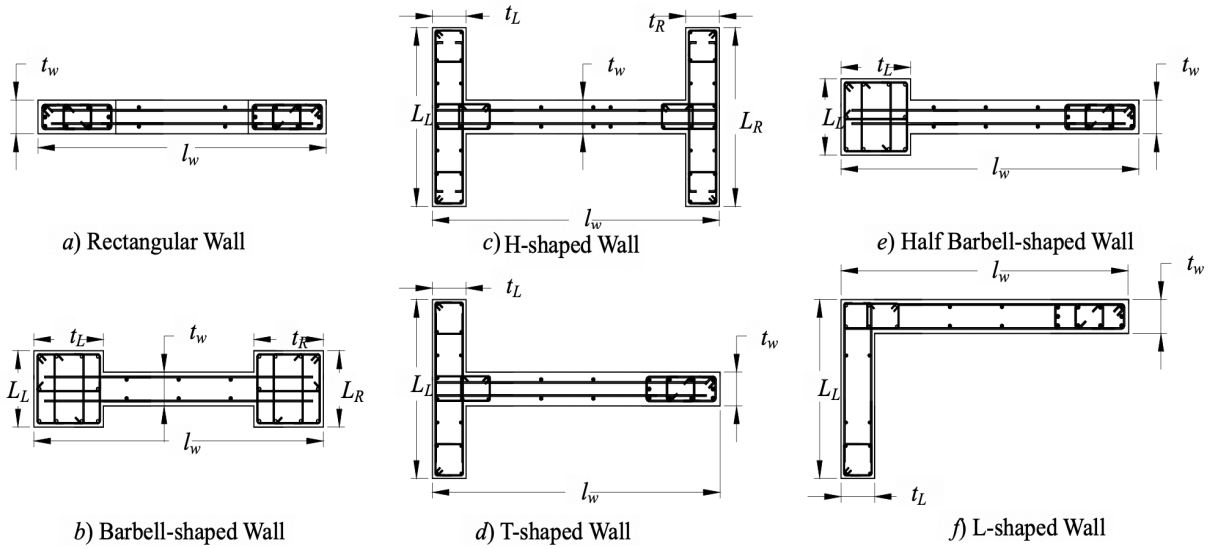

Fig. 2-8–Wall cross-section shapes included UCLA-RCWalls.

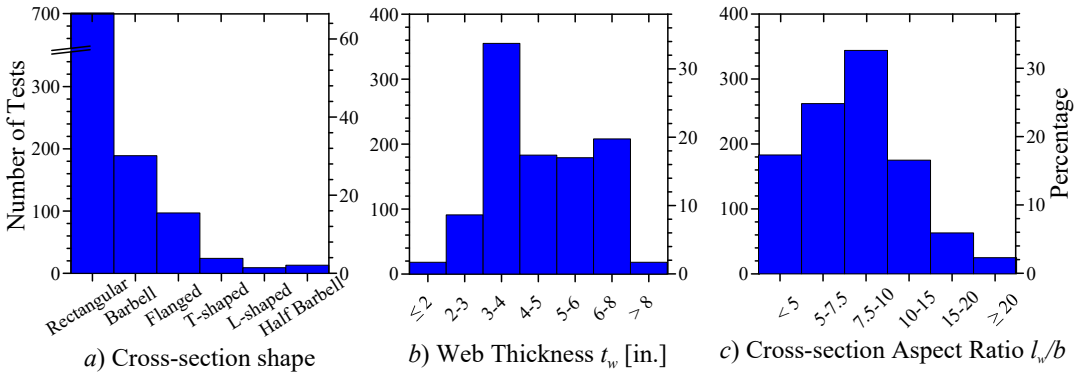

a) Cross-section shape *b*) Web Thickness t_w [in.] *c*) Cross-section Aspect Ratio l_w/b

Fig. 2-9–Histograms of wall cross-section shape and geometry.

2.5.4. Material Properties

Materials strength properties, both specified (nominal) and tested (measured), are contained in the database for both concrete (i.e., compressive strength, f'_c) and steel reinforcement (i.e., yield strength, f_y, and, tensile strength, f_u). Tested concrete compressive strength is recorded as strength of standard cylinders with length-to-diameter ratio of 2:1, which is the commonly used compressive strength test in most countries including the US, Canada, Japan, Australia, New Zealand, etc. However, some test programs, especially in Europe (e.g., from Great Britain and Germany) and Chinese, concrete strength is based on cube tests. In such cases, cylinder concrete compressive strength is taken as 80% of cube compressive strength, which is a commonly assumed value (Mindess et al. 2003) and a reasonable approximation for the purpose of this database. As shown in Fig. 2-10, there are a significant number of wall tests for a wide range of tested material strengths for both concrete and reinforcement in the boundary elements.

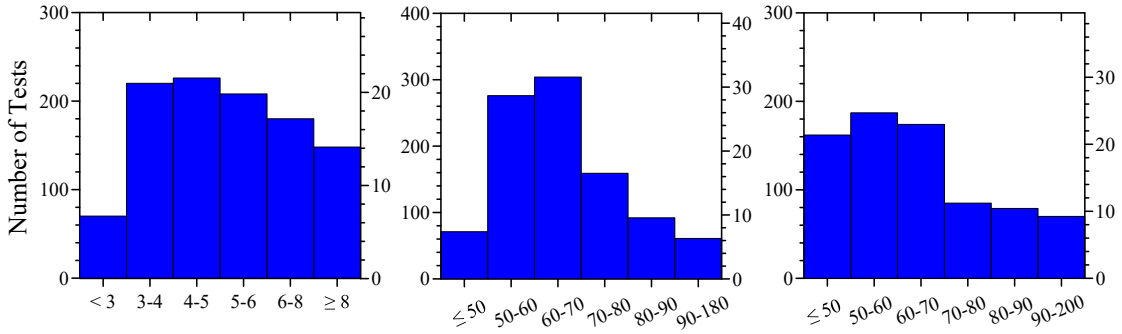

a) Concrete Compressive Strength f'_c [ksi]

b) Yield strength of boundary longitudinal bars f_{yl} [ksi]

c) Yield strength of boundary transverse bars f_{yt} [ksi]

Fig. 2-10–Histograms of tested material strength properties.

Specified strength properties are especially important to determine if walls are code compliant, as ACI 318-14 code provisions are based on specified material strengths; however, these properties are not always reported. Therefore, it was of interest to know the variation of tested and specified material strengths (especially f'_c and f_y) for walls whose both tested and specified strengths are reported. Fig. 2-11(*a*) shows that, on average, tested concrete compressive strength is about 9% larger than specified strength. Tested yield strength of longitudinal and transverse reinforcement within boundary elements is on average about 10% larger than specified minimum yield strength (Fig. 2-11(*b*) and Fig. 2-11(*c*)). This yield overstrength factor (1.10) is about 88% of the factor specified by ASCE 41-17 for expected yield strength of reinforcing steel in existing concrete construction (i.e., $f_{yE} = 1.25f_y$).

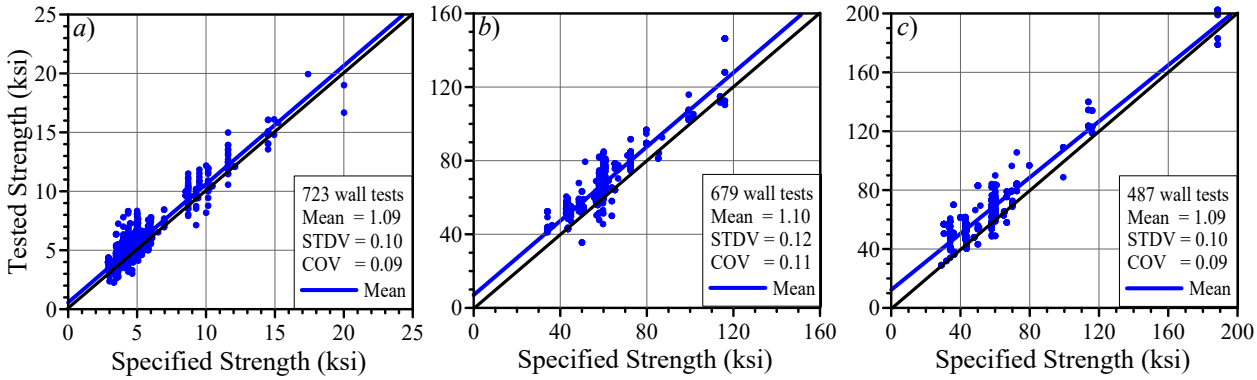

Fig. 2-11–Tested versus specified material strengths: a) concrete compressive strength, f'_c, b) yield strength of boundary longitudinal reinforcement, f_{yl}, and c) yield strength of boundary transverse reinforcement, f_{yt}.

2.5.5. Boundary Elements Details

The *boundary element* section of the database contains by far the largest body of data. This is because, in flexure-controlled structural walls, the detailing at the wall boundaries is used to provide nonlinear deformation capacity (ductility) in lateral-force resisting systems (e.g., Special Structural Walls according to ACI 318-14). In addition to geometric information (location and spacing of reinforcement, and provided concrete cover), example details parameterized in the database include perimeter hoop with intermediate legs of crossties, types of overlapping hoops/spiral (Fig. 2-12(*a*)), types of hooks used on crossties or headed bar crossties (Fig. 2-12(*b*)), layout and lateral support of vertical bars (Fig. 2-12(*c*)), anchorage type of vertical bars in the plastic hinge region (i.e., continuous bars, lap-spliced bars, or mechanical couplers), embedment type and length of vertical bars into the foundations block (types of hooks or headed bars used), and distribution of vertical reinforcement (concentrated at boundary elements or uniformly distributed throughout cross section). Availability of the above information is critical to allow researchers to assess the role of various parameters and the effectiveness of code provisions.

Histograms of boundary element longitudinal reinforcement ratio $\rho_{long.BE}$, ratio of provided-to-required (per ACI 318-14 §18.10.6.4) area of boundary transverse reinforcement, $A_{sh,provided}/A_{sh,required}$, and ratio of vertical spacing of boundary transverse reinforcement to minimum diameter of longitudinal boundary reinforcement, s/d_b are shown in Fig. 2-13. A great deal of tests have been conducted on a large range of $A_{sh,provided}/A_{sh,required}$, with the majority not satisfying ACI 318-14 §18.10.6.4 required transverse reinforcement partly due to re-instating expression 18.10.6.4a in the 2014 version of the code which tends to govern for walls with thin boundary zones.

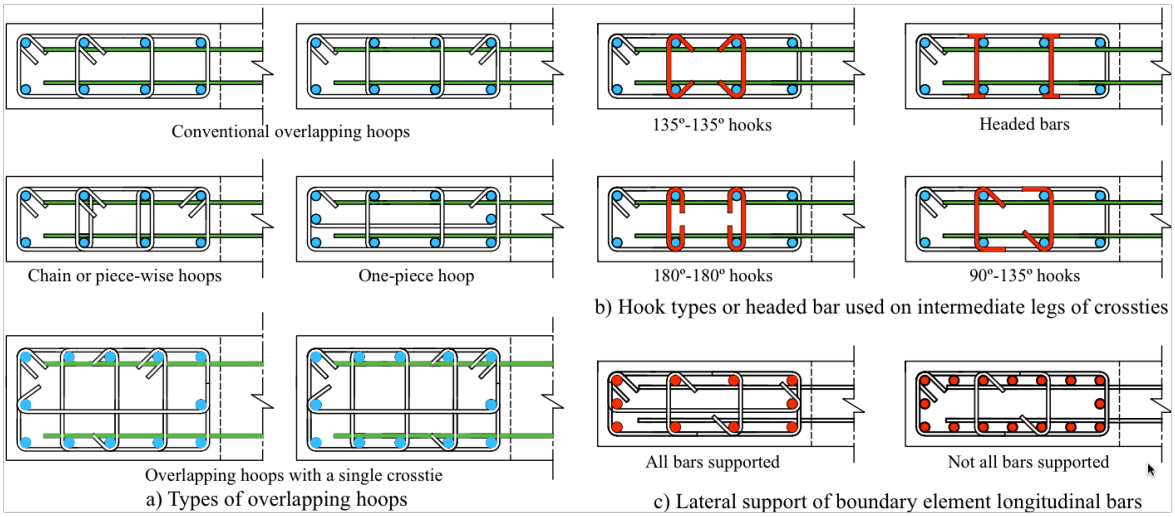

Fig. 2-12–Examples of wall boundary element details parameterized in UCLA-RCWalls.

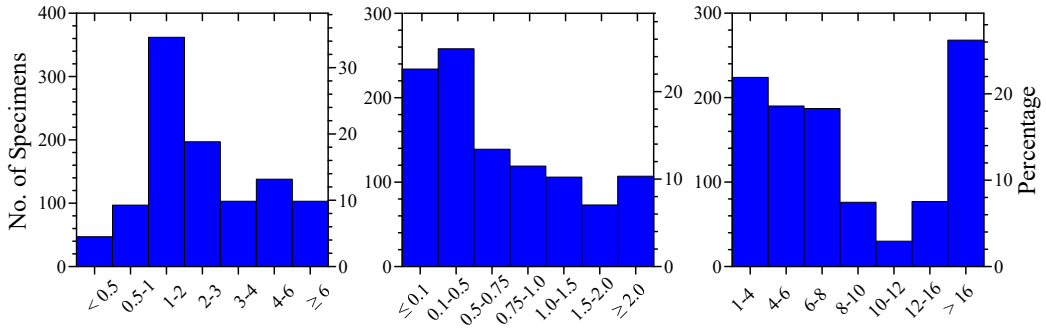

a) Reinf. Ratio, $\rho_{long.\ BE}$ [%] *b*) $A_{sh,\ provided}/A_{sh,required}$: X-Dir. *c*) Bar slenderness s/d_b

Fig. 2-13–Histograms of boundary element details.

2.5.6. Web Details

The database contains thorough information about wall web reinforcements (i.e., vertical, horizontal, diagonal, and confinement reinforcement). Details such as number of curtains, end anchorage condition for horizontal web reinforcement (Fig. 2-14(*a*)), location of web vertical bars (Fig. 2-14(*b*)), anchorage type of web vertical bars in the plastic hinge region, and embedment type and length of web vertical bars in the foundations block are few examples of web details parameterized in UCLA-RCWalls.

Fig. 2-15(*a*)and Fig. 2-15(*b*) show that the vast majority of the wall tests have web horizontal and vertical reinforcement ratios, ρ_h and ρ_l, greater than 0.0025, which has been the required minimum web reinforcement ratio in ACI 318 since the 1971 version of the code. Fig. 2-15(*c*) also indicates that there are about 120 walls with one curtain and five walls with more than two curtains of web reinforcement in the database, leaving the rest of the walls (~920 walls) having two curtains.

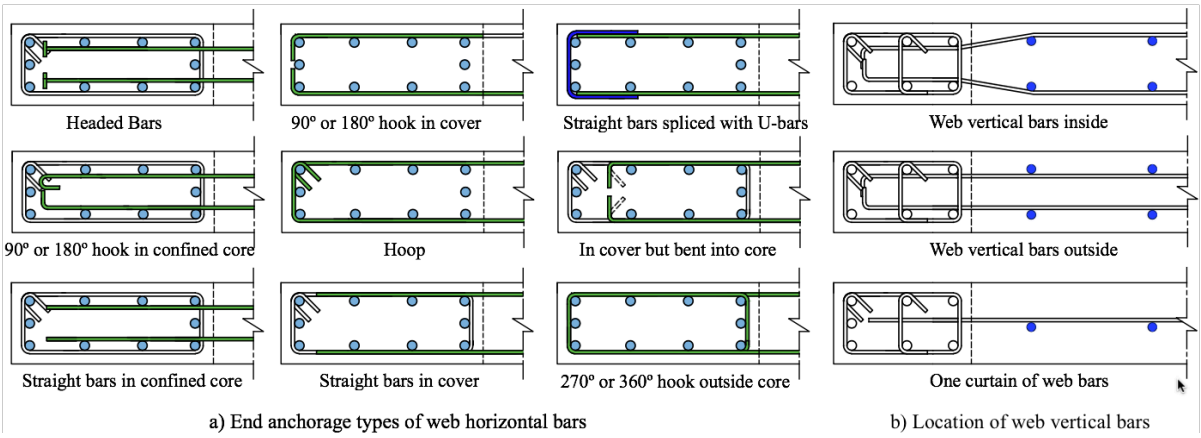

Fig. 2-14–Examples of wall web details parameterized in UCLA-RCWalls.

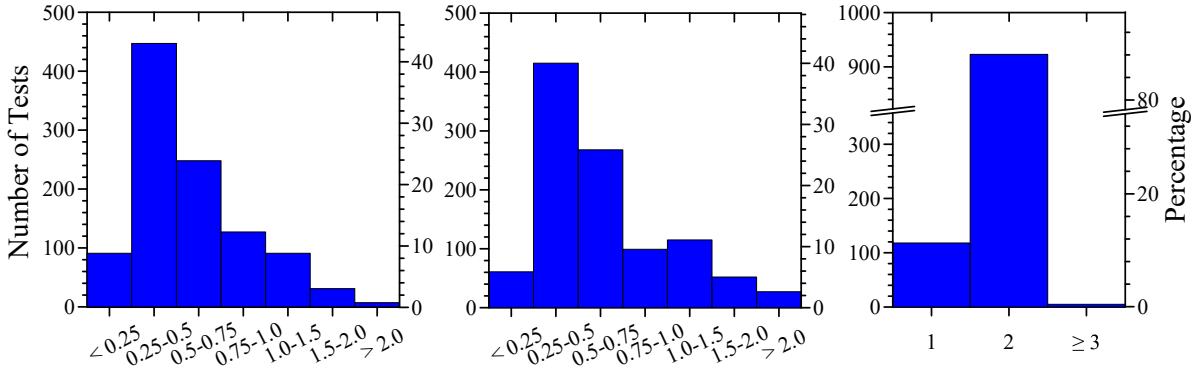

a) Horizontal reinf. ratio, ρ_h [%] *b*) Vertical reinf. ratio, ρ_l [%] *c*) Number of curtains

Fig. 2-15–Histograms of web details.

2.5.7. Experimental Results

Backbone curves of base shear-top displacement, base moment-rotation, and base shear-shear displacement responses are generated and included in the database. The backbone curves provide a significant amount of information about wall deformation, strength, and stiffness. As shown in Fig. 2-16, the backbone curves consist of seven points, namely, *Origin, Cracking, General Yield, Peak*, *Ultimate, Residual,* and *Collapse*, corresponding to the first cycle at each load/displacement level. *Cracking* point represents the state at which horizontal flexural or diagonal shear cracks are first observed in the test. This information is reported for the majority of the tests in the database. However, in cases where cracking load and displacement are not reported, attempts were made to visually identify the cracking point on the load-displacement curve (a significant change in stiffness). *General Yield* is defined as the point where the hysteretic loops (or the response curve in case of monotonic loading) begin to abruptly lose stiffness, as illustrated in Fig. 2-16. It should be noted that this point does not necessarily correspond to first yielding of longitudinal bars, but rather is associated with yielding of most of the longitudinal bars. *Peak* is the point at which the maximum lateral strength occurred. *Ultimate* (*or deformation capacity*) is defined as the deformation at which strength degraded by 20% in the first cycle from peak, which is widely

accepted among researchers. *Residual* and *Collapse* points are defined as the state at which the wall reaches its residual strength and loses its axial load-carrying capacity, respectively. The majority of the tests, especially earlier tests, do not have *Residual* and *Collapse* points due to termination of the test before reaching residual strength and axial collapse.

In addition to backbone curves, reported drift at key damage states such as cover spalling, onset of bar buckling, and bar fracture are recorded based on reported information at those stages. However, a large number of the programs do not report such details, especially programs for which there are no available report, thesis, or dissertation, where detailed information is typically reported.

The reported failure modes are also contained in the database, which are classified as flexure failure modes (i.e., *bar buckling and concrete crushing*, *bar fracture*, *or global or local lateral instability*), shear failure modes (i.e., *diagonal tension, diagonal compression* (web crushing), or *shear sliding at the base*), flexure-shear failure (i.e., yielding in flexure and failing in shear), and *lap-splice failure.* The authors did their best to validate that the reported failure mode was consistent with the observed response and wall damage before recording that information in the database. Fig. 2-17(*a*) shows that half of the walls in the database are classified as flexure failure; the other tests are recorded as either flexure-shear or shear failure modes. Although the database contains about 30 walls with lap-splices of boundary element longitudinal bars (Fig. 2-17), there are only about 10 tests that failed due to insufficient lap-splice. Walls not tested to some degree of lateral strength degradation due to either limited available actuator stroke/capacity or pushing the wall to a repairable level of damage are flagged as “No Failure”. These tests are included because they are useful for wall strength and.

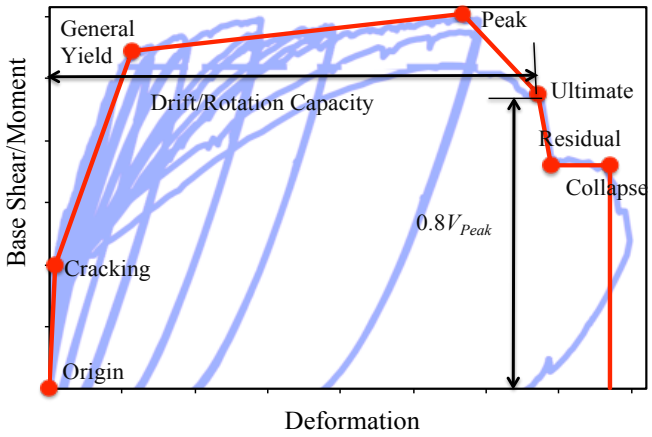

Fig. 2-16–An example of backbone derivation (Tran, 2012).

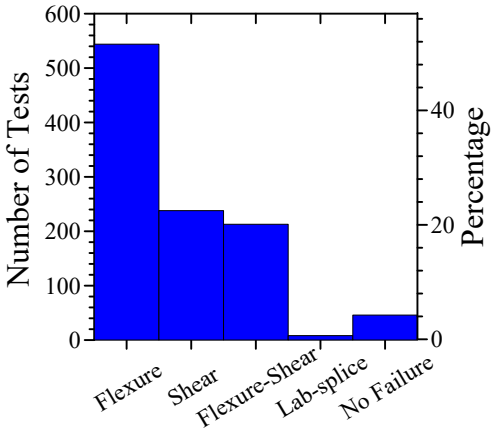

Fig. 2-17–Wall failure modes.

2.5.8. Analytical Results

Another important feature of UCLA-RCWalls database is that it contains computed data for both flexural and shear responses, and numerous other calculated parameters, e.g., axial load ratio, reinforcement ratios in the web and boundary elements, ratio of provided-to-required area of boundary transverse reinforcements, and normalized shear stresses. These computed data are essential to facilitate filtering process, determine code compliancy, assess code provisions, and, ultimately, assist in developing new design recommendations.

Analytical moment-curvature $(M-\phi)$ analysis was performed for each wall using tested material properties (f'_c, f_y, and f_u) and assuming 1) linear strain variation (plane sections), 2) maximum extreme fiber concrete compressive strain of 0.004, 3) stress-strain behavior of unconfined concrete given by Hognestad (1951) (Fig. 2-18(*a*)), 4) steel stress-strain relationship given in Fig. 2-18(*b*), where ε_y, ε_{sh}, and ε_u are steel strains at yield, strain hardening, and ultimate, respectively. Although the $M-\phi$ response of each wall is available in a spreadsheet for each test, values of nominal and first yield moment strength (M_n and M_y) and curvature (ϕ_n and ϕ_y) and depth of neutral axis (c) at concrete compressive strain of 0.003 are extracted from the curves and recorded in the database. Fig. 2-19 shows histograms of computed c normalized by wall length (c/l_w) and width of compression zone (c/b). It can be seen that very few walls have been tested with $c/b > 4$, with the majority having $c/b \leq 2$. ACI 318-14 wall shear strength parameters, e.g., α_c, shear strength contributed by concrete and reinforcement (V_c and V_s), and nominal shear strength (V_n) computed from equation 18.10.4.1, are also included in the database.

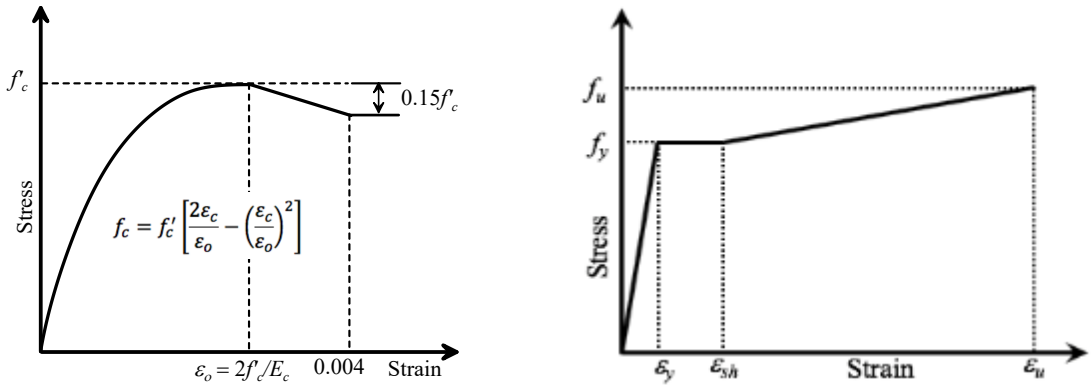

(*a*) Concrete (*b*) Reinforcement

Fig. 2-18–Steel stress-strain relationships used to compute moment-curvature relations.

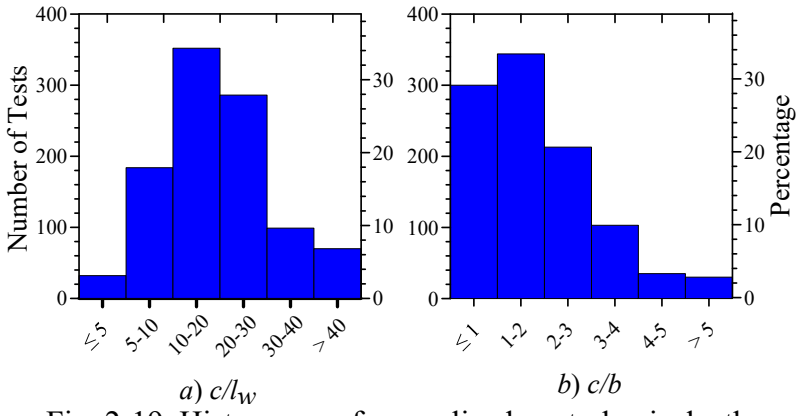

a) c/l_w *b*) c/b

Fig. 2-19–Histograms of normalized neutral axis depth

2.6. Recommendations for Future Wall Tests

Based on the gaps observed in the test results assembled in the UCLA-RCWalls database, it is recommended that future test programs of RC walls address on the following items:

1. Walls in new building constructions are commonly characterized by more slender cross-section profiles $\left(l_w/b>15\right)$ and higher compression demands $\left(c/b>4\right)$, at least on the West Coast of the US. This trend has been accelerated by the availability of high strength concrete. However, test results on walls with $l_w/b>15$ and $c/b>4$ are relatively sparse in the literature. Therefore, it is recommended that future wall test programs focus on ACI 318-14 code-compliant walls with $l_w c/b^2>60$.
2. Abdullah and Wallace (2019a) investigated the impact of using different boundary transverse reinforcement configurations on drift capacity and noted that there are relatively few code-compliant walls with large compression zones $\left(c/b>4\right)$, high shear demands, and transverse reinforcement consisting of either overlapping hoops or a combination of a single perimeter hoop and crossties with 135º-135º hooks.

3. Walls with lap-splices of web horizontal reinforcement are common; however, there are currently no wall tests that could be used to evaluate the impact of lap-splicing the web horizontal reinforcement on strength and deformation capacity of walls.
4. Wall tests under bi-directional (or multi-directional) quasi-static, cyclic loading are very scare, especially tests on rectangular walls, and are limited to tests reported by Almeida et al. (2014), Brueggen (2009), Imanishi (1996), Imanishi et al. (1996), Kabeyasawa et al. (2012), Idosako et al. (2017), and Niroomandi et la. (2018).
5. Wall tests that utilize headed bars as crossties with a single perimeter hoop for boundary element confinement (Fig. 2-12(*b*)) are limited to tests reported by Mobeen (2002) and Seo et al. (2010). However, these walls have relatively small ratios of l_w/b and c/b, such that $l_w c / b^2 \leq 6$; therefore, these tests, by themselves, do not provide sufficient insight into the effectiveness of headed bars for use as crossties within SBEs.

2.7. Summary

This paper presents a robust and large database of RC walls known as UCLA-RCWalls. Unlike other existing databases, the database is designed and developed using sophisticated software and framework that not only makes the database a secure tool but also enables efficient filtering and manipulation of data. UCLA-RCWalls currently contains detailed and parameterized information and test results of over 1000 wall tests from more than 200 experimental programs reported in the literature around the world. The database can serve as a valuable resource for the structural/earthquake engineering community to assess behavior of RC walls against a wide range of design parameters, develop empirical models that capture data trends, and validate analytical studies.

2.8. Acknowledgement

Our endless thanks go to Pshtiwan A. Hassan, a software developer at Farouk Holdings in Sulaymaniyah, Kurdistan-Iraq, for his outstanding assistance and extensive knowledge and expertise throughout developing the structure of the database. Funding for this work was provided, in part, by the National Science Foundation Grant CMMI-1446423, which focused on promoting and enhancing US and international collaboration on performance assessment of structural wall systems and development of databases. Any opinions, findings, and conclusions or recommendations expressed in this paper are those of the authors and do not necessarily reflect the views of others mentioned here.

2.9. References

Abdullah S. A., and Wallace J. W., 2019a. Drift capacity of RC structural walls with special boundary elements, *ACI Structural Journal* **116**, 183–194.

Abdullah S. A., and Wallace J. W., 2019b. A reliability-based design methodology for RC structural walls with special boundary elements, *ACI Structural Journal*, submitted for review and possible publication, May 4, 33pp.

Ali, A., and Wight, J. K., 1991. RC structural walls with staggered door openings, *Journal of Structural Engineering* **117**, 1514–1531.

Almeida, J. P., Prodan, O., Rosso, A., and Beyer, K., 2017. Tests on thin reinforced concrete walls subjected to in-plane and out-of-plane cyclic loading, *Earthquake Spectra* **33**, 323–345.

American Concrete Institute (ACI 318-71), 1971. *Building code requirements for reinforced concrete (ACI 318-71)*, Detroit, MI, 78 pp.

American Concrete Institute (ACI 318-83), 1983. *Building Code Requirements for Reinforced Concrete (ACI 318-83)*, Detroit, MI, 155 pp.

American Concrete Institute (ACI 318-99), 1999. *Building Code Requirements for Structural Concrete (ACI 318-99) and Commentary (318R-99)*, Farmington Hills, MI, 391 pp.

American Concrete Institute (ACI 318-14), 2014. *Building Code Requirements for Structural Concrete (ACI 318-14) and Commentary (318R-14)*, Farmington Hills, MI, 519 pp.

American Concrete Institute (ACI 369-17), 2017. *Standard Requirements for Seismic Evaluation and Retrofit of Existing Concrete Buildings (ACI 369.1-17) and Commentary*, Farmington Hills, MI, 110 pp.

Architectural Institute of Japan (AIJ), 2010. *Standard for Structural Calculation of Reinforced Concrete Structures*, Japan. (in Japanese).

American Society of Civil Engineers (ASCE 41-17), 2017. *ASCE/SEI 41-17: Seismic Evaluation and Retrofit of Existing Buildings*, Reston, VA, 576 pp.

Arteta, C., To, D., and Moehle, J., 2014. Experimental response of boundary elements of code-compliant reinforced concrete shear walls, *Proceedings of the 10th U.S. National Conference on Earthquake Engineering*, Anchorage, Alaska.

ASP.NET MVC4, 2013. *Microsoft*, framework, https://www.asp.net/mvc/mvc4.

Barda, F., 1972. Shear Strength of Low-Rise Walls with Boundary Elements, Ph.D. Thesis, Lehigh University, Bethlehem, Pennsylvania.

Beekhuis, W. J., 1971. *An Experimental Study of Squat Shear Walls*, M.E. *Report,* Department of Civil Engineering, University of Canterbury, Christchurch, New Zealand.

Benjamin, J. R., and Williams, H. A., 1953. *Investigation of Shear Walls, Part–Experimental and Mathematical Studies of Reinforced Concrete Walled Bents under Static Shear Loading, Report No. 1*, Department of Civil Engineering, Stanford University, Stanford, CA.

Benjamin, J. R., and Williams, H. A., 1954. *Investigation of Shear Walls, Part 6–Continued Experimental and Mathematical Studies of Reinforced Concrete Walled Bents under Static Shear Loading, Report No. 4*, Department of Civil Engineering, Stanford University, Stanford, CA.

Benjamin, J. R., and Williams, H. A., 1956. *Investigation of Shear Walls, Part 12–Studies of Reinforced Concrete Shear Wall Assemblies, Report No. 10*, Department of Civil Engineering, Stanford University, Stanford, CA.

Birely, A. C., Lowes, L.N., and Lehman, D. E., 2014. Evaluation of ASCE 41 modeling parameters for slender reinforced concrete structural walls, *Special Publication of American Concrete Institute*, **SP-297-4**, 4.1–4.18

Birely, A. C., 2012. Seismic Performance of Slender Reinforced Concrete Structural Walls, Ph.D. Dissertation, University of Washington, Seattle, WA.

Brueggen, B. L., 2099. Performance of T-shaped Reinforced Concrete Structural Walls under Multi-Directional Loading, PhD Thesis, University of Minnesota, Minnesota.

Elwood, K. J., Pampanin, S., and Kam, W. Y., 2012. 22 February 2011 Christchurch earthquake and implications for the design of concrete structures, *Proceedings of the International Symposium on Engineering Lessons Learned from the 2011 Great East Japan Earthquake*, Tokyo, Japan.

Federal Emergency Management Agency (FEMA), 1997. *Guidelines to the Seismic Rehabilitation of Existing Buildings (FEMA 273)*, Washington, D.C, 444 pp.

Federal Emergency Management Agency (FEMA), 2000. *Prestandard and Commentary for the Seismic Rehabilitation of Buildings (FEMA 356)*, Washington, D.C, 518.

Galletly, G. D., 1952. *Behavior of Reinforced Concrete Shear Walls Under Static Load, Report Submitted to Office of the Chief of Engineers, Department of the Army*, Department of Civil and Sanitary Engineering, Massachusetts Institute of Technology, Cambridge, MA.

Hirosawa, M., 1975. *Past Experimental Results on Reinforced Concrete Shear Walls and Analysis on Them, Kenchiku Kenkyu Shiryo, No. 6*, Building Research Institute, Ministry of Construction, Tokyo, Japan. (in Japanese)

Hognestad, E., 1951. *A Study of Combined Bending and Axial Load in Reinforced Concrete Members*, *Bulletin No. 399*, University of Illinois Engineering Experimental Station, IL.

Idosako, Y., Sakashita, M., Tani, M., Nishiyama, M., 2017. Bi-directional lateral loading tests on RC shear-dominant walls, *Journal of Structural and Construction Engineering (Transactions of AIJ)* **82**, 683–692.

Illiya, R., and Bertero, V., 1980. *Effect of Amount and Arrangement of Wall-Panel Reinforcement on Hysteretic Behavior of Reinforced Concrete Walls, Report No. 80-04*, University of California, Berkeley, CA.

Imanishi T., Nishinaga M., Itakura Y., and Morita S., 1996. Experimental study of post-yield behavior of reinforced concrete shear walls subjected to bilateral deformation under axial loading, *Proceedings of the Japan Concrete Institute* **18**, 1055–1060.

Imanishi, T., 1996. Post-yield behaviors of multi-story reinforced concrete shear walls subjected to bilateral deformations under axial loading, *Proceedings of the 11th World Conference on Earthquake Engineering*, Acapulco, Mexico.

Kabeyasawa, T., Kato, S., Sato, M., Kabeyasawa, T., Fukuyama, H., Tani, M., Kim, Y., and Hosokawa, Y., 2014. Effects of bi-directional lateral loading on the strength and deformability of reinforced concrete walls with/without boundary columns, *Proceedings of the 10th U.S. National Congress on Earthquake Engineering*, Anchorage, Alaska.

Lopes, M., and Elnashi, A., 1992. A new experimental setup for high shear loading of reinforced concrete walls, *Proceedings of the 10th World Conference on Earthquake Engineering*, Madrid, Spain.

Lu, X., Zhou, Y., Yang, J., Qian, J., Song, C., and Wang, Y., 2010. NEES Shear Wall Database, Network for Earthquake Engineering Simulation, Dataset, available at https://nees.org/resources/1683.

Massone, L. M., and Wallace, J. W., 2004. Load – deformation responses of slender reinforced concrete walls, *ACI Structural Journal* **101**, 103-113.

Microsoft SQL Server, 2014. *Microsoft*, Software, https://www.microsoft.com/en-us/sql-server.

Mindess, S., Young, J. F., and Darwin, D., 2003. *Concrete*, 2nd edition, Prentice Hall, Englewood Cliffs, NJ, 644 pp.

Motter, C. J., Abdullah, S. A., and Wallace, J. W., 2018. Reinforced concrete structural walls without special boundary elements, *ACI Structural Journal* **115**, 723–733.

Nagae, T., Tahara, K., Taiso, M., Shiohara, H., Kabeyasawa, T., Kono, S., Nishiyama, M., Wallace, J. W., Ghannoum, W. M., Moehle, J. P., Sause, R., Keller, W., and Tuna, Z., 2011. *Design and Instrumentation of the 2010 E-Defense Four-Story Reinforced Concrete and Post-Tensioned Concrete Buildings*, *PEER Report 2011/104*, Pacific Earthquake Engineering Research Center, Berkeley, CA.

Niroomandi, A., S.Pampanin, S., Dhakal, R. P., and Ashtiani, M. S., 2018. Experimental study on slender rectangular RC walls under bi-directional loading, *Proceedings of the 11th U.S. National Conference on Earthquake Engineering*, Los Angeles, California.

Oesterle, R.G., Fiorato, A.E., Johal, L.S., Carpenter, J.E., Russell, H.G., and Corley, W.G., 1976. *Earthquake Resistant Structural Walls–Tests of Isolated Walls, Report to National Science Foundation,* Construction Technology Laboratories, Portland Cement Association, Skokie, IL, 315 pp.

Oesterle, R. G., Aristizabal-Ochoa, J. D., Fiorato, A. E., Russell, H. G., and Corley, W. G., 1979. *Earthquake Resistant Structural Walls–Phase II. Report to National Science Foundation*, Construction Technology Laboratories, Portland Cement Association, Skokie, IL, 336 pp.

Oesterle, R. G., 1986. Inelastic Analysis for In-plane Strength of Reinforced Concrete Shear Walls, PhD Thesis, Northwestern University, Evanston, IL, 332 pp.

Orakcal, K., Massone, L., Wallace, J., 2009. Shear strength of lightly reinforced wall piers and spandrels, *ACI Structural Journal* **106**, 455–465.

Paulay, T. and Goodsir, W. J., 1985. The ductility of structural walls, *Bulletin of the New Zealand National Society for Earthquake Engineering* **18**, 250–269.

Segura, C. L., and Wallace, W. J., 2018. Seismic performance limitations and detailing of slender RC walls, *ACI Structural Journal*, **115**, 849–860.

Seismic Engineering Research Infrastructures For European Synergies (SERIES), 2013. SERIES RC Walls Database, available at http://www.dap.series.upatras.gr.

Shiu, K. N., Aristizabal-Ochoa, J. D., Barney, G. B., Fiorato, A. E., and Corley, W. G., 1981a. *Earthquake Resistant Structural Walls—Coupled Wall Tests, Report to the National Science Foundation*, Portland Cement Association, Skokie, IL.

Shiu, K. N., Daniel, J. I., Aristizabal-Ochoa, J. D., Fiorato, A. E., and Corley, W. G., 1981b. *Earthquake Resistant Structural Walls—Tests of Walls with and Without Openings, Report to the National Science Foundation*, Portland Cement Association, Skokie, IL.

Synge A. J., 980. *Ductility of Squat Shear Walls*, *Technical Report No. 80-8*, Department of Civil Engineering, University of Canterbury, Christchurch, New Zealand.

Thomsen, J. H. and Wallace, J. W., 1995. *Displacement-Based Design of Reinforced Concrete Structural Walls: Experimental Studies of Walls with Rectangular and T-Shaped Cross Sections, Report No. CU/CEE-95/06*, Department of Civil and Environmental Engineering, Clarkson University, Potsdam, NY.

Tran, T. A., 2012. Experimental and Analytical Studies of Moderate Aspect Ratio Reinforced Concrete Structural Walls, Ph.D. Dissertation, University of California, Los Angeles, CA, 300 pp.

Vallenas, J. M., Bertero, V. V., and Popov, E. P., 1979. *Hysteretic Behavior of Reinforced Concrete Structural Walls, Report No. EERC 79-20*, University of California, Berkeley, CA.

Wallace, J. W., 2012. Behavior, design, and modeling of structural walls and coupling beams–lessons from recent laboratory tests and earthquakes, *International Journal of Concrete Structures and Materials* **6**, 3–18.

Wallace, J. W., 2011. February 27, 2010 Chile Earthquake: Preliminary observations on structural performance and implications for U.S. building codes and standards, *Proceedings of the ASCE Structures Congress*, Las Vegas, Nevada.

Wallace, J. W., and Orakcal, K., 2002. ACI 318-99 provisions for seismic design of structural walls, *ACI Structural Journal* **99**, 499–508.

Wallace, J. W., Massone, L. M., Bonelli, P., Dragovich, J., Lagos, R., Luders, C., and Moehle, J., 2012. Damage and implications for seismic design of RC structural wall buildings, *Earthquake Spectra* **28**, 281–289.

Wang, T. Y., Bertero, V. V., and Popov, E. P., 1975. *Hysteretic Behavior of Reinforced Concrete Framed Walls, Report No. EERC 75-23*, University of California, Berkeley, CA.

CHAPTER 3. Drift Capacity of RC Structural Walls with Special Boundary Elements

3.1. Abstract

Performance of reinforced concrete (RC) walls in recent laboratory tests and in recent strong earthquakes has revealed that thin wall boundaries are susceptible to concrete crushing, rebar buckling, and lateral instability. To address this concern, a wall database with detailed information on more than 1000 tests was assembled to enable the study of the impact of various parameters on wall deformation capacity. For this study, the data are filtered to identify and analyze a dataset of 164 tests on well-detailed walls generally satisfying ACI 318-14 provisions for special structural walls. The study indicates that wall deformation capacity is primarily a function of the ratio of wall neutral axis depth-to-compression zone width $\left(c/b\right)$, the ratio of wall length-to-compression zone width $\left(l_w/b\right)$, wall shear stress ratio $\left(v_{max}/\sqrt{f'_c}\right)$, and the configuration of boundary transverse reinforcement. Based on these observations, an expression is developed to predict wall drift capacity with low coefficient of variation.

3.2. Introduction

Reinforced concrete (RC) structural walls are commonly used as lateral force-resisting elements in tall and moderately tall buildings because they provide substantial lateral strength and stiffness and are assumed to provide the needed nonlinear deformation capacity if detailed according to ACI 318. Major updates to ACI 318 design provisions for slender walls occurred in 1983, 1999, and 2014. In 1983, an extreme compression fiber stress limit of $0.2f'_c$ under bending and axial stress was introduced to determine if special boundary transverse reinforcement was required, whereas in 1999, an alternative to the stress-based approach, a displacement-based approach, was

introduced to evaluate the need for special boundary transverse reinforcement for slender, continuous walls. In 2014, more stringent detailing requirements for slender ($h_w / l_w \geq 2.0$) walls were introduced to address issues associated with detailing and lateral stability of thin walls, and to include a minimum wall thickness for sections that are not tension-controlled. The ACI 318-83 provisions were based on research conducted by the Portland Cement Association (PCA) (e.g., Oesterle et al., 1976 & 1979) and Paulay and Goodsir (1985) which demonstrated that large lateral drift ratios could be achieved when compression zones in yielding regions were adequately detailed to remain stable, whereas the 1999 additions were based primarily on the work by Wallace and Moehle (1992), Wallace (1994), and Thomsen and Wallace (2004) to develop a displacement-based approach to assess wall boundary detailing requirements. The 2014 changes to ACI 318 were based on observations from recent earthquakes and laboratory tests (Wallace 2012, Wallace et al., 2012; Nagae et al., 2011; Lowes et al., 2012).

Even with the 2014 updates, the underlying premise of the ACI 318-14 approach to design and detailing of Special Structural Walls is that walls satisfying the provisions of §18.10.6.2 through §18.10.6.4 possess drift capacities in excess of the expected drift demands. However, recent research has shown that wall drift capacity is impacted by wall geometry, configuration of boundary transverse reinforcement, and level of wall shear stress. For example, Segura and Wallace (2018a) studied the relationship between wall thickness and lateral drift capacity and found that thin walls possess smaller lateral drift capacities than thicker walls that are otherwise similar. Furthermore, it has been found that thin, rectangular sections confined by an outer hoop and intermediate legs of crossties, which is a detail allowed by ACI 318-14 §18.10.6.4 at wall boundaries, is less stable in compression than sections that utilize overlapping hoops for confinement (Welt, 2015; Segura and Wallace, 2018a). Finally, Whitman (2015) suggested, using

finite element analysis, that the confined length of a boundary element should be increased over that currently required, to address the increase in compression demands that result from higher shear demands.

This research focuses on assessing which wall design parameters have the greatest impact on wall lateral drift capacity by assembling a detailed database that includes data from more than 1000 large-scale tests. The data are filtered to identify a dataset of 164 tests on walls that are ACI 318-14 code-compliant, or nearly code-compliant, and results for these tests are analyzed. The data analysis is then used to develop an expression to predict mean wall drift capacity prior to substantial lateral strength loss with low coefficient of variation (COV).

3.3. Research Significance

Recent research has indicated that wall lateral drift capacity is significantly impacted by wall geometry, detailing, and compression and shear stress demands; however, current ACI 318-14 provisions do not adequately address the role of these parameters on wall drift capacity. Instead, it is assumed that all walls satisfying requirements of ACI 318-14 §18.10.6.1 through §18.10.6.4 possess adequate drift capacity to meet the estimated drift demands determined from analysis. A test database is assembled and analyzed to study the impact of various design parameters and derive an expression for the lateral drift capacity of slender walls with ACI 318-14 special boundary elements.

3.4. Experimental RC Wall Database

Prior to the mid-1990's, relatively few large-scale experimental studies had been conducted on relatively slender reinforced concrete structural walls (Oesterle et al., 1976, 1979, Paulay and

Goodsir, 1985). However, since then, a substantial number of experimental studies have been conducted to assess the impact of various design parameters on wall load-deformation responses and failure modes. Several attempts have been made to assemble wall databases (e.g., NEEShub Shear Wall Database (Lu et al., 2010) and the SERIES Database, 2013) to assist in the development of code provisions and to validate analytical models for RC walls; however, these databases do not contain sufficient information to allow detailed and robust assessment of wall lateral drift capacity. In addition, a significant number of tests have been conducted since the 2010 Chile and 2011 New Zealand earthquakes, and data from these more recent tests are typically not included in these databases. To address these issues, a new database was developed, referred to as UCLA-RCWalls, which includes information from more than 1000 wall tests from more than 200 experimental programs reported in the literature. The database includes detailed information about the tests, i.e., wall cross-section, loading protocol, configuration of boundary transverse reinforcement, and material properties. The database also includes backbone relations (base shear-total top displacement, base moment-base rotation, and/or base shear-top shear displacement), consisting of seven points (*origin, cracking, general yielding, peak*, *ultimate, residual*, and *collapse*). Ultimate deformation capacity is defined as the total displacement or rotation at which strength degrades 20% from the peak strength, which has been widely used to define deformation at strength loss (e.g., Elwood et al., 2009). Finally, the database also contains analytical (or computed) data, such as moment-curvature relationships, nominal and yield moment strength ($\boldsymbol{M_n}$ and $\boldsymbol{M_y}$) and curvature (ϕ_n and ϕ_y), neutral axis depth, $\boldsymbol{c}$, and wall shear strength computed according to ACI 318-14.

An important aspect of the database involved addressing the impact of different test setups (cantilever wall tests, e.g., Thomsen and Wallace, 2004, versus panel/partial height wall tests, e.g.,

Segura Wallace, 2018a) on wall lateral drift capacity. For the wall panel tests and partial wall height tests, the UCLA-RCWalls database includes the drift capacity at the effective height $\left(M_{u,base}/V_{u,base}\right)$, determined as sum of the measured displacement at the top of the panel (experimental) and the estimated contribution of elastic bending deformations between the top of the test specimen and the effective height (e.g., see Segura and Wallace, 2018b).

For this study, which focuses on the drift capacity of walls with Special Boundary Elements (SBEs), the UCLA-RCWalls database was filtered to include only wall tests satisfying the following requirements:

a) Quasi-static, reversed cyclic loading,

b) Measured concrete compressive strength, $f_c' \geq 3$ ksi [20.7 MPa],

c) Ratio actual tensile-to-yield strength of boundary longitudinal reinforcement, $f_u/f_y \geq 1.2$,

d) Rectangular, or nearly rectangular, compression zone, b,

e) Wall web thickness, $t_w \geq 3.5$ in. [90 mm],

f) A minimum of two curtains of web vertical and horizontal reinforcement,

g) Shear span ratio, $M/Vl_w \geq 1.0$,

h) Boundary longitudinal reinforcement ratio, $\rho_{Long,BE} \geq 6\sqrt{f_c'(\text{psi})}/f_y \left[0.5\sqrt{f_c'(\text{MPa})}/f_y\right]$,

i) Ratio of provided-to-required (per ACI 318-14 §18.10.6.4) area of boundary transverse reinforcement, $A_{sh,provided}/A_{sh,required} \geq 0.7$,

j) Ratio of vertical spacing of boundary transverse reinforcement to minimum diameter of longitudinal boundary reinforcement, $s/d_b \leq 8.0$,

k) Centerline distance between laterally supported boundary longitudinal bars, h_x, between 1.0 in. and 9.0 in. [25 to 230 mm].

l) Reported strength loss due to flexural tension or compression failure, i.e., tests were excluded if some noticeable strength loss was not observed (only three tests were excluded for this reason), or if walls exhibited shear (i.e., diagonal tension, diagonal compression, sliding at the base) or lap slice failures prior to yielding of longitudinal reinforcement.

Based on the selected filters, a total of 164 test specimens were identified. Histograms for various database parameters for the 164 tests are shown in Fig. 3-1, where $P/(A_g f'_c)$ is the axial load normalized by concrete compressive strength (f'_c) and gross concrete area (A_g) and M/Vl_w is the ratio of base moment-to-base shear normalized by wall length (l_w). The filters were selected to identify walls that satisfied, or nearly satisfied, ACI 318-14, Chapter 18 provisions for Special Structural Walls, including requirements for boundary transverse reinforcement in §18.10.6.4. A concrete compression strength limit of 3 ksi [20.7 MPa] was specified in accordance with requirements of ACI 318-14 §18.2.5 for special seismic systems. Walls with web thickness, t_w, less than 3.5 in. [90 mm] were not included because use of two layers of web reinforcement along with realistic concrete cover is not practical. At least two curtains of web reinforcement was specified to be consistent with ACI 318-14 §18.10.2.2. The limit on ratio f_u/f_y is slightly less restrictive than the limit of 1.25 specified in ACI 318-14 §20.2.2.5. The specified limits on s/d_b ≤ 8.0 and $A_{sh,provided}/A_{sh,required}$ ≥ 0.7 are slightly less restrictive than the current limits in ACI 318-14 §18.10.6.4 of 6.0 and 1.0, respectively, to include more data. The limit on $\rho_{Long.BE}$ was included

to avoid brittle tension failures (Lu et al., 2016). ACI 318-14 §18.10.6.4e requires $h_{x,max}$ not exceeding the lesser of 14 in. [355 mm] or 2b/3; however, most of the tests in the database were conducted at 25 to 50% scale; therefore, $h_{x,max}$ for the wall tests should generally be between 3.5 to 7.0 in. [89 to 178 mm] for the 14 in. [355 mm] limit. Based on the range of h_x used to filter the data, 95% of the specimens have $h_x \leq 6$ in. [152 mm], which is reasonable, whereas the histogram for h_x/b presented in Fig. 3-1(*f*) indicates that a majority of tests have $h_x/b < 3/4$, which is slightly higher than the current limit of $h_x/b < 2/3$.

The histogram for the parameter M/Vl_w, presented in Fig. 3-1(*d*), indicates that 44 tests in the reduced database have $1.0 \leq M/Vl_w < 2.0$, and 120 tests with $M/Vl_w \geq 2.0$. Tests with $M/Vl_w \geq 2.0$ are generally appropriate for assessing the drift capacity of walls designed using ACI 318-14 §18.10.6.2, which requires $M/Vl_w \geq 2.0$, whereas the other tests are more appropriate for walls designed according to ACI 318-14 §18.10.6.3. Walls with $M/Vl_w < 1.0$ are not included because they are generally governed by shear failure. In subsequent assessments presented here, either the entire dataset of 164 tests is used, or subsets for $1.0 \leq M/Vl_w < 2.0$ and $M/Vl_w \geq 2.0$ are used, as deemed appropriate.

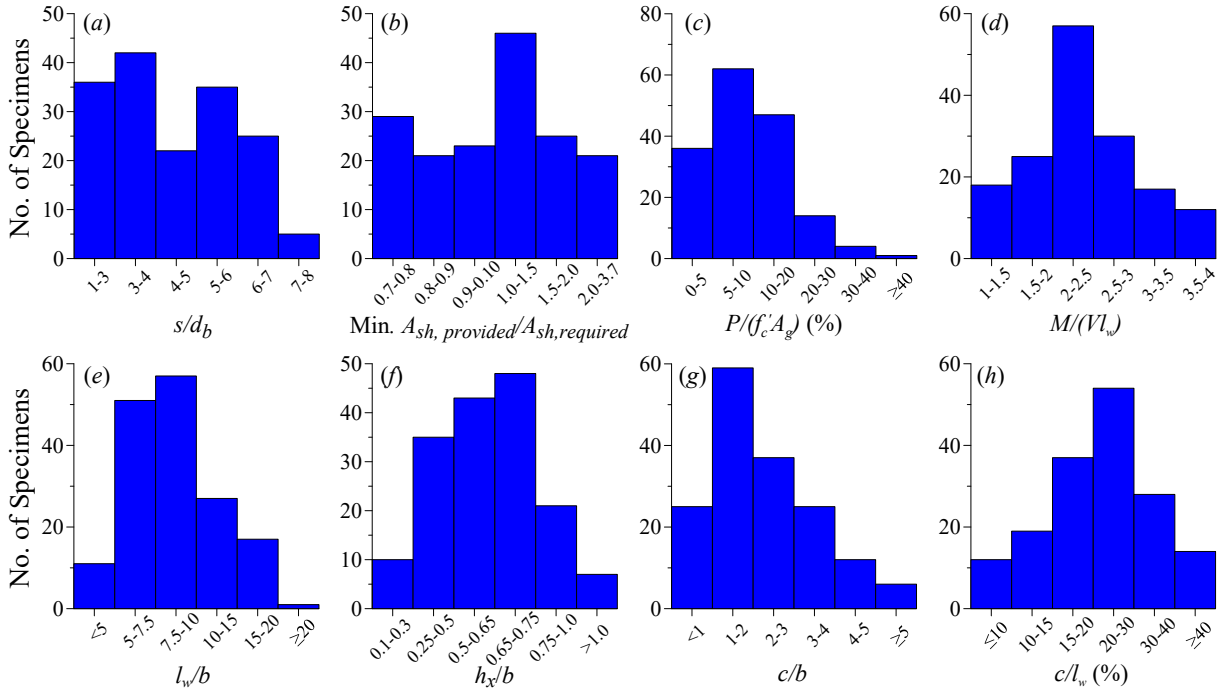

Fig. 3-1–Histograms of the dataset (164 tests) used in this study.

In ACI 318-14 Equation 18.10.6.2, roof drift demand $\left(\delta_u / h_w\right)$ determined using ASCE 7 analysis procedures is used to assess the need for SBEs; however, no specific check is required to ensure that the roof drift capacity of a wall with SBEs exceeds the roof drift demand. An alternative approach, to use plastic rotation was not considered in this study, because ACI 318-14 does not include a definition for plastic hinge rotation and plastic hinge rotation capacities from wall tests are not always measured in tests or reported in the literature. However, it would be a relatively simple task to covert roof drift to rotation (elastic and plastic) over an assumed plastic hinge length. To facilitate comparison of test drift capacities with drift demands determined from analysis, drift capacities for the 164 tests corresponding to the effective height $\left(h_{eff} \approx 0.7 h_w\right)$ were adjusted to determine roof-level (h_w) drift ratios to be consistent with ACI 318-14 Equation 18.10.6.2, which uses roof level drift demand to assess the need for special boundary elements. To accomplish this

task, the increase in elastic drift between h_{eff} and h_w was estimated analytically based on the ASCE 7-10 §12.8 Equivalent Lateral Force procedure for a Class B site in Los Angeles with number of stories estimated based on h_{eff} (Fig. 3-2) and an approximate test scale. The wall effective bending stiffness between h_{eff} and h_w was determined at first yield of boundary longitudinal reinforcement based on a computed moment-curvature relation included in the database. Use of this approach typically increased the elastic roof level displacements by 10 to 20%, which is relatively small compared to nonlinear displacements, which are due to plastic hinge rotation at the wall base, and thus, nonlinear drift at h_{eff} and h_w are equal.

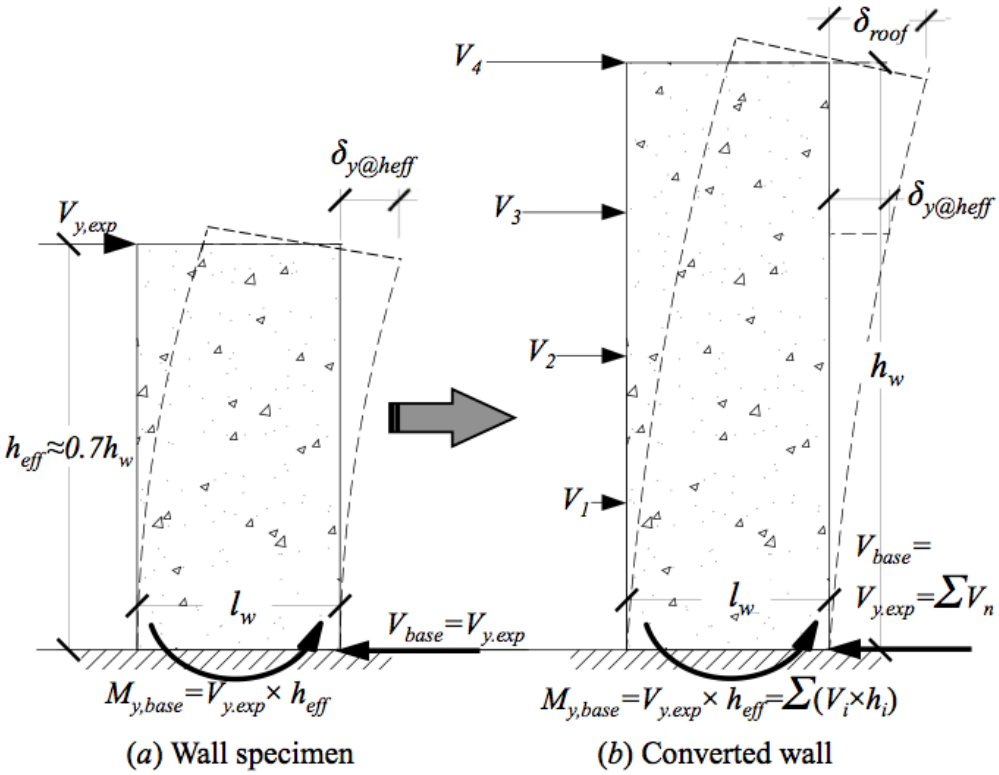

Fig. 3-2–Conversion of elastic drift from h_{eff} and h_w.

3.5. Parameters That Impact Wall Lateral Drift Capacity

Parameters likely to impact the lateral drift capacity of walls with SBEs (Table 3-1) were selected based on a review of current codes/standards and available literature (e.g., ACI 318-14; ASCE 41-13; Oesterle et al., 1976 & 1979, Brown et al., 2006; Birely, 2012; Segura and Wallace, 2018a). Based on this review, the following parameters were expected to have the greatest impact on wall lateral drift capacity: (1) ratio of wall neutral axis depth-to-width of the compression zone, c/b, where c is computed for an extreme fiber concrete compressive strain of 0.003, (2) ratio of the wall length-to-width of the compression zone, l_w/b, (3) ratio of the maximum wall shear stress ratio, $v_{max}/\sqrt{f'_c}$, and (4) the configuration of the boundary transverse reinforcement used, e.g., use of overlapping hoops versus a single perimeter hoop with intermediate crossties. Other parameters investigated (Table 3-1) did not significantly impact wall lateral drift capacity, as will be shown in subsequent paragraphs.

Table 3-1–Correlation coefficients, R, for design parameters and wall drift capacity

Design Parameter	$\frac{c}{b}$	$\frac{l_w}{b}$	$\frac{v_{max}}{\sqrt{f'_c}}$	$\frac{P}{A_g f'_c}$	$\frac{A_{sh,provided}}{A_{sh,required}}$	$\frac{s}{d_b}$	$\frac{h_x}{b}$	$\rho_{long.\,BE}$	$\rho_{t,web}$ *	$\frac{f_u}{f_y}$	$\frac{l_{BE}}{l_w}$ *	$\frac{c}{l_w}$	$\frac{l_w c}{b^2}$
Correlation coefficient, R	-0.66	-0.56	-0.30	-0.08	0.13	-0.02	-0.25	-0.32	-0.14	-0.07	0.06	-0.32	-0.68

* $\rho_{t,web}$ = web transverse reinforcement ratio, and $\frac{l_{BE}}{l_w}$ = length of confined boundary normalized by wall length.

A series of linear regression analyses were performed to identify the most influential parameters on wall drift capacity. Correlation coefficients, R, for the complete dataset of 164 tests for various parameters are presented in Table 3-1. Parameters c/b, l_w/b, and $v_{max}/\sqrt{f'_c}$, produce the highest

correlation coefficients with wall drift capacity, with R = 0.66, 0.56, and 0.30, respectively. A similar approach indicated that use of overlapping hoops versus a single perimeter hoop with supplemental legs of crossties impacted lateral drift capacity. Other parameters, such as $\rho_{Long.BE}$, h_x/b, and c/l_w produce modest R-values; however, the impact of these parameters are already incorporated into c/b and l_w/b. Other parameters, within the range of the filtered data, had little impact on lateral drift capacity. A more detailed assessment of the four more significant parameters is presented in the following paragraphs by using results from companion tests and results from the dataset of 164 tests. Following this presentation, a general expression to predict wall drift capacity is presented that includes the influence of these four parameters.

3.5.1. Impact of l_w/b

Brown et al. (2006) assembled a building inventory of post-1991 designed mid-rise buildings utilizing structural walls as the primary lateral load resisting system on the West Coast of the United States. The building inventory indicated that walls with $l_w/b \geq 15$ are quite common; however, due to limitations associated with laboratory testing, it is noted that there are only a handful of test specimens (6 tests) with SBEs and very slender cross-sections $(l_w/b \geq 20)$ in the selected dataset, as seen from Fig. 3-1(*e*). The complete database of more than 1000 tests includes 38 tests with $l_w/b \geq 20$; however, 32 of them do not meet the filtering criteria for the reduced dataset because they either failed in shear, did not have sufficient boundary transverse reinforcement, or were tested under monotonic loading.

Although the linear regression analysis indicated a fairly strong correlation between l_w/b and drift capacity, various parameters are changing, and it is not always clear which variables are impacting

drift capacity. Therefore, the reduced dataset (164 tests) was examined to find "companion" tests, i.e., tests where the change in ratio l_w/b is due to changes of primarily one parameter at a time (either wall length l_w or wall compression zone width b). Results for drift capacity versus l_w/b are presented in Fig. 3-3 for four series of companion test specimens with SBEs (Chun, 2015; Chun and Park, 2016; Chun et al., 2013; Segura and Wallace, 2018a; Xiao and Guo, 2014; Zhi et al., 2015) and indicate substantial reductions in wall drift capacity. The reason for this is not obvious. For example, consider two cantilever walls constructed with the same materials and of the same height h_w pushed to the same top displacement $\delta_u > \delta_y$, with identical values of wall length l_w, neutral axis depth c/l_w, and wall shear stress $v_{max}/\sqrt{f_c'}$, where l_w/b is varied by changing only b. For this to be the case, wall longitudinal reinforcement would have to be changed to maintain the ratios of c/l_w and $v_{max}/\sqrt{f_c'}$ as b changes. Because yield displacement (e.g., associated with first yield of boundary longitudinal reinforcement) is related to c/l_w, the yield displacements are equal, and therefore, the inelastic displacements are equal. Based on the common assumption that wall plastic hinge length, l_p, is related to wall length l_w, e.g., $l_p = 0.5l_w$, and assuming plane sections remain plane after loading (which has been shown to be reasonably true, see Thomsen and Wallace, 2004), then the strain gradient along the cross section at all locations would be identical. Under these conditions and assumptions, there is no reason to expect that the drift capacities of the two walls should be different. The one important parameter that is not constant in this example is the ratio of neutral axis depth to the wall compression zone thickness c/b. Segura and Wallace (2018b) has shown that, for slender walls that fail due to flexural compression (concrete crushing, reinforcement buckling, and lateral instability of the compression zone), ratio c/b is, as shown in the subsequent section, an important variable as the compressive

strains tend to concentrate over a wall height that is more closely related to b than l_w. The walls tested by Segura and Wallace (2018a) have similar drift capacities to the other companion test specimens presented in Fig. 3-3, which have lower values of l_w/b, because other parameters are influencing drift capacity, as mentioned above and discussed below.

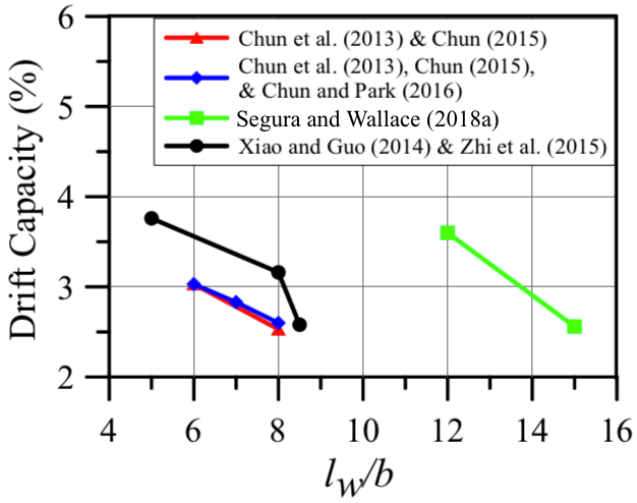

Fig. 3-3–Drift capacity of companion specimens against cross-section slenderness ratio.

3.5.2. Impact of c/b

Segura and Wallace (2018b) show that larger values of c/b impact drift capacity because thicker walls increase the spread of plasticity and provide increased lateral stability under nonlinear compression yielding. Takahashi et al. (2013) observed that c/b correlates well with plastic drift capacity for slender walls with modest boundary transverse reinforcement. The histogram plotted in Fig. 3-1**(g)** indicates that only 18 tests have been conducted with $c/b > 4$.

As noted previously in Table 3-1, use of a combined slenderness parameter $\lambda_b = (l_w/b)(c/b)$ provided an efficient means to account for slenderness of the cross section (l_w/b) and the slenderness of the compression zone on the cross section (c/b). This combined parameter, as noted previously, considers the impact of concrete and reinforcement material properties, axial load, wall geometry, and quantities and distributions of longitudinal reinforcement at the boundary and in the web. Fig. 3-4 and Table 3-1 indicate that wall drift capacity is strongly correlated with λ_b, with drift capacity varying between 1.25% and 3.25% as λ_b reduces from 80 to zero. The cluster of data points with $\lambda_b \approx 80$ includes the tests by Birely (2012), which have a rather slender cross section $(l_w/b \approx 20)$ and a relatively large ratio of $c/b \approx$ 4 to 5, although the ratio of $c/l_w \approx$0.20 to 0.25 is not vastly different than many other tests included in the dataset (see Fig. 3-1).

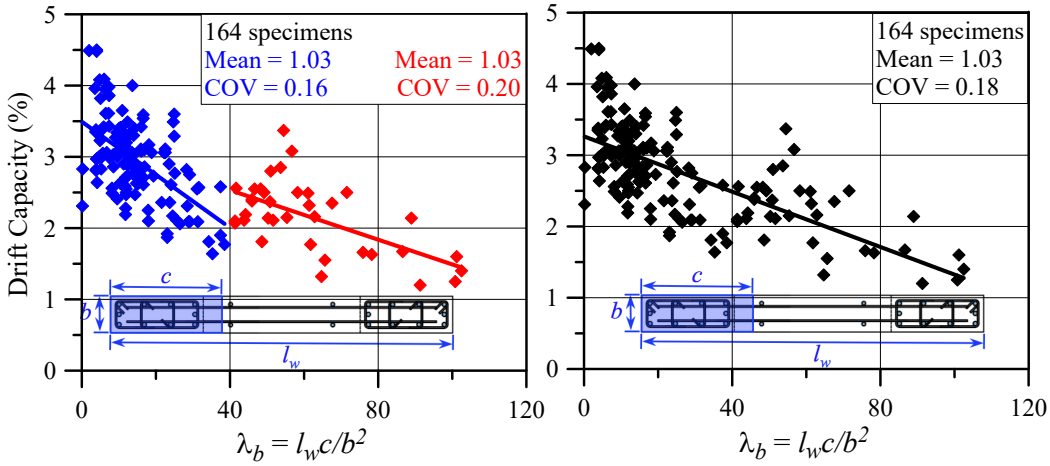

(*a*) $0 \le \lambda_b \le 40$ and $40 < \lambda_b$ (*b*) $0 \le \lambda_b$

Fig. 3-4–Wall drift capacity variation versus λ_b.

The results plotted in Fig. 3-4 have very important design implications. For design level shaking (**DE**), ASCE 7-10 §12.12.1 limits allowable interstory drift ratio to 0.02 for typical RC buildings

in Risk Category I & II that are taller than four stories and utilize structural walls as a lateral-force-resisting system. At Maximum Considered Earthquake (**MCE**) level shaking, which is commonly used to assess collapse prevention, this limit is typically taken as 0.03. If roof drift is approximated as three-quarters of peak interstory drift, then the peak roof drift demand allowed by ASCE 7-10 is approximately 0.0225. Results presented in Fig. 3-4 indicate that the drift capacities of RC walls with SBEs vary substantially, i.e., all RC walls with SBEs do not have the same drift capacity, and walls with $\lambda_b > 50$ have a mean drift capacity less than that allowed by ASCE 7-10. Results are presented for two ranges of λ_b in Fig. 3-4(***a***) and for the entire dataset in Fig. 3-4(***b***), to show that trends are similar. The findings suggest strongly that changes to ACI 318-14 are needed to address this issue. A possible approach to address this issue would be to include a drift demand versus drift capacity provision in ACI 318, e.g., similar to demand-to-capacity checks for moment or shear strengths, or drift capacity of slab-column connections (ACI 318-14 §18.14.5), to meet a specified level of reliability.

3.5.3. Impact of $v_{max}/\sqrt{f_c'}$

As noted earlier, wall shear stress demand, expressed as $v_{max}/\sqrt{f_c'}$, has a significant impact on wall lateral drift capacity, where $v_{max} = V_{max}/A_{cv}$ and V_{max} is taken as the maximum shear force that develops in the wall where yielding of tension reinforcement under combined bending and axial stresses limits the shear force demand, and $A_{cv} = l_w \times t_w$. It is noted that, because the database includes only walls tested under quasi-static loading, the impact of dynamic shear amplification is not considered (e.g., Keintzel, 1990; Eberhard and Sozen, 1993). Even for relatively slender walls, which are defined in ACI 318-14 as $h_w/l_w \geq 2.0$, there is ample evidence that wall lateral drift capacity is impacted by shear, e.g., see experimental studies presented in Fig. 3-5 and Table 3-2and

trends shown in Fig. 3-6(***b***). Kolozvari et al. (2015) used a shear-flexure interaction model to demonstrate that shear transfer from diagonal compressive struts into the flexural compression zone results in higher concrete compressive strains than would result from bending and axial load alone, and also tends to increase the neutral axis depth modestly. As well, ASCE 41-13 Tables 10-19 and 10-21 include wall modeling parameters (e.g., plastic rotation capacities at lateral strength loss and at axial failure) that depend on the level of wall shear stress, with values of $4\sqrt{f_c'\ \text{psi}}\ \left(0.33\sqrt{f_c'\ \text{MPa}}\right)$ and $6\sqrt{f_c'\ \text{psi}}\ \left(0.5\sqrt{f_c'\ \text{MPa}}\right)$ for walls with lower and higher shear demands, respectively. Currently, ACI 318-14 §18.10.4.4 allows wall shear stress demands as high as $10\sqrt{f_c'\ \textbf{psi}}\ \left(0.83\sqrt{f_c'\ \text{MPa}}\right)$ for individual wall segments, although the average shear stress demand on walls resisting a common shear force is limited to $8\sqrt{f_c'\ \text{psi}}\ \left(0.67\sqrt{f_c'\ \text{MPa}}\right)$.

As was done earlier for parameter l_w/b, the impact of shear stress on wall lateral drift capacity is first evaluated by using "companion" tests, where the primary test variable is wall shear stress. In general, for the companion specimens, a change in shear stress demand was accomplished by either varying M/Vl_w or the quantity of longitudinal reinforcement (e.g., see programs presented in Table 3-2); for this latter condition, in addition to shear stress, wall moment capacity and neutral axis depth are also impacted. Fig. 3-5 shows wall drift capacity versus shear stress ratio $\left(\text{i.e., } v_{\max}/\sqrt{f_c'}\right)$ for 13 pairs of companion specimens and indicates that higher shear demands have a detrimental impact on wall drift capacity, even for relatively low shear demands, i.e., $v_{max}/\sqrt{f_c'\ \text{psi}} \le 5\left[v_{max}/\sqrt{f_c'\ \text{MPa}}\ \le\ 0.42\right]$. Table 3-2 provides detailed information about the results plotted in Fig. 3-5. It also is noted that the impact (slope) of shear stress is different from

one pair of companion specimens to another, indicating that other parameters may also be at play (e.g., c/b, since increasing this ratio also tends to reduce drift capacity). Drift capacities versus λ_b are plotted in Fig. 3-6(***a***) for the entire dataset (164 tests) with $M/Vl_w \geq 1.0$ and in Fig. 3-6(***b***) for the slender walls (120 tests) in the dataset with $M/Vl_w \geq 2.0$ to demonstrate that shear stress demand impacts drift capacity beyond what can be attributed to changes in other variables. The tests are separated into two bins, one for low-to-modest and the other for higher shear stress demands. The trend lines plotted in Fig. 3-6(***a***) and Fig. 3-6(***b***), which are offset by approximately 0.5% drift, clearly indicate that higher shear demand has a significant negative impact on wall drift capacity. Therefore, it is appropriate that the level of shear stress demand on a wall should be considered when assessing drift capacity, which is consistent with ASCE 41-13 Table 10-19, where the modeling parameters and acceptance criteria vary with level of wall shear stress.

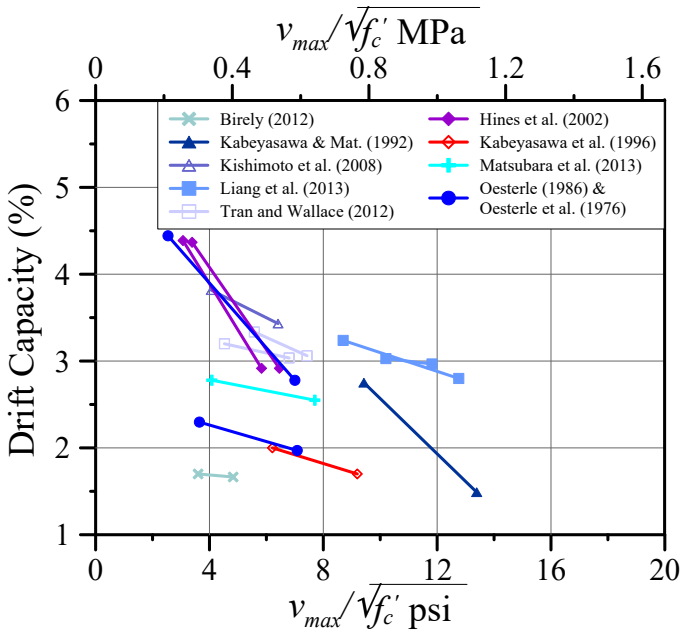

Fig. 3-5–Companion specimens with special detailing and different levels of wall shear stress.

Table 3-2–Companion wall specimens with special detailing and different levels of shear stress

Ref.	Test ID	$\frac{P}{A_g f'_c}$ (%)	$\frac{M}{Vl_w}$	$\rho_{long.BE}$ (%)	$\frac{V_{n,ACI}}{A_{cv}\sqrt{f'_c}}$ in psi	$\frac{V_{test}}{A_{cv}\sqrt{f'_c}}$ in psi	$\frac{V_{@Mn}}{A_{cv}\sqrt{f'_c}}$ in psi	$\frac{c}{l_w}$ (%)	$\frac{l_w}{b}$	$\frac{c}{b}$	Drift Capacity (%)
Kishimoto et al., 2008	No. 5	18.3	2.0	4.0	7.2	6.4	5.7	35	8.0	2.8	3.43
	No. 6	17.7	3.0			4.1	3.7				3.82
Kabeyasawa & Matsumoto 1992	NW-1	10.9	2.0	2.1	8.9	9.4	7.5	20	8.5	1.7	2.75
	NW-2	10.2	1.3		9.6	13.4	10.9				1.49
Liang et al., 2013	DHSCW-02	21.0	2.1	2.7	9.3	8.7	8.9	34	5.0	1.7	3.24
	DHSCW-04		1.5		9.7	12.8	12.4	33		1.6	2.80
Tran and Wallace 2015	RW-A20-P10-S38	7.3	2.0	3.0	4.4	4.5	3.6	17	8.0	1.4	3.20
	RW-A20-P10-S63			6.7	6.7	6.8	6.1	22		1.7	3.04
Tran and Wallace, 2015	RW-A15-P10-S51	7.7	1.5	3.0	5.9	5.6	4.9	18	8.0	1.4	3.34
	RW-A15-P10-S78	6.4		5.7	8.2	7.4	6.9	21		1.7	3.06
Hines et al., 2002	1A	9.3	4.0	1.6	7.6	3.4	2.8	20	4.5	0.9	4.37
	2A	9.7	2.0		7.9	6.5	5.8				2.92
Hines et al., 2002	1B	8.3	4.0	1.6	3.6	3.1	2.7	20	4.5	0.9	4.39
	2B	8.5	2.0			5.8	5.4				2.92
Kabeyasawa et al., 1996	HW1	-8.0	2.3	4.3	7.2	6.2	4.1	12	11	1.3	2.00
	HW2	-7.9	2.0			9.2	6.1	17		1.9	1.70
Matsubara et al., 2013[1]	N	4.5	1.5	1.6	7.5	7.7	6.2	22	14.5	3.2	2.55
	N(M/Qd3.1)	5.3	3.1	1.5	7.1	4.1	3.1	24		3.5	2.78
Oesterle 1986	R3	6.9	2.4	5.9	7.3	7.1	6.1	25	18.7	4.7	1.97
	R4	7.4		3.4	6.1	3.6	3.5	19		3.6	2.30
Oesterle et al., 1976	B3	0.0	2.4	1.1	4.6	2.5	2.3	5	6.3	0.3	4.44
	B5			3.7	7.6	7.0	6.2	10		0.6	2.78
Liang et al., 2013[1]	DHSCW-01	28.0	2.1	2.7	10.0	10.2	10.0	46	5.0	2.3	3.03
	DHSCW-03	21.0	1.5			11.8	12.5	34		1.7	2.97
Birely, 2012[1]	PW1	9.5	2.8	3.4	4.9	3.6	3.2	22	20	4.3	1.70
	PW2	13.0	2.2		4.7	4.8	4.6	25		5.1	1.66

[1]Although these specimens were intended to be companion specimens, there is a moderate variation between the two specimens.

$V_{n,ACI}$ = the nominal wall shear strength in accordance with ACI 318-14 §18.10.4.

$V_{@Mn}$ = wall shear strength corresponding to nominal flexural strength (M_n),

1 ksi = 1000 psi = 6.895 MPa.

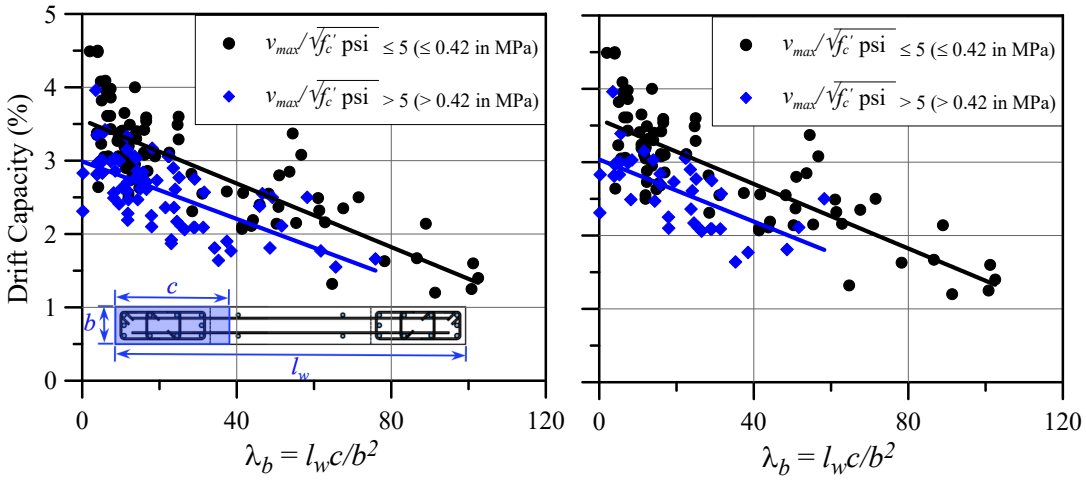

(*a*) Entire dataset ($M/Vl_w \geq 1.0$) (*b*) $M/Vl_w \geq 2.0$

Fig. 3-6–Impact of wall shear stress on wall drift capacity.

3.5.4. Overlapping Hoops

As noted earlier, one of the primary reasons to develop the database was to assess the impact of different detailing options on wall drift capacity. ACI 318-14 §18.7.5.2(a) states that "transverse reinforcement shall comprise either single or overlapping spirals, circular hoops, or rectilinear hoops with or without crossties"; therefore, both configurations are allowed and are assumed to be equivalent. To assess the impact of overlapping hoops on lateral drift capacity, very detailed information on the configuration of boundary transverse reinforcement used in each test was included in the database. Different types of overlapping hoop configurations observed in the database are shown in Fig. 3-7**,** whereas different configurations used for supplemental crossties combined with a single perimeter hoop are shown in Fig. 3-8. It is noted that ACI 318-14 §25.3.5 requires that crossties shall have a seismic hook (135º) at one end and a 90º hook at the other end, and that the 90º hooks on successive crossties engaging the same longitudinal bars must be alternated end for end vertically and along the perimeter of the boundary element. For columns, ACI 318-14 §18.7.5.2 requires use of seismic hooks (135º) on both ends of crossties for high axial

load ratios and high concrete compressive strengths (f_c'≥10,000 psi; 69 MPa); however, this provision does not apply to walls. As noted in Fig. 3-8, a range of crosstie configurations are included in the database. Tests with 135º-135º hooks on crossties were primarily conducted in Japan, where the Architectural Institute of Japan (AIJ 2010) requires their use, and China. Test results that utilize a single perimeter hoop with headed bar crossties for wall boundary transverse reinforcement (Fig. 3-8(*c*)) are limited to the studies by Mobeen (2002) and Seo et al. (2010). However, walls tested utilizing headed bars for crossties have relatively small ratios of (l_w/b) and (c/b), such that $\lambda_b \leq 6$, and strength degradation for these tests resulted from longitudinal bar fracture; therefore, these tests, by themselves, do not provide sufficient insight into the effectiveness of headed bars used for transverse reinforcement within SBEs.

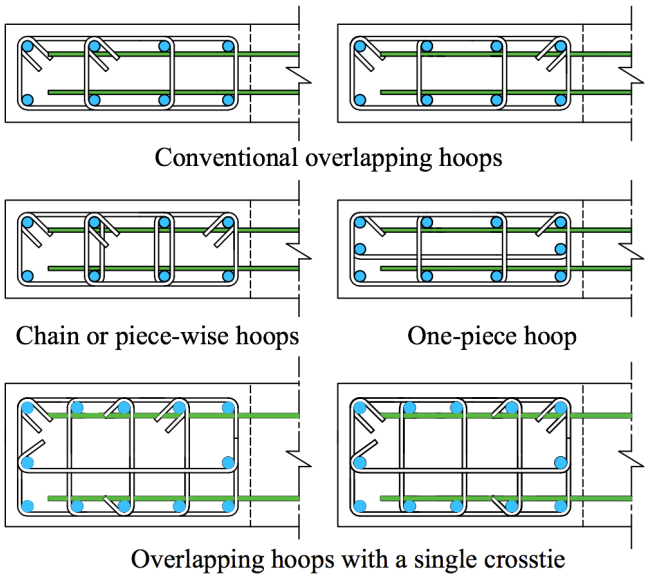

Fig. 3-7–Types of overlapping hoop configurations observed in the database.

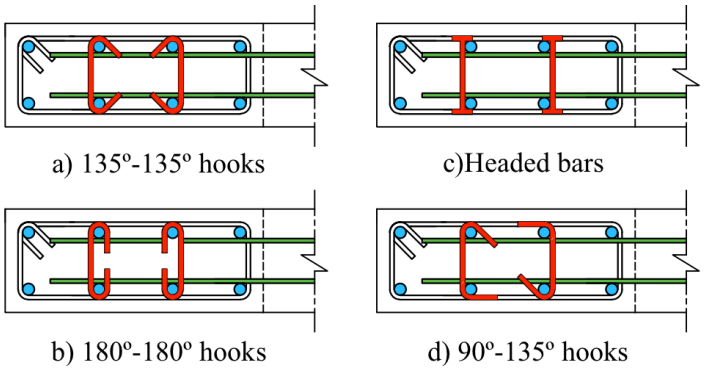

Fig. 3-8–Types of crossties observed in the database.

Of the 164 tests, analysis of the dataset indicates that 51 tests utilized overlapping hoop configurations such as those shown in Fig. 3-7, whereas 51 and 31 tests used a combination of a perimeter hoop and crossties with 90º-135º and 135º-135º hooks, respectively. Twenty-eight tests utilized a single hoop without intermediate legs of crossties, and the rest (3 tests) used headed bars as intermediate legs combined with a single perimeter hoop such as that shown in Fig. 3-8(***c***); however, these three tests have $\boldsymbol{c/b} \leq 1.3$ and $\boldsymbol{\lambda_b} \leq 6$. Drift capacity versus $\boldsymbol{c/b}$ and $\boldsymbol{\lambda_b}$, for $\boldsymbol{v_{max}} / \sqrt{\boldsymbol{f_c'}\ \text{psi}} \leq 5 \left[\boldsymbol{v_{max}} / \sqrt{\boldsymbol{f_c'}\ \text{MPa}} \leq 0.42\right]$ and $\boldsymbol{v_{max}} / \sqrt{\boldsymbol{f_c'}\ \text{psi}} > 5 \left[\boldsymbol{v_{max}} / \sqrt{\boldsymbol{f_c'}\ \text{MPa}} > 0.42\right]$ are shown in Fig. 3-9(***a***) and Fig. 3-9(***b***), respectively. For the lower shear stress range, use of overlapping hoops provides improved drift capacity if, $c/b \geq 2.5$ or $\lambda_b \geq 40$ (Fig. 3-9(***a***)), whereas the use of a perimeter hoop with 135º-135º crossties results in only a slight increase in drift capacity over the use of 90º-135º crossties. It is noted that, for $c/b \geq 2.5$, the provided length of confinement was, on average, 118% of that required by ACI 318-14, which is defined as at least the greater of $c - 0.10 l_w$ and $c/2$; therefore, the test results in the database were not significantly overdesigned with respect to length of confinement provided. The phenomenon of "90º hook opening prematurely" for walls with larger λ_b ratios has been observed in recent laboratory

programs, e.g., Birely (2012), with approximately $80 \le \lambda_b \le 100$ and Segura and Wallace (2018a), with approximately $45 \le \lambda_b \le 60$. For the Segura and Wallace (2018b) tests, $2.0 \le c/b \le 4.0$ and $0.2 \le c/l_w \le 0.3$. Observations indicated that once cover concrete spalled and longitudinal bar buckling initiated, crosstie hooks opened and the long leg of the perimeter hoop was ineffective in resisting the forces exerted on it by the buckling longitudinal reinforcement, leading to concrete crushing of the core of the SBE and subsequent lateral instability of the boundary. For values of $\lambda_b \ge 50$, use of overlapping hoops results in a 50 to nearly 100% increase in drift capacity (Fig. 3-9(***a***)). Interestingly, use of overlapping hoops for the tests with high shear stresses i.e., $v_{max} / \sqrt{f_c'} \text{ psi} > 5 \left[v_{max} / \sqrt{f_c'} \text{ MPa} > 0.42 \right]$ does not indicate a clear trend of increased drift capacity (Fig. 3-9(***b***)); however, it is noted that relatively few tests exist for $\lambda_b \ge 40$ to evaluate this trend. Given these observations, it would seem prudent to require the use of overlapping hoops for ratios of $c/b \ge 2.5$; alternatively, the impact of the reduced drift capacity of the wall could be accounted for in the design process. This issue is addressed later.

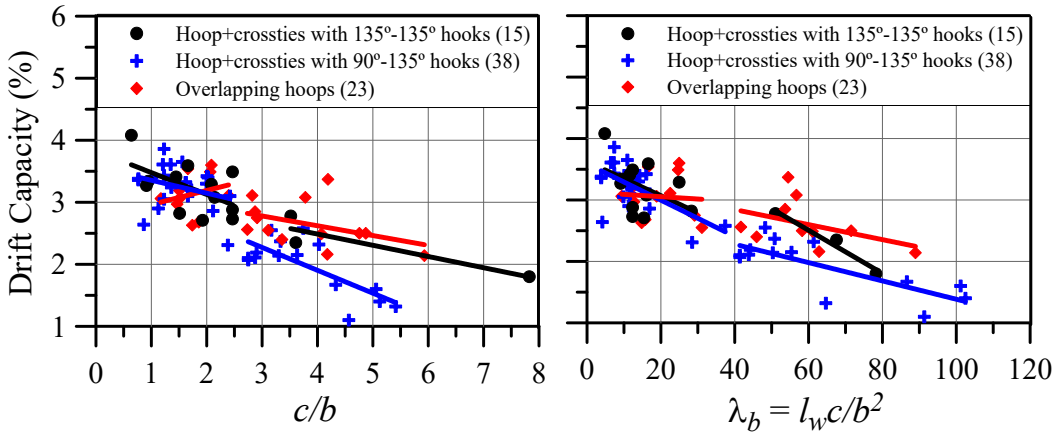

(a) $v_{max}/\sqrt{f_c'}$ psi ≤ 5 (≤ 0.42 in MPa)

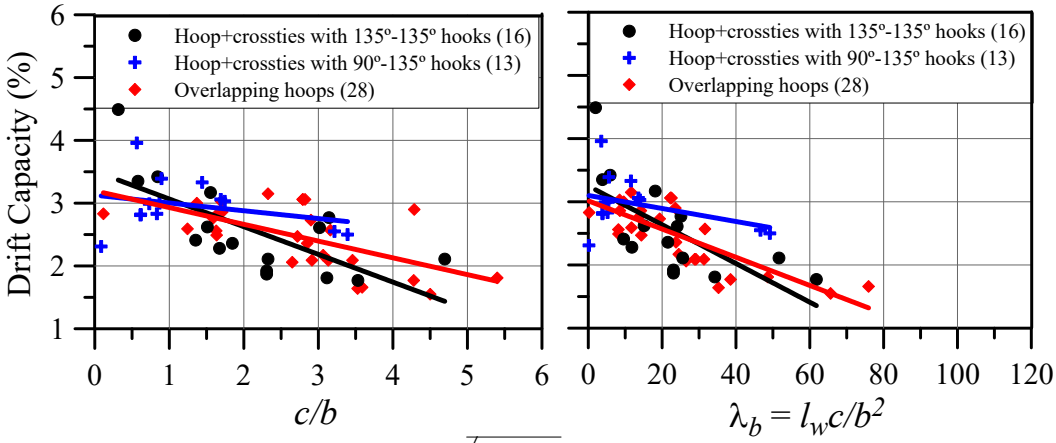

(b) $v_{max}/\sqrt{f_c'}$ psi > 5 (> 0.42 in MPa)

Fig. 3-9–Comparison of different boundary transverse reinforcement configurations (Note: number of tests for each case is given in parentheses).

3.5.5. Other Factors

As noted earlier, the primary variables impacting wall lateral drift capacity were c/b, l_w/b, $v_{max}/\sqrt{f_c'}$, and configuration of the boundary transverse reinforcement used. However, for completeness, the influence of other variables on lateral drift capacity is presented here to demonstrate that they do not significantly impact lateral drift capacity. Parameters considered include: (1) minimum $A_{sh,provided}/A_{sh,required}$, (2) s/d_b, (3) $h_x/h_{x,max}$, (4) degree of lateral support provided (support for all boundary longitudinal bars versus every other bar), and (5) $P/A_g f'_c$.

For these variables, the dataset of 164 tests was further reduced to include only those tests that fully satisfy the ACI 318-14 provisions, particularly those related to quantities $A_{sh,provided}$, s, s/d_b, h_x, and l_{be}, resulting in a reduced dataset of 78 code-compliant wall test specimens. Results are discussed in subsequent paragraphs.

Results presented in Fig. 3-10(***a***) indicate that providing ratios of $A_{sh,provided}/A_{sh,required}$ modestly greater than 1.0, does not significantly increase wall lateral drift capacity. Similarly, results presented in Fig. 3-10(***b***) demonstrate that variations in s/d_b (and s) also have little influence on wall lateral drift capacity, particularly for the practical range of $3 \leq s/d_b \leq 6$, suggesting that the current ACI 318-14 limits are sufficient. Additional investigation indicated no significant difference in drift capacity trends for $3 \leq s/d_b \leq 4$ and $4 < s/d_b \leq 6$. Comparison of test results where lateral support was provided for every boundary longitudinal bar by corners of a crosstie or hoop leg versus for every other longitudinal boundary bar (e.g., Fig. 3-10(***c***)), indicates only a slight improvement in drift capacity when all bars are supported, although data are limited for $\lambda_b > 60$ for configurations where all bars are supported. It is noted that, for columns with high axial load $\left(P_u > 0.3A_g f_c'\right)$ or high concrete strength ($f_c' \geq 10{,}000$ psi; 69 MPa), ACI 318-14 §18.7.5.42(f) requires that every longitudinal bar around the perimeter of a column have lateral support provided by the corner of a hoop or by a seismic hook, and the value of h_x cannot exceed 8 in. [200 mm]. For wall with SBEs, ACI 318-14 §18.10.6.4(e) requires h_x not exceed the least of 14 in. [356 mm] or 2***b***/3. The 14 in. [356 mm] limit governs only for relatively thick walls (***b*** ≥ 21 in. [533 mm]); no walls within the reduced database fell into this category. Fig. 3-10(***d***) indicates that, for the range of h_x within the dataset (i.e., $0.3 \leq h_x / h_{x,max} \leq 1.0$), and assuming an

average test scale factor of 40% for all tests, $h_{x,max}$ = 0.4x14 in. = 5.6 in. [142 mm], variations in h_x had no impact on wall drift capacity. An alternative approach, where h_x was normalized to the wall compression zone width (***b***), did not alter the trends noted in Fig. 3-10(***d***)**.** Based on the information provided here, requiring wall SBEs to satisfy the same requirements (ACI 318-14 §18.7.5.2(f)) for columns with high axial load $\left(P_u > 0.3 A_g f_c'\right)$ or high concrete strength (f_c' ≥10,000 psi; 69 MPa) would be expected to only slightly improve wall lateral drift capacity. However, as noted, due to the lack of data, adding such a requirement might be prudent.

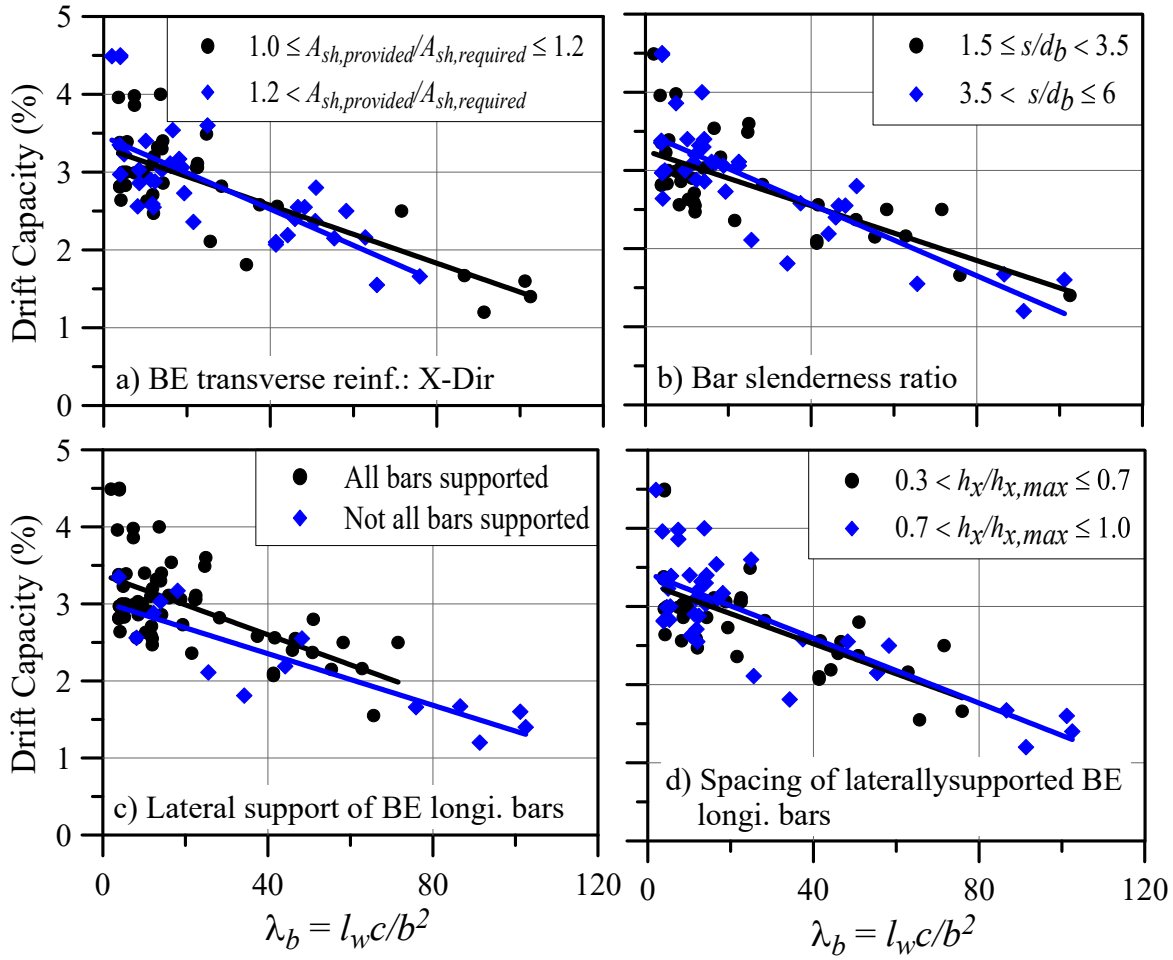

Fig. 3-10–Impact of some boundary element details on drift capacity of walls with SBEs.

Axial load is typically assumed to have a significant impact on wall (or column) lateral drift (or plastic rotation) capacity. For example, in UBC 1997 §1921.6.6.3 and ASCE 41-13 §10.7.1.1, if axial load on a wall exceeded $\mathbf{0.3}A_g f_c'$, the lateral strength of the wall could not be considered. Additionally, ASCE 41-13 Tables 10-19 and 10-20 use axial load ratio as a primary term for selecting modeling parameters and acceptance criteria for both flexure- and shear-controlled walls. However, as noted earlier in Table 3-1, axial load ratio by itself had no clear correlation with wall drift capacity (correlation coefficient, $\boldsymbol{R}$ = 0.08). Variation of wall drift capacity against axial load ratio $\left(\boldsymbol{P}/\boldsymbol{A_g f_c'}\right)$ is shown in **Fig. 11**(***a***) for the entire dataset with $\boldsymbol{M/Vl_w} \geq 1.0$ and in Fig. 3-11(***b***) for slender walls in the dataset with $\boldsymbol{M/Vl_w} \geq 2.0$, whereas trends for two levels of $\boldsymbol{P}/\boldsymbol{A_g f_c'}$ are shown in Fig. 3-11(***c***). From Fig. 3-11, it is clear that there is no significant trend between axial load ratio (ranging from 0.0 to 0.35) and wall drift capacity. It is noted that the slenderness parameter $\left(\lambda_b\right)$ described earlier incorporates the impact of axial load through neutral axis depth.

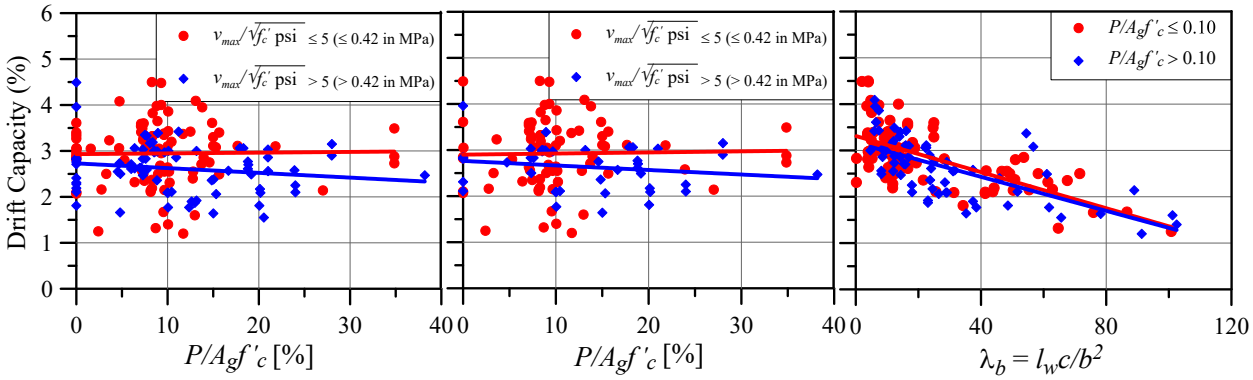

(*a*) Entire dataset ($M/Vl_w \geq 1.0$) (*b*) $M/Vl_w \geq 2.0$ (*c*) Entire dataset ($M/Vl_w \geq 1.0$)

Fig. 3-11–Impact of axial load ratio $\left(P / A_g f'_c\right)$on drift capacity of walls with SBEs.

3.6. Drift Capacity Prediction

A primary objective of this study was to develop an empirical model to predict lateral drift capacity of structural walls with SBEs. Key variables impacting lateral drift capacity have been identified, such as: $\lambda_b = l_w c / b^2$, $v_{max} / \sqrt{f_c'}$, and the use of overlapping hoops versus a single perimeter hoop with intermediate legs of crossties. Other variables also were investigated and found to not substantially influence lateral drift capacity for cases were ACI 318-14 detailing provisions for SBEs are satisfied. It is important to note here that the authors are not saying that these parameters do not influence lateral drift capacity, defined as a 20% drop in strength from the peak lateral load, only that changes in these parameters within ranges that are permissible or reasonable for SBEs do not influence (or change significantly) the lateral drift capacity. Application of linear regression analyses for the dataset of 164 tests, including the variables that significantly impact lateral drift capacity, resulted in the following predictive equation for mean drift capacity $\left(\delta_c / h_w\right)$of walls with SBEs:

$$\frac{\delta_c}{h_w}(\%) = 3.85 - \frac{\lambda_b}{\alpha} - \frac{v_{max}}{10\sqrt{f_c'(\text{psi})}} \qquad \text{(Eq. 3-1a)}$$

$$\frac{\delta_c}{h_w}(\%) = 3.85 - \frac{\lambda_b}{\alpha} - \frac{v_{max}}{0.83\sqrt{f_c'(\text{MPa})}} \qquad \text{(Eq. 3-1b)}$$

Where $\lambda_b = l_w c / b^2$; α = 60 where overlapping hoops are used and 45 where a combination of a single perimeter hoop with supplemental crossties is used. The first term in **Eq. 3-1** represents the maximum mean drift capacity, whereas the second term represents the impact of c/b and l_w/b, which incorporate the influence of material properties (e.g., f_y and f_c'), axial load, geometry, and

quantities and distribution of longitudinal reinforcement at the boundaries and within the web, on lateral drift capacity, whereas the third term incorporates the reduction in wall drift capacity due to the level of wall shear stress normalized by the maximum shear stress allowed by ACI 318-14 §18.10.4.4 for an isolated wall. The drift capacities predicted with **Eq. 3-1** are compared with experimental drift capacities in Fig. 3-12(***a***) for the entire dataset of 164 walls and for the 44 walls with $1.0 \leq \boldsymbol{M/Vl_w} < 2.0$. The mean and coefficient of variation (COV) are 1.0 and 0.15, respectively, over the entire range of drift values, from roughly 1.25% drift to 3.5% drift. In addition, **Eq. 3-1** was applied to the subset of 78 fully ACI 318-14 code-complaint walls identified previously, and the mean and COV of 1.03 and 0.137 are obtained, indicating that the result is not sensitive to the dataset used to derive **Eq. 3-1**. For the majority of the test specimens in the dataset, ***b*** did not vary over ***c*** (in a few cases for walls with boundary columns and thinner webs, ***c*** did extend modestly into the thinner web); however, for more complex cases, e.g., biaxial loading on a flanged wall, an average or representative value of ***b*** would need to be defined to compute drift capacity. In such cases, the drift capacity is likely to be relatively large, such that this case is not critical, whereas cases with flanges in tension producing large compression on a narrow compression zone are likely to be critical.

To facilitate the implementation of **Eq. 3-1** into design recommendations or ACI 318, **Eq. 3-1** was simplified modestly as **Eq. 3-2**:

$$\frac{\delta_c}{h_w}(\%) = 4.0 - \frac{\lambda_b}{\alpha} - \frac{v_{max}}{10\sqrt{f_c'(\text{psi})}} \qquad \text{(Eq. 3-2a)}$$

$$\frac{\delta_c}{h_w}(\%) = 4.0 - \frac{\lambda_b}{\alpha} - \frac{v_{max}}{0.83\sqrt{f_c'(\text{MPa})}} \qquad \text{(Eq. 3-2b)}$$

Where α = 50 where overlapping hoops are used and 40 where a combination of a single perimeter hoop with supplemental crossties are used. The drift capacities predicted with the simplified equation (**Eq. 3-2**) are compared with experimental drift capacities observed in Fig. 3-12(***b***) for the entire dataset of 164 walls and for the 44 walls with $1.0 \leq \boldsymbol{M/Vl_w} < 2.0$. The drift capacities predicted with **Eq. 3-2** are slightly conservative, with mean and COV of 0.97 and 0.16, respectively.

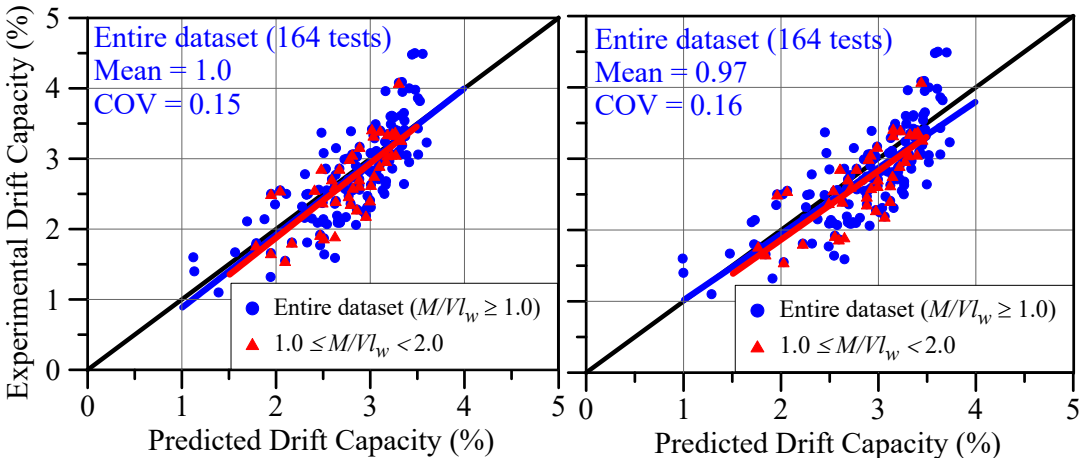

Fig. 3-12–Comparison of predicted drift capacity with experimental drift capacity.

3.7. Conclusions and Recommendations

Based on the findings of this study, the following conclusions with regards to behavior of structural walls with SBEs can be drawn:

1. Displacement capacity of special structural walls that satisfy the detailing requirements of ACI 318-14 §18.10.6.4 is primarily a function of $\boldsymbol{c/b}$, $\boldsymbol{l_w/b}$, $\boldsymbol{v_{max}/\sqrt{f'_c}}$, and use of

overlapping hoops versus a single perimeter hoop with supplemental crossties. Depending on these variables, the lateral drift capacity can be as low as 1.25% and as high as 3.5%. In general, lower drift capacities result for walls with $\ell_w/b \geq 15$, $c/b \geq 3.0$, and wall shear stress levels approaching the ACI 318-14 limit of $10\sqrt{f'_c}$ psi $\left(0.83\sqrt{f'_c}\text{ MPa}\right)$ for an individual wall.

2. ACI 318-14 §18.10 provisions for Special Structural Walls do not ensure that the walls have roof drift capacity at 20% strength loss greater than the maximum roof drift demand allowed by ASCE 7-10, which is approximated as three-quarters of the allowable story drift of 0.02 x 1.5 = 0.03 for MCE level demands, or 0.0225. Drift capacities for a significant number of walls in the dataset are less than 0.0225.

3. A slenderness parameter, $\lambda_b = \ell_w c/b^2$, was defined that provides an efficient means to account for the impact of slenderness of the cross section $\left(\ell_w/b\right)$ and the slenderness of the compression zone on the cross section $\left(c/b\right)$ on wall lateral drift capacity. The slenderness parameter λ_b considers the impact of concrete and reinforcement material properties, axial load, wall geometry, and quantities and distributions of longitudinal reinforcement at the boundary and within the web.

4. The drift capacity of walls with higher shear stress ratio (i.e., $v_{max}/\sqrt{f'_c\text{ psi}} > 5$ [$v_{max}/\sqrt{f'_c\text{ MPa}} > 0.42$]) is approximately 0.5% drift less than walls with low-to-moderate shear stress ratios (i.e., $v_{max}/\sqrt{f'_c\text{ psi}} \leq 5$ [$v_{max}/\sqrt{f'_c\text{ MPa}} \leq 0.42$]). Over the full range of shear stress ratios, shear demand can reduce wall drift capacity by as much as 1.0% drift.

5. For low-to-modest shear stress ratios, i.e., $v_{max} / \sqrt{f_c'}$ psi ≤ 5 [$v_{max} / \sqrt{f_c'}$ MPa ≤ 0.42], use of overlapping hoops, as opposed to use of a single perimeter hoop with supplemental crossties, provides improved drift capacity if, $c/b \geq 2.5$ or $\lambda_b \geq 40$. No clear trend of increased drift capacity is observed where overlapping hoops are used for walls with higher shear stress ratios, i.e., $v_{max} / \sqrt{f_c'}$ psi > 5 [$v_{max} / \sqrt{f_c'}$ MPa > 0.42]; however, given the relatively sparse data for higher shear stresses, use of overlapping hoops is recommended for all cases.
6. The drift capacity of SBEs with a single perimeter hoop and crossties with 135º-135º hooks is slightly higher than for SBEs with a single perimeter hoop and crossties with alternating 90º-135º hooks; however, neither is as effective as using overlapping hoops because crossties with either 90º or 135º hooks are prone to opening that leads to rebar buckling and crushing of the entire boundary region. Use of overlapping hoops results in an increase in drift capacity from 0.2% to 0.5% drift as λ_b increases from 40 to 100.
7. A drift capacity equation that depends on $\lambda_b = l_w c / b^2$, level of wall shear stress, and configuration of boundary transverse reinforcement was developed that accurately predicts the lateral drift capacity of walls with SBEs, with mean and coefficient of variation of approximately 1.0 and 0.15, respectively.
8. There is no real correlation between axial load ratio (ranging from 0.0 to 0.35) and wall drift capacity; therefore, limits on wall axial load (stress) alone are not recommended.
9. It is recommended that future experimental programs focus on walls with $l_w / b \geq 20$ and $c/b \geq 4$ (or walls with $\lambda_b \geq 80$), to address gaps in the test database given that walls with these parameters are common in practice.

3.8. References

ACI Committee 318, 2014, "Building Code Requirements for Structural Concrete (ACI 318-14) and Commentary," American Concrete Institute, Farmington Hills, MI, 519 pp.

ACI Committee 318, 1999, "Building Code Requirements for Structural Concrete (ACI 318-99) and Commentary (318R-99), American Concrete Institute, Detroit, MI, 391 pp.

ACI Committee 318, 1983, "Building Code Requirements for Reinforced Concrete (ACI 318-83), American Concrete Institute, Detroit, MI, 155 pp.

Architectural Institute of Japan, 2010, "AIJ Standard for Structural Calculation of Reinforced Concrete Structures," Maruzen, Tokyo, Japan. (in Japanese)

ASCE/SEI Standards, 2013, "Seismic Evaluation and Retrofit of Existing Buildings (ASCE/SEI 41-13)," American Society of Civil Engineers, Reston, VA, 518 pp.

ASCE/SEI Standards, 2010, "Minimum Design Loads for Buildings and Other Structures (ASCE/SEI 7-10)," American Society for Civil Engineers, Reston, VA, 518 pp.

Birely, A. C., 2012, "Seismic Performance of Slender Reinforced Concrete Structural Walls," Ph.D. Dissertation, University of Washington, Seattle, WA, 983 pp.

Brown, P., Ji, J., Sterns, A., Lehman, D. E., Lowes, Kuchma, D., and Zhang, J., 2006 "Investigation of the seismic behavior and analysis of reinforced concrete walls," *Proceedings*, 8th US National Conference on Earthquake Engineering, San Francisco, CA.

Chun, Y. S., 2015, "Seismic performance of special shear wall with the different hoop reinforcement detail and spacing in the boundary element," *LHI Journal*, Vol. 6, No. 1, pp. 11-19. (in Korean)

Chun, Y. S., and Park, J. Y., 2016, "Seismic performance of special shear wall with modified details in boundary element depending on axial load ratio," *LHI Journal*, Vol. 7, No. 1, pp. 31-41. (in Korean)

Chun, Y. S., Lee, K. H., Lee, H. W., Park, Y. E., and Song, J. K., 2013, "Seismic performance of special shear wall structural system with effectively reduced reinforcement detail," *Journal of the Korea Concrete Institute*, Vol. 25, No. 3, pp. 271-281. (in Korean).

Eberhard, M. O., and Sozen, M. A., 1993, "Behavior-based method to determine design shear in earthquake-resistant walls," *Journal of Structural Engineering*, Vol. 119, No. 2, pp. 619-639.

Elwood, K. J., Maffei, J. M., Riederer, K. A., and Telleen, K., 2009, "Improving Column Confinement—Part 1: Assessment of design provisions," *Concrete International*, Vol. 31, No. 11, pp. 32-39.

Hines, E. M., Seible, F., and Priestley, M. J. N., 2002, "Seismic Performance of Hollow Rectangular Reinforced Concrete Piers with Highly Confined Corner Elements—Phase I: Flexural Tests, and Phase II: Shear Tests," *Structural Systems Research Project 99/15*, University of California, San Diego, CA, 266 pp.

Kabeyasawa, T., and Matsumoto, K., 1992, "Tests and analyses of ultra-high strength reinforced concrete shear walls," *Proceedings*, 10th World Conference on Earthquake Engineering, Madrid, Spain, pp. 3291-3296.

Kabeyasawa, T., Ohkubo, T., and Nakamura, Y., 1996, "Tests and analysis of hybrid wall systems," *Proceedings*, 11th World Conference on Earthquake Engineering, Acapulco, Mexico.

Keintzel, E., 1990, "Seismic design shear forces in RC cantilever shear wall structures," *European Earthquake Engineering*, Vol. 3, pp. 7–16.

Kishimoto, T., Hosoya, H., and Oka, Y., 2008, "Study on structural performance of R/C rectangular section core walls (Part 3 and 4)", *Summaries of Technical Papers of Annual Meeting*, Architectural Institute of Japan, Vol. C-2, pp. 355-358. (in Japanese)

Kolozvari, K., Orakcal, K., and Wallace, J. W., 2015a, "Modeling of cyclic shear-flexure interaction in reinforced concrete structural walls. Part I: Theory," *Journal of Structural Engineering*, Vol. 141, No. 5, 10 pp.

Liang, X., Che, J., Yang, P., and Deng, M., 2013, "Seismic Behavior of High-Strength Concrete Structural Walls with Edge Columns," *ACI Structural Journal*, Vol. 110, No. 6, pp. 953-963.

Lowes, L. N., Lehman, D. E., Birely, A. C., Kuchma, D. A., Marley, K. P., and Hart, C. R., 2012, "Earthquake Response of Slender Concrete Planar Concrete Walls with Modern Detailing" *Engineering Structures*, Vol. 34, pp. 455-465.

Lu, X., Zhou, Y., Yang, J., Qian, J., Song, C., and Wang, Y., 2010, "NEES Shear Wall Database," Network for Earthquake Engineering Simulation, Dataset, available at https://nees.org/resources/1683.

Lu, Y., Gultom, R., Henry, R. S., and Ma, Q. T., 2016, "Testing of RC walls to investigate proposed minimum vertical reinforcement limits in NZS 3101:2006 (A3)", *Proceedings*, 2016 NZSEE Annual Conference, Christchurch, New Zealand.

Matsubara, S., Sanada, Y., Tani, M., Takahashi, S., Ichenose, T., and Fukuyama, H., 2013, "Structural parameters of confined area affect flexural deformation capacity of shear walls that fail in bending with concrete crushing," *Journal of Structural and Construction Engineering*, Vol. 78, No. 691, pp. 1593-1602.

Mobeen, S., 2002, "Cyclic Tests of Shear Walls Confined with Double Head Studs," MS Thesis, University of Alberta, Canada, 194 pp.

Nagae, T., Tahara, K., Taiso, M., Shiohara, H., Kabeyasawa, T., Kono, S., Nishiyama, M., Wallace, J. W., Ghannoum, W. M., Moehle, J. P., Sause, R., Keller, W., and Tuna, Z., 2011, "Design and Instrumentation of the 2010 E-Defense Four-Story Reinforced Concrete and Post-Tensioned Concrete Buildings," *PEER Report 2011/104*, Pacific Earthquake Engineering Research Center (PEER), Berkeley, CA, 234 pp.

Oesterle, R. G., Aristizabal-Ochoa, J. D., Fiorato, A. E., Russell, H. G., and Corley, W. G., 1979, "Earthquake Resistant Structural Walls–Phase II," *Report to National Science Foundation (ENV77-15333)*, Construction Technology Laboratories, Portland Cement Association, Skokie, IL, 331 pp.

Oesterle, R.G., Fiorato, A.E., Johal, L.S., Carpenter, J.E., Russell, H.G., and Corley, W.G., 1976, "Earthquake Resistant Structural Walls–Tests of Isolated Walls," *Report to National Science Foundation (GI-43880),* Construction Technology Laboratories, Portland Cement Association, Skokie, IL, 315 pp.

Paulay, T. and Goodsir, W. J., 1985, "The ductility of structural walls," *Bulletin of the New Zealand National Society for Earthquake Engineering*, Vol. 18, pp. 250-269.

Segura, C. L., and Wallace, W. J., 2018a, "Seismic performance limitations and detailing of slender RC walls," *ACI Structural Journal*, Vol. 115, No. 03, pp. 849-860.

Segura, C. L., and Wallace, W. J., 2018b, "Impact of geometry and detailing on drift capacity of slender walls," *ACI Structural Journal*, Vol. 115, No. 03, pp. 885-896.

Seismic Engineering Research Infrastructures For European Synergies (SERIES), 2013, "SERIES RC Walls Database," available at http://www.dap.series.upatras.gr.

Seo, S., Oh, T., Kim, K., and Yoon, S., 2010, "Hysteretic behavior of RC shear wall with various lateral reinforcements in boundary columns for cyclic lateral load," *Journal of the Korea Concrete Institute*, Vol. 22, No. 3, pp. 357-366.

Takahashi, S., Yoshida, K., Ichinose, T., Sanada, Y., Matsumoto, K., Fukuyama, H., and Suwada, H., 2013, "Flexural drift capacity of reinforced concrete wall with limited confinement," *ACI Structural Journal*, Vol. 110, No. 1, pp. 95-104.

Thomsen, J. H. IV, and Wallace, J. W., 2004, "Displacement-based design of slender reinforced concrete structural walls—experimental verification," *Journal of Structural Engineering*, V. 130, No. 4, pp. 618-630.

Uniform Building Code, 1997, "International Council of Building Code Officials (UBC-97)," Whittier, CA.

Wallace J. W., and Moehle, J. P., 1992, "Ductility and detailing requirements of bearing wall buildings," *Journal of Structural Engineering*, Vol. 6, pp. 1625-1644.

Wallace, J. W., 1994, "A new methodology for seismic design of RC shear walls," *Journal of Structural Engineering*, Vol. 120, No. 3, pp. 863-884.

Wallace, J. W., 2012, "Behavior, design, and modeling of structural walls and coupling beams–lessons from recent laboratory tests and earthquakes," *International Journal of Concrete Structures and Materials*, Vol. 6, No. 1, pp. 3-18.

Wallace, J. W, Massone, L. M., Bonelli, P., Dragovich, J., Lagos, R., Luders, C., and Moehle, J., 2012, "Damage and implications for seismic design of RC structural wall buildings," *Earthquake Spectra*, Vol. 28, No. S1, pp. 281-289.

Welt, T. S., 2015, "Detailing for Compression in Reinforced Concrete Wall Boundary Elements: Experiments, Simulations, and Design Recommendations," PhD Thesis, University of Illinois, Urbana-Champaign, IL, 530 pp.

Whitman, Z., 2015, "Investigation of Seismic Failure Modes in Flexural Concrete Walls Using Finite Element Analysis," MS Thesis, University of Washington, Seattle, WA, 201 pp.

Xiao, Q., and Guo, Z., 2014, "Low-cyclic reversed loading test for double-wall precast concrete shear wall," *Journal of Southeast University*, Vol. 44, No., 4, pp. 826-831. (in Chinese)

Zhi, Q., Song J., and Guo Z., 2015, "Experimental study on behavior of precast shear wall using post-cast at the connection," *Proceedings*, 5th International Conference on Civil Engineering and Transportation (ICCET 2015), Guangzhou, China, pp. 1089-1092.

CHAPTER 4. A Reliability-Based Design Methodology for Structural Walls with SBEs

4.1. Abstract

The underlying premise of the ASCE 7-10 and ACI 318-14 provisions is that special structural walls satisfying the provisions of ACI 318-14 §18.10.6.2 through §18.10.6.4 possess adequate deformation capacity to exceed the expected deformation demand determined using ASCE 7-10 analysis procedures. However, observations from recent laboratory tests and strong earthquakes, where significant damage occurred at wall boundaries due to concrete crushing, rebar buckling, and lateral instability, have raised concerns that current design provisions are inadequate. Recent studies have identified that deformation capacity of code compliant walls is primarily a function of wall cross-section geometry, neutral axis depth, shear stress demands, and the configuration of boundary transverse reinforcement, and that, in some cases, the provisions of ACI 318-14 may not result in buildings that meet the stated performance objectives. To address this issue, this study proposes a new reliability-based design methodology for structural walls where a drift demand-to-capacity ratio check is performed to provide a low probability that roof drift demands exceed roof drift capacity at strength loss for a specified hazard level.

4.2. Introduction

Reinforced concrete (RC) structural walls are commonly used as lateral force-resisting systems (LFRS) in tall and moderately tall buildings because they provide substantial lateral strength and stiffness and are assumed to provide the needed deformation capacity if detailed according to provisions of ACI 318-14 §18.10 for Special Structural Walls. ACI 318 provisions for wall design and detailing have undergone three major updates, which occurred in the 1983, 1999, and 2014

versions of the code. In 1983, an extreme fiber compression stress limit of $\mathbf{0.2}f'_c$ under combined gravity loads and earthquake overturning moment was introduced to determine if special boundary element transverse reinforcement was required. This approach was implemented based on research conducted by the Portland Cement Association (e.g., Oesterle et al., 1976 and 1979; Paulay and Goodsir, 1985), which indicted that lateral drift ratios as large as 0.03 or 0.04 could be achieved if the wall boundary zones were adequately detailed to remain stable while yielding in compression. This approach still exists in 318-14 §18.10.6.3. In 1999, an alternative to the stress-based limit, a displacement-based approach, which applies to continuous (or effectively continuous), cantilever walls with a single critical section, was introduced to evaluate the need for Special Boundary Element (SBE) detailing (Wallace and Moehle, 1992; Wallace, 1994; and Thomsen and Wallace, 2004). More recently, in 2014, extensive revisions were introduced to require more stringent detailing requirements for thin, slender walls $\left(h_w/l_w \geq \mathbf{2.0}\right)$, include a limit on wall slenderness $\left(h_u/b \leq \mathbf{16}\right)$, require a minimum width of flexural compression zone ($b \geq \mathbf{12}$ in., 300 mm) for sections that are not tension-controlled $\left(c/l_w \geq \mathbf{3}/\mathbf{8}\right)$, and require that more walls be detailed with SBEs by adding a 1.5 factor in the denominator of ACI 318-14 Equation 18.10.6.2. These more recent changes were a result of the unsatisfactory performance of many walls in the 2010 Chile and 2011 New Zealand earthquakes, as well as observations from recent large-scale laboratory tests (Wallace, 2012; Wallace et al., 2012; Nagae et al., 2011; Lowes et al., 2012).

Even with these updates, the underlying premise of the ACI 318-14 approach to design and detailing of Special Structural Walls is that walls satisfying the provisions of §18.10.6.2 through §18.10.6.4 possess adequate displacement capacity to exceed the expected displacement demands from ASCE 7-10 analysis procedures when subjected to design-level ground motions. However, recent research has shown that wall drift capacity is impacted by parameters that are not adequately

addressed in ACI 318-14. For example, Segura and Wallace (2018a) studied the relationship between wall thickness and lateral drift capacity of planar walls and concluded that thin walls possess smaller lateral drift capacities than thicker walls that are otherwise similar. Furthermore, it has been found that thin, rectangular boundary regions confined by an outer hoop and crossties, which is a detail allowed by ACI 318-14 §18.10.6.4, may be substantially less stable in compression than sections that utilize overlapping hoops for confinement (Welt, 2015; Segura and Wallace, 2018a). The studies by Segura and Wallace (2018b) and Abdullah and Wallace (2018a) showed that lateral drift capacity of walls with SBEs is significantly influenced by parameters, such as width of flexural compression zone b, wall length l_w, neutral axis depth c (i.e., compression demands), wall shear demand V_u, and configuration of boundary transverse reinforcement (overlapping hoops versus a single perimeter hoop with intermediate crossties). The findings of these studies indicated that, depending on these variables, drift capacity of walls with SBEs varies by a factor of three, ranging between approximately 1.2% and 3.5%. These results have very important design implications. For instance, at Design Earthquake (**DE**) level shaking, ASCE 7-10 §12.12.1 limits allowable story drift ratio to 0.02 for typical RC buildings in Risk Category I & II that are taller than four stories and utilize structural walls for a LFRS. At Maximum Considered Earthquake (**MCE**) level shaking, which is used to assess collapse prevention, this limit is typically taken as 1.5 times the **DE** limit, or 0.03. If roof drift demand is approximated as three-quarters of peak story drift, which is a reasonable approximation for buildings with walls, then the peak roof drift demand allowed by ASCE 7-10 is approximately 0.0225, which is about 87% greater than the minimum wall drift capacity of 0.012 observed by Abdullah and Wallace (2018a) and Segura and Wallace (2018b). These findings suggest that current ACI 318 code provisions do not adequately address concerns related to brittle compression failure of walls, nor

do they ensure that walls have adequate drift capacity to exceed the expected drift demands under **DE** shaking with a reasonable level of reliability (e.g., 90%); therefore, ACI 318-14 wall provisions should be updated to address this critical issue.

To address the above issue, a new reliability-based design methodology is proposed where a drift demand-to-capacity ratio (DDCR) check is performed to provide a low probability that roof drift demands exceed roof drift capacity at strength loss for a given hazard level (e.g., 10% probability of lateral strength loss for the **DE** or **MCE** level shaking). In general, walls with slender cross sections $\left(l_w/b > 15\right)$, large neutral axis depth relative to width of flexural compression zone $\left(c/b > 3\right)$, shear stress demands approaching the ACI 318 §18.10.4.4 limit $\left(10\sqrt{f'_c}\right)$, and roof drift demands approaching the maximum value allowed by ASCE 7-10 (i.e., 0.75×0.02 = 0.015) tend to be screened out for redesign using the proposed methodology to prevent strength loss under **DE** level shaking and reduce the probability of collapse under **MCE** level shaking. Finally, two design examples are presented to highlight the deficiencies in the current code provisions and to illustrate application of the proposed methodology.

4.3. Research Significance

Current provisions of ACI 318-14 assume that walls satisfying Special Structural Wall provisions of 18.10.6 possess adequate drift capacity to exceed the expected drift demands from analysis under **DE** level shaking defined in ASCE 7, without critical strength decay. However, recent research has indicated that this underlying premise is not always correct, and that wall deformation capacity is significantly impacted by wall cross-section geometry, detailing, and compression and shear demands, and that these factors are not adequately addressed in ACI 318. A drift demand-

to-capacity ratio (DDCR) check is proposed for ACI 318 to require that wall drift capacity exceed expected drift demands under a prescribed hazard level with a low probability of strength loss.

4.4. Wall Deformation Capacity

Abdullah and Wallace (2018b) developed a comprehensive database that summarizes results from more than 1000 RC wall tests reported in the literature. The database was filtered to identify walls that satisfied, or nearly satisfied, the provisions of ACI 318-14 §18.10 for Special Structural Walls, resulting in a reduced dataset of 164 wall tests, in which about one-half of the walls fully satisfied requirements for special boundary transverse reinforcement in ACI 318-14 §18.10.6.4 (see Abdullah and Wallace, 2018a and 2019). The walls in the dataset included 108 rectangular, 34 barbell, 2 Flanged, 15 T-shaped (web in compression), 2 L-shaped (web in compression), and 3 half-barbell (web in compression) cross-sectional shapes. Histograms for various parameters for the 164 tests are shown in Fig. 4-1, where s/d_b is the ratio of vertical spacing of boundary transverse reinforcement to minimum diameter of longitudinal boundary reinforcement, $A_{sh,provided}/A_{sh,required}$ is the ratio of provided-to-required (per ACI 318-14 §18.10.6.4) area of boundary transverse reinforcement, $P/\left(A_g f'_c\right)$ is the axial load normalized by concrete compressive strength $\left(f_c^{'}\right)$ and gross concrete area $\left(A_g\right)$, $M/\left(Vl_w\right)$ is the ratio of base moment-to-base shear normalized by wall length $\left(l_w\right)$, b is the width of flexural compression zone, h_x is the centerline distance between laterally supported boundary longitudinal bars, and c is the depth of neutral axis computed at concrete compressive strain of 0.003. Wall displacement capacity $\left(\delta_c\right)$ in the database is defined as the lateral displacement corresponding to wall effective height

$\left(h_{eff} \approx 0.7h_w\right)$ at which lateral strength degrades by 20% from peak strength. To facilitate comparison of test drift capacities $\left(\delta_c / h_w\right)$ with drift demands determined from analysis, which is the roof level $\left(h_w\right)$ drift demand $\left(\delta_u / h_w\right)$for ACI 318-14 Equation 18.10.6.2, test drift capacities $\left(\delta_c / h_{eff}\right)$ at h_{eff} were adjusted to include the elastic displacement contributed by the wall height between h_{eff} and h_w. This adjustment was accomplished using a representative lateral load distribution in ASCE 7-10 §12.8 consistent with a prototype building height for the tested wall, and typically increased the elastic roof level displacements by 10 to 20% over the value at h_{eff}. The adjustments tended to be small compare to nonlinear roof level displacements. More details of this adjustment are available in Abdullah and Wallace (2019).

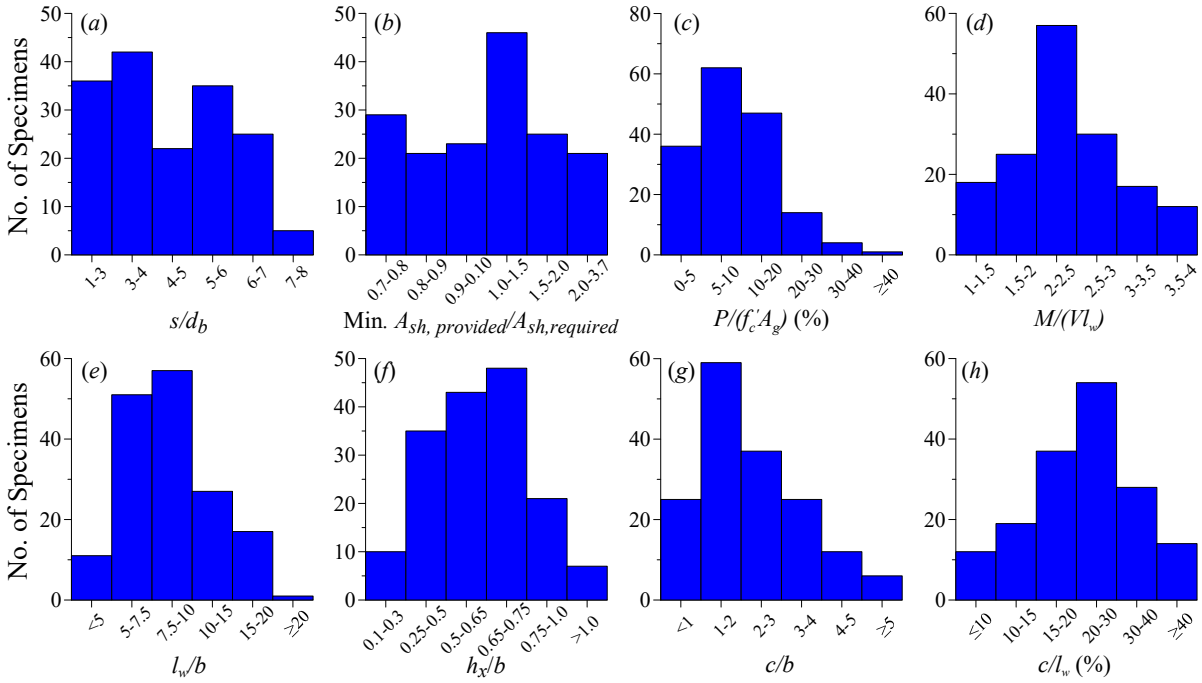

Fig. 4-1–Histograms of the dataset of 164 wall tests with special detailing.

A series of regression analyses (linear and nonlinear) were performed on the dataset of 164 walls to identify design parameters that significantly impact in-plane lateral drift capacity $\left(\delta_c / h_w\right)$ of walls with SBEs. Based on the results, it was concluded that wall drift capacity is primarily a function of: (1) ratio of wall neutral axis depth-to-width of flexural compression zone, c/b, (2) ratio of wall length-to-width of flexural compression zone, l_w/b, (3) ratio of the maximum wall shear stress to square-root of concrete compressive strength, $v_{max}/\sqrt{f'_c}$, and (4) the configuration of the boundary transverse reinforcement used, i.e., overlapping hoops versus a single perimeter hoop with intermediate legs of crossties (see Abdullah and Wallace, 2018b for examples of boundary transverse reinforcement configurations). The impacts of other parameters were also considered, such as: (5) $A_{sh,provided}/A_{sh,required}$, (6) s/d_b, (7) h_x, (8) degree of lateral support provided to the boundary longitudinal reinforcement (i.e., support for all boundary longitudinal bars versus every other bar), and (9) $P/\left(A_g f'_c\right)$; however, it was found that the items (5) through (9) did not significantly impact lateral drift capacity of fully code-compliant walls with SBEs. These findings suggest that a majority of the current detailing provisions of ACI 318-14 §18.10.6.4 are adequate, and that minor-to-moderate adjustments to these parameters would not likely result in an appreciable improvement of wall lateral deformation capacity. The results also indicated that $P/\left(A_g f'_c\right)$, by itself (ranging from 0.0 to 0.35), has low correlation with wall drift capacity, and that its impact is best accounted for in the c/b parameter. A summary of the impact of first four (more significant) parameters is presented in the following paragraphs; however, a more detailed assessment can be found in Abdullah and Wallace (2019; 2018c).

A combined slenderness parameter, $\lambda_b = (l_w/b)(c/b) = l_w c/b^2$, was identified, which provides an efficient means to account for the slenderness of the cross section (l_w/b) and the slenderness of the compression zone of the cross section (c/b). In addition to wall cross-section geometry, this parameter, through depth of neutral axis (***c***), considers the impact of concrete and reinforcement material strengths, axial load, and quantities and distributions of longitudinal reinforcement at the wall boundaries and in the web (Wallace, 1994). Fig. 4-2 indicates that lateral drift capacity of walls with SBEs is highly correlated with λ_b, with drift capacity varying roughly between 1.2% and 3.5% as λ_b decreases from 80 to zero. Fig. 4-2 also shows trends for two levels of shear stress demand, represented by $v_{max}/\sqrt{f'_c}$, to demonstrate the impact of wall shear stress beyond what can be attributed to changes in other variables. For the shear stress demand levels considered, the trend lines are offset by approximately 0.5% drift, indicating that higher shear stress demand has a significant negative impact on wall drift capacity, even for relatively slender walls (Fig. 4-2(***b***)). Fig. 4-3 highlights the impact of different boundary element transverse reinforcement configurations on wall drift capacity. For low-to-moderate shear stress demands, use of overlapping hoops provides improved drift capacity if $\lambda_b \geq 40$ (Fig. 4-3(***a***)), whereas the use of a perimeter hoop with 135º-135º crossties results in only a slight increase in drift capacity over the use of 90º-135º crossties due to ineffectiveness of 90º hooks used on crossties for walls with large λ_b (Segura and Wallace, 2017a). On the other hand, Fig. 4-3(***b***) indicates that use of overlapping hoops for the walls with high shear stresses does not necessarily lead to increased drift capacity; however, it is noted that relatively few tests exist for $\lambda_b \geq 40$ to evaluate this trend.

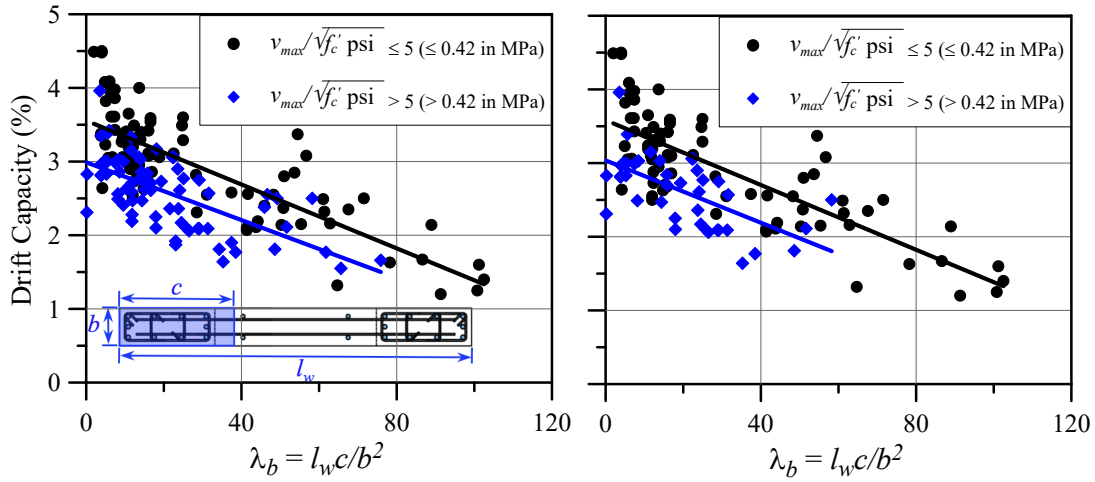

(*a*) $M/Vl_w \geq 1.0$ (164 walls) (*b*) $M/Vl_w \geq 2.0$ (120 walls)

Fig. 4-2–Impact of slenderness parameter (λ_b) and wall shear stress ratio $\left(v_{max}/\sqrt{f'_c}\right)$ on wall drift capacity.

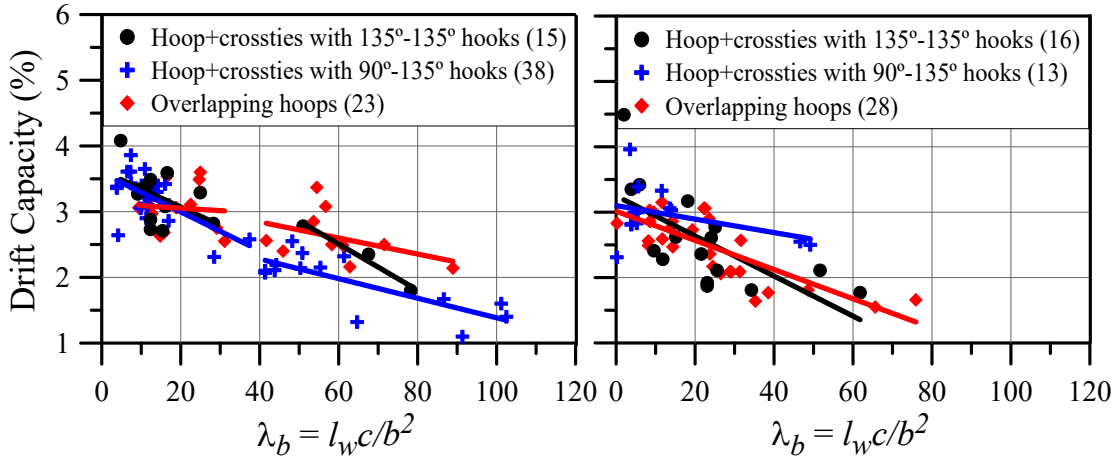

(*a*) $v_{max}/\sqrt{f_c'}$ psi ≤ 5 (*b*) $v_{max}/\sqrt{f_c'}$ psi > 5

Fig. 4-3–Comparison of different configurations of boundary transverse reinforcements (Note: number of tests for each case is given in parentheses).

4.5. Wall Deformation Capacity Predictions

Linear regression analysis was applied to the 164-wall dataset considering only the four important variables that significantly impact wall lateral drift capacity $\left(\delta_c/h_h\right)$, and the following predictive equation for mean drift capacity $\left(\bar{\delta}_c/h_w\right)$ of walls with SBEs is proposed:

$$\frac{\bar{\delta}_c}{h_w}(\%) = 3.85 - \frac{\lambda_b}{\alpha} - \frac{v_{max}}{10\sqrt{f_c'(\text{psi})}} \geq \min\frac{\bar{\delta}_c}{h_w} \qquad \text{(Eq. 4-1a)}$$

$$\frac{\bar{\delta}_c}{h_w}(\%) = 3.85 - \frac{\lambda_b}{\alpha} - \frac{v_{max}}{0.83\sqrt{f_c'(\text{MPa})}} \geq \min\frac{\bar{\delta}_c}{h_w} \qquad \text{(Eq. 4-1b)}$$

Where $\lambda_b = l_w c/b^2$; α = 60 where overlapping hoops are used and 45 where a single perimeter hoop with supplemental crosstie legs are used; minimum drift capacity ($\bar{\delta}_c/h_w$) = 1.75% where overlapping hoops are used and 1.25% where a single perimeter hoop with supplemental crosstie legs are used. **Eq. 4-1** results in mean and coefficient of variation (COV) of 1.0 and 0.15, respectively, over the entire range of drift capacity values, from roughly 1.2% to 3.5% drift (Fig. 4-4(*a*)).

An alternative format, where displacement capacities of the walls in the dataset were converted to total curvatures over an assumed plastic hinge length, also is presented, since this format is convenient for nonlinear response history analysis. Total curvature $\left(\phi_t\right)$ was computed for an assumed plastic hinge length $\left(l_p\right)$ of $l_w/2$ as the sum of elastic (first yield) and plastic curvatures over the assumed plastic hinge length. It is noted that the contribution of hinge yield curvature to the total hinge curvature $\left(\phi_t\right)$ was on average 10% for the dataset. Similar to drift capacity, linear regression analysis was applied to the dataset to develop the following predictive equation:

$$\phi_t\left(rad/in\right)=\left(a_1-\frac{\lambda_b}{a_2}-0.2\frac{v_{max}}{\sqrt{f_c^{'}(\text{psi})}}\right)\times10^{-4}\geq\phi_{t,min} \qquad \text{(Eq. 4-2a)}$$

$$\phi_t\left(rad/mm\right)=\left(a_1-\frac{\lambda_b}{a_2}-0.95\frac{v_{max}}{\sqrt{f_c^{'}(\text{MPa})}}\right)\times10^{-5}\geq\phi_{t,min} \qquad \text{(Eq. 4-2b)}$$

Where the values of parameters $\boldsymbol{a_1}$ and $\boldsymbol{a_2}$ are obtained from Table 4-1based on the wall length $\left(\boldsymbol{l_w}\right)$, which ranges from 27.5 in. (700 mm) to 120 in. (3048 mm) in the dataset, and minimum total curvature ($\phi_{t,min}$) = 2.8×10^{-4} rad/in. (1.1×10^{-5} rad/mm). **Eq. 4-2** results in a mean and COV of 1.0 and 0.20, respectively, for the entire range of curvature capacities (Fig. 4-4(***b***)). It should be noted that this model is developed based on an assumed plastic hinge length of $l_w/2$, and if the nonlinear analysis results show that nonlinear curvature demands spread over a distance greater than $l_w/2$, the total curvature capacities obtained from **Eq. 4-2** or the curvature demands need to be adjusted.

Table 4-1–Parameters to be used in **Eq. 4-2**

l_w in. (m)		≤ 40 (1.0 m)	40-60 (1.0-1.5 m)	> 60 (1.5 m)
a_1		20 (7.9)	15 (5.9)	10 (3.9)
a_2	Overlapping Hoops	11 (27.9)		13 (33)
	Hoop + Crossties	6 (15.2)		8 (20.3)

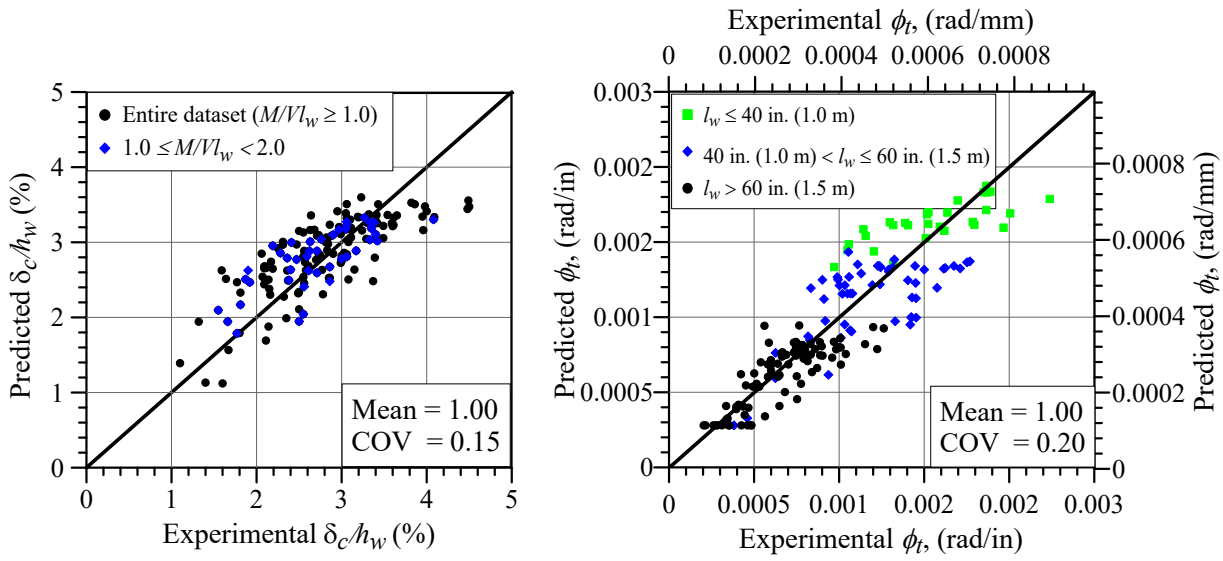

(*a*) **Eq. 4-1** (*b*) **Eq. 4-2**

Fig. 4-4–Comparison of predicted drift and curvature capacities with experimental drift and curvature capacities.

For the purpose of preliminary analysis, **Eq. 4-3** can be used to compute the approximate depth of neutral axis ***c***, corresponding to concrete compressive strain of 0.003. **Eq. 4-3** was derived based on data from 696 walls in the overall database with $\boldsymbol{P/\left(A_g f'_c\right) > 0}$, including the wall test results included in **Fig. 1**.

$$\frac{c}{l_w} = k_1 + k_2 \frac{P}{A_g f'_c} \qquad \text{(Eq. 4-3)}$$

Where values of $\boldsymbol{k_1}$ and $\boldsymbol{k_2}$ are obtained from Table 4-2 based on the cross-section shape of the wall. In **Eq. 4-3**, the first term considers the impact of longitudinal reinforcement (ratio and strength) and concrete strength, whereas the second term addresses the impact of axial load. Fig 4-5 compares the depth of neutral axis computed from **Eq. 4-3** with that computed from detailed sectional analysis using as-tested material properties.

Table 4-2–Neutral axis depth parameters in **Eq. 4-3**

Wall cross-section shape	k_1	k_2	Mean	COV
Rectangular	0.10*	1.2	1.04	0.17
Barbell and Flanged	0.03	1.4	1.05	0.27
T-, L-shaped, and half-barbell: flange in compression	0.03	0.7	1.00	0.30
T-, L-shaped, and half-barbell: web in compression	0.20	2.0	1.01	0.24

*This value is for walls with longitudinal reinforcement concentrated in the boundary elements. For wall with uniformly distributed reinforcement, k_1 = 0.05 and 0.20 when longitudinal reinforcement ratio < 0.005 and ≥ 0.015, respectively. For intermediate values, linear interpolation is applied.

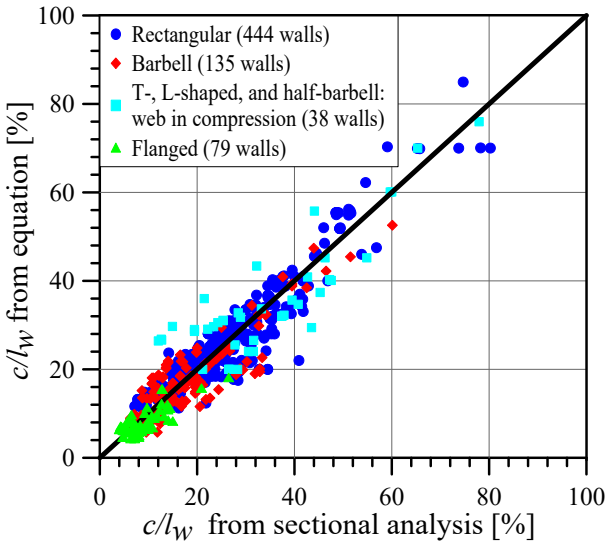

Fig 4-5–Comparison of c computed from **Eq. 4-3** with that from detailed sectional analysis.

In addition, since the specified (design) material strengths are not always reported, the ***c*** values included in the database are based on the as-tested (actual) concrete and steel strengths. Given this, the sensitivity of the calculation of ***c*** was investigated to assess the impact of using specified versus as-tested material properties (Fig. 4-6). A random subset of 35 tests from different tests programs was selected for a more detailed comparison. Results presented in Fig. 4-7 indicate that the value

of ***c*** is insensitive to the use of specified versus as-tested material properties, since the ratios for as-tested-to-specified for reinforcement yield strength and concrete strength are similar (Fig. 4-6).

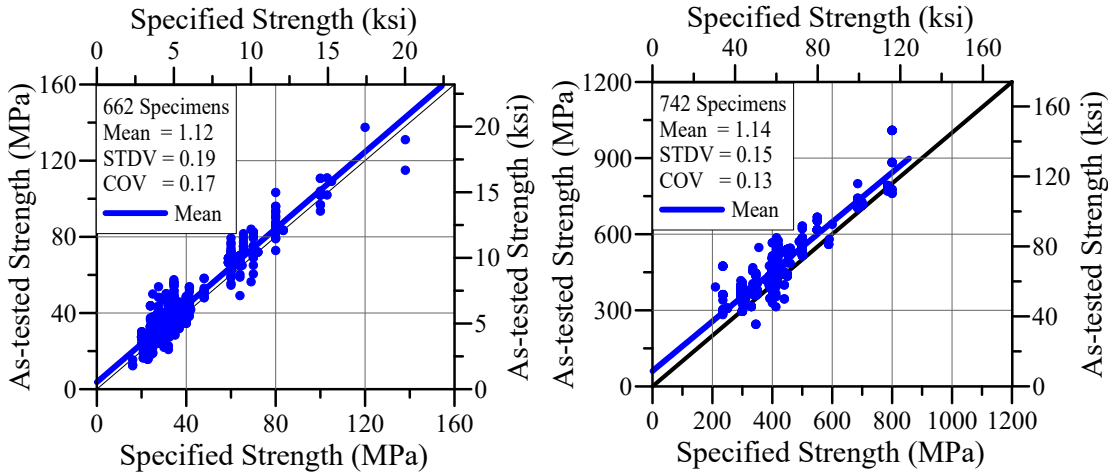

(*a*) Concrete compressive strength (*b*) Reinforcement yield strength

Fig. 4-6–Variation of specified and as-tested material strengths in the overall database.

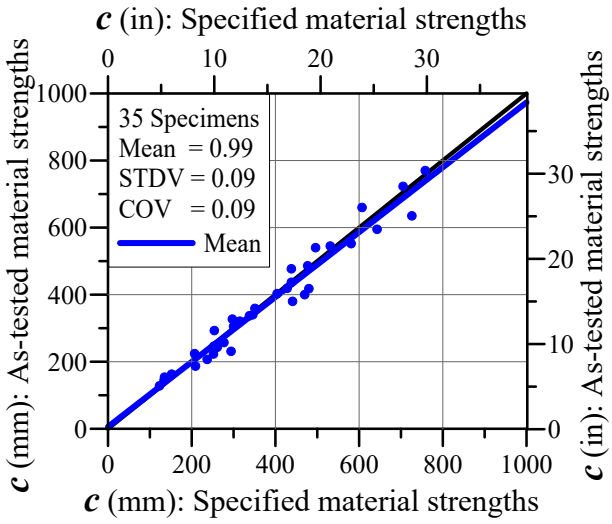

Fig. 4-7–Computed value of **c** using specified versus as-tested material strengths.

The expressions presented here are intended to apply to walls with rectangular, flanged, and barbell cross sectional shapes (Fig. 4-8(***a***) through (***f***)). For cases with a large ***b***, e.g., where the barbell or

flange of the wall is in compression (Fig. 4-8(***a***) through (***h***)), drift capacity is likely to be relatively large (low λ_b); however, for cases with a barbell or flange in tension, and a thin wall web in compression (Fig. 4-8(***b***) and (***e***) through (***h***)), relatively large values of c/b, and thus λ_b, and higher shear demands are likely, and thus, lower drift capacities will result. For cases where b varies over c, or where c varies over b, a representative (e.g., weighted average) value of b or c should be used, as shown in Fig. 4-8(***c***), (***d***), (**e**) and (***h***).

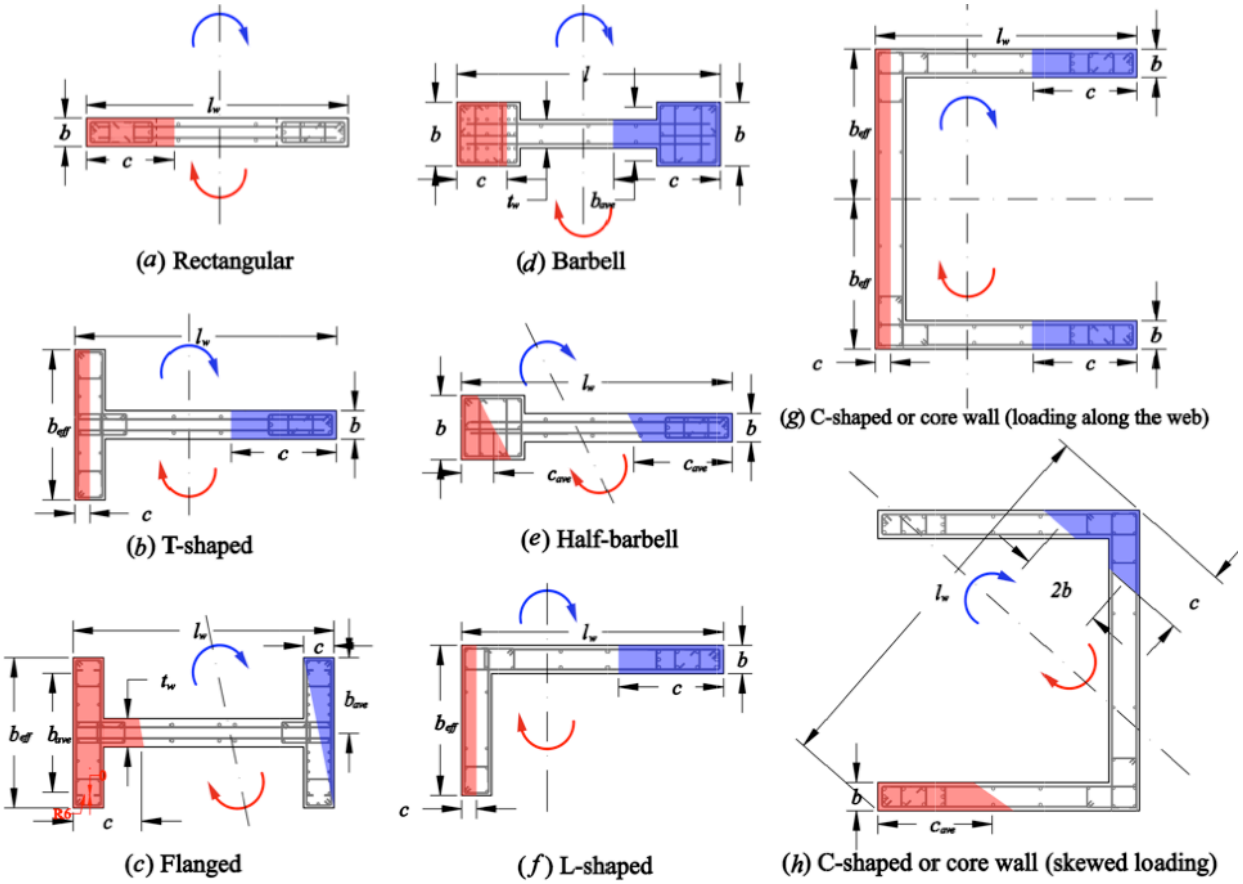

Fig. 4-8–Definition of width (b) and length (c) of flexural compression zone. (b_{ave} = average width of compression zone, c_{ave}= average depth of neutral axis, and b_{eff}= effective with of wall flange; the blue and red arrows indicate the direction of bending)

4.6. Roof Drift Demand

Roof drift (or displacement) demand at the top of a wall, referred to as Design Displacement (δ_u) in ACI 318-14, is used in Equation 18.10.6.2 to assess the need for SBEs. The design displacement is computed using ASCE 7-10 analysis procedures for lateral loads, such as the Equivalent Lateral Force (ELF) procedure of §12.8, the Modal Response Spectrum Analysis (RSA) of §12.9, or the Linear Response History Analysis (LRHA) of §16.1. For reinforced concrete buildings, the influence of concrete cracking is considered, resulting in the use of effective stiffness values for flexure $E_c I_{eff}$ and shear $G_c A_{eff}$.

Because the design methodology presented is based on a low probability that mean wall drift capacity at significant strength loss is less than mean wall drift demand, dispersion estimates in drift capacity and demand are required. Dispersion in drift capacity was estimated from **Eq. 4-1** (Fig. 4-4) presented in the prior section. Dispersion in roof drift demand was estimated based on limited results of nonlinear response history analyses (NL-RHA) of 28 buildings with planar structural walls (Wallace and Safdari, 2018), as well as results reported in the literature. Seven different building heights (4-, 6-, 8-, 10-, 12-, 16-, and 20-stories) were designed and analyzed for suites of ground motion records scaled to match the ASCE 7-10 **DE** spectra for site classes B, C, D, and E. COVs for mean roof drift demand of each building is presented in Table 4-3, and range from 0.23 to 0.50, with an overall mean value of 0.38.

Additional information was gleaned from studies reported in the literature that reported mean and COV of roof drift demands from NL-RHA of wall buildings. Kim (2016) reports dispersion in mean roof drift demands for a 30-story RC core wall system at both **DE** and **MCE** hazard levels, using two suites of ground motions (suite **A** and **B** containing 15 and 30 ground motions,

respectively). The COVs in mean roof drift demand for **DE** hazard level were 0.26 and 0.39 for suite **A** and **B**, respectively; whereas the COVs for **MCE** hazard level were 0.29 and 0.40 for Suite **A** and **B**, respectively. Moehle et al. (2007) reports a COV of 0.23 for mean roof drift demand of a 40-story building with RC core walls subjected to 14 ground motions scaled to **DE** hazard level. Similar results are reported by Haselton (2009) and Dezhdar (2012) for **MCE** level shaking. Based on these results, the COV for mean roof drift demand under **DE** level shaking generally ranges from 0.20 to 0.40. A COV of 0.30 was adopted for the reliability analysis presented in the next section, and the sensitivity of the results to modest variations in the COVs is considered later.

Table 4-3–COVs for mean roof drift demand from NRHA at DE level shaking

Building	4-story	6-story	8-story	10-story	12-story	16-story	20-story
Site Class B	0.50	0.43	0.52	0.30	0.47	0.47	0.39
Site Class C	0.30	0.47	0.38	0.40	0.37	0.32	0.23
Site Class D	0.23	0.40	0.30	0.40	0.34	0.34	0.34
Site Class E	0.41	0.48	0.42	0.39	0.32	0.31	0.38
Mean	0.36	0.45	0.40	0.37	0.37	0.36	0.33
	0.38						

4.7. Proposed Design Approach

ACI 318-14 §18.10.6 includes two design approaches to assess whether SBE detailing is required at wall boundaries, a simplified displacement-based design approach (§18.10.6.2) and a stress-based approach (§18.10.6.3). The present study focuses on a DDCR approach for more slender walls with a single critical section; therefore, the discussion that follows is limited to the

displacement-based design approach of §18.10.6.2, which applies to walls with $h_w/l_w \geq 2.0$ that are effectively continuous from a single critical section to the top of the wall.

Wallace and Orakcal (2002) provide background on the displacement-based approach to evaluate the need for SBEs. The approach is based on the model shown in Fig. 4-9(***a***), whereas a simplified approach shown in Fig. 4-9(***b***) was adopted for ACI 318-99. The simplified model neglects the contribution of elastic and shear deformations to the top displacement, and it moves the centroid of the plastic hinge to critical section, which is the base of the wall in Fig. 4-9(***b***). Using the simplified model, with the assumption that the wall plastic hinge length, l_p, can be approximated as $l_w/2$, the following relationship for the top (roof) displacement, δ_u, can be derived:

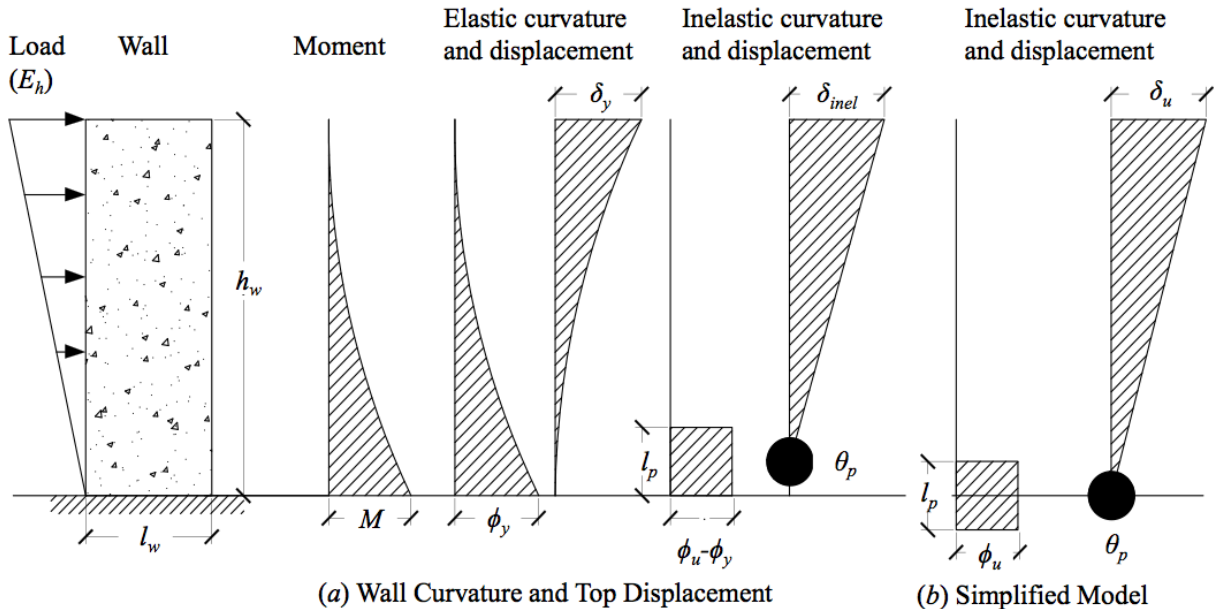

Fig. 4-9–Illustration of the current displacement-based design approach.

$$\delta_u = \theta_p h_w = \left(\phi_u l_p\right) h_w = \left(\frac{\varepsilon_{cu}}{c}\frac{l_w}{2}\right) h_w \qquad \text{(Eq. 4-4)}$$

Where θ_p is the plastic rotation at the base of the wall, and ε_{cu} is the extreme concrete fiber compression strain associated with the inelastic curvature ϕ_u. If $c_{critical}$ is defined as the neutral axis depth associated with ε_{cu} = 0.003 and a 1.5 factor is applied to $\left(\delta_u\right)$, then **Eq. 4-4** can be rearranged as:

$$c_{critical} = \frac{l_w}{667\left(1.5\delta_u / h_w\right)} \approx \frac{l_w}{600\left(1.5\delta_u / h_w\right)} \qquad \text{(Eq. 4-5)}$$

If maximum value of c computed for the factored axial load and nominal moment strength $\left(P_{u,max}, M_n\right)$ consistent with the direction of the design roof displacement $\left(\delta_u\right)$ exceeds $c_{critical}$ from **Eq. 4-5**, then SBEs are required. The 1.5 multiplier on δ_u was added in ACI 318-14 to account for dispersion in the computed drift demands under **DE** level shaking and to produce detailing requirements more consistent with the ASCE 7 code intent of a low probability of collapse for **MCE** level shaking.

If a structural wall is determined to require an SBE based on **Eq. 4-5**, the SBE is required to satisfy the detailing requirements of ACI 318-14 §18.10.6.4. If these requirements are satisfied, the underlying premise of the code is that the wall drift capacity exceeds the expected wall drift demands determined from analysis when subjected to **DE**-level ground motions, without critical strength decay. However, as presented earlier, this is not necessarily the case. In particular, walls with $l_w / b \geq 15$ and $c / b \geq 3$ (i.e., $\lambda_b \geq 45$), and high shear stresses (e.g., approaching the ACI

318-14 §18.10.4.4 average wall shear stress limit of $10\sqrt{f'_c\,\mathbf{(psi)}}$ ($0.83\sqrt{f'_c\,\mathbf{(MPa)}}$)), would be expected to have a $\overline{\delta}_c/h_w$ less than the maximum drift demand allowed by ASCE 7-10. Walls with these attributes are fairly common in modern wall buildings (Brown et al., 2006). In the following paragraphs, a new reliability-based design approach is proposed that has been implemented in the ACI 318-19 code to address this issue.

4.7.1. Proposed approach: drift demand-to-capacity ratio (DDCR) check

One strategy that could be adopted to address the deficiencies identified in the previous paragraph would be to require sufficient detailing such that all walls have a roof drift capacity that exceeds a "worst-case" for a story drift demand of 0.03 for **MCE**-level demands (a roof level drift demand of approximately 0.03(3/4) = 0.0225). This approach was used recently to update column detailing requirements in the ACI 318-14 §18.7.5.4 (Elwood et al., 2009); however, this approach would be overly conservative for structural walls where story drift demands are often considerably less than 0.03, e.g., for a building with many walls. Therefore, an alternative approach, to introduce a DDCR check for Special Structural Walls is proposed. This approach is somewhat similar to demand-to-capacity checks in ACI 318 code for moment and shear strengths, or drift capacity of slab-column connections (ACI 318-14 §18.14.5), to meet a specified level of reliability. The basis for the new design approach is expressed in **Eq. 4-6**:

$$\phi_d\left(\frac{\overline{\delta}_c}{h_w}\right) \geq \left(1.5\frac{\overline{\delta}_u}{h_w}\right) \qquad \text{(Eq. 4-6)}$$

Where $\left(\overline{\delta}_c/h_w\right)$ is the mean wall lateral drift capacity estimated from **Eq. 4-1**, ϕ_d is a "displacement" reduction factor, and $\left(\overline{\delta}_u/h_w\right)$ is the mean roof drift demand estimated using ASCE 7 analysis approaches, multiplied by 1.5 to convert the **DE** mean roof drift demands to mean

MCE demands (see ASCE 7-10 §11.4.4). This format also is consistent with 1.5 multiplier used in the current ACI 318-14 Equation 18.10.6.2 to assess the need for SBEs. Considering COV of 0.3 on $\overline{\delta}_u/h_w$ based on the results presented previously and COV of 0.15 on $\overline{\delta}_c/h_w$ based on the results obtained from **Eq. 4-1**, a simple reliability analysis of **Eq. 4-6**, assuming lognormal distributions in $\overline{\delta}_u/h_w$ and $\overline{\delta}_c/h_w$, results in a probability of strength loss of approximately 10% and 50% for **DE** and **MCE** level demands, respectively, for ϕ_d = 1.0. If the COVs on $\overline{\delta}_u/h_w$ and $\overline{\delta}_c/h_w$ are increased to 0.40 and 0.2, respectively, the probability of strength loss under **DE** demands increases modestly from about 10% to 17%, indicating the strength loss probabilities are not overly sensitive to the estimated COVs. These levels of probability of collapse appear to be high, given the target collapse probabilities of ASCE 7-16 §1.3.1.3 of 10% for Risk Category I and II buildings and 5% for Risk Category III building under **MCE** level demands. To reduce the probability of strength loss to 10% for **MCE** level demands Risk Category I and II buildings, a ϕ_d of 0.65 is required. Selection of an appropriate ϕ_d value requires a definition for collapse, since drift capacity at 20% strength loss is not necessarily associated with building collapse, which is more commonly associated with loss of axial load capacity.

Use of a low probability (10%) of strength loss for **MCE** level demands would be a conservative estimate of collapse, since axial failure models in the literature for columns (Elwood and Moehle, 2005) and for walls (Wallace et al., 2008), as well as ASCE 41 backbone relations, generally indicate that drift ratios at axial failure exceed those at significant strength loss. A review of the dataset of 164 tests with lower drift capacities (i.e., λ_b > 40) revealed that lateral strength loss in these walls was abrupt and typically much greater than 20%, and that axial failure was observed to occur soon after loss of lateral strength (i.e., Segura and Wallace, 2018a; Shegay et al., 2016).

Although tests of well-detailed, isolated cantilever walls in the database show that axial failure may follow soon after substantial lateral strength loss under continued lateral loading, collapse of buildings with structural walls has rarely been reported following earthquakes or shake table tests, even for walls with substantial damage (Wallace et al., 2008; Nagae et al., 2015). Given these observations, use of a low probability of strength loss (i.e., 10%) for **DE** level shaking is suggested here as a minimum criterion for collapse (i.e., ϕ_d = 1.0). This approach will screen out walls with high likelihood of strength loss at **DE** shaking for redesign, which will reduce the likelihood of severe damage at shaking levels less than **DE** and reduce the potential for collapse for **MCE** level shaking.

If **Eq. 4-6** is not satisfied for a given wall, then the designer would be required to revise the design for that wall. The most likely change would be to increase the width of the flexural compression zone ***b*** (i.e., wall thickness, t_w), which would increase the drift capacity obtained with **Eq. 4-1** by reducing the slenderness parameter $\lambda_b = l_w c / b^2$ and also likely reducing the shear and drift demands. **Eq. 4-6** can be rearranged to determine the required minimum width of compression zone (b_{min}) as:

$$\left(b_{min}\right)^2 \geq \frac{l_w c}{\alpha\left(3.85 - \frac{v_{max}}{10\sqrt{f_c'(\text{psi})}} - \frac{1.5\delta_u}{h_w}\right)} \qquad \text{(Eq. 4-7a)}$$

$$\left(b_{min}\right)^2 \geq \frac{l_w c}{\alpha\left(3.85 - \frac{v_{max}}{0.83\sqrt{f_c'(\text{MPa})}} - \frac{1.5\delta_u}{h_w}\right)} \qquad \text{(Eq. 4-7b)}$$

An upper-bound width of the flexural compression zone $\left(\boldsymbol{b_{upper}}\right)$ can be approximated using **Eq. 4-7**, which is based on assuming the shear stress term approaches 1.0 and $\boldsymbol{1.5\delta_u / h_w}$ approaches 0.0225, resulting in the following:

$$b_{upper} = \sqrt{0.025 c l_w} \qquad \text{(Eq. 4-8)}$$

Note that, if $\boldsymbol{c} = 0.20\boldsymbol{l_w}$, then **Eq. 4-8** requires walls with $\boldsymbol{b_{upper}}$ of 17 in. (432 mm) and 26 in. (660 mm) for walls with length of 20 ft (6096 mm) and 30 ft (9144 mm), respectively. Two design examples are presented in the following section to illustrate the proposed approach.

4.8. Example Application

4.8.1. Description of the buildings

In the following, two residential buildings (6-story and 10-story) located in Los Angeles, California are used to illustrate the application of the proposed design methodology, as well as to highlight the significant deficiency in the current design provisions of ACI 318. The building footprint (Fig. 4-10) is 150×75 ft. (45.75×22.9 m), and the typical story height is 12 ft. (3.66 m). A summary of seismic design parameters is provided in Table 4-4. Design concrete compressive strength $\left(\boldsymbol{f'_c}\right)$ of 5 ksi (34.5 MPa) and Grade 60 reinforcement with yield strength $\left(\boldsymbol{f_y}\right)$ of 60 ksi (414 MPa) are specified, consistent with requirements of ACI 318-14 §18.2.5 for concrete and §18.2.5 for reinforcement in structural walls. A total uniformly distributed floor dead load (in addition to self-weight of walls) of 150 psf (7.18 kN/m^2) and floor live load of 40 psf (0.2 kN/m^2) per ASCE 7-10 §4.3.1 are used as the loading criteria.

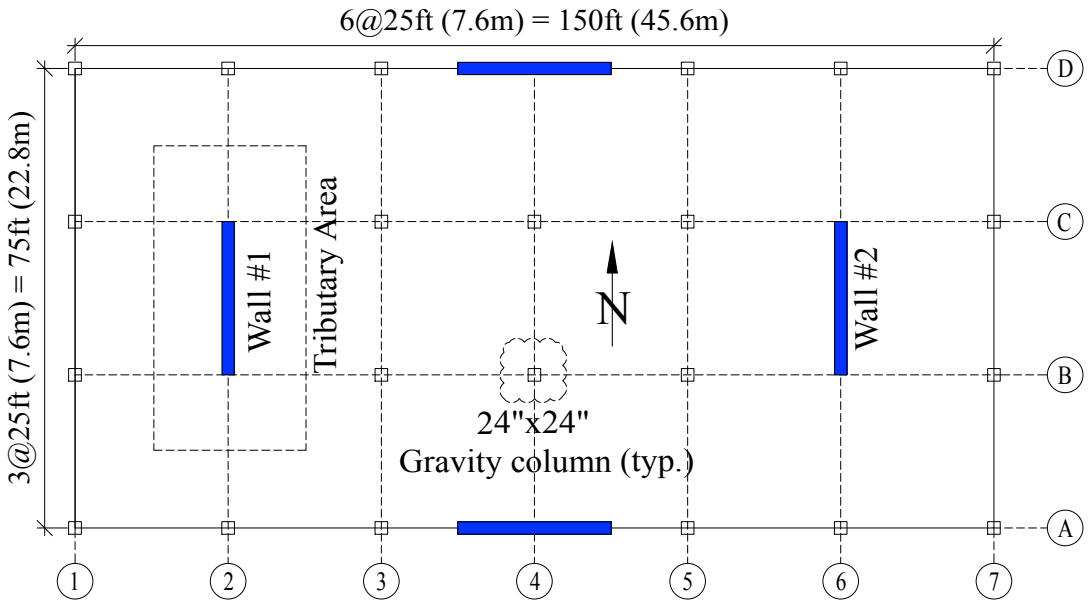

Fig. 4-10–Typical plan view of the buildings.

Table 4-4–ASCE 7-10 seismic parameters

Parameter	Value
Building Location	34.058°N, 118.445°W
Risk Category	II
Importance Factor	1.0
Site Class	D
S_S; S_{DS} (g)	2.253; 1.502
S_1; S_{D1} (g)	0.829; 0.829
SDC	E
$R = C_d$	5
Redundancy factor ρ	1.3

4.8.2. Lateral load analysis

ASCE 7-10 §12.9 Modal Response Spectrum Analysis (RSA) was utilized to determine design lateral forces on the walls under **DE** level shaking. For the purposes of this study, only analysis and design of the LFRS in the north-south direction, which consists of planar RC Special Structural Walls, was considered. A wall effective stiffness, $\boldsymbol{E_c I_{eff}}$, of $\boldsymbol{0.5 E_c I_g}$ was assumed for the lateral analysis, consistent with ACI 318-14 §6.6.3.1.2. The contribution of the gravity columns to the lateral strength and stiffness of the system was ignored. The lateral analysis included the impact of accidental torsional moment $\left(\boldsymbol{M_{ta}}\right)$ required by ASCE 7-10 §12.8.4.2. Inclusion of accidental torsion generally resulted in an increase of both roof drift and base shear demands by about 15%. The ASCE 7-10 strength level load combinations (LC) defined in §2.3.2 and §12.14.3.1 were used to compute the ultimate force demands. Additionally, a redundancy factor $\left(\rho\right)$ of 1.3 was applied to the load combinations that include seismic loads $\left(\boldsymbol{E}\right)$ in accordance with ASCE 7-10 §12.3.4.2, resulting in a 30% increase in base shear and moment demands, and a redundancy factor $\left(\rho\right)$ of 1.0 was used for drift calculations in accordance with ASCE 7-10 § 12.3.4.1. A summary of the force and drift demands obtained from different applicable Load Combinations (LC) is given in Table 4-5 for Wall #1 of building **6A**. It can be seen from Table 4-5 that LC 5, with negative accidental eccentricity (i.e., moving CM closer to the wall) produces the largest force and drift demands.

Detailed information for the LFRS and the analysis results (maximum story and roof drifts, base moment, and base shear demands) are summarized in Table 4-6 under columns **A6** and **A10** for the 6-story and 10-story buildings, respectively. The walls were proportioned such that the allowable story drift demands $\left(\Delta_{story}/\boldsymbol{h_x}\right)$, computed at CM in accordance with ASCE 7-10

§12.8.6, were smaller than the allowable story drift (i.e., $\Delta_a/h_x = 0.02$) given in ASCE 7-10 §12.12.1 for **DE** level shaking. The **DE** roof drift demands (δ_u/h_w), given in Table 4-6, were taken at the top of the wall (not at CM), consistent with wall design displacements used in ACI 318-14 Equation 18.10.6.2. A factor of 1.5 was used to convert the **DE** roof drift demands to **MCE** demands, as noted previously. Base moment, shear, and axial demands given in Table 4-6 are for a critical section at the base of the walls.

Table 4-5–Demands from ASCE 7-10 LCs for Wall #1 in Building 6A

ASCE 7-10 LC No.	LC	$P_{u,base}$ (kips)	M_{base} (kips-ft)	V_{base} (kips)	δ_u (in.)	δ_u/h_w (%)
1	1.4D	2102	-	-	-	-
2	1.2D + 1.6L	2337	-	-	-	-
5	$(1.2+0.2S_{DS})$D + 0.5L + ρQ_{E1}	2420	58166	-1196	8.465	0.98
5	$(1.2+0.2S_{DS})$D + 0.5L + ρQ_{E2}	**2420**	**85523**	**-1767**	**12.466**	**1.44**
5	$(1.2+0.2S_{DS})$D + 0.5L - ρQ_{E1}	2420	-758063	1194	-8.44	-0.98
5	$(1.2+0.2S_{DS})$D + 0.5L - ρQ_{E2}	**2420**	**-85420**	**1766**	**-12.444**	**-1.44**
7	$(1.2-0.2S_{DS})$D + ρQ_{E1}	901	58133	-1196	8.458	0.98
7	$(1.2-0.2S_{DS})$D + ρQ_{E2}	**901**	**85490**	**-1766**	**12.459**	**1.44**
7	$(1.2-0.2S_{DS})$D - ρQ_{E1}	901	-58095	1194	-8.45	-0.98
7	$(1.2-0.2S_{DS})$D - ρQ_{E2}	**901**	**-85452**	**1766**	**-12.451**	**-1.44**

Note:
(1) Q_{E1} = Effect of horizontal seismic forces with negative accidental eccentricity (i.e., moving CM towards Wall #1), and Q_{E2} = Effect of horizontal seismic forces with positive accidental eccentricity (i.e., moving CM away from Wall #1).
(2) The negative and positive signs indicate the direction of the seismic forces.
(3) $\rho = 1.3$ for base moment and shear demands and = 1.0 for drift demands.
(4) δ_u is the design displacement at the top of the wall $(\delta_{elastic} \times C_d/I)$.

4.8.3. Walls design

Based on the demands from the preceding section, two identical planar structural walls are proposed as the LFRS in the north-south direction for each building. The walls are 24 ft. (7.3 m) long and 12 in. (0.30 m) thick for building **A6** and 26 ft. (7.9 m) long and 18 in. (0.46 m) thick for building **A10**, resulting in wall cross-section aspect ratio $\left(\boldsymbol{l_w}/\boldsymbol{t_w}\right)$ of 24 and 17.33, respectively. Because the buildings are assigned to SDC E in accordance with ASCE 7-10 §11.6, the walls are required to be designed and detailed to satisfy the provisions of ACI 318-14 §18.10 for Special Structural Walls. Wall design details are shown in Table 4-6 under columns **6A** and **10A** for the 6-story and 10-story buildings, respectively. Since $\boldsymbol{c} > \boldsymbol{c_{critical}}$, the compression zones of the walls must be reinforced with SBE details that satisfy the requirements of ACI 318-14 §18.10.6.4 over a distance of $\boldsymbol{l_{be,required}} = \mathbf{max}\left(\boldsymbol{c}/\mathbf{2}; \boldsymbol{c} - \mathbf{0.1}\boldsymbol{l_w}\right)$. The wall boundary element details are shown in Fig. 4-11(***a***) and Fig. 4-11(***c***) for building **6A** and **10A**, respectively.

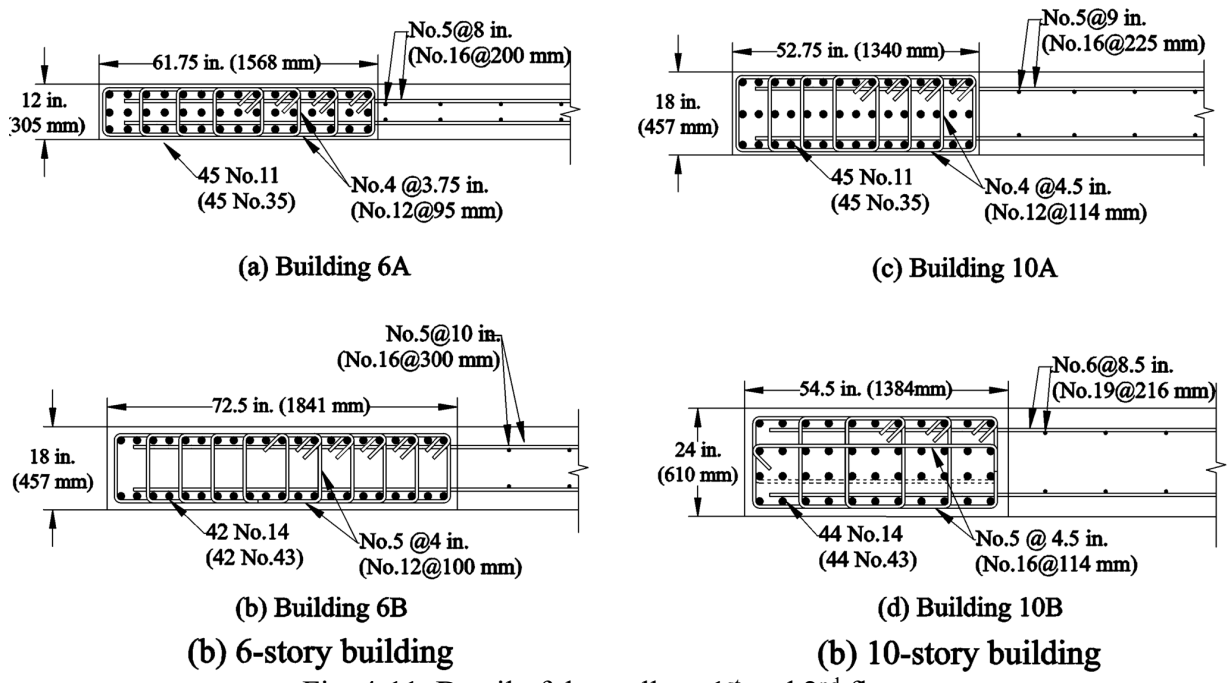

Fig. 4-11–Detail of the walls at 1st and 2nd floors.

4.8.4. Reliability analysis

Wall roof drift capacities, defined at 20% strength degradation, were computed from **Eq. 4-1** for two boundary transverse reinforcement configurations, namely, overlapping hoops (OH) and a single perimeter hoop with supplemental legs of crossties (HC), as shown in Table 4-6. The lower bound (minimum) drift capacity from **Eq. 4-1** governs for both walls. To determine the probabilities of strength loss, simple reliability analyses were performed using **Eq. 4-6** assuming lognormal distributions in drift demand and capacity and considering COVs of 0.30 and 0.15 for roof drift demand and capacity, respectively. The probabilities of strength loss under **DE** and **MCE** level shaking are given in Table 4-6**.** The resulting values of 28% and 66% for OH and HC configurations, respectively, for building **6A**, and 46% and 83% for OH and HC configurations, respectively, for building **10A**, for **DE** level shaking, are unacceptably high given the current target reliabilities of ASCE 7-16 §1.3.1.3. It is important to note that the walls in both buildings (**6A** and

10A) satisfy the provisions of ASCE 7-10 and ACI 318-14 for Special Structural Walls (i.e., code compliant walls). These results highlight that the current code provisions do not adequately address concerns related to brittle compression failure of walls under **DE** shaking, and that these wall designs should be revised.

4.8.5. Revised design

To reduce the probability of strength loss to an acceptable level (e.g., 10% or lower for **DE** level shaking), either **Eq. 4-7** $\left(b_{min}\right)$ or **Eq. 4-8** $\left(b_{upper}\right)$ can be employed. For the given c/l_w demands, the upper bound compression zone width $\left(b_{upper}\right)$ is 25.4 in. (645 mm) for the 6-story building and 27.9 in. (709 mm) for the 10-story building. An alternative approach is used here, where b_{min} is determined using **Eq. 4-7** assuming a change in wall thickness results in proportional reductions in δ_u/h_w, $v_{max}/\sqrt{f'_c}$, and c/l_w. For building **6A** with HC configuration $\left(\alpha = \mathbf{45}\right)$, revised demand values for an estimated 15% reduction are: δ_u/h_w ≈ 1.44×0.85 = 1.22%, $v_{max}/\sqrt{f'_c \textbf{ psi (MPa)}}$ ≈ 7.21(0.6)×0.85 = 6.13 (0.51), and c/l_w ≈ 0.31×0.85 = 0.26.

Substituting these values in **Eq. 4-7** results in b_{min} = 0.064 l_w ≈ 18 in. (457 mm) for the 6-story building and, similarly, b_{min} = 23 in. (584 mm) for the 10-story building. Therefore, wall thickness values were increased to 18 in. (457 mm) for the 6-story building and to 24 in. (610 mm) for 10-story building. Using the new wall thickness values, the analyses were rerun to determine the new force and drift demands, as well as to determine whether **Eq. 4-6** is satisfied (i.e., probability of strength loss is 10% or lower for **DE** level shaking). The revised design details are given in Table 4-6 under columns **6B** and **10B** for the 6-story and 10-story building, respectively. As can be seen

from Table 4-6, increasing in the wall thickness for building **6A** resulted in: (1) reduction of δ_u / h_w by about 18%, (2) reduction of $v_{max} / \sqrt{f'_c}$ by about 16%, and (3) significant increase in δ_c / h_w, because a portion of the drift capacity is proportional to b^2. The new probabilities of strength loss for **DE** level shaking have reduced to below 10% for both the 6-story building (**6B**) and the 10-story building (**10B**), for both OH and HC configurations. The wall boundary element details are shown in Fig. 4-11(***b***) and Fig. 4-11(***d***) for building **6B** and building **10B**, respectively.

4.9. Conclusions and Recommendations

Based on the findings of this study, the following conclusions with regards to design of structural walls with SBEs resulted:

1. Displacement capacity of ACI 31-14 code-compliant walls is primarily a function of parameters that are not adequately addressed in ACI 318-14 code, such as wall cross-section geometry, neutral axis depth, wall shear stress demand, as well as the configuration of the boundary transverse reinforcement (use of overlapping hoops versus a single perimeter hoop with supplemental crosstie legs). Based on these variables, drift capacity of walls with SBEs varies roughly by a factor of 3, ranging from approximately 0.012 to 0.035.

Table 4-6–Design details of the walls in each building

Building	6-story		10-story	
	6A	**6B**	**10A**	**10B**
$h_w \times l_w \times t_w$, ft. (m)	72×24×1.0 (21.95×7.3×0.30)	72×24×1.5 (21.95×7.3×0.46)	120×26×1.5 (36.5×7.9×0.46)	120×26×2.0 (36.5×17.9×0.61)
h_w/l_w; $M_{base}/(V_{base}l_w)$	3.0; 2.02		4.62; 2.39	
$l_{be} \times b$, in. (mm)	61×12 (1,550×305)	52×18 (1,321×457)	71×18 (1,778×457)	53×24 (1,346×610)
$l_{be,required}$, in. (mm)	60.2 (1,529)	41.2 (1,046)	69.8 (1,773)	50 (1,270)
Boundary longitudinal reinforcement	45 No.11 (45 No.35)	45 No.11 (45 No.35)	42 No.14 (42 No.43)	44 No.14 (44 No.43)
Boundary transverse reinforcement	No.4@3.75in. (No.12@95mm)	No.4@4.5in. (No.12@114mm)	No.5@4in. (No.16@100mm)	No.5@4.5in. (No.16@114mm)
$A_{sh,prov.}/A_{sh,req.}$; $S_{prov.}/S_{req.}$	1.05; 0.9	1.02; 0.8	1.00; 0.7	1.05; 0.8
Web vertical and horizontal reinforcement	2 layers No.6@8in. (No.19@200mm)	2 layers No.6@9in. (No.19@229mm)	2 layers No.6@10in. (No.19@200mm)	2layers No.6@8.5in. (No.19@216mm)
Min ϕM_n, kips-ft. (kN-m)	88,139 (119,578)	95,570 (129,660)	133,039 (180,494)	152,076 (206,321)
$V_{@Mn}/\left(A_{cv}\sqrt{f'_c \text{ psi (MPa)}}\right)$	8.3 (0.69)	6.0 (0.5)	6.0 (0.5)	5.1 (0.43)
$V_{n,ACI}$, kips (kN)	2,408 (10,710)	2,440 (10,854)	2,884 (12,830)	3,032 (13,486)
$V_{n,ACI}/\left(A_{cv}\sqrt{f'_c \text{ psi (MPa)}}\right)$	9.8 (0.82)	6.6 (0.55)	7.2 (0.6)	5.7 (0.48)
T_a; T_u; T_1 (sec)	0.49; 0.69; 0.94	0.49; 0.69; 0.78	0.73; 1.02; 1.79	0.73; 1.02; 0.1.58
P_{u1}, kips (kN); $P_{u1}/\left(A_g f'_c\right)$	2,420 (10,765); 0.14	2,649 (11,780); 0.10	4,606 (20.488); 0.16	5,022 (22,339); 0.13
P_{u2}, kips (kN); $P_{u2}/\left(A_g f'_c\right)$	901 (4,008); 0.05	991 (4,408); 0.038	1,724 (7,669); 0.06	1,888 (8,398); 0.05
M_{base}, kips-ft. (kN-m)	85,356 (115,803)	92,050 (124,884)	132,213 (179,373)	146,073 (198,177)
V_{base}, kips (kN)	1,762 (7,838)	1,835 (8,162)	2,127 (9,461)	2,222 (9,884)
$V_{base}/\left(A_{cv}\sqrt{f'_c \text{ psi (MPa)}}\right)$	7.21 (0.6)	6.0 (0.50)	5.36 (045)	4.2 (0.35)
Max c, in. (mm)	89 (2,261)	70 (1,778)	101 (2,565)	81 (2,057)
$c_{critical}$, in. (mm)	22.2 (564)	26.7 (678)	20.3 (515)	23 (584)
Max c/l_w; c/l_w from **Eq. 4-3**	0.31; 0.27	0.24; 0.22	0.32; 0.29	0.26; 0.26
c/b; l_w/b	7.5; 24	3.89; 16	5.6; 17.33	3.38; 13
$\lambda_b = l_w c/b^2$	180	62	97	44
Max Δ_{story}/h_x (%) at **DE**	1.92	1.56	1.93	1.70
ASCE 7-10 Δ_a/h_x (%)	2.00	2.00	2.00	2.00
Roof δ_u/h_w (%) at **DE**	1.44	1.20	1.71	1.51
Roof δ_u/h_w (%) at **MCE**	1.44×1.5 = 2.16	1.20×1.5 = 1.80	1.71×1.5 = 2.56	1.51×1.5 = 2.27
δ_c/h_w (%): OH	1.75	2.21	1.75	2.70
δ_c/h_w (%): HC	1.25	1.87	1.25	2.45
Probability of strength loss (%) at **DE** (**MCE**): OH	28 (73)	3 (26)	46 (87)	4 (30)
Probability of strength loss (%) at **DE** (**MCE**): HC	66 (95)	9 (45)	83 (98)	8 (41)

OH = Overlapping hoop configuration, HC = Single perimeter hoop with supplemental crossties.

2. Considering parameters with the greatest impact on wall lateral deformation capacity, equations **Eq. 4-1** and **Eq. 4-2** were developed to accurately predict drift and total curvature capacities of walls with SBEs, with mean values of 1.0 and COVs of 0.15 and 0.18, respectively.
3. The underlying premise of the ASCE 7-10 and ACI 318-14 provisions is that special structural walls satisfying the provisions of ACI 318-14 §18.10.6.2 through §18.10.6.4 possess adequate drift capacity to exceed the expected drift demand determined from ASCE 7-10 analysis procedures. However, results presented in this study show that this assumption is not always correct, and that, in some case, the intended performance objectives may not be achieved.
4. To address the above deficiencies, a new reliability-based design methodology is proposed where a drift demand-capacity ratio (DDCR) check is performed to provide a low probability (i.e., 10% or lower) that roof drift demands exceed roof drift capacity at strength loss for the **DE** level shaking. In general, walls with slender cross sections $\left(\boldsymbol{l_w/b > 15}\right)$, large neutral axis depth relative to width of flexural compression zone $\left(\boldsymbol{c/b > 3}\right)$, shear stresses approaching the ACI 318 §18.10.4.4 limit $\left(\mathbf{10}\sqrt{\boldsymbol{f'_c}}\right)$, and roof drift demands approaching the maximum story drift allowed by ASCE 7-10 are screened out for redesign. Preventing strength loss under **DE** level shaking is assumed to reduce the probability of collapse under **MCE** level shaking; however, for improved performance, a lower (or specified) probability of strength loss for **MCE** level shaking could be used.

5. Example applications are presented to highlight concerns that, in some cases, the provisions of ACI 318-14 may not result in buildings that meet the stated performance objectives. To assist in cases where redesign is required, expressions for minimum and upper-bound width of flexural compression zone are provided.

4.10. Acknowledgements

Funding for this study was provided, in part, by the National Science Foundation Grant CMMI-1446423, which focused on promoting and enhancing US and international collaboration on performance assessment of structural wall systems. Any opinions, findings, and conclusions or recommendations expressed in this paper are those of the authors and do not necessarily reflect the views of others mentioned here. The authors would also like to thank members of ACI Committee 318H for providing thoughtful comments on the proposed design approach.

4.11. References

ACI Committee 318, 2014, "Building Code Requirements for Structural Concrete (ACI 318-14) and Commentary," American Concrete Institute, Farmington Hills, MI, 519 pp.

ACI Committee 318, 1999, "Building Code Requirements for Structural Concrete (ACI 318-99) and Commentary (318R-99), American Concrete Institute, Detroit, MI, 391 pp.

ACI Committee 318, 1983, "Building Code Requirements for Reinforced Concrete (ACI 318-83), American Concrete Institute, Detroit, MI, 155 pp.

Abdullah, S. A., and Wallace, J. W., 2018a, "Drift capacity prediction of RC structural walls with special boundary elements," *Proceedings, 11th National Conference in Earthquake Engineering*, Earthquake Engineering Research Institute, Los Angeles, CA.

Abdullah, S. A., and Wallace, J. W., 2018b, "UCLA-RCWalls database for reinforced concrete structural walls," *Proceedings, 11th National Conference in Earthquake Engineering*, Earthquake Engineering Research Institute, Los Angeles, CA.

Abdullah, S. A., and Wallace, J. W., 2018c, "A Reliability-based deformation capacity model for ACI 318 compliant special structural walls," *Proceedings, 2018 Structural Engineers Association of California (SEAOC) Convention*, Palm Springs, CA.

Abdullah S. A., Wallace J. W., 2019, "Drift capacity of RC structural walls with special boundary elements," *ACI Structural Journal*, Vol. 116, No. 1, pp. 183–194.

ASCE/SEI Standards, 2013, "Seismic Evaluation and Retrofit of Existing Buildings (ASCE/SEI 41-13)," American Society of Civil Engineers, Reston, VA, 518 pp.

ASCE/SEI Standards, 2010, "Minimum Design Loads for Buildings and Other Structures (ASCE/SEI 7-10)," American Society for Civil Engineers, Reston, VA, 518 pp.

ASCE/SEI Standards, 2016, "Minimum Design Loads for Buildings and Other Structures (ASCE/SEI 7-16)," American Society for Civil Engineers, Reston, VA, 690 pp.

Brown, P., Ji, J., Sterns, A., Lehman, D. E., Lowes, L. N., Kuchma, D., and Zhang, J., 2006 "Investigation of the seismic behavior and analysis of reinforced concrete walls," *Proceedings*, 8th National Conference on Earthquake Engineering, San Francisco, CA.

Dezhdar, E., 2012, "Seismic Response of Cantilever Shear Wall Buildings," Ph.D. Dissertation, University of British Columbia, Vancouver, Canada, 287 pp.

Elwood, K. J., Maffei, J. M., Riederer, K. A., and Telleen, K., 2009, "Improving Column Confinement–Part 2: Proposed New Provisions for the ACI 318 Building Code," *Concrete International*, Vol. 31, No. 12, pp. 41–48.

Elwood, K. J. and Moehle, J. P., 2005, "Drift capacity of reinforced concrete columns with light transverse reinforcement," *Earthquake Spectra*, Vol. 21, No. 1, pp. 71–89.

Haselton, C. B., 2009, "Evaluation of Ground Motion Selection and Modification Methods: Predicting Median Interstory Drift Response of Buildings," *PEER Report 2009/01,* Pacific Engineering Research Centre (PEER), Berkeley, CA, 288 pp.

Kim, S., 2016, "Reliability of Structural Wall Shear Design for Tall Reinforced Concrete Core Wall Buildings," Ph.D. Dissertation, University of California, Los Angeles, CA, 246 pp.

Lowes, L. N., Lehman D. E., Birely A. C., Kuchma D. A., Marley K. P., and Hart C. R., 2012, "Earthquake response of slender concrete planar concrete walls with modern detailing" *Engineering Structures*, Vol. 34, pp. 455–465.

Moehle, J., Bozorgnia, Y., and Yang, T. Y., 2007, "The tall buildings initiative," *Proceedings*, SEAOC 2007 Convention, Squaw Creek, California, USA.

Nagae, T., Tahara, K., Taiso, M., Shiohara, H., Kabeyasawa, T., Kono, S., Nishiyama, M., Wallace, J. W., Ghannoum, W. M., Moehle, J. P., Sause, R., Keller, W., and Tuna, Z., 2011, "Design and Instrumentation of the 2010 E-Defense Four-Story Reinforced Concrete and Post-Tensioned Concrete Buildings," *PEER Report 2011/104*, Pacific Earthquake Engineering Research Center (PEER), Berkeley, CA, 234 pp.

Oesterle, R. G., Aristizabal-Ochoa, J. D., Fiorato, A. E., Russell, H. G., and Corley, W. G., 1979, "Earthquake Resistant Structural Walls–Phase II," *Report to National Science Foundation (ENV77-15333)*, Construction Technology Laboratories, Portland Cement Association, Skokie, IL, 331 pp.

Oesterle, R. G., Fiorato, A. E., Johal, L. S., Carpenter, J. E., Russell, H. G., and Corley, W. G., 1976, "Earthquake Resistant Structural Walls–Tests of Isolated Walls," *Report to National Science Foundation (GI-43880),* Construction Technology Laboratories, Portland Cement Association, Skokie, IL, 315 pp.

Paulay, T. and Goodsir, W. J., 1985, "The ductility of structural walls," *Bulletin of the New Zealand National Society for Earthquake Engineering*, Vol. 18, pp. 250–269.

Segura, C. L., and Wallace, W. J., 2018a, "Seismic performance limitations and detailing of slender reinforced concrete walls," *ACI Structural Journal*, V. 115, No. 3, pp. 849–860.

Segura, C. L., and Wallace, W. J., 2018b, "Impact of geometry and detailing on drift capacity of slender walls," *ACI Structural Journal*, V. 115, No. 3, pp. 885–896.

Shegay, A. S., Motter, C. M., Henry, R. S., and Elwood, K. J., 2016, "Large scale testing of a reinforced concrete wall designed to the amended version of NZS3101: 2006," *Proceedings*, The New Zealand Concrete Industry Conference, Auckland, New Zealand.

Thomsen, J. H. IV, and Wallace, J. W., 2004, "Displacement-based design of slender reinforced concrete structural walls—experimental verification," *Journal of Structural Engineering*, Vol. 130, No. 4, pp. 618–630.

Wallace, J. W. and Moehle, J. P., 1992, "Ductility and detailing requirements of bearing wall buildings," *Journal of Structural Engineering*, Vol. 6, pp. 1625–1644.

Wallace, J. W., 1994, "A new methodology for seismic design of RC shear walls," *Journal of Structural Engineering*, Vol. 120, No. 3, pp. 863–884.

Wallace, J. W., 2012, "Behavior, design, and modeling of structural walls and coupling beams–lessons from recent laboratory tests and earthquakes," *International Journal of Concrete Structures and Materials*, Vol. 6, No. 1, pp. 3–18.

Wallace, J. W., and Orakcal, K., 2002, "ACI 318-99 provisions for seismic design of structural walls," *ACI Structural Journal*, Vol. 99, No. 4, pp. 499–508.

Wallace, J. W, Massone, L. M., Bonelli, P., Dragovich, J., Lagos, R., Luders, C., and Moehle, J., 2012, "Damage and implications for seismic design of RC structural wall buildings," *Earthquake Spectra*, Vol. 28, No. S1, pp. 281–289.

Wallace, J. W., Elwood, K. J., and Massone, L. M., 2008, "Investigation of the axial load capacity for lightly reinforced wall piers," *Journal of Structural Engineering,* Vol. 134, No. 9, pp. 1548–1557.

Wallace, J. W., and Safdari, A., 2018, "Design of slender reinforced concrete walls," *Proceedings,* 11th National Conference in Earthquake Engineering, Earthquake Engineering Research Institute, Los Angeles, CA.

Welt, T. S., 2015, “Detailing for Compression in Reinforced Concrete Wall Boundary Elements: Experiments, Simulations, and Design Recommendations,” Ph.D. Thesis, University of Illinois, Urbana-Champaign, IL, 530 pp.

CHAPTER 5. Drift Capacity at Axial Failure of RC Structural Walls and Wall Piers

5.1. Abstract

A large number of reinforced concrete (RC) buildings constructed prior to the mid-1970s in earthquake-prone regions rely on lightly reinforced or perforated, perimeter structural walls to resist earthquake-induced lateral loads. These walls are susceptible to damage when subjected to moderate-to-strong shaking; a number of such cases were observed in Chi Chi and Kocaeli Earthquakes in 1999, and more recently in 2010 Maule and 2011 Christchurch earthquakes. Despite these observations, there have been limited studies reported in the literature to investigate the loss of axial (gravity) load carrying capacity of damaged walls and wall piers, primarily due to limited experimental data. However, over the last decade, a large number of experimental studies examining the behavior of RC walls, including axial failure, have become available. A comprehensive database was developed that includes detailed information on more than 1100 RC wall tests. To study axial failure of structural walls, the database was filtered to identify and analyze datasets of tests on shear- and flexure-controlled walls. Based on the results, expressions were derived to predict lateral drift capacity at axial failure of RC walls and piers.

5.2. Introduction

Reinforced concrete (RC) structural walls (also known as shear walls) have commonly been used as lateral force-resisting elements in buildings in regions of moderate-to-high seismic hazard because they provide substantial lateral strength and stiffness when buildings are subjected to strong ground shaking. Although test programs on RC walls initiated in the 1950s in the US, relatively few test programs were reported in the literature through the late-1990s. Those limited

test programs focused primarily on addressing issues related to peak shear strength of squat walls and the influence of boundary element detailing, cross-section shape, and wall shear stress on the load versus deformation behavior and failure modes of slender walls. Observations from major earthquakes in the US and Japan in the mid-1990s, and the expansion of experimental testing facilities around the world have since led to a significant increase in the available wall test results reported in the literature. However, one common aspect of the experimental programs conducted prior to around the mid-2000s is that the tests were generally terminated after peak strength or relatively minor loss of lateral strength (~20 to 40%); therefore, the issue of loss of axial load carrying capacity (referred to as axial failure in this paper) was not studied. Although axial failure has rarely been reported for walls (Wallace et al, 2008), wall axial failure could trigger partial or total building collapse, especially in buildings with significant torsional irregularities and no redundancy. The lack of data may also result in conservatively low estimates of lateral drift capacity at axial failure for ASCE 41 acceptance criteria, which would result in most intrusive and costly seismic retrofits. Therefore, it is important to be able to adequately evaluate the lateral drift capacity of walls associated with axial failure.

Observations of column axial failures in the 1995 Kobe earthquake led to a number of test programs to investigate the axial failure of shear-critical columns (Kabeyasawa et al., 2002; Kato and Ohnishi, 2002; Nakamura and Yoshimura 2002; Tasai, 1999; Tasai, 2000; Yoshimura and Yamanaka, 2000). Subsequently, theoretical and empirical or semi-empirical models were proposed to assess axial failure of shear-damaged columns (e.g., Elwood and Moehle, 2005; Ousalem, 2006; Tran, 2010; Uchida and Uezono, 2003; Nakamura and Yoshimura, 2002). Research efforts focused on axial failure of RC walls were initiated in the early 2000s to extend the model developed by Elwood and Moehle (2005) to predict axial failure of shear-controlled

columns to lightly reinforced, shear-controlled wall and wall-piers based on observations from the Chi-Chi, Taiwan and Kocaeli, Turkey earthquakes in 1999 (Wallace et al, 2008). These walls are typically found in buildings constructed prior to the mid-1970s; however, limited data existed to calibrate and validate the model for shear-controlled walls. Recently, Looi and Su (2018) formulated a model based on Mohr's circle to assess axial failure of heavily reinforced, short shear-span RC coupled shear walls, designed for moderate intensity earthquake ground shaking and primarily used to control lateral drift in strong wind events.

ASCE 41-17 is commonly used to evaluate the expected performance of existing buildings subjected to earthquake ground motions. Generally, shear- and flexure-controlled walls are treated as deformation-controlled components, where ASCE 41-17 provides modeling parameters (backbone relations) and acceptance criteria. However, the provided backbones were developed in late 1990s (FEMA 273/274-1997) based on limited experimental data and engineering judgment. Studies by Abdullah and Wallace (2019), Motter et al. (2018), and Segura and Wallace (2018) have indicated that the current modeling parameters tend to be overly conservative and are influenced by variables that are not considered in ASCE 41-17. Wall axial failure models are needed to update and improve the modeling parameters (currently the *b*-parameter) of ASCE 41-17, which could result in considerable savings during seismic evaluation and retrofit of existing RC buildings.

Over the last ten years, a large number of laboratory studies examining the behavior of RC structural walls have been reported in the literature. A comprehensive wall database, UCLA-RCWalls, has been developed at University of California, Los Angeles (UCLA) that includes detailed information on more than 1100 tests reported in the literature (Abdullah and Wallace, 2018). The database was utilized to develop an approach to determine the expected failure mode

for RC structural walls, and then to study axial failure of walls, by filtering the main database to identify and analyze datasets of test results on shear- and flexure-controlled walls. Based on the results, relationships were developed to predict wall lateral drift capacity at axial failure. Given that the study is based on test results for individual walls, the predictive expressions do not take into account the impact of gravity load redistribution and torsional irregularity on potential for axial failure of the wall and the building. The lack of test data on complete buildings, either laboratory or in earthquakes, limits these studies.

5.3. Experimental RC Wall database

5.3.1. Overview

A comprehensive database, referred to as the UCLA-RCWalls database, was developed by the authors that compiles detailed data on more than 1100 RC wall tests reported in the literature. The database includes three major clusters of data: 1) information about the test specimen, test setup, and axial and lateral loading protocols, 2) analytically computed data, e.g., moment-curvature relationships (c, M_n, M_y, ϕ_n, ϕ_y) and wall shear strengths according to ACI 318-19, and 3) test results, e.g., backbone relations and failure modes. Database information related to the objectives of this study (i.e., failure mode classification and axial failure) are briefly presented below; however, detailed information about the content and structure of the database can be found elsewhere (Abdullah and Wallace, 2018; Abdullah and Wallace, 2019).

Fig. 5-1 shows a typical backbone curve for the experimental base shear versus total top displacement (curvature, shear, and bar slip/extension) from a wall test (Tran and Wallace, 2015). The *collapse* point represents the state at which axial failure occurs and was identified based on

either reported axial failure from the test (e.g., Fig. 5-2 and Fig. 5-3) or observed concrete crushing and damage along the entire length of the wall and/or out-of-plane instability such that no portion of the wall is left intact or stable to carry the applied axial load (e.g., Fig. 5-4). In some tests, complete loss of axial load carrying capacity was not observed or reported, in these cases, the data represent a lower bound deformation capacity for axial failure. If reported axial failure occurred at deformations smaller than the maximum deformation reached prior to axial failure, then the maximum deformation is reported in the database for axial failure (e.g., Fig. 5-2 and Fig. 5-3). As noted previously, many wall tests, especially earlier tests (prior to mid-2000s), do not have information on axial failure because the test was terminated prior to an observed axial failure.

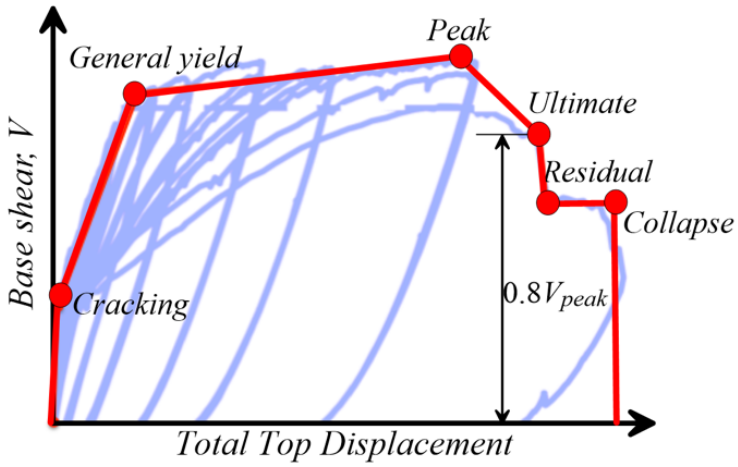

Fig. 5-1–Typical wall backbone curve contained in UCLA-RCWalls database.

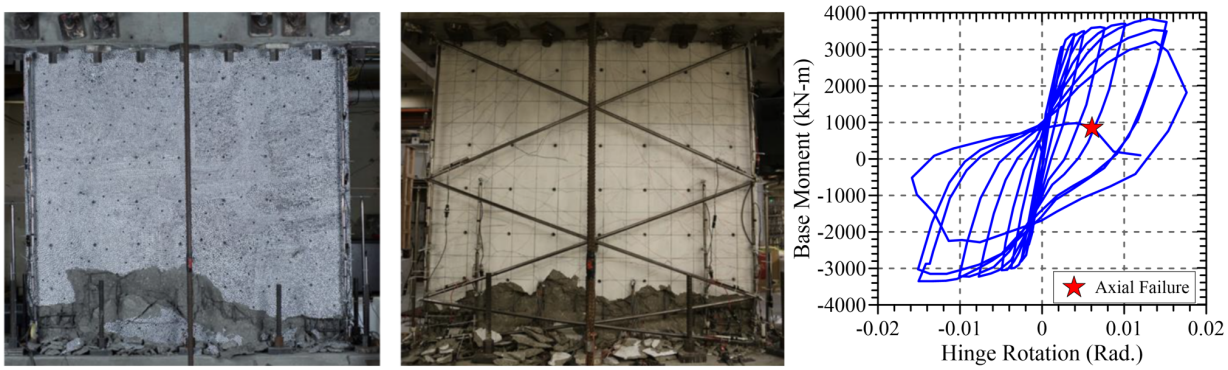

(*a*) Damage at the end of testing (*b*) Load-deformation response

Fig. 5-2–Reported axial failure of a wall test reported by Segura and Wallace (2018). (*Note*: for (*b*) only the first cycle at each displacement is shown)

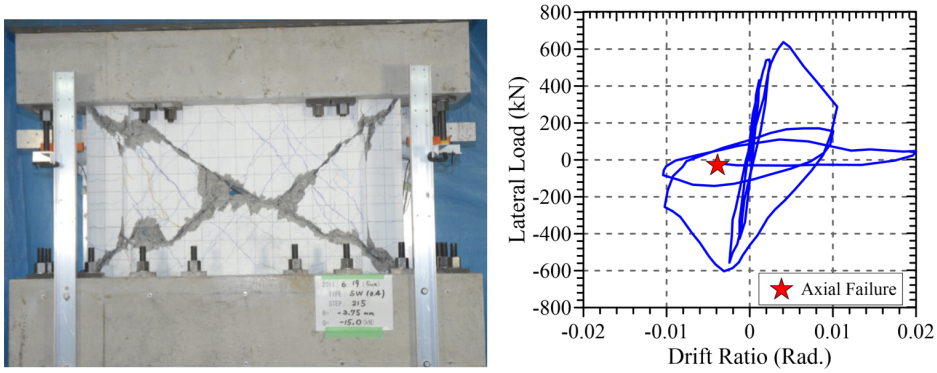

(*a*) Damage at the end of testing (*b*) Load-deformation response

Fig. 5-3–Reported axial failure of a shear-controlled wall test reported by Sanada et al. (2012).

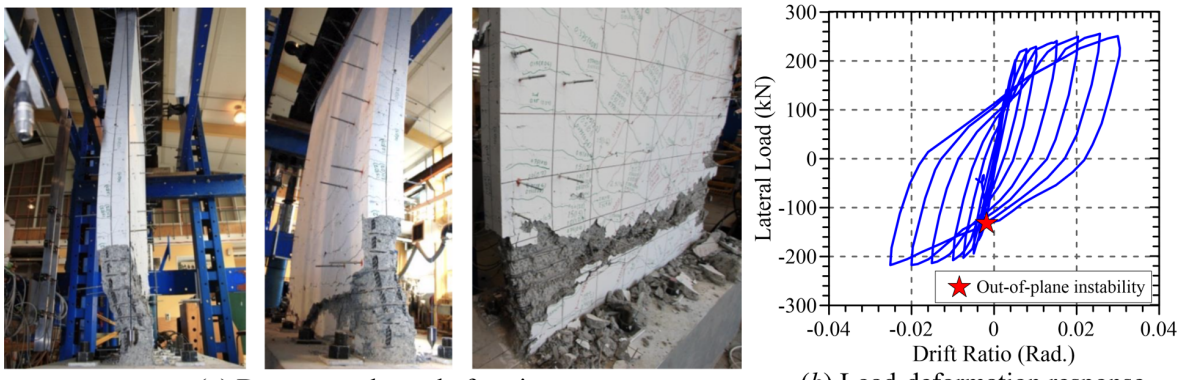

(*a*) Damage at the end of testing (*b*) Load-deformation response

Fig. 5-4–Out-of-plane instability and concrete crushing of a wall test reported by Dashti et. (2018). (*Note*: for (*b*) only the first cycle at each displacement is shown)

The reported failure modes are classified in the database as either flexure failure modes, i.e., flexural compression (bar buckling and concrete crushing), flexural tension (bar fracture), or global or local lateral instability (Fig. 5-5), shear failure modes, i.e., diagonal tension, diagonal compression (web crushing), or shear sliding at the base (Fig. 5-6), flexure-shear failure modes, i.e., yielding in flexure and failing in one of the shear failure modes (Fig. 5-7), and lap-splice failure mode. The authors did their best to validate that the reported failure mode was consistent with the observed wall response and damage before recording that information in the database.

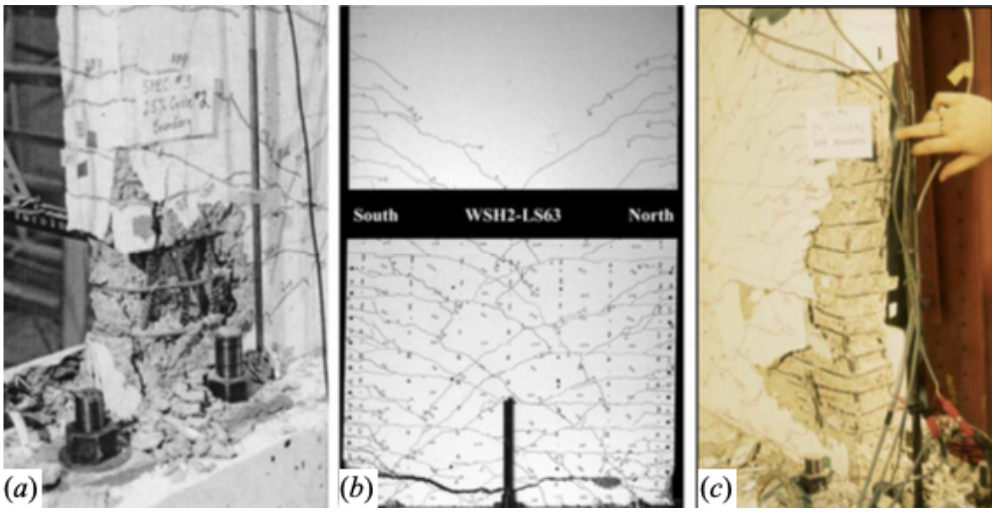

Fig. 5-5–Wall flexural failure modes: (*a*) bar buckling and concrete crushing (Thomsen and Wallace, 1995), (*b*) bar fracture (Dazio et al., 2009), and (*c*) lateral instability (Thomsen and Wallace, 1995).

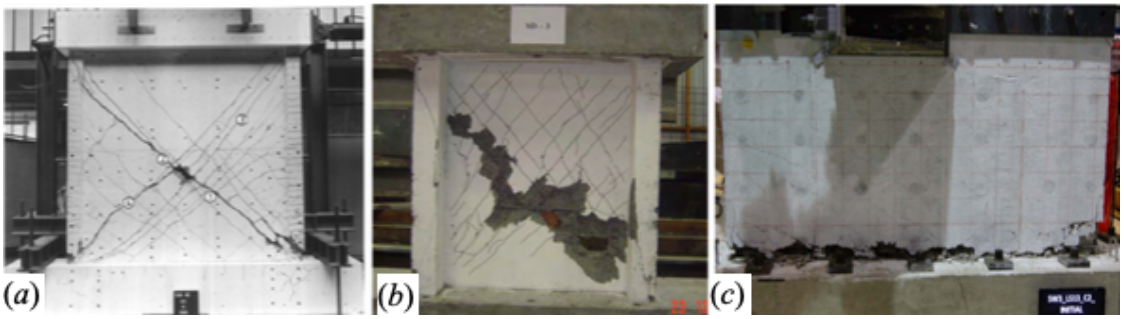

Fig. 5-6–Wall shear failure modes: (*a*) diagonal tension (Mestyanek, 1986), (*b*) diagonal compression (Dabbagh, 2005), and (*c*) shear-sliding (Luna, 2015).

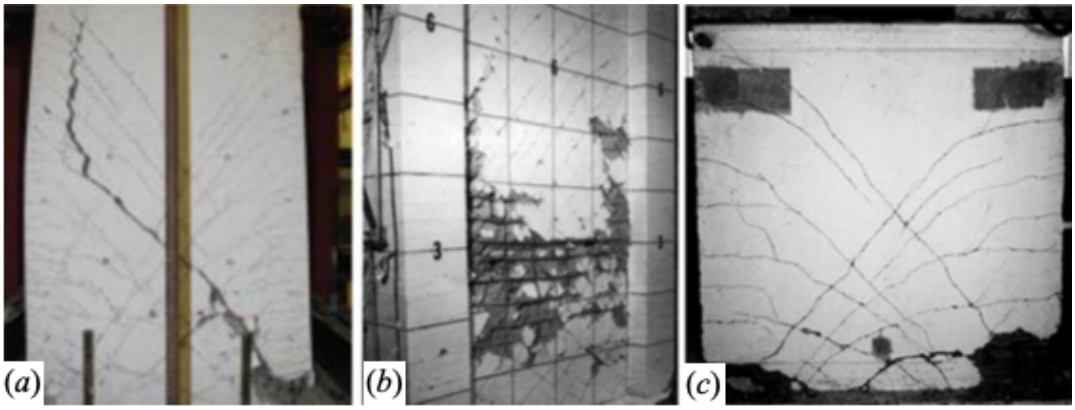

Fig. 5-7–Wall flexure-shear failure modes: (*a*) flexure-diagonal tension (Tran and Wallace, 2015), (*b*) flexure-diagonal compression (Oesterle et al., 1976), and (*c*) flexure-shear-sliding (Salonikios et al., 1999).

Furthermore, the database contains computed data for both flexural and shear responses. Analytical moment-curvature $(M-\phi)$ analysis was performed for each wall using tested material properties and the sustained axial load, if present. Although the moment-curvature response of each wall is available in a spreadsheet, values of nominal moment strength (M_n) and depth of neutral axis (c) at concrete compressive strain of 0.003 and first yield moment strength (M_y) and curvatures corresponding to M_n and M_y are recorded in the database. Additionally, the database includes the following diagonal and sliding shear friction strengths:

1. Diagonal shear strength, $V_{n,d}$

The wall shear strength corresponding to the strength associated with diagonal tension or compression strut ($V_{n,d}$) is computed from **Eq. 5-1** (ACI 318-19 Equation 18.10.4.1 without restrictions on spacing, reinforcement ratio, and the number of curtains of reinforcement):

$$V_{n,d} = A_{cv}\left(\alpha_c\sqrt{f_c'} + \rho_t f_{yt}\right) \le 10A_{cv}\sqrt{f_c'} \qquad \text{(Eq. 5-1)}$$

Where A_{cv} is the gross area of concrete section bounded by web thickness and wall length (A_{cv}= $t_w l_w$), f'_c is the tested concrete compressive strength, ρ_t is the web transverse (horizontal) reinforcement ratio, f_{yt} is the tested yield strength of the web transverse reinforcement, and α_c is a coefficient that depends on h_w/l_w of the wall. However, walls are generally tested as cantilevers with a single lateral load applied at the top of the wall (with or without axial load) or as panel or partial height walls under a combined effects of lateral load(s), axial load, and bending moment at the top of the panel, and thus h_w/l_w is not always a relevant parameter. Therefore, the test shear-span-ratio (M/Vl_w) was used instead, where α_c is taken as 3.0 for $M/Vl_w \leq 1.5$, as 2.0 for $M/Vl_w \geq 2.0$, and varies linearly between 3.0 and 2.0 for M/Vl_w between 1.5 and 2.0.

2. Sliding shear friction strength at the base, $V_{n,f}$

The wall shear strength corresponding to the shear friction strength at the wall-foundation interface ($V_{n,f}$) is computed from **Eq. 5-2** (ACI 318-19 Equation 22.9.4.2) including the impact of sustained axial load (ACI 318-19 §22.9.4.5):

$$V_{n,f} = \mu\left(A_{vf} f_{yl} + P\right) \leq 0.2 f'_c A_c \qquad \text{(Eq. 5-2)}$$

Where A_{vf} is the area of all reinforcement crossing the wall-foundation interface, f_{yl} is the tested yield strength of the reinforcement crossing the wall-foundation interface, μ is the coefficient of friction and is taken as 0.6 in accordance with ACI 318-19 Table 22.9.4.2, A_c is the area of concrete section resisting shear transfer, and P is the sustained axial load applied during the experiment. It is noted that the upper limit of $800A_c$ given in ACI 318-19 §22.9.4.4 for **Eq. 5-2** was not considered, as it was found to under predict wall shear friction strength, especially for walls with high strength concrete.

To enable classifying walls based on their failure mode, an approach is proposed below and is then used to obtain datasets of flexure- and shear-controlled walls from the database to study wall axial failure.

5.3.2. Failure Mode Classification

The reported failure modes in the database are presented in Fig. 5-8(about 1000 wall tests, excluding walls that failed due to inadequate lap-splices and walls not tested to failure), where V_n is the least shear strength computed from **Eq. 5-1** and **Eq. 5-2**, $V_{@Mn}$ is the wall shear demand corresponding to the development of M_n computed based on the shear-span-ratio used in the test, and $V_{@test}$ is the peak shear strength obtained during the test. Fig. 5-8(***a***) indicates that the vast majority of flexure- and shear-controlled walls have a shear-to-flexure strength ratio ($V_n/V_{@Mn}$) > 1.0 and < 1.0, respectively. Walls with failure modes reported as flexure-shear are mainly scattered between $0.7 < V_n/V_{@Mn} < 1.3$. The flexure-shear-controlled walls with $V_n/V_{@Mn} < 1.0$ generally have limited flexural nonlinearity (i.e., barely experiencing first yield of longitudinal reinforcement) and, therefore, could realistically be classified as shear-controlled walls. On the other hand, for the flexure-shear-controlled walls with $V_n/V_{@Mn} > 1.0$, the behavior is initially governed by flexural cracking and yielding similar to flexure-controlled walls because V_n is initially greater than $V_{@Mn}$, but the wall shear strength gradually reduces, as the wall is cycled through large nonlinear displacement excursions, until it drops below $V_{@Mn}$, and then the wall fails in shear. Depending on the level of shear and flexural demands, these walls could exhibit drift capacities comparable to those of flexure-controlled walls (e.g., Tran and Wallace, 2015). Fig. 5-8(***a***) also reveals that the maximum strength (M_{ult}) obtained during the test for the flexure-controlled walls is approximately 1.15 times the shear corresponding to the development of M_n. A similar conclusion can be observed for shear-controlled walls.

An alternative presentation of failure modes is given in Fig. 5-8(***b***), where the Y-axis is the shear friction strength computed from **Eq. 5-2** ($V_{n,f}$) normalized by the diagonal shear strength from **Eq. 5-1** ($V_{n,d}$). It can be seen that the data are divided between three regions: 1) blue region: flexure-controlled walls with $V_n/V_{@Mn} > 1.0$, 2) red region: diagonal shear-controlled walls (due to failure of diagonal tension or compression strut) with $V_n/V_{@Mn} \leq 1.0$ and $V_{n,f}/V_{n,d} \geq 1.0$, and 3) yellow region: sliding shear-controlled walls with $V_n/V_{@Mn} \leq 1.0$ and $V_{n,f}/V_{n,d} < 1.0$.

Therefore, for the purpose of obtaining datasets to study axial failure, walls with $V_n/V_{@Mn} > 1.0$ and ≤ 1.0 are considered as flexure- and shear-controlled walls, respectively, as presented below.

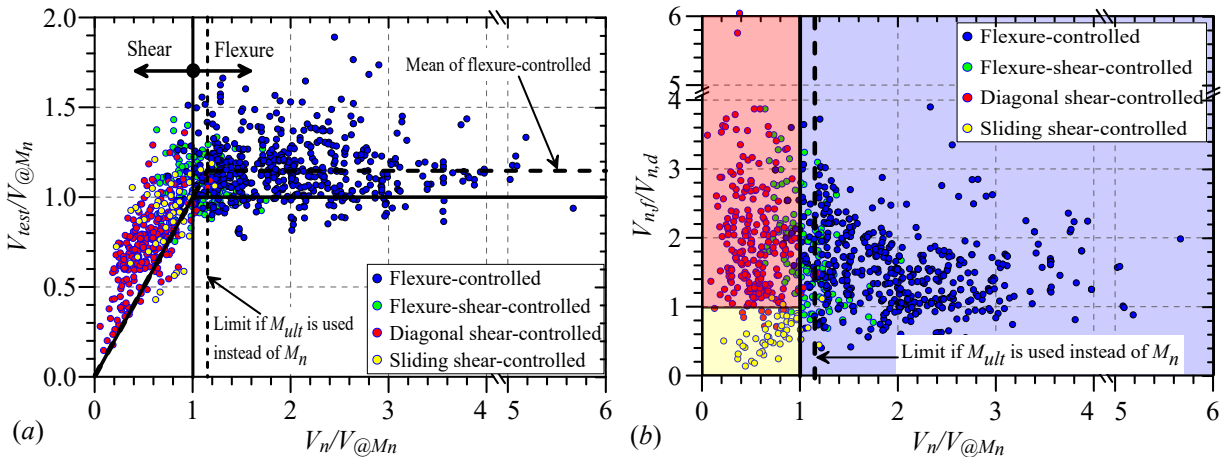

Fig. 5-8–Wall failure modes results from a dataset of 1000 wall tests: (*a*) Shear (diagonal and sliding) versus flexural failure mode; (*b*) Blue region = flexure-controlled; red region = diagonal shear-controlled; and yellow region = sliding shear-controlled.

5.3.3. Datasets of Flexure-Controlled Walls

The following two datasets, for special and ordinary (non-special) flexure-controlled walls, were filtered from the UCLA-RCWalls database:

Special Walls: Design of RC structural walls is currently governed by the requirements of ASCE 7-16 and ACI 318-19, which includes provision for special structural walls with well-detailed special boundary elements (SBE) that satisfy ACI 318-19 §18.10.6.4 for buildings assigned to Seismic Design Category D, E, and F. Detailing requirements for SBEs have changed over the years and are likely to keep change in the future; therefore, the UCLA-RCWalls database was filtered using the following criteria to obtain a dataset of ACI 318-19 code- or nearly code-compliant walls. It is noted that the detailing criteria are less restrictive than the detailing requirements of ACI 318-19 §18.10.6.4:

m) General criteria:
   i. Flexure-controlled walls, i.e., $V_n / V_{@Mn} > 1.0$,
   ii. Walls with different cross-sections were included (i.e., rectangular, barbell, H-shaped, T-shaped, L-Shaped, or half-barbell),
   iii. Walls tested under quasi-static, reversed cyclic loading,
   iv. Tests were excluded if information on axial failure was not available in the database.
   v. Walls with measured concrete compressive strength, $f_c^{'} \geq 3$ ksi,
   vi. Walls with ratio of measured tensile-to-yield strength for boundary longitudinal reinforcement, $f_u / f_y \geq 1.2$, and
   vii. Walls with web thickness, $t_w \geq 3.5$ in.,

n) Detailing criteria:
   i. A minimum of two curtains of web vertical and horizontal reinforcement,
   ii. Boundary longitudinal reinforcement ratio, $\rho_{l,BE}, \geq 6\sqrt{f_c^{'}(\text{psi})} / f_y$,

iii. Min ratio of provided-to-required (per ACI 318-19 §18.10.6.4) area of boundary transverse reinforcement, $A_{sh,provided} / A_{sh,required} \geq 0.7$,

iv. Ratio of vertical spacing of boundary transverse reinforcement to minimum diameter of longitudinal boundary reinforcement, $s/d_b < 8.0$, and

v. Centerline distance between laterally supported boundary longitudinal bars, h_x, between 1.0 in. and 9.0 in.

Based on the above selected filters, a total of 88 wall tests were identified. Histograms for various dataset parameters for the 88 tests are shown in Fig. 5-9, where $P/\left(A_g f_c^{'}\right)$ is the compressive axial load normalized by the measured concrete compressive strength $\left(f_c^{'}\right)$ and gross concrete area $\left(A_g\right)$, and M/Vl_w is the ratio of base moment-to-base shear normalized by wall length $\left(l_w\right)$. A limit of 3 ksi was specified on $f_c^{'}$ in accordance with requirements of ACI 318-19 §18.2.5 for conforming seismic systems. At least two curtains of web reinforcement were specified to be consistent with ACI 318-19 §18.10.2.2. Walls with t_w less than 3.5 in. were not included because use of two curtains of web reinforcement along with realistic concrete cover is not practical in such thin walls. The limit on ratio f_u/f_y is slightly less restrictive than the limit of 1.25 specified in ACI 318-19 §20.2.2.5. The specified limits on $s/d_b \leq 8.0$ and $A_{sh,provided} / A_{sh,required} \geq 0.7$ are slightly less restrictive than the current limits in ACI 318-19 §18.10.6.4 of 6.0 and 1.0, respectively. The limit on $\rho_{long,BE}$ was included to avoid brittle tension failures (Lu et al., 2016), based on what was adopted in ACI 318-19 §18.10.2.4. ACI 318-19 §18.10.6.4e requires $h_{x,max}$ not exceeding the lesser

of 14 in. or 2*b*/3; however, most of the tests in the database were conducted at less than full scale (typically 25 to 50%). Therefore, $h_{x,max}$ for the wall tests should generally be between 3.5 to 7.0 in. for the 14 in. limit. Based on the range of h_x used to filter the data, 95% of the specimens have h_x ≤ 6 in., which is reasonable, whereas the histogram for h_x/b presented in Fig. 5-9(***l***) indicates that a majority of the tests have h_x/b < 3/4, which is only slightly higher than the current limit of h_x/b < 2/3.

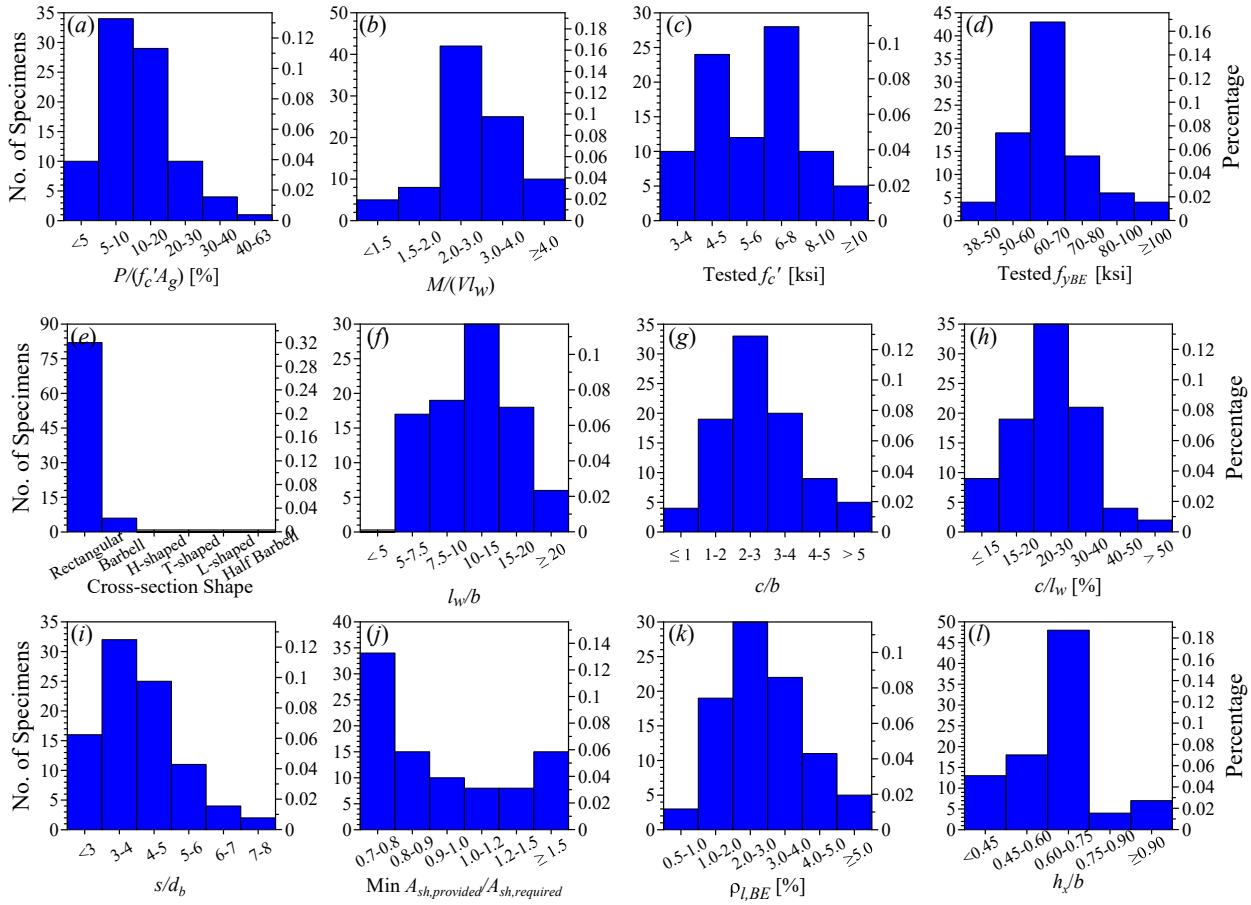

Fig. 5-9–Histograms of the dataset with 88 special, flexure-controlled walls.

Ordinary Walls: Walls with detailing not conforming to Special Structural Wall provisions of ACI 318-19 are common in older constructions designed prior to the establishment of detailing requirements for Special Structural Walls, which were introduced in ACI 318-77 and were updated significantly in ACI 318-83, 318-99, and 318-14. Additionally, the special detailing requirements of ACI 318-19 are relaxed where wall displacements or force demands are low; however, if the boundary longitudinal reinforcement ratio exceeds $400/f_y$ (psi), modest detailing is required by ACI 318-19 §18.10.6.5 (introduced in ACI 318-99 in §21.6.6.5) to prevent bar buckling at smaller deformation demands. These walls are sometimes referred to as walls with Ordinary Boundary Elements, or OBEs (e.g., see NIST 2011). Based on these considerations, the following (a) general and (b) detailing criteria were used to obtain a dataset of "Ordinary Walls":

(a) General criteria:

i. Flexure-controlled walls, i.e., $V_n / V_{@Mn} > 1.0$,

ii. Walls with different cross-sections were included (i.e., rectangular, barbell, H-shaped, T-shaped, L-Shaped, or half-barbell),

iii. Walls tested under quasi-static, reversed cyclic loading, and

iv. Tests were excluded if information on axial failure was not available in the database.

(b) Detailing criteria:

i. Walls with one or more curtains of web vertical and horizontal reinforcement,

ii. Min ratio of provided-to-required (per ACI 318-19 §18.10.6.4) area of boundary transverse reinforcement $A_{sh,provided} \big/ A_{sh,required} < 0.7$, and/or ratio of vertical spacing of boundary transverse reinforcement to minimum diameter of longitudinal boundary reinforcement, $s \big/ d_b \geq 8.0$.

Based on the above selected filters, a total of 68 wall tests were identified. Histograms for various dataset parameters for those 68 tests are shown in Fig. 5-10.

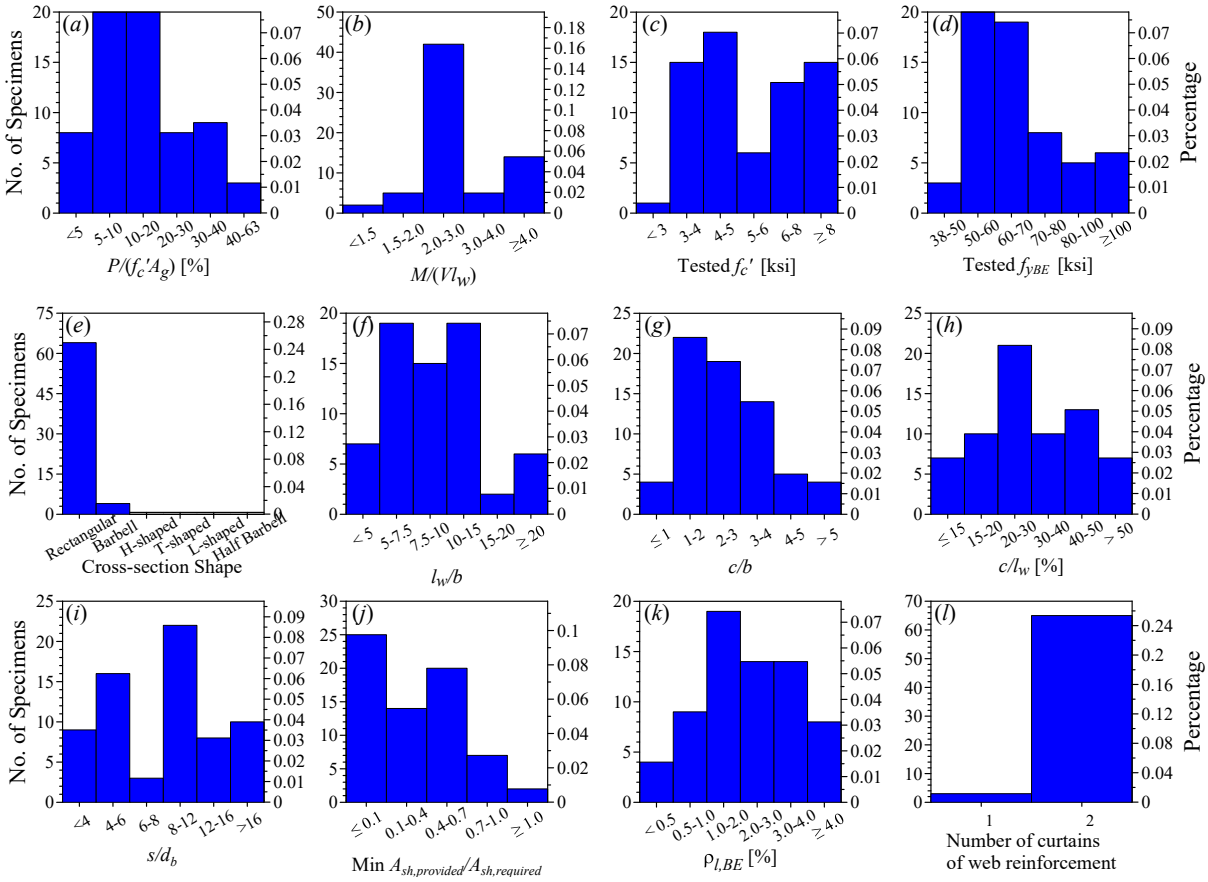

Fig. 5-10–Histograms of the dataset with 68 ordinary, flexure-controlled walls.

5.3.4. Dataset of Shear-Controlled Walls

Similar to flexure-controlled wall, the UCLA-RCWalls database was filtered to obtain a subset of shear-controlled wall or wall pier tests:

(a) Shear-controlled walls, i.e., $V_n / V_{@Mn} \leq 1.0$,

(b) Walls with different cross-sections were included (i.e., rectangular, barbell, H-shaped, T-shaped, L-Shaped, or half-barbell),

(c) Walls tested under quasi-static, reversed cyclic loading, and

(d) Tests were excluded if information on axial failure was not available in the database.

It is noted that no detailing criteria were applied to the dataset. Based on the above selected filters, a total of 53 wall tests were identified, which include a range of parameters (axial load level, geometry, reinforcement), as shown in Fig. 5-11, where ρ_l and ρ_t are the web vertical and horizontal reinforcement ratios, respectively, and f_{yt} is tested yield strength of the web horizontal reinforcement.

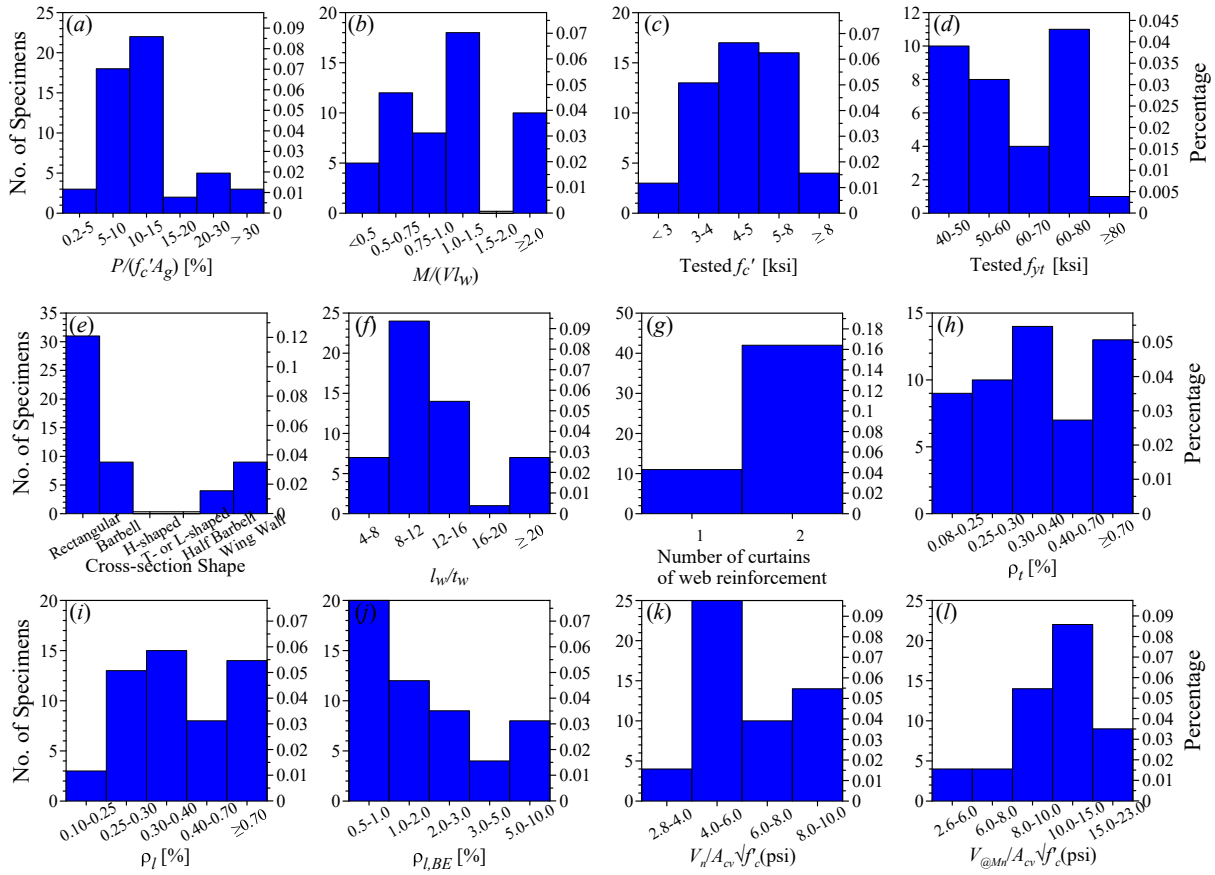

Fig. 5-11–Histograms of the dataset of 53 shear-controlled wall/pier tests.

5.4. Axial Failure of Flexure-Controlled Walls

5.4.1. Special Walls

Abdullah and Wallace (2019) studied the drift capacity at 20% lateral strength loss of flexure-controlled walls with special boundary elements (SEBs) and found that drift capacity is primarily a function of: (1) ratio of wall neutral axis depth-to-width of the flexural compression zone, c / b, where c is computed for an extreme fiber concrete compressive strain of 0.003, (2) ratio of the wall length-to-width of the flexural compression zone, l_w / b, (3) ratio of the maximum wall shear stress, $v_{max} / \sqrt{f_c'}$, and (4) the configuration of the boundary transverse reinforcement used, e.g., use of

overlapping hoops versus a single perimeter hoop with intermediate crossties. They also found that a combined slenderness parameter, $\lambda_b = (l_w / b)(c / b) = l_w c / b^2$, provides an efficient means to account for the slenderness of the cross section (l_w / b) and the slenderness of the flexural compression zone of the cross section (c / b). In addition to wall cross-section geometry, this parameter, through depth of neutral axis (c), considers the impact of concrete and reinforcement material strengths, axial load, and quantities and distributions of longitudinal reinforcement at the wall boundaries and in the web (Wallace, 1994).

The reduced subset of 88 flexure-controlled special walls described in Fig. 5-9 was studied to identify parameters that primarily influence lateral drift capacity at axial failure. The results showed that, similar to drift capacity at 20% lateral strength loss, $\lambda_b = l_w c / b^2$ significantly influences drift capacity at axial failure, with a correlation coefficient (R) of 0.70, as shown in Fig. 5-12, with drift capacity varying on average between 1.5 and 4.0% as λ_b reduces from 100 to zero.

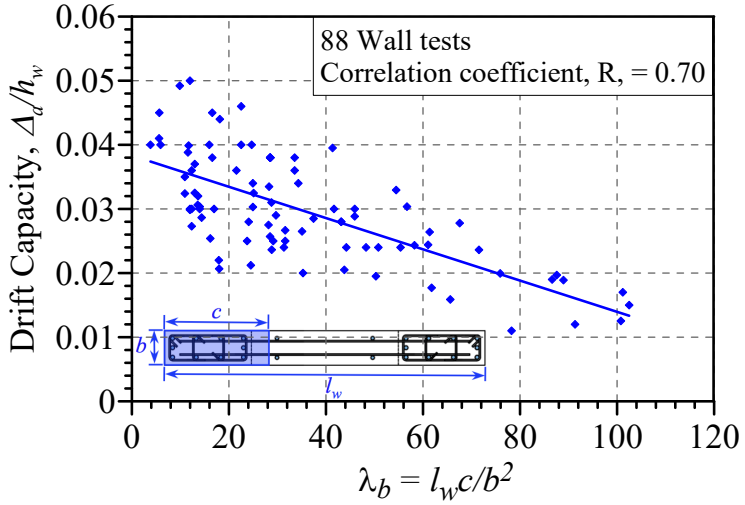

Fig. 5-12–Variation of wall drift capacity at axial failure versus λ_b for special walls.

Additionally, although the axial load is included in the $\lambda_b = l_w c / b^2$ parameter through depth of neutral axis, *c*, it was found that the level of axial load has a significant impact on post-strength loss deformation capacity, as shown in Fig. 5-13. This is because, once strength degradation initiates, the level of axial load accelerates the rate of deterioration such that walls with high $P / A_g f_c'$ have a steep post-peak slope on the backbone relation shown in Fig. 5-1, where little to no additional deformation capacity beyond the *Ultimate* point is achieved prior to axial failure (i.e., no residual strength plateau). Insufficient data existed to evaluate the impact of using overlapping hoops in the boundary elements, as opposed to a single perimeter hoop with crossties, on drift capacity at axial failure. Segura and Wallace (2018a) reported that providing lateral restraint in the form of crossties for the web longitudinal reinforcement in the plastic hinge region increased the rotation capacity at axial failure; however, tests on walls with such detailing are rare and would not allow statistical analysis. Further data are needed to help explain the role of detailing variables (e.g., overlapping hoops versus a perimeter hoops with crossties in the boundary elements and lateral restraint in the form of 135º-135º crossties in the web) and loading protocol (i.e., number of cycles) on deformation capacity at axial failure.

Linear regression analyses performed on the dataset of 88 special walls, including λ_b and $P / A_g f_c'$ as predictor variables, resulted in the following predictive equation for mean drift capacity at axial failure (Δ_a / h_w):

$$\frac{\Delta_a}{h_w}(\%) = 4.10 - \left(\frac{l_w c}{40 b^2}\right) - \left(2.5\frac{P}{A_g f_c'}\right) \geq 1.5\% \qquad \text{(Eq. 5-3)}$$

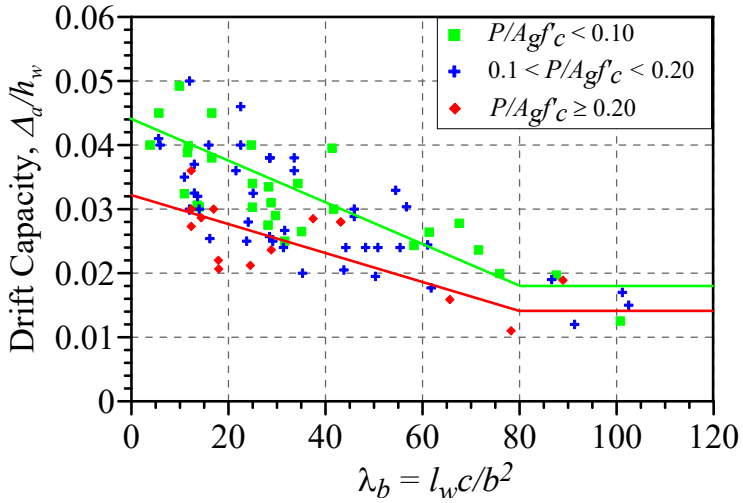

Fig. 5-13–Variation of wall drift capacity at axial failure as a function of including λ_b and $P / A_g f'_c$ for special walls.

The drift capacities predicted with **Eq. 5-3** are compared with experimental drift capacities for the dataset of 88 special walls in Fig. 5-14. The mean of ratios of predicted-to-experimental values, standard deviation (STDV), and coefficient of variation (COV) are 1.03, 0.20, and 0.19, respectively, over the entire range of drift values, from roughly 1.5 to 4.5% drift.

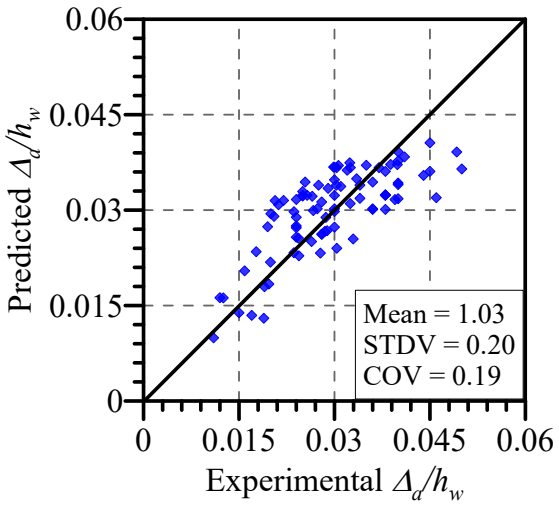

Fig. 5-14–Comparison of predicted drift capacities (**Eq. 5-3**) with experimental drift capacities.

5.4.2. Ordinary Walls

After studying the reduced dataset of ordinary walls (Fig. 5-10), it was found that, similar to special walls, $\lambda_b = l_w c / b^2$ and $P / A_g f_c'$ significantly influence drift capacity at axial failure. Fig. 5-15 shows the variation of drift capacity at axial failure as a function of $\lambda_b = l_w c/b^2$ and $P/A_g f_c'$ for the dataset of 68 ordinary walls. The trends of Fig. 5-15 are generally similar to those of Fig. 5-13, with two main differences. First, at low values of $\lambda_b = l_w c/b^2$, the drift capacity values of the ordinary walls are lower than those of special walls by about 0.01 drift, which highlights the impact of special detailing on the performance of structural walls. Second, the slope of the trends of Fig. 5-15 are steeper than those of Fig. 5-13. This is likely because an increase in value of $\lambda_b = l_w c/b^2$ means an increase in compression demands, and having more compression demands in such walls means faster deterioration of both lateral and axial strength due to lack of proper detailing to restrain bar buckling and prevent concrete curushing.

Application of linear regression analyses for the dataset of 68 ordinary wall tests, including $\lambda_b = l_w c/b^2$ and $P/A_g f_c'$ as variables that significantly impact lateral drift capacity, resulted in the following predictive equation for drift capacity at axial failure:

$$\frac{\Delta_a}{h_w}(\%) = 3.65 - \left(\frac{l_w c}{30 b^2}\right) - \left(3.5\frac{P}{A_g f_c'}\right) \geq 0.8\% \qquad \text{(Eq. 5-4)}$$

Comparison of predicted drift capacities from **Eq. 5-4** with experimentally obtained drift capacities at axial failure from the dataset of 68 ordinary walls results in a mean of 1.01 and COV of 0.20 (Fig. 5-16).

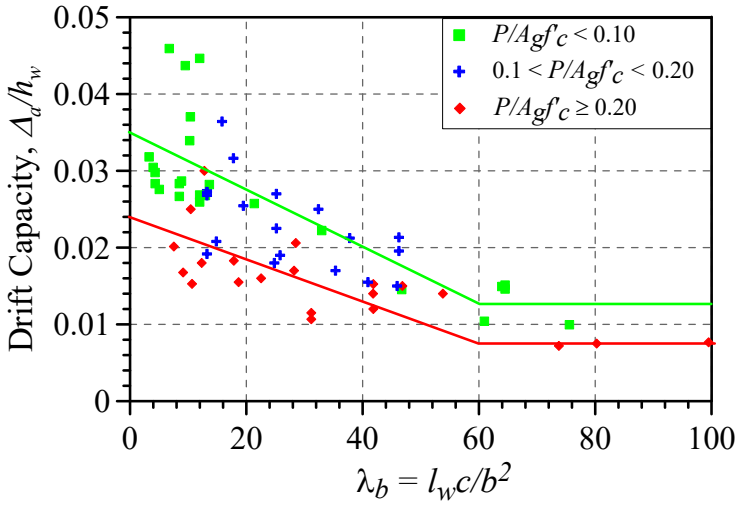

Fig. 5-15–Variation of drift capacity at axial failure as a function of λ_b and $P / A_g f'_c$ for ordinary walls.

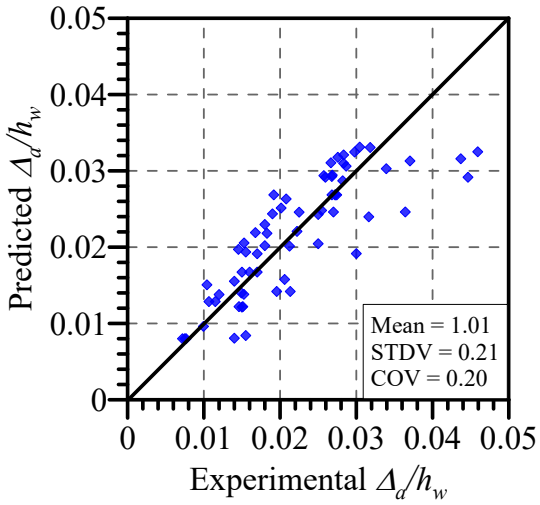

Fig. 5-16–Comparison of predicted drift capacities (**Eq. 5-4**) with experimental drift capacities.

For walls with asymmetric cross-sections, such as T-shaped, L-shaped, and half-barbell cross-sections (Fig. 5-17), the drift capacity should be evaluated for both directions of loading (i.e., flange/barbell in compression and web in compression), and the larger drift value should be used to assess axial failure. This is because, for cases that result in a large ***b***, e.g., where the

barbell or flange of the wall is in compression (low λ_b), drift capacity is relatively large (Abdullah and Wallace, 2019). Additionally, it is unlikely that these walls lose axial load capacity since tests observations have shown that, although the web experiences extensive damage, the flange or the barbell remains mostly intact (unless it is subjected to a bi-directional loading) and thus could carry the axial load (Fig. 5-18).

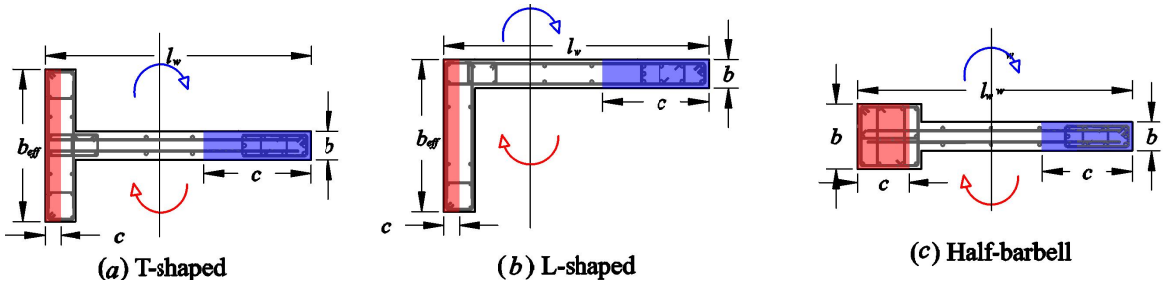

(*a*) T-shaped (*b*) L-shaped (*c*) Half-barbell

Fig. 5-17–Asymmetric wall cross-sections.

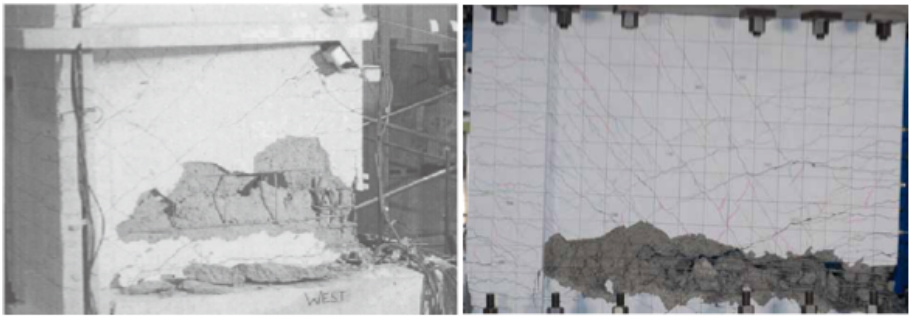

(*a*) T-shaped (Thomson & Wallace, 1995) (*b*) Half-barbell (Takahashi et al., 2013)

Fig. 5-18–Damage in walls tests with flanged and barbell shaped cross-sections.

5.5. Axial Failure of Shear-Controlled Walls and Piers

5.5.1. Shear Friction Model - Background

Research conducted by Elwood and Moehle (2005) suggested that the axial load-carrying capacity of shear-controlled RC columns can be investigated using a shear friction model, where the axial load supported by a column must be transferred across a diagonal crack through shear friction. Wallace et al. (2008) extended the model by Elwood and Moehle (2005) to investigate the axial failure of shear-controlled wall piers, where the critical crack is assumed to extend diagonally over the clear height of the pier (Fig. 5-19), and the axial failure is assumed to result from sliding along the critical crack plane when the shear friction demand exceeds the shear friction capacity. Using vertical and horizontal equilibrium for the free body diagram in Fig. 5-19 and the classical shear friction model of ACI 318 (i.e., $V_{sf} = \mu N$), they developed the following model for axial capacity of shear-controlled walls and wall piers (**Eq. 5-5**). Further details of formulation of **Eq. 5-5** can be found in Wallace et al. (2008).

$$P = \left(\frac{A_{st} f_{yt} h}{s_v} - V_r \right) \left(\frac{1 + \mu_m \tan\theta}{\tan\theta - \mu_m} \right) \qquad \text{(Eq. 5-5)}$$

Where P is the axial load demand on the wall, $A_{st} f_{yt}$ is the force developed in the web horizontal bars crossing the critical crack (Fig. 5-19), s_v is the vertical spacing of the horizontal web bars, V_r is the residual lateral shear resistance at the onset of axial failure, h is the height over which the diagonal crack extends, $\theta$is the angle of the critical crack relative to the horizontal plane, and μ_m is the coefficient of friction which includes aggregate interlock and reinforcement dowel action.

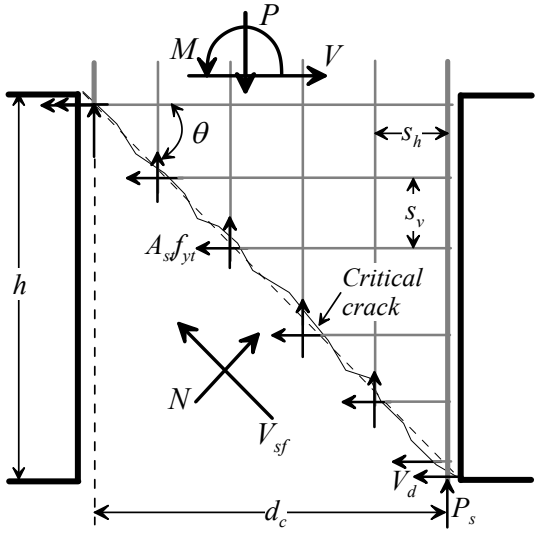

Fig. 5-19–Free body diagram of a cracked wall pier.

By rearranging **Eq. 5-5**, the coefficient of friction can be calculated as

$$\mu_m = \frac{P - \frac{A_{st} f_{yt} h}{s_v} \frac{1}{\tan\theta} + \frac{V_r}{\tan\theta}}{\frac{P}{\tan\theta} + \frac{A_{st} f_{yt} h}{s_v} - V_r} \qquad \text{(Eq. 5-6)}$$

For columns, Elwood and Moehle (2005) and Wallace et al. (2008) were able to develop a relationship between μ_m determined from **Eq. 5-6** and observed drift capacity at axial failure based on limited sets of test data of shear- and flexure-shear-controlled columns. The data revealed that μ_m decreases as the drift ratio at axial failure increases, which makes sense, and that the relationship can be captured by a linear fit in the form of **Eq. 5-7**:

$$\mu_m = C_1 - C_2 \left(\frac{\Delta_a}{h} \right) \geq 0 \qquad \text{(Eq. 5-7)}$$

Where Δ_a / h is the lateral drift ratio at axial failure, and the coefficients C_1 and C_2 define the intercept (shear friction coefficient at zero drift ratio) and slope (reduction in shear friction

coefficient due to increase in lateral drift) of the trend. Substitution of **Eq. 5-7** into **Eq. 5-5**, and rearranging, results in the following general expression for drift capacity at axial failure:

$$\frac{\Delta_a}{h_w} = \frac{\left(1 + C_1 \tan\theta\right) + \left(P / C_3\right)\left(C_1 - \tan\theta\right)}{C_2\left(P / C_3 + \tan\theta\right)} \qquad \text{(Eq. 5-8)}$$

In which

$$C_3 = \frac{A_{st} f_{yt} h_w}{s_v} - V_r \qquad \text{(Eq. 5-9)}$$

Due to the lack of experimental data of walls, Wallace et al. (2008) used results from Elwood and Moehle (2005) and additional column test data to propose values for C_1 and C_2 (i.e., $C_1 = 1.6$ and $C_2 = 30$ or 50). The proposed values produced relatively high estimates of lateral drift capacity at axial failure, in the range of 0.03 to 0.10, for shear-controlled walls and wall piers, suggesting that axial failure is unlikely. Therefore, the following section provides a more detailed assessment of the model and its assumptions using experimental data of wall and pier tests described in Fig. 5-11.

5.5.2. Shear Friction Model – Calibration and Validation

In the following section, the experimental results from the dataset of shear-controlled walls described in Fig. 5-11 are used to provide a more detailed assessment of the shear friction model, particularly with respect to the relation used for shear friction versus lateral drift capacity, as well as critical crack angle and residual lateral strength. The dataset includes 28 walls with diagonal tension failure (with no flexural yielding), 17 walls with diagonal compression failure (or web crushing with no flexural yielding), and eight walls with flexure-shear failures (flexural yielding prior to diagonal shear failure), six of which are Japanese wing wall tests (i.e., large and generally well detailed columns with thin wing walls on one or both side of the column, e.g., see Kabeyasawa

et al., 2008). Walls that fail in sliding shear at the base typically have no or low axial loads and low longitudinal reinforcement ratios, and they tend to slide along the shear plane at the base, leading to sequential fracture of some of the longitudinal bars crossing the shear plane (Ramarozatovo et al., 2016), while the wall portion above the shear plane remains relatively intact; therefore, axial failure is unlikely. Therefore, axial failure of shear-friction-controlled walls is not addressed in this study.

Review of the results of the dataset of 53 shear-controlled walls revealed the following three major observations:

Critical diagonal crack: The critical diagonal crack generally extends diagonally over the clear height of the wall or pier when aspect ratio (h_w/l_w) is equal to, or smaller than, 1.5 (i.e., crack angle $\theta \leq 56^o$), especially for diagonal tension-controlled walls, which is consistent with post-earthquake reconnaissance observations [e.g., Fig. 5-20(***a***) and (***b***)]. However, for walls with h_w/l_w greater than 1.5, experimental evidence indicates that the critical crack extends diagonally over a height that is approximately 1.5 times the wall length, i.e., $\theta \approx 56^o$ [e.g., Fig. 5-20(***c***) and (***d***)]. Therefore, the critical crack angle is limited to be less than, or equal to, 56º.

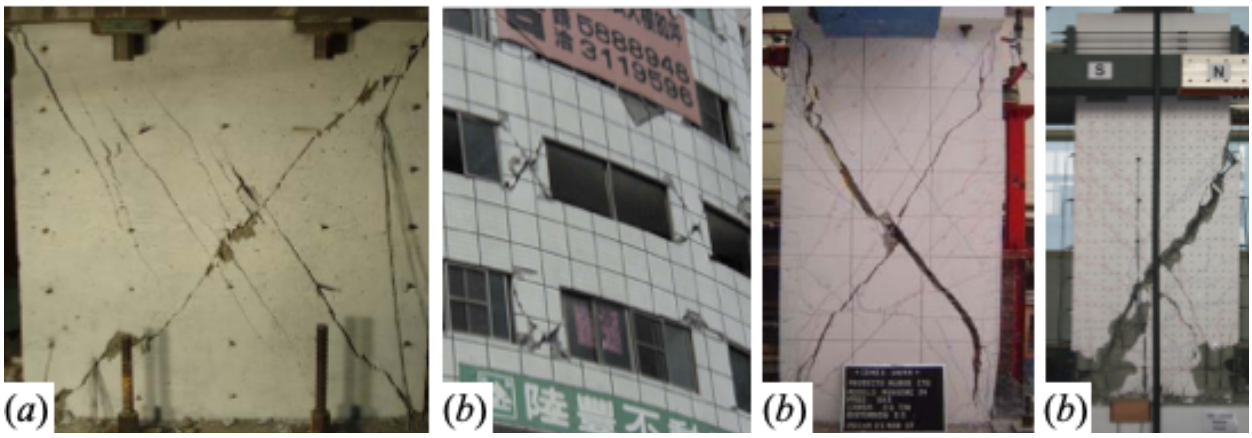

Fig. 5-20–Angle of critical diagonal shear cracks observed from experimental tests and earthquake reconnaissance: (*a*) Pier tests by Massone (2006); (*b*) Five-story building in Dungshr, Taiwan, after 1999 Chi-Chi Earthquake (Wallace et al., 2008); (*c*) Wall test by Flores (2007); (*d*) Wall test by Bimschas (2010).

Residual lateral shear resistance (V_r): When axial failure occurs, the residual lateral shear resistance (V_r) typically is close to zero (only three out of the 53 wall tests in the dataset showed residual lateral strength, ranging from 10% to 30% of the nominal shear strength, V_n). Wallace et al. (2008) performed sensitivity analyses to highlight the impact of residual lateral strength on drift capacity at axial failure and observed that lateral drift ratios are reduced modestly where V_r is taken as $0.2V_n$, as opposed to no residual strength. Although in the results presented herein the residual lateral resistance is taken as zero, consideration of residual shear strength of equal to 10 or 20% of V_n for walls with low axial loads (e.g., $< 0.05 A_g f'_c$) would introduce a modest level of conservatism in the results predicted using the shear friction model.

Coefficient of friction (μ_m): Similar to columns, μ_m calculated using **Eq. 5-6** correlates well with Δ_a / h and failure mode. Fig. 5-21 presents the relationship between μ_m and the observed Δ_a / h for the different failure modes and Fig. 5-21(***a***) and Fig. 5-21(***b***) show linear and logarithmic trends fitted to the data, respectively. Fig. 5-21(***a***) reveals that C_1 is about 1.1 for walls with diagonal tension and flexure-shear failure modes and 0.70 for walls with diagonal compression failure mode, that the trends for the diagonal tensions- and compression-controlled walls have the same slope (i.e., C_2= 40), and that the trend for the flexure-shear-controlled walls has a significantly smaller slope (i.e., C_2= 8). Alternatively, the logarithmic trends shown in Fig. 5-21(***b***) can be used, which result in higher shear friction coefficients at zero or near zero drift ratios. However, axial failure at drift ratios smaller than 0.5% might be unlikely, as it is less than the lateral drift ratio

corresponding to yield. Therefore, for ease of implementation of μ_m in **Eq. 5-8**, the shear friction variables (C_1 and C_2) associated with the linear trends are selected, as shown in Table 5-1. It should be noted that relatively few tests are available to derive the relationship between μ_m and Δ_a / h for flexure-shear-controlled walls, and most of the test results are from tests of wing walls. The resulting trend line shown in Fig. 5-21 for this case is very flat and would produce significant estimates of drift capacity. This result is shown for completeness; however, the author does not recommend using this trend until additional data are available to sufficiently validate the model.

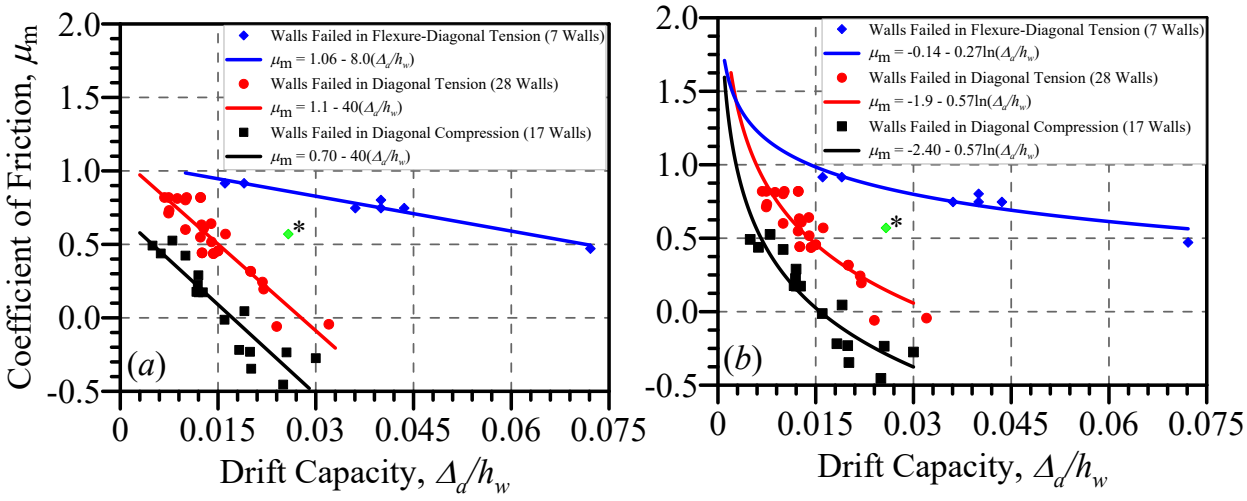

Fig. 5-21–Shear friction relations derived from wall tests: (*a*) linear fits to data; (*b*) logarithmic fits to data. (* the green diamond-shaped data point is a wall with only a slight yielding of longitudinal bars)

Table 5-1. Shear friction variable in **Eq. 5-4**

Expected failure mode[a]	C_1	C_2
Diagonal tension	1.1	40
Diagonal compression	0.70	40
Flexure-shear	1.1	8

[a]the limited data presented here suggests that shear-controlled walls with can be assumed as diagonal-compression-controlled.

The drift capacities (Δ_a/h_w) predicted with **Eq. 5-8** using the variables given in Table 5-1 are compared with the experimental drift capacities of the 53-test dataset in Fig. 5-22. The mean of ratios of predicted-to-experimental values, STDV, and COV are 1.00, 0.19, and 0.19, respectively, over the entire range of drift values, from roughly 0.005 to 0.70 drift.

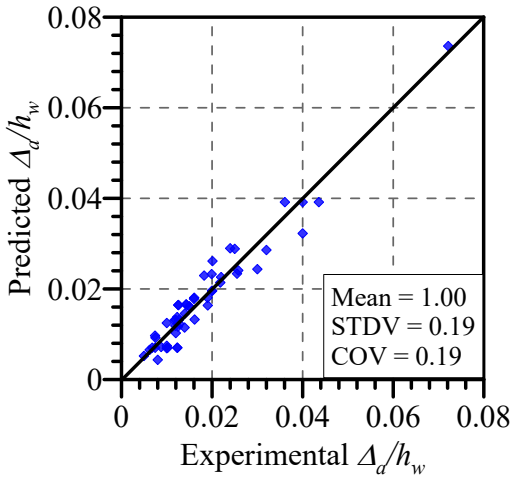

Fig. 5-22–Comparison of predicted drift capacities (**Eq. 5-8**) with experimental drift capacities.

5.5.3. Simplified Model

For the purpose of preliminary analysis, a simplified drift capacity model is developed that is only a function of axial load ratio. Axial load is one of the primary terms in the shear friction model (**Eq. 5-8**) and is used to assess the drift capacity of shear-controlled walls in ASCE 41-17. The observed drift capacities at axial failure of the wall tests are plotted against $P / A_g f_c'$ in Fig. 5-23,

along with logarithmic trend lines fitted to the data. Trend lines shown in Fig. 5-23 for walls with diagonal tension and compression failure modes are only slightly different, and there is a significant scatter in the data for walls with flexure-shear failure modes. It is noted that there are only seven data points with flexure-shear failure modes, five which are wing walls; therefore, the data for wing walls are not considered.

Extrapolating the trends in Fig. 5-23 indicates that drift capacity reaches about zero at $P/A_g f_c^{'}$ of approximately 0.85 (i.e., axial stress of ~ 0.85 $f_c^{'}$), which is commonly used as the maximum pure axial compression strength of compression members (ACI 318-19), ignoring the presence of the longitudinal reinforcement.

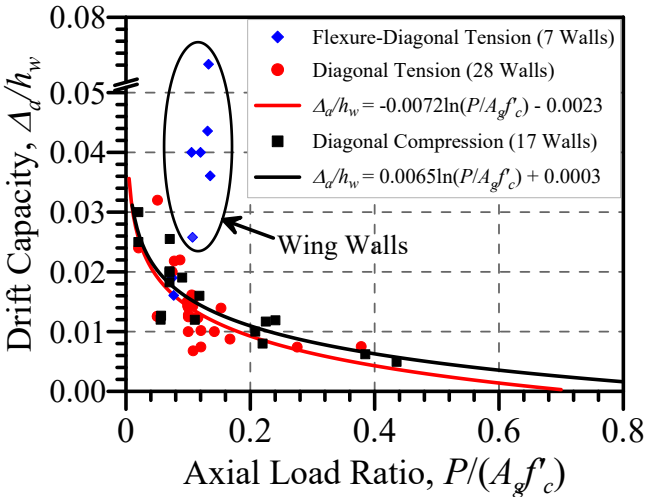

Fig. 5-23–Drift capacity of shear-controlled walls as a function of $P/A_g f_c^{'}$.

An average logarithmic fit through the data results in the following predictive equation for Δ_a/h_w of shear-controlled walls and piers (**Eq. 5-10**):

$$\frac{\Delta_a}{h_w} = -0.006 \ln\left(P/A_g f_c^{'}\right) \qquad \text{(Eq. 5-10)}$$

The drift capacities predicted with **Eq. 5-10** are compared with experimental drift capacities in Fig. 5-24 for the walls with diagonal tension or compression failures. The mean of ratios of predicted-to-experimental values, STDV, and COV are 1.00, 0.28, and 0.28, respectively. It is noted that the dispersion of the simplified model is significantly higher than that of the shear friction model, which explains the role of other parameters on drift capacity.

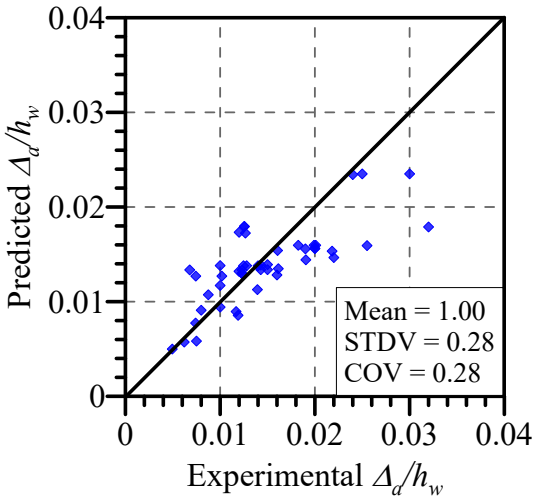

Fig. 5-24–Comparison of predicted drift capacities (**Eq. 5-10**) with experimental drift capacities.

5.6. Walls with Spirally Reinforced Columns

Use of walls with barbell shaped cross-sections (i.e., walls with a thin web and large columns at boundary regions) was common in low- to medium-rise concrete buildings till late 1980s, where the boundary columns were typically reinforced with spiral transverse reinforcement spaced at, or smaller than, 3 in. center-to-center (Wang et al., 1975). Post-earthquake reconnaissance observations (e.g., 1971 San Fernando earthquake) has revealed that columns reinforced with closely spaced spiral reinforcement performed significantly better than columns with non-spiral transverse reinforcement. Although test results of axial failure of walls with spirally reinforced

boundary columns are not available in the database, it is plausible that such walls have greater drift capacities than walls reinforced with non-spirally reinforced boundary columns or non-barbell shaped walls, and that use of expressions proposed earlier for such walls might result in conservative drift values for axial failure. Nonetheless, to provide some insight into performance of these walls, the UCLA-RCWalls database was searched, and subsets of 11 and 19 flexure- and shear-controlled wall tests were identified, respectively. As noted, one key limitation of these tests, which were mostly conducted in 1990s or earlier, is that they are not tested to axial failure (and in some cases, only modest lateral strength degradation).

5.6.1. Flexure-Controlled Walls

Review of test results and damage of the 11 flexure-controlled walls revealed that at lateral strength loss the damage in most cases included concrete cover spalling of the boundary columns and concrete crushing in the web next to the columns [Fig. 5-25(***a***)], and in rare cases bar fracture (fatigue) and concrete crushing in the column cores. This is consistent with post-earthquake reconnaissance observations of columns reinforced with closely spaced spirals (e.g., 1971 San Fernando earthquake). Fig. 5-25(***b***) shows that the drift capacities at ~ 20% lateral strength loss of these 11 wall tests, which ranges from 2.7 to 5.0% on average (green dots), are comparable with the trends of Fig. 5-13 (i.e., drift capacities at axial failure of special walls with no spirally reinforced columns). This is because the closely spaced spirals prevent early strength degradation due to bar buckling and concrete core crushing. It is also noted that since the width of flexural compression zone, *b*, is relatively large for these walls, λ_b for these 11 tests is equal, or smaller, than 15. Abdullah and Wallace (2019) found that walls that have $\lambda_b < 20$ can exhibit moderate to significant post-20% strength loss deformation capacity. Therefore, there is a potential for these 11 tests to develop moderate-to-significant additional drift capacities prior to axial failure.

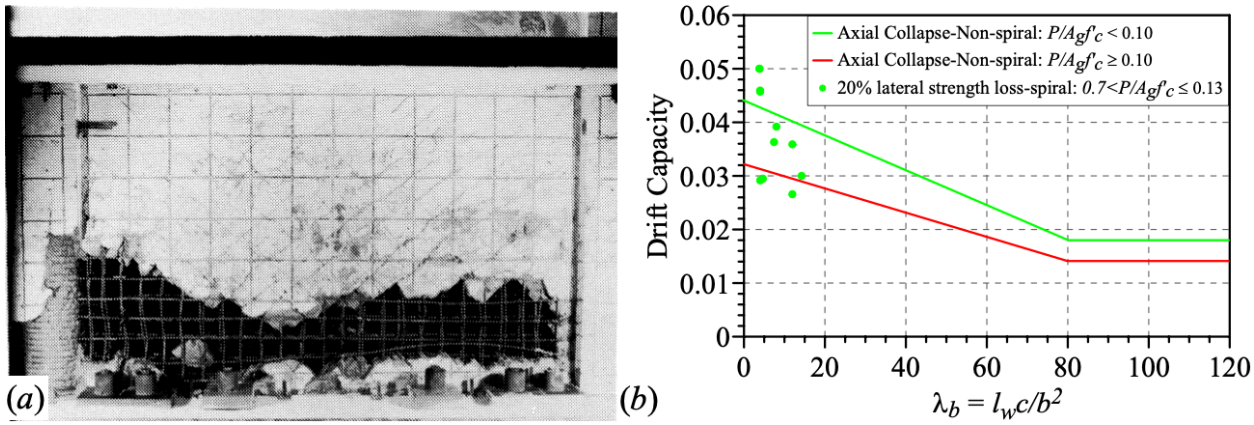

Fig. 5-25–Test results of flexure-controlled walls with spiral transverse reinforcement in the boundary columns: (*a*) Damage of a wall tests by Wang et al. (1975) (*b*) Comparison of drift capacity of walls with spirally- vs non-spirally reinforced columns.

5.6.2. Shear-Controlled Walls

For the 28 shear-controlled walls, the test results showed that the damage at lateral strength loss generally includes crushing concrete in the thinner web and in some cases spalling concrete cover of the columns, as seen in Fig. 5-26(***a***). However, the core of the boundary columns appears to be mostly intact and can, therefore, resist axial load. After the web is crushed, it is possible that the wall becomes flexible and can deform significantly before the columns fail in a sliding shear failure mode along the crushed plane. Fig. 26(***b***) compares drift capacities of the 28 tests at either peak strength or 20% lateral strength loss with drift capacities at axial failure of the walls shown in Fig. 5-23. This figure shows that it is plausible that walls with spirally reinforced columns have larger drift capacities than those predicted by the shear friction or simplified model presented earlier. Furthermore, tests results reported by Nakachi et al. (1992) revealed that providing confinement

in the form of crossties or closed hoops in the web of barbell-shaped walls results in significantly increased drift capacity.

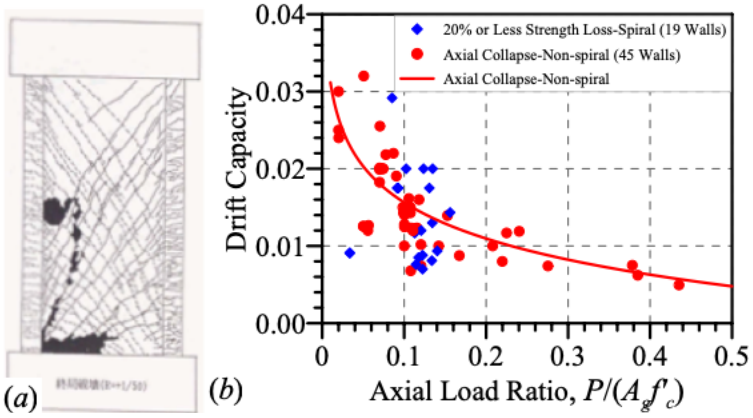

Fig. 5-26–Test results of shear-controlled walls with spiral transverse reinforcement in the boundary columns: (*a*) Damage of a wall tests by Kabeyasawa and Matsumoto (1992), and (*b*) Comparison of drift capacity of walls with spirally- vs non-spirally reinforced columns.

5.7. Conclusions and Recommendations

A comprehensive wall database, UCLA-RCWalls, that includes detailed information on more than 1100 tests reported in the literature was utilized to develop an approach to determine the expected failure mode for RC structural walls and study axial failure of shear- and flexure-controlled walls. Based on the findings of this study, the following conclusions and recommendations are made:

1. Analysis of reported failure modes of about 1000 wall tests indicated that the flexure- and shear-controlled walls have a shear-to-flexure strength ratio ($V_n/V_{@Mn}$) > 1.0 and < 1.0, respectively, whereas walls with failure modes reported as flexure-shear are mainly scattered between $0.7 < V_n/V_{@Mn} < 1.3$.

2. Displacement capacity at axial failure of flexure-controlled special structural walls that generally satisfy the detailing requirements of ACI 318-14, §18.10.6.4, is primarily a function of $\lambda_b = l_w c / b^2$ and $P / A_g f_c^{'}$. Depending on these variables, the lateral drift capacity can be as low as 1.2% and as high as 5.0%. Although the axial load is indirectly included in the $\lambda_b = l_w c / b^2$ parameter through depth of neutral axis, *c*, it was found that the level of axial load has a significant impact on post-lateral strength loss deformation capacity. This is because, once strength degradation initiates, the level of axial load accelerates the rate of deterioration such that walls with high $P / A_g f_c'$ have a steep post-peak slope on the backbone relation, where little to no additional deformation capacity beyond the deformation at initiation of lateral strength loss is achieved prior to axial failure (i.e., no residual strength plateau), which is consistent with observations from column tests.
3. Similar to special walls, it was found that $\lambda_b = l_w c / b^2$ and $P / A_g f_c'$ significantly influenced drift capacity at axial failure for flexure-controlled ordinary walls. At low values of $\lambda_b = l_w c / b^2$, the drift capacity values of the ordinary walls are lower than those of special walls by about 0.01 drift, which highlights the impact of special detailing on the performance of structural walls.
4. Drift capacity equations that depends on $\lambda_b = l_w c / b^2$ and $P / A_g f_c'$ were developed to predicts the lateral drift capacity of flexure-controlled walls with special and ordinary detailing, with mean and coefficient of variation of approximately 1.0 and 0.20, respectively.
5. For flexure-controlled walls with asymmetric cross-sections such as T-shaped, L-shaped, and half-barbell cross-sections, drift capacity at axial failure is controlled by the case where the barbell or flange of the wall is in compression (low λ_b). Additionally, it is unlikely that these

walls lose axial load capacity since tests observations have shown that, although the web experiences extensive damage, the flange or the barbell remains mostly intact (unless it is subjected to a bi-directional loading) and thus could carry the axial load.

6. Further data are needed to help explain the role of detailing variables (e.g., overlapping hoops versus a perimeter hoops with crossties in the boundary elements and lateral restraint in the form of 135º-135º crossties in the web) and loading protocol (i.e., number of cycles) on deformation capacity at axial failure for flexure-controlled walls.
7. Review of the results of the dataset of 53 shear-controlled walls revealed that the critical diagonal crack generally extends diagonally over the clear height of the wall or pier when $h_w/l_w \leq 1.5$ (i.e., crack angle $\theta \leq 56º$), which is consistent with post-earthquake reconnaissance observations. However, for walls with h_w/l_w greater than 1.5, experimental evidence indicates the critical crack angle be limited to $\leq 56º$.
8. Similar to columns, coefficient of friction (μ_m) calculated using **Eq. 5-6** correlates well with drift capacity at axial failure (Δ_a / h) and failure mode. Results from the dataset of 53 shear-controlled walls were used to derive relations between μ_m and Δ_a / h for walls controlled by diagonal tension or compression to use in the shear friction model developed by Wallace et al. (2008). Relatively few tests were available to derive the relationship between μ_m and Δ_a / h for flexure-shear-controlled walls, and most of the test results were from tests of wing walls. The resulting trend line shown in Fig. 5-21 for this case is very flat and would produce significant estimates of drift capacity. This result is shown for completeness; however, the authors do not recommend using this trend until additional data are available to sufficiently validate the model.

9. Although the results presented in this study for shear-controlled walls indicated that when axial failure occurs, the residual lateral shear resistance typically is close to zero, consideration of residual shear strength of equal to 10 or 20% of nominal shear strength for walls with low axial loads (e.g., $< 0.05A_g f'_c$) would introduce a modest level of conservatism in the results predicted using the shear friction model.
10. Lastly, given that the study is based on test results for individual walls, the predictive expressions do not take into account the impact of gravity load redistribution and torsional irregularity on potential for axial failure of the wall and the building. The lack of test data on complete buildings, either laboratory or in earthquakes, limits these studies.

5.8. Acknowledgements

Funding for this study was provided, in part, by the National Science Foundation Grant CMMI-144642, which focused on promoting and enhancing US and international collaboration on performance assessment of structural wall systems, and ATC Project 78, and the University of California, Los Angeles. The authors would also like to thank members of ATC 78 Project for providing thoughtful comments on the proposed approach. Any opinions, findings, and conclusions or recommendations expressed in this paper are those of the authors and do not necessarily reflect the views of others mentioned here.

5.9. References

Abdullah, S. A., and Wallace, J. W. (2018). "UCLA-RCWalls database for reinforced concrete structural walls." *Proceedings, 11th National Conference in Earthquake Engineering*, Earthquake Engineering Research Institute, June 25-29, Los Angeles, CA.

Abdullah S. A., and Wallace J. W. (2019). "Drift capacity of RC structural walls with special boundary elements." *ACI Structural Journal*, 116(1), 183–194.

ACI (American Concrete Institute). (2019). "Building code requirements for structural concrete." *ACI 318-19*, Farmington Hills, MI, 623 pp.

ACI (American Concrete Institute). (2014). "Building code requirements for structural concrete." *ACI 318-14*, Farmington Hills, MI, 519 pp.

ACI (American Concrete Institute). (1999). "Building code requirements for structural concrete." *ACI 318- 99*, Detroit, MI, 391 pp.

ACI (American Concrete Institute). (1983). "Building code requirements for reinforced concrete." *ACI 318-83*, Detroit, MI, 155 pp.

ACI (American Concrete Institute). (2017). "Standard requirements for seismic evaluation and retrofit of existing concrete buildings." *ACI 369.1-17,* Farmington Hills, MI, 110 pp.

ASCE (American Society of Civil Engineers). (2017). "Seismic evaluation and retrofit of existing buildings." *ASCE/SEI 41-17*, Reston, VA, 576 pp.

ASCE (American Society of Civil Engineers). (2016). "Minimum design loads for buildings and other structures." *ASCE/SEI 7-16,* Reston, VA, 690 pp.

Bimschas, M. (2010). "Displacement based seismic assessment of existing bridges in regions of moderate seismicity." PhD dissertation, ETH Zurich, Zürich, Switzerland.

Dabbagh, H. (2005). "Strength and ductility of high-strength concrete shear walls under reversed cyclic loading." *PhD Dissertation*, The University of New South Wales, Sydney, Australia.

Dazio, A., Beyer, K., and Bachmann, H. (2009). "Quasi-static cyclic tests and plastic hinge analysis of RC structural walls." *Engineering Structures*, 31(7), 1556–1571.

Elwood, K. J., and Moehle, J. P. (2005). "Axial capacity model for shear-damaged columns." *ACI Structural Journal*, 102(4), 578–587.

FEMA (Federal Emergency Management Agency). (1997). "Guidelines to the seismic rehabilitation of existing buildings." *FEMA 273*, Washington, D.C.

Flores, L., Alcocer, S., and Carrillo, J. (2007). "Tests of concrete walls with various aspect ratios and small steel ratios, to be used for housing." *Proceedings, XVI National Conference on Earthquake Engineering*, Ixtapa-Zihuatanejo, Mexico (in Spanish).

Kabeyasawa, T., Tasai, A., and Igarashi, S. (2002). "An economical and efficient method of strengthening reinforced concrete columns against axial load collapse during major earthquake." PEER Report 2002/02, Third US-Japan Workshop on Performance-Based Earthquake Engineering Methodology for RC Building Structures, Pacific Earthquake Engineering Research Center, University of California, Berkeley, CA.

Kabeyasawa, T., and Matsumoto, K. (1992). "Tests and analyses of ultra-high strength reinforced concrete shear walls." *Proceedings*, *10th World Conference on Earthquake Engineering*, Madrid, Spain, July 19–24, 3291–3296.

Kato, D., and Ohnishi, K. (2002). "Axial load carrying capacity of RC columns under lateral load reversals." PEER Report 2002/02, Third US- Japan Workshop on Performance-Based Earthquake Engineering Methodology for RC Building Structures, Pacific Earthquake Engineering Research Center, University of California, Berkeley, CA.

Looi, D. T. W., and Su, R. K. L. (2018). "Seismic axial collapse of shear damaged heavily reinforced shear walls experiencing cyclic tension–compression excursions: a modified Mohr's axial capacity model." *Journal of Earthquake Engineering*, DOI: 10.1080/13632469.2018.1475314.

Lu, Y., Gultom, R., Henry, R. S., and Ma, Q. T. (2016). "Testing of RC walls to investigate proposed minimum vertical reinforcement limits in NZS 3101:2006 (A3)." *Proceedings*, *2016 NZSEE Annual Conference*, Christchurch, New Zealand.

Luna, B. N. (2015). "Seismic response of low aspect ratio reinforced concrete walls for building and safety-related nuclear applications." Ph.D. Dissertation, University at Buffalo, NY.

Massone, L. M. (2006). "RC wall shear–flexure interaction: analytical and experimental responses." PhD Dissertation, University of California, Los Angeles, CA.

Mestyanek, M. (1986). "The earthquake of resistance of reinforced concrete structural walls of limited ductility." MS Thesis, University of Canterbury, Christchurch, New Zealand.

Motter, C. J., Abdullah, S. A., and Wallace, J. W. (2018). "Reinforced concrete structural walls without special boundary elements." *ACI Structural Journal*, 115(3), 723-733.

Nakachi, T., Toda, T., and Makita, T. (1992). "Experimental study on deformation capacity of reinforced concrete shear walls after flexural yielding." *Proceedings, 10th World Conference on Earthquake Engineering*, July 19-24, Madrid, Spain, 3231-3236.

Nakamura, T., and Yoshimura, M. (2002). "Gravity load collapse of reinforced concrete columns with brittle failure modes." *Journal of Asian Architecture and Building Engineering*, 1(1), 21–27.

NIST (National Institute of Standards and Technology). (2011). “Seismic design of cast-in-place concrete special structural walls and coupling beams: a guide for practicing engineers.” *NIST GCR 11-917-11 REV-1*, NEHRP Consultants Joint Venture, Gaithersburg, Maryland.

Oesterle, R.G., Fiorato, A.E., Johal, L.S., Carpenter, J.E., Russell, H.G., and Corley, W.G. (1976). “Earthquake resistant structural walls–tests of isolated walls.” Report to NSF (GI-43880), Construction Technology Laboratories, Portland Cement Association, Skokie, IL.

Ousalem, H. (2006). “Experimental and analytical study on axial load collapse assessment and retrofit of reinforced concrete columns.” PhD Dissertation, The University of Tokyo, Tokyo, Japan.

Ramarozatovo, R., Hosono, J., Kawai, T., Takahashi, S., and Ichinose T. (2016). “Effects of construction joints and axial loads on slip behavior of RC shear walls.” *International Journal of Civil, Structural, Environmental and Infrastructure Engineering Research and Development (IJCSEIERD)*, 6(4), 1-10.

Salonikis, T., Kappos, A., Tegos, I. and Penelis, G. (1999). “Cyclic load behavior of low-slenderness reinforced concrete walls: design basis and test results.” *ACI Structural. Journal*, 96(4), 649–661.

Sanada, Y., Takahashi, H., and Toyama, H. (2012). “Seismic strengthening of boundary columns in RC shear walls.” *Proceedings*, *15th World Conference on Earthquake Engineering*, Sept. 24-28, Lisbon, Portugal.

Segura, C. L., and Wallace, W. J. (2018). “Seismic performance limitations and detailing of slender reinforced concrete walls.” *ACI Structural Journal*, 115(3), 849-860.

Takahashi, S., Yoshida, K., Ichinose, T., Sanada, Y., Matsumoto, K., Fukuyama, H., and Suwada, H. (2013). "Flexural drift capacity of reinforced concrete wall with limited confinement." *ACI Structural Journal*, 110(1), 95-104.

Tasai, A. (2000). "Residual axial capacity of reinforced concrete columns during shear deterioration." PEER Report 2000/10*,* Second US-Japan Workshop on Performance-Based Earthquake Engineering Methodology for RC Building Structures, Pacific Earthquake Engineering Research Center, University of California, Berkeley, CA.

Tasai, A. (1999). "Residual axial capacity and restorability of reinforced concrete columns damaged due to earthquake." PEER Report 1999/10, US-Japan Workshop on Performance-Based Earthquake Engineering Methodology for RC Building Structures, Pacific Earthquake Engineering Research Center, University of California, Berkeley, CA.

Thomsen, J. H. and Wallace, J. W. (1995). "*Displacement-based design of reinforced concrete structural walls: experimental studies of walls with rectangular and T-shaped cross sections*." Report No. CU/CEE-95/06, Clarkson University, Potsdam, N.Y.

Tran, T. A., and Wallace, J. W. (2015). "Cyclic testing of moderate-aspect-ratio reinforced concrete structural walls." *ACI Structural Journal*, 112(6), 653–666.

Tran, C. (2010). "Experimental and analytical studies on the seismic behavior of reinforced concrete columns with light transverse reinforcement." PhD Dissertation, Nanyang Technological University, Singapore.

Uchida, Y., and Uezono, Y. (2003). "Method of judging collapse of SRC and RC columns failed by shear and axial force." *Proceedings*, *ASSCCA'03 International Conference Advances in Structures (ASCCS-7)*, June 22–25, Sydney, NSW, Australia, 1209–1215.

Wallace, J. W., Elwood, K. J., and Massone, L. M. (2008). "Investigation of the axial load capacity for lightly reinforced wall piers." *Journal of Structural Engineering,* 134(9), 1548-1557.

Wallace, J. W. (1994). "A new methodology for seismic design of RC shear walls." *Journal of Structural Engineering*, 120(3), 863–884.

Wang, T. Y., Betero, V. V., and Popov, E. P. (1975). "*Hysteretic behavior of reinforced concrete framed walls*." Report No. EERC 75-23, Earthquake Engineering Research Center, University of California, Berkeley.

Yoshimura, M., and Yamanaka, N. (2000). "Ultimate limit state of RC columns." PEER Report 2000/10, Second US-Japan Workshop on Performance-Based Earthquake Engineering Methodology for Reinforced Concrete Building Structures, Pacific Earthquake Engineering Research Center, University of California, Berkeley, CA.

CHAPTER 6. Structural Wall Classification Based Failure Mode

6.1. Abstract

The shear and flexural behaviors of a reinforced concrete (RC) structural wall are accounted for in a lumped plasticity model using shear (translational) and flexural (rotational) springs, respectively. In a nonlinear analysis, these springs will exhibit either linear or nonlinear behavior depending on the dominant wall behavior mode. Therefore, it is important to quantitatively distinguish between flexure-controlled (generally slender) walls and shear-controlled (generally low-rise or squat) walls/piers. ASCE 41-17 Tables 10-19 and 10-20 (Structural wall tables) include "components controlled by flexure" and "components controlled by shear" in the table captions, but the standard does not provide the user with an approach to determine whether a wall is controlled by flexure or shear. The commentary of ASCE 41-17 (C10.7.1) defines slender and squat walls as walls with aspect ratio (h_w/l_w) $\geq$ 3.0 and $\leq$ 1.5, respectively, and walls with intermediate aspect ratios are defined as flexure-shear-controlled walls. However, the results presented show that shear span ratio (h_{eff}/l_w), which is similar to h_w/l_w, is not a good indicator of the expected wall dominant behavior and failure mode. Therefore, an approach, which is based on the shear-to-flexure strength ratio ($V_{yE}/V_{@MyE}$), is proposed using results from a large database, known as UCLA-RCWalls database. The proposed approach accurately captures the predominant behavior and failure mode of walls.

6.2. Background of ASCE 41-17 / ACI 369-17 Methodology

In ASCE 41-17 (§ 7.5.1.2) and ACI 369-17 (§7.2.4.1) Standards, both shear and flexure actions in RC structural walls are treated as deformation-controlled actions, with acceptance criteria

tabulated for linear approaches (deformation-based m factors) and nonlinear approaches (plastic hinge rotations). Other actions, such as axial, shear sliding, as well as shear in walls with a transverse reinforcement ratio < 0.0015 (ASCE 41-17 § 10.7.2.3) and flexure in walls where the cracking moment strength exceeds the yield strength (ASCE 41-17 § 10.7.2.3), are currently treated as force-controlled actions, unless component testing is performed to demonstrate otherwise. The approach presented herein for wall classification based on expected dominant behavior (shear or flexure) and failure mode does not result in changes to the modeling parameters for force and deformation-controlled actions.

ASCE 41-17 §7.5.1.3 also explicitly denotes whether to use expected or lower-bound strengths based on whether an action is classified as deformation- or force-controlled. For evaluating the behavior of deformation-controlled actions, expected strength is used, whereas for evaluating the behavior of force-controlled actions, a lower bound estimate of strength is used. Because wall shear and flexure actions are generally treated as deformation-controlled actions, the proposed classification is based on tested (expected) material strengths. The ASCE 41-17 and ACI 369-17 standards use the notation of M_{yE} to denote wall nominal moment strength associated with expected material properties obtained consistent with ACI 318-14 approach for M_n, using expected material strengths. The notations M_{yE} and c_E, which imply the use of expected material properties, are used hereafter instead of the ACI 318-14 notation for nominal moment strength, M_n, and the associated depth of neutral axis, c, respectively.

6.3. Wall Database–UCLA-RCWalls

The database currently contains detailed information and test results on more than 1000 wall tests reported in the literature (Abdullah and Wallace, 2018). The database includes three major clusters

of data: 1) detailed information about the test specimen and loading protocols, 2) test results, e.g., backbone relations and failure modes; and 3) computed data, e.g., moment-curvature relationships and wall shear strength parameters.

The reported failure modes are classified in the database as either flexure failure modes, i.e., bar buckling and concrete crushing, bar fracture, or global or local lateral instability (Fig. 6-1), shear failure modes, i.e., diagonal tension, diagonal compression (web crushing), or shear sliding at the base (Fig. 6-2), flexure-shear failure modes, i.e., yielding in flexure prior to failing in one of the shear failure modes (Fig. 6-3), and lap-splice failure mode. Wall not tested to some level of lateral strength loss are flagged as "not tested to failure". The authors did their best to validate that the reported failure mode was consistent with the observed wall response and damage before recording that information in the database.

(*a*) (*b*) (*c*)

Fig. 6-1–Wall flexural failure modes: (*a*) bar buckling and concrete crushing (Thomsen and Wallace, 1995), (*b*) bar fracture (Dazio et al., 2009), and (*c*) lateral instability (Thomsen and Wallace, 1995).

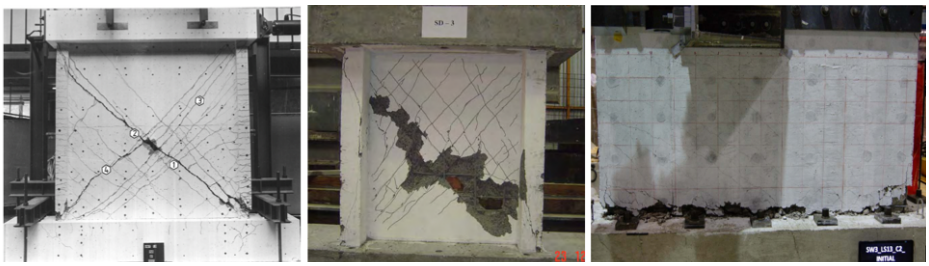

(*a*) (*b*) (*c*)

Fig. 6-2–Wall shear failure modes: (*a*) diagonal tension (Mestyanek, 1986), (*b*) diagonal compression (Dabbagh, 2005), and (*c*) shear-sliding (Luna, 2015).

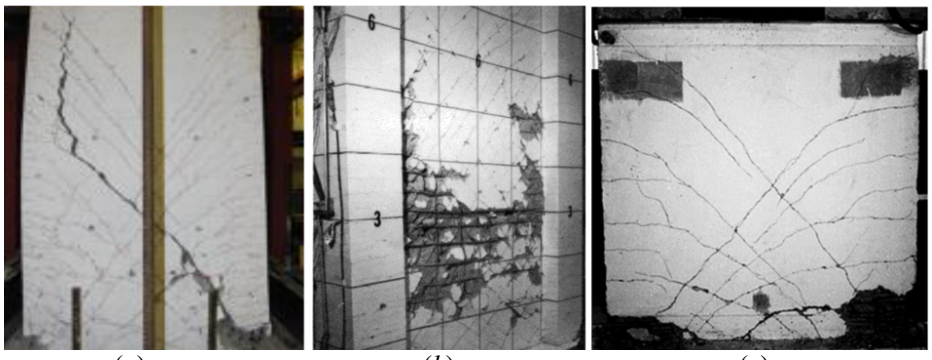

(*a*) (*b*) (*c*)

Fig. 6-3–Wall flexure-shear failure modes: (*a*) flexure-diagonal tension (Tran, 2012), (*b*) flexure-diagonal compression (Oesterle et al., 1976), and (*c*) flexure-shear-sliding (Salonikios et al., 1999).

Furthermore, the database contains computed data for both flexural and shear responses. Analytical moment-curvature $(M-\phi)$ analysis was performed for each wall test using tested material properties and the sustained axial load if present, and assuming 1) linear strain gradient (plane sections), 2) compressive stress-strain behavior for unconfined concrete given by Hognestad (1951) in Fig. 6-4(***a***), and 3) steel stress-strain relationship given in Fig. 6-4(***b***), where ε_y, ε_{sh}, and ε_u are steel strains at yield, initiation of strain hardening, and peak strength, respectively. Although the moment-curvature response of each wall is available in a spreadsheet, values of nominal moment strength (M_n) and depth of neutral axis (c) at concrete compressive strain of 0.003

and first yield moment strength (M_y) and the corresponding curvatures (i.e., ε_n at M_n and ε_y at M_y) are recorded in the database.

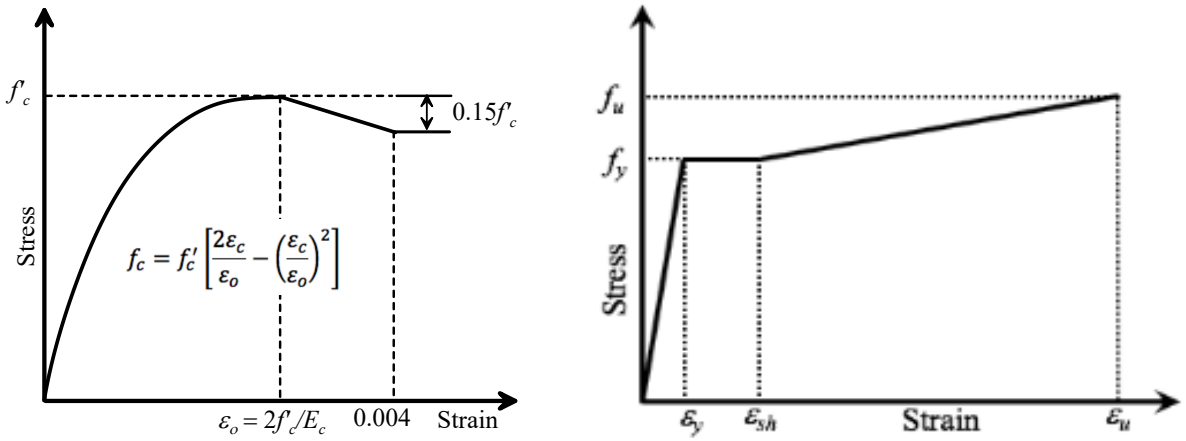

(*a*) Concrete (*b*) Reinforcement

Fig. 6-4–Stress-strain relationships used to compute moment-curvature relations.

As noted, the steel stress-strain relationship used to produce the moment-curvature relations includes the impact of strain hardening of longitudinal reinforcement. However, ACI 318-14 §20.2.2.1 stipulates that the increase in M_n due to the effect of strain hardening of the reinforcement be neglected. Thus, to evaluate the impact of strain hardening of longitudinal reinforcement on the value of M_{yE} and c_E, a randomly selected subset of 200 walls with different cross-sections and attributes was examined. For this data subset, M_{yE} and c_E were computed with and without the impact of strain hardening. The results are shown in Fig. 6-5, which demonstrates that including strain hardening of longitudinal reinforcement increased M_{yE} and c_E by only 3% and 1%, respectively. In general, the increase in M_{yE} due to strain hardening was observed for walls with T-shaped, L-shaped, or half barbell-shaped cross-sections for the case where the flange or barbell

is in compression. Nonetheless, a 3% increase in M_{yE} due to strain hardening of longitudinal reinforcement is negligible for seismic retrofit and could be ignored.

The wall shear demand corresponding to the development of yield moment strength (M_{yE}) is computed based on the shear-span-ratio (SSR) used in the tests, as follows:

$$V_{@M_{yE}} = \frac{M_{yE}}{SSR \times l_w} \quad \text{(Eq. 6-1)}$$

Where l_w is the total length of the wall.

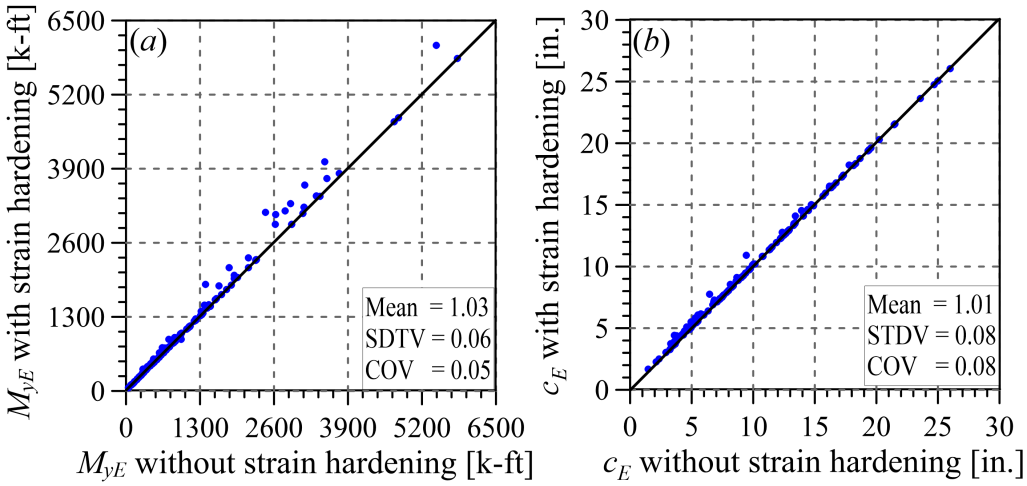

Fig. 6-5–Impact of strain hardening of longitudinal reinforcement at concrete compressive strain of 0.003 on: (*a*) yield moment strength (M_{yE}), and (*b*) depth of neutral axis (*c*)–results from 200 walls.

The database also includes the following strengths computed using tested material properties:

1. Shear strength at failure of diagonal tension or compression strut, $V_{yE,d}$

The wall shear strength corresponding to the strength associated with diagonal tension or compression strut ($V_{yE,d}$) is computed from **Eq. 6-2** (ACI 318-14 Equation 18.10.4.1 without restrictions on spacing, reinforcement ratio, and the number of curtains of reinforcement):

$$V_{yE,d} = A_{cv}\left(\alpha_c\sqrt{f'_{cE}} + \rho_t f_{ytE}\right) \le 10A_{cv}\sqrt{f'_{cE}} \quad \text{(Eq. 6-2)}$$

Where A_{cv} is the gross area of concrete section bounded by web thickness and wall length (A_{cv}= $t_w l_w$), f'_{cE} is the tested concrete compressive strength, ρ_t is the web transverse (horizontal) reinforcement ratio, f_{ytE} is the tested yield strength of the web transverse reinforcement, and α_c is a coefficient that depends on h_w/l_w of the wall. However, walls are generally tested as cantilevers with a single lateral load applied at the top of the wall (with or without axial load) or as panel or partial height walls under a combined effects of lateral load(s), axial load, and bending moment at the top of the panel, and thus h_w/l_w is not always a relevant parameter. Therefore, the test shear-span-ratio, SSR, (M/Vl_w or h_{eff}/l_w) was used instead, where α_c is taken as 3.0 for $M/Vl_w \le 1.5$, as 2.0 for $M/Vl_w \ge 2.0$, and varies linearly between 3.0 and 2.0 for M/Vl_w between 1.5 and 2.0.

2. Shear friction strength at the base, $V_{yE,f}$

The wall shear strength corresponding to the shear friction strength at the wall-foundation interface ($V_{yE,f}$) is computed from **Eq. 6-3** (ACI 318-14 Equation 22.9.4.2) including the impact of sustained axial load (ACI 318-14 §22.9.4.5):

$$V_{yE,f} = \mu\left(A_{vf} f_{ylE} + P\right) \le 0.2 f'_{cE} A_c \quad \text{(Eq. 6-3)}$$

Where A_{vf} is the area of all reinforcement crossing the wall-foundation interface, f_{ylE} is the tested yield strength of the reinforcement crossing the wall-foundation interface, μ is the coefficient of friction and is taken as 0.6 in accordance with ACI 318-14 Table 22.9.4.2, A_c is the area of concrete

section resisting shear transfer, and P is the sustained axial load applied during the experiment. It is noted that the upper limit of $800A_c$ given in ACI 318-14 §22.9.4.4 for **Eq. 6-3** was not considered, as it was found to under predict wall shear friction strength, especially for walls with high strength concrete. The same conclusion is reported by Mattock (2001), who also proposed a model that performs well for walls with high strength concrete.

6.4. Discussion of Wall Failure Mode Classification in Database

The database was filtered to obtain a dataset of approximately 1000 wall tests with reported flexure, shear, or flexure-shear failure modes (i.e., basically all the walls in the database except those that failed due to inadequate lap-splice of longitudinal reinforcement and walls that were not tested to failure or some significant (> ~10%) degree of lateral strength degradation). Fig. 6-6 presents histograms of wall attributes associated with the dataset.

The results obtained using the 1000 wall dataset are presented in Fig. 6-7 for each reported failure mode separately and in Fig. 6-8 for the entire dataset, where V_{yE} is the least shear strength computed from **Eq. 6-2** and **Eq. 6-3**, and $V_{@test}$ is the peak wall shear obtained during the test. From these figures, it can be seen that almost all flexure- and shear-controlled walls have a shear-to-flexure strength ratio ($V_{yE}/V_{@MyE}$) > 1.0 (Fig. 6-7(*a*)) and < 1.0 (Fig. 6-7(***b***) and (***c***)), respectively. Walls with failure modes reported as flexure-shear are mainly scattered between $0.7 < V_{yE}/V_{@MyE} < 1.3$ (Fig. 6-7(***d***)). The flexure-shear-controlled walls with $V_{yE}/V_{@MyE} < 1.0$ generally have limited flexural nonlinearity (i.e., barely experiencing first yield of longitudinal reinforcement) and, therefore, could realistically be classified as shear-controlled walls. On the other hand, for the flexure-shear-controlled walls with $V_{yE}/V_{@MyE} > 1.0$, the behavior is initially governed by flexural

cracking and yielding similar to flexure-controlled walls because V_{yE} is initially greater than $V_{@MyE}$, but the wall shear strength gradually reduces, as the wall is cycled through large nonlinear displacements, until it drops below $V_{@MyE}$, and then the wall fails in shear. Depending on the level of shear and flexural demands, these walls could exhibit drift capacities comparable to those of flexure-controlled walls. Fig. 6-8 also reveals that the ratio $V_{@Mult}/V_{@MyE}$ for the flexure-controlled walls is approximately 1.15.

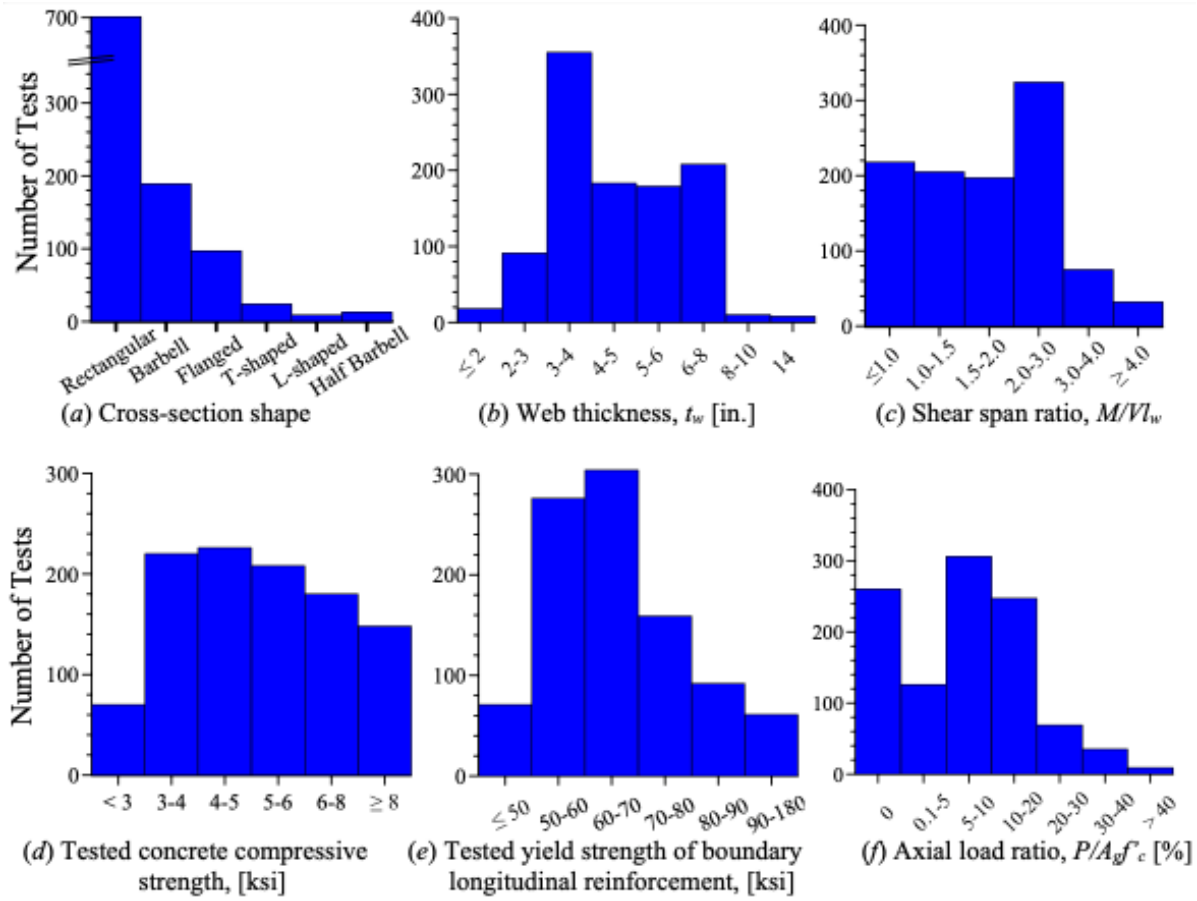

Fig. 6-6–Histograms of wall tests in the UCLA-RCWalls database.

A rearranged presentation of the results is given in Fig. 6-9, where the Y-axis is the shear friction strength computed from **Eq. 6-3** ($V_{yE,f}$) normalized by the diagonal shear strength from **Eq. 6-2** ($V_{yE,d}$). It can be seen that the data are divided between three regions: 1) blue region: flexure-controlled walls with $V_{yE}/V_{@MyE} > 1.0$, 2) red region: diagonal shear-controlled walls (due to failure of diagonal tension or compression strut) with $V_{yE}/V_{@MyE} \leq 1.0$ and $V_{yE,f}/V_{yE,d} \geq 1.0$, and 3) yellow region: sliding shear-controlled walls with $V_{yE}/V_{@MyE} \leq 1.0$ and $V_{yE,f}/V_{yE,d} < 1.0$.

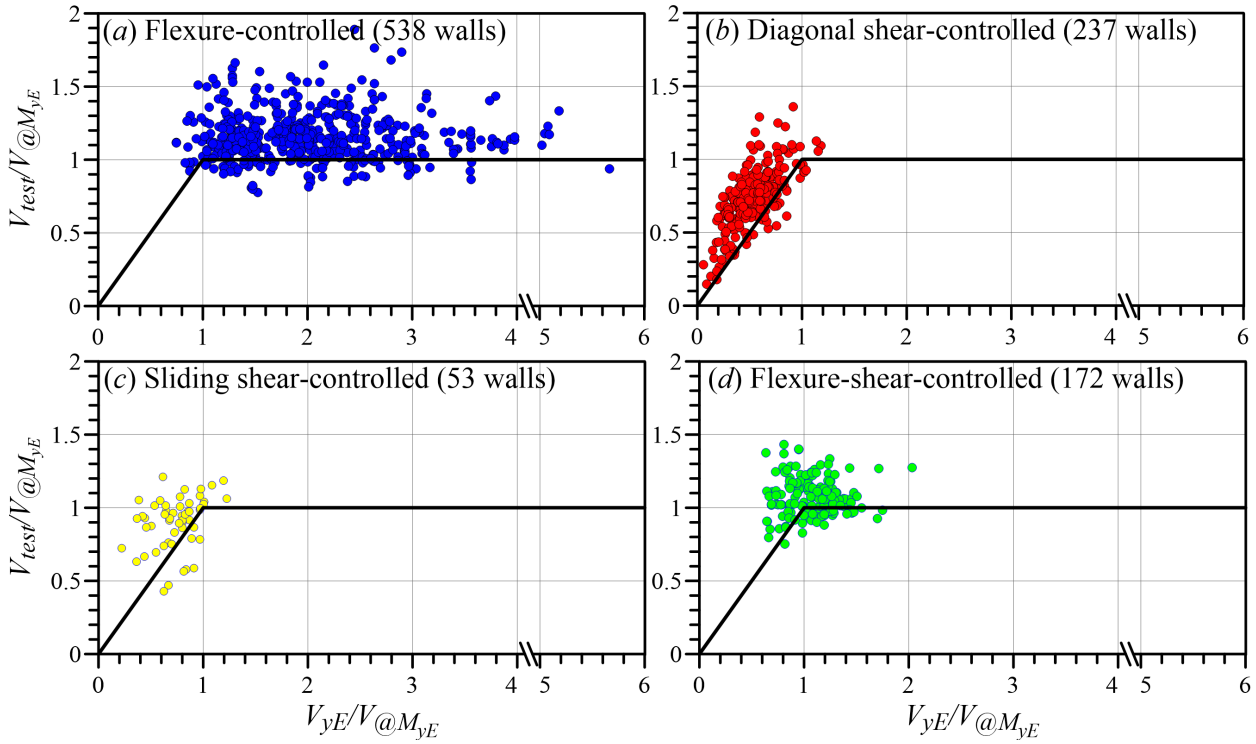

Fig. 6-7–Wall failure modes results from a dataset of 1000 wall tests: failure modes separated.

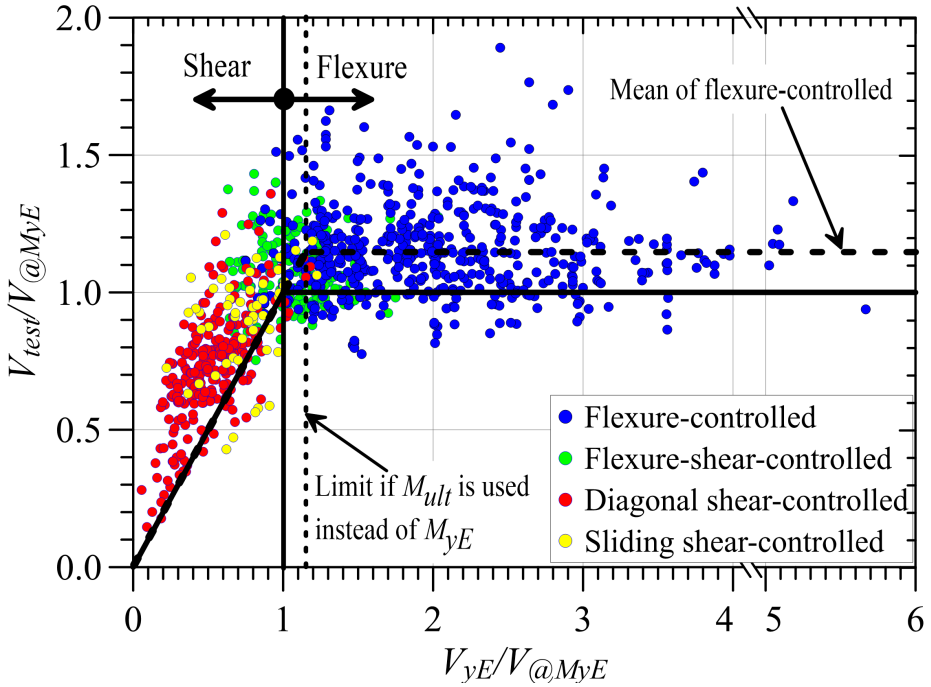

Fig. 6-8–Wall failure modes results from a dataset of 1000 wall tests: failure modes combined.

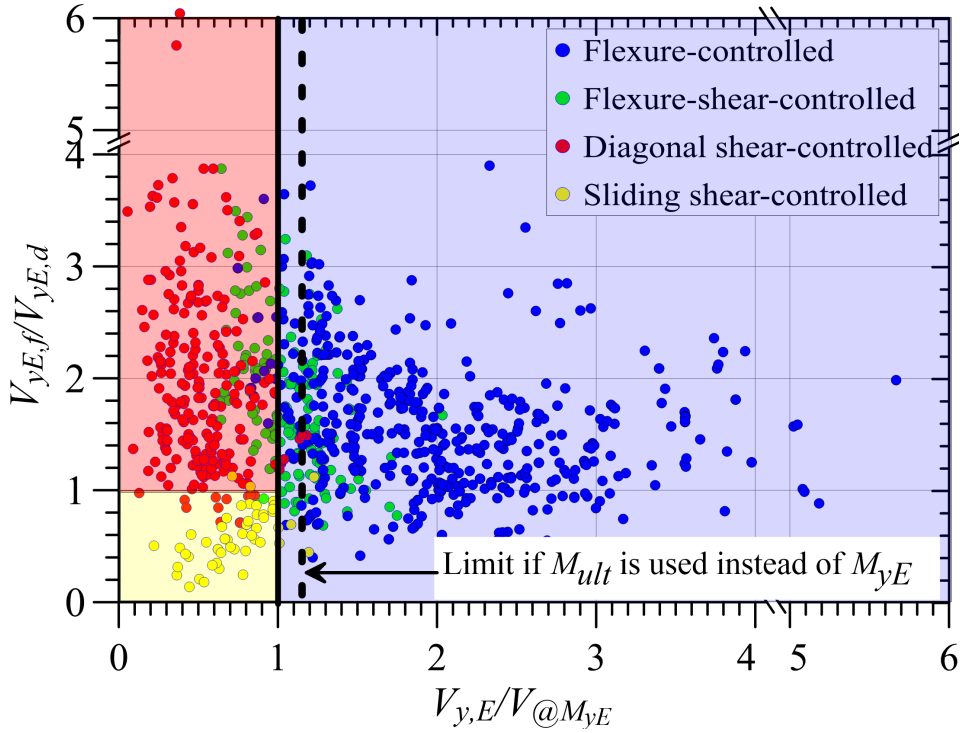

Fig. 6-9–Wall classification: blue region = flexure-controlled, red region= shear-controlled (diagonal tension or compression), and yellow region= shear sliding at the base.

Fig. 6-10 shows the distribution of failure modes of the walls in the dataset versus test shear-span-ratio (M/Vl_w or h_{eff}/l_w) and $V_{yE}/V_{@MyE}$, reveals that M/Vl_w, which is closely related to aspect ratio (h_w/l_w), is not as good of an indicator of wall dominant behavior and failure mode; therefore, it is proposed to use $V_{yE}/V_{@MyE}$ as a criterion to classify walls based on expected dominant behavior and failure mode. However, this figure also shows that walls with $M/Vl_w \geq 3.0$ and < 1.0 fail in flexure and shear failure modes, respectively.

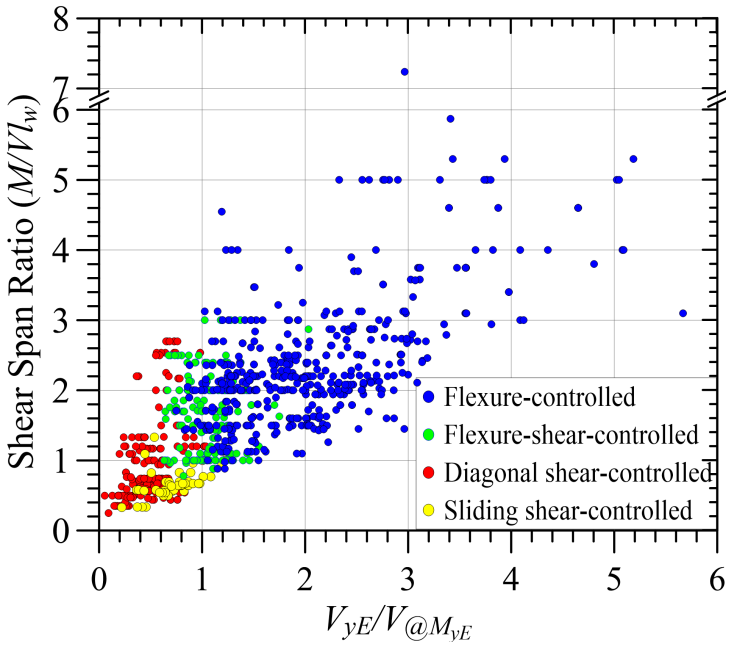

Fig. 6-10–Variation of wall failure mode versus shear-span-ratio and shear-flexure strength ratio.

6.5. Proposed Wall Classification Approach

Results presented in the preceding section indicate that walls can be classified as shear- or flexure-controlled walls based on their shear-to-flexure strength ratio. However, for an actual building

(versus a laboratory test), the distribution of lateral forces along the height of the building (wall) needs to be known to enable calculation of the shear demands (i.e., $V_{@MyE}$ and $V_{@Mult}$). Linear analysis approaches of ASCE 7-16 (i.e., ELF in §12.8 and RSA and LRHA in §12.9) or ASCE 41-17 (i.e., LDP in §7.4.2) could be used to determine the effective height of the wall (h_{eff}), from which $V_{@MyE}$ and $V_{@Mult}$ are calculated as M_{yE}/h_{eff} and M_{ult}/h_{eff}, respectively. This approach does not account for the dynamic amplification of wall shear demands due to higher mode responses of a wall that develops its flexural strength. Currently, ASCE 41-17 §10.7.2.4 and ACI 369-17 §7.2.4.1 allow use of a simplified approach where linear analysis approaches are used to account for the impact of higher mode responses on the shear demand by assuming uniform distribution of lateral forces over the height of the wall (i.e., h_{eff} is one-half of the total wall height, h_w).

Research has shown that dynamic shear amplification is strongly correlated with building period, which is a function of building height. Therefore, the following simplified dynamic shear amplification factor (ω_v) computed from **Eq. 6-4** is proposed to amplify $V_{@MyE}$ and $V_{@Mult}$. This approach, which is aligned with the approaches in New Zealand and Canadian codes (NZS 3101-2006 and CSA A23.3-2014, respectively), has been adopted in ACI 318-19 in §18.10.3.

$$\omega_v = 0.9 + \frac{n_s}{10} \text{ for } n_s \le 6$$
$$\omega_v = 1.3 + \frac{n_s}{30} \text{ for } n_s > 6 \qquad \text{(Eq. 6-4)}$$

Where n_s is the number of stories above the critical section and should not be taken less than 0.007 times the wall height above the critical section (h_{wcs}) measured in inches. This limit is imposed on n_s to account for buildings with large story heights (i.e., >12 ft. (144 in.)). Dynamic shear amplification is not significant in walls with $h_w/l_w < 2.0$.

It is noted that this new provision in ACI 318-19 also includes shear amplification due to moment overstrength. However, since the expected material strengths are used to compute M_{yE}, and M_{yE} is amplified to obtain M_{ult}, the moment overstrength amplification factor is not considered here.

Based on the results presented above, the approach given in Table 6-1 is proposed to distinguish between flexure- and shear-controlled walls. It is noted that to ensure pure flexural behavior (i.e., shear yielding does not occur following flexural yielding), the ratio $V_{yE}/(\omega_v V_{@MyE})$ was selected to be equal to and greater than 1.15 (i.e., $V_{yE}/(\omega_v V_{@Mult}) \geq 1.0$). To use Table 6-1, the user needs to estimate the shear demands at the wall critical section using either linear static or linear dynamic analysis approach, amplify the estimated shear demands to account for the effects of higher modes on shear demands, if applicable, and then compare these demands to the wall shear strength to determine the expected dominant behavior. According to the expected dominant behavior, wall nonlinearity can be modeled using the applicable modeling parameters.

Table 6-1–Criteria for determining the expected wall dominant behavior

Criterion		Expected Dominant Behavior
$\frac{V_{yE}}{w_v V_{@M_{yE}}} < 1.15$	$V_{yE,d} \leq V_{yE,f}$	Diagonal shear -controlled
	$V_{yE,d} > V_{yE,f}$	Sliding shear-controlled
$\frac{V_{yE}}{w_v V_{@M_{yE}}} \geq 1.15$		Flexure-controlled

Note: V_{yE} is the least of $V_{yE,d}$ and $V_{yE,f}$ per **Eq. 6-2** and **Eq. 6-3**, respectively, and ω_v is computed from **Eq. 6-4**.

6.6. Summary and Conclusions

This study involves developing an approach to quantitatively distinguish between flexure-controlled (generally slender) walls and shear-controlled (generally low-rise or squat) walls/piers using the experimental results included in the UCLA-RCWalls databse. ASCE 41-17 standard does not provide the user with an approach to determine whether a wall is controlled by flexure or shear. The commentary of ASCE 41-17 (C10.7.1) defines slender and squat walls as walls with aspect ratio (h_w/l_w) $\geq$ 3.0 and $\leq$ 1.5, respectively, and walls with intermediate aspect ratios are defined as flexure-shear-controlled walls. However, results from a dataset of about 1000 wall tests indicated that shear span ratio at (h_{eff}/l_w), which is similar to aspect ratio (h_w/l_w) for cantilever walls, is not a good indicator of the expected wall dominant behavior and failure mode. Based on the results of about 1000 wall tests, an approach, which is based on the shear-to-flexure strength ratio ($V_{yE}/V_{@MyE}$), is proposed, which accurately captures the predominant behavior and failure mode of walls.

6.7. Acknowledgements

Funding for this study was provided, in part, by ATC 140 Project, and the University of California, Los Angeles. The authors would also like to thank the other member of Working Group 3 (WG3) of ATC 140 Project, which include Wassim Ghannoum, Garrett Hagen, Mohamed Talaat, Laura Lowes, and Afshar Jalalian for providing thoughtful comments on the work presented. Any opinions, findings, and conclusions or recommendations expressed in this paper are those of the authors and do not necessarily reflect the views of others mentioned here.

6.8. References

Abdullah, S. A., and Wallace, J. W., 2018. UCLA-RCWalls database for reinforced concrete structural walls. *Proceedings, 11th National Conference in Earthquake Engineering*, Earthquake Engineering Research Institute, June 25-29, Los Angeles, CA.

American Concrete Institute (ACI 318-14), 2014. *Building Code Requirements for Structural Concrete (ACI 318-14) and Commentary (318R-14)*, Farmington Hills, MI, 519 pp.

American Concrete Institute (ACI 369-17), 2017. *Standard Requirements for Seismic Evaluation and Retrofit of Existing Concrete Buildings (ACI 369.1-17) and Commentary*, Farmington Hills, MI, 110 pp.

American Society of Civil Engineers (ASCE 41-17), 2017. *Seismic Evaluation and Retrofit of Existing Buildings (ASCE/SEI 41-17)*, Reston, VA, 576 pp.

Canadian Standards Association (CSA) (2014). CAN/CSA-A23.3-14 Design of concrete structures. 352 pp.

Dabbagh, H., 2005. Strength and Ductility of High-Strength Concrete Shear Walls Under Reversed Cyclic Loading, PhD Dissertation, School of Civil and Environmental Engineering, The University of New South Wales, Sydney, Australia.

Dazio, A, Beyer, K., and Bachmann, H, 2009. Quasi-static cyclic tests and plastic hinge analysis of RC structural walls, Engineering Structures, Vol.31, No. 7, pp. 1556-1571.

Hognestad, E., 1951. *A Study of Combined Bending and Axial Load in Reinforced Concrete Members*, *Bulletin No. 399*, University of Illinois Engineering Experimental Station, IL.

Luna, B. N., 2015. Seismic Response of Low Aspect Ratio Reinforced Concrete Walls for Building and Safety-Related Nuclear Applications, Ph.D. Dissertation, Department of Civil, Structural and Environmental Engineering, University at Buffalo.

Mattock, A.H., 2001. Shear friction and high-strength concrete, *ACI Structural Journal*, Vol. 98, No. 1, pp. 50–59.

Mestyanek, J. M., 1986. The earthquake of resistance of reinforced concrete structural walls of limited ductility, Master Thesis, University of Canterbury, Christchurch, New Zealand.

NZS 3101 (2006). Concrete Structures Standard, Part 1: The Design of Concrete Structures: Part 2: Commentary on the Design of Concrete Structures, Standards New Zealand, Wellington, New Zealand. ISBN 1-86975-043-8.

Oesterle, R.G., Fiorato, A.E., Johal, L.S., Carpenter, J.E., Russell, H.G., and Corley, W.G., 1976. *Earthquake Resistant Structural Walls–Tests of Isolated Walls, Report to National Science Foundation,* Construction Technology Laboratories, Portland Cement Association, Skokie, IL, 315 pp.

Salonikis, T., Kappos, A., Tegos, I. and Penelis, G. (1999), Cyclic load behavior of low-slenderness reinforced concrete walls: design basis and test results, ACI Structural Journal, Vol. 96, No. 4, pp. 649–661.

Thomsen, J. H. and Wallace, J. W., 1995. *Displacement-Based Design of Reinforced Concrete Structural Walls: Experimental Studies of Walls with Rectangular and T-Shaped Cross Sections, Report No. CU/CEE-95/06*, Department of Civil and Environmental Engineering, Clarkson University, Potsdam, NY.

Tran, T. A., 2012. Experimental and Analytical Studies of Moderate Aspect Ratio Reinforced Concrete Structural Walls, Ph.D. Dissertation, University of California, Los Angeles, CA, 300 pp.

CHAPTER 7. Stiffness of Flexure-Controlled RC Structural Walls

7.1. Abstract

Current requirements of ACI 369-17 §7.2.2 allow "cracked" effective flexural stiffness ($E_{cE}I_{eff}$) of RC structural walls to be calculated in accordance with Table 5 of the standard, which is 35% of the gross flexural stiffness ($0.35E_{cE}I_g$). However, use of a constant value does not adequately consider variables that influence wall effective flexural stiffness. Also, ACI 369-17 §7.2.2 requires that shear response in flexure-controlled walls be modeled using 100% of the gross "uncracked" shear stiffness ($0.4E_{cE}A_w$), which research has shown that significantly overestimates effective shear stiffness. As an alternative to the use of §7.2.2 Table 5, ACI 369-17 C7.2.2 provides additional guidance on modeling wall flexural stiffness for fiber-section and lumped-plasticity modeling approaches, which are based on moment-curvature analysis of the wall cross-section with and without consideration of the effect of bond slip of the wall longitudinal reinforcement anchored in the foundation. However, these recommendations have only been verified using a limited set of test results. Furthermore, there is currently no explicit provision in ACI 369-17 to estimate "uncracked" wall flexural stiffness for cases where little to no cracking is expected. For such cases, ACI 369.1-17 C7.2.2 allows the licensed design professional to use an iterative approach to obtain a more accurate estimate of the wall flexural stiffness. Therefore, the objectives of this study are to: 1) evaluate the wall stiffness provisions and recommendations of ACI 369-17 §7.2.2 and C7.2.2, and 2) develop provisions and recommendations for appropriate flexural and shear stiffness values that account for the effect of various parameters using results from a large database of RC structural walls.

7.2. Wall Database

To accomplish the aforementioned objectives, a comprehensive database of RC wall tests (called UCLA-RCWalls) is utilized (Abdullah and Wallace, 2018a and 2018b), which includes data from more than 1000 wall tests reported in the literature. The database includes three major clusters of data: 1) detailed information about the test specimen and loading, i.e., wall cross-section, web reinforcement, parameterized information of boundary transverse reinforcement, and material properties, loading protocol; 2) test results, e.g., backbone relations, key damage details, and failure modes; and 3) analytically computed data, such as moment-curvature relationships and wall shear strength according to ACI 318-14.

Fig. 7-1shows a typical backbone curve for base shear versus total top displacement (flexural, shear, and bar slip/extension deformation). The *cracking* point represents the state at which horizontal flexural cracks are first observed in the test. The cracking load and displacement is contained in the database for the majority of the tests based on information reported by the authors who performed the tests. However, in cases where this information is not reported, attempts were made to visually identify the cracking point on the load-displacement curve (i.e., a significant change in stiffness). If this was not possible, the cracking information was left blank in the database. The *general yield* point is defined as the point where the hysteretic loops (or the response curve in case of monotonic loading) begin to abruptly lose stiffness, as shown in Fig. 7-1. The value in the database was visually identified. It should be noted that this point does not necessarily correspond to first yielding of longitudinal bars, but rather is associated with yielding of most of the longitudinal bars in the boundary region for tension-yielding walls or onset of concrete nonlinearity for compression-yielding walls. *Peak* is the point at which the maximum lateral strength occurred. *Ultimate* (or *deformation capacity*) is defined as the deformation at which lateral

strength degraded by 20% in the first cycle from the peak. *Residual* and *Collapse* points are defined as the state at which the wall reaches its residual strength (if any) and loses its axial load-carrying capacity, respectively. The majority of the tests, especially earlier tests, do not have *Residual* and *Collapse* points due to termination of the tests before reaching residual strength and axial collapse.

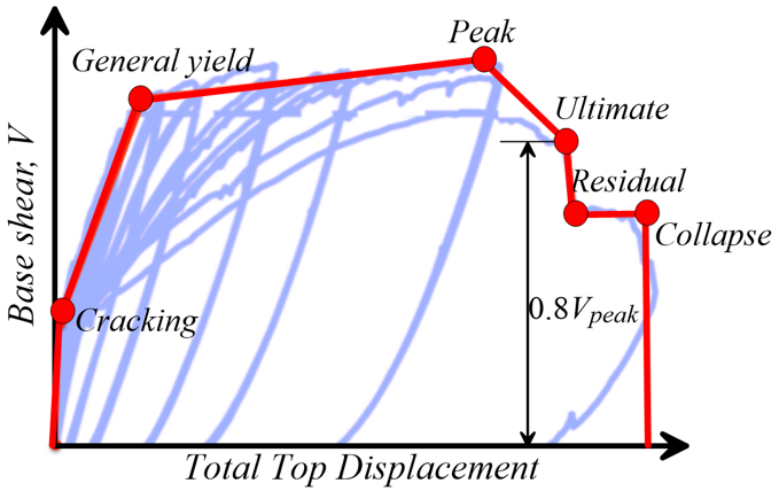

Fig. 7-1–Typical backbone curve for base shear versus total top displacement in UCLA-RCWalls database.

For the purpose of this study, the UCLA-RCWalls database was filtered to obtain a subset of wall tests that satisfied the following requirements:

(a) Flexure-controlled walls (i.e., shear-to-flexure strength ratio, $V_{yE}/V_{@MyE} \geq 1.15$),

(b) Walls tested under quasi-static, monotonic or cyclic loading (in-plane or bi-directional),

(c) Walls containing one or two curtains of web reinforcement,

(d) Walls with conforming or non-conforming detailing, and

(e) Walls with different cross-sections (i.e., rectangular, barbell, I-shaped, T-shaped, L-Shaped, or half-bar bell).

Based on the selected filters, a total of 527 wall tests were identified. Histograms for various dataset parameters are shown in Fig. 7-2, where $P/A_g f'_c$ is the sustained axial load applied during the experiment normalized by tested concrete compressive strength (f'_c) and gross concrete area (A_g), $M/(Vl_w)$ is the ratio of base moment-to-base shear used in the test normalized by wall length (l_w), $\rho_{l,BE}$ and $\rho_{l,web}$ are the longitudinal reinforcement ratios in the boundary elements and the web, respectively, $f_{y,BE}$ is the tested yield strength of the boundary longitudinal reinforcement, t_w is the wall web thickness, and b is the width of flexural compression zone. Walls tested under monotonic or bidirectional loading are included because it is assumed that the loading protocol does not have a significant influence on the wall behavior up to yielding. Nonetheless, walls tested under monotonic and bidirectional loading constitute only 6% and 2.5% of the walls in the dataset of 527 walls, as shown in Fig. 7-2(***l***).

Due to the lack of information on first flexural cracking, a total of 132 of the 527 wall tests were excluded from the uncracked stiffness scope, leaving 395 tests.

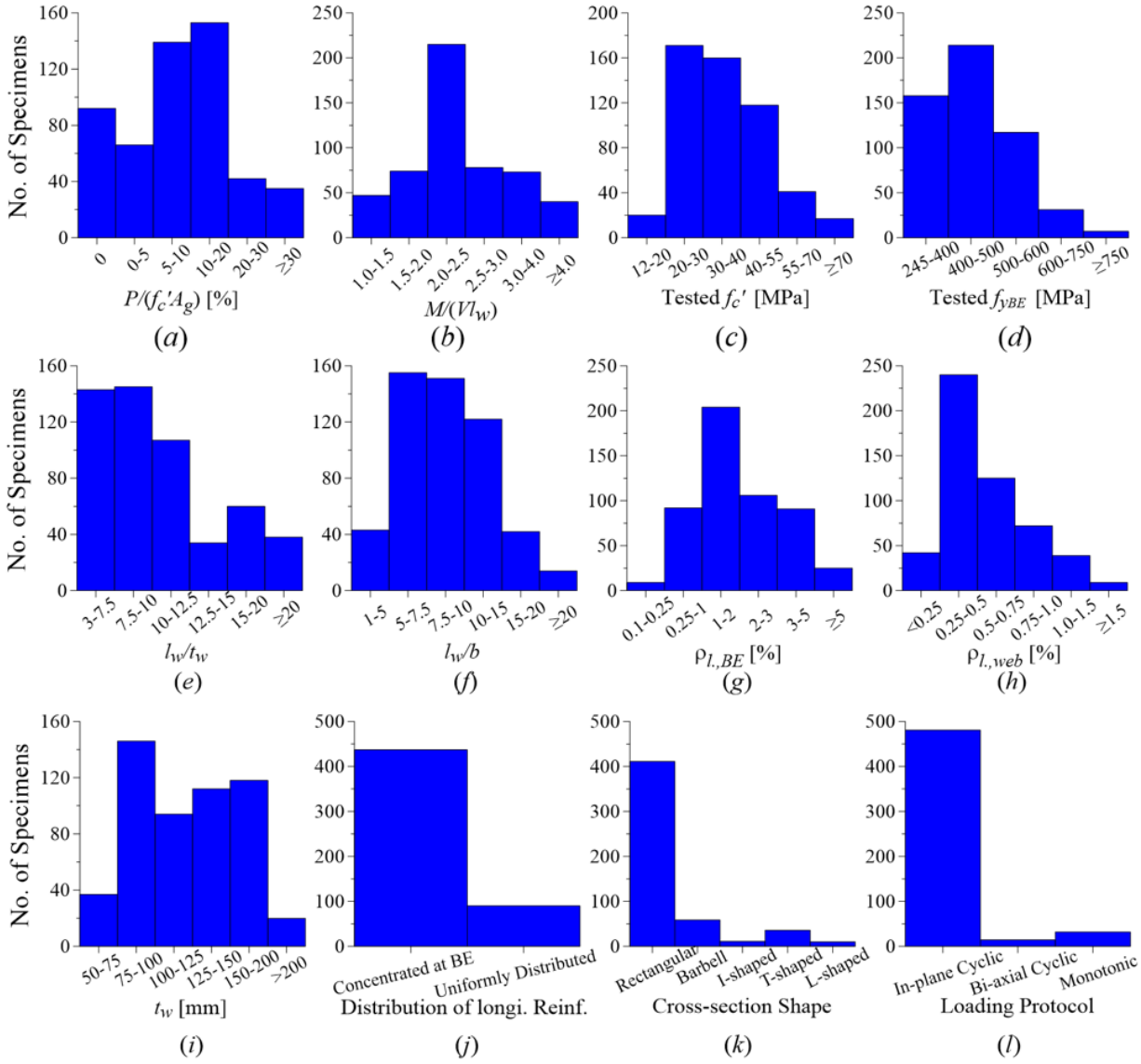

Fig. 7-2–Histograms of the dataset (527 wall tests).

In the results presented here, the flexural stiffness values are normalized by gross section flexural stiffness (E_cI_g), in which Young's modulus of concrete (E_c) is computed from **Eq. 7-1** (ACI 318-14 Equation 19.2.2.1a) for normal strength concrete (NSC) and **Eq. 7-2** (ACI 363R-10) for high strength concrete (HSC). ACI CT-13 defines high strength concrete as concrete that has a specified compressive strength of 8000 psi or greater. However, **Eq. 7-1** is intended to only be used for concrete compressive strength up to 6000 psi. Therefore, the break point between normal and high

strength concrete was adopted as 6000 psi for the purpose of calculating E_c using tested f'_c. I_g is the gross section moment of inertia, for which presence of reinforcement in the cross-sections is ignored, consistent with the I_g definition given in ACI 369-17.

$$E_c = w_c^{1.5} 33\sqrt{f'_c \text{psi}} \left(= w_c^{1.5} 0.043\sqrt{f'_c \text{MPa}}\right) \quad \text{Normal strength concrete} \quad \text{(Eq. 7-1)}$$

$$E_c = 40000\sqrt{f'_c \text{psi}} + 10^6 \left(= 3320\sqrt{f'_c \text{MPa}} + 6900\right) \quad \text{High-strength concrete} \quad \text{(Eq. 7-2)}$$

Where w_c is unit weight of concrete, assumed to be equal to 150 pcf (24 kN/m^3) and 120 pcf (19.2 kN/m^3) for normal weight and light weight concrete, respectively.

7.3. Derivation of Wall Stiffnesses from Data in the Database

In this study, uncracked and effective "cracked" flexural stiffnesses of the walls in the dataset are derived from the experimental backbone curves, with some approximations and assumptions, as discussed below:

7.3.1. Uncracked Flexural Stiffness

Not to be confused with the gross sectional stiffness, the uncracked "or initial" stiffness (K_{uncr}) is defined as the slope of the backbone curve from *origin* to a point at which flexural cracking is first observed (reported). However, the deformation at *cracking* point shown in Fig. 7-1 includes shear deformation ($\delta_{cr,s}$). Therefore, the $\delta_{cr,s}$ corresponding to the base shear at flexural cracking was analytically computed using **Eq. 7-3** (assuming no shear cracking at this loading stage and thus using the gross shear stiffness, $G_g A_{cv}$) and is subtracted from the total experimental cracking deformation ($\delta_{cr,t}$) to obtain the cracking flexural deformation ($\delta_{cr,f}$) using **Eq. 7-4** (Fig. 7-3):

$$\delta_{cr,s} = \frac{V_{cr} h_w f}{A_{cv} G_g} \quad \text{(Eq. 7-3)}$$

$$\delta_{cr,f} = \delta_{cr,t} - \delta_{cr,s} \quad \text{(Eq. 7-4)}$$

Where V_{cr} is the base shear corresponding to cracking moment of the wall (experimental), h_w is the wall height, A_{cv} is the shear resisting (web) area of the wall ($=l_w t_w$), G_g is the gross shear modulus taken as $0.4E_c$, E_c is the concrete Young's modulus computed from **Eq. 7-1** or **Eq. 7-2** using tested f'_c, and f is a shape factor allowing the non-uniform distribution of shear stresses in the cross-section and is taken as 1.2 for rectangular sections and 1.0 for flanged or barbell-shaped sections.

The uncracked flexural stiffness ($E_c I_{uncr}$) is then computed as follows, for a cantilever wall (**Eq. 7-5**), as an example:

$$E_c I_{uncr} = \frac{V_{cr} h_w^3}{3\delta_{cr,f}} \quad \text{(Eq. 7-5)}$$

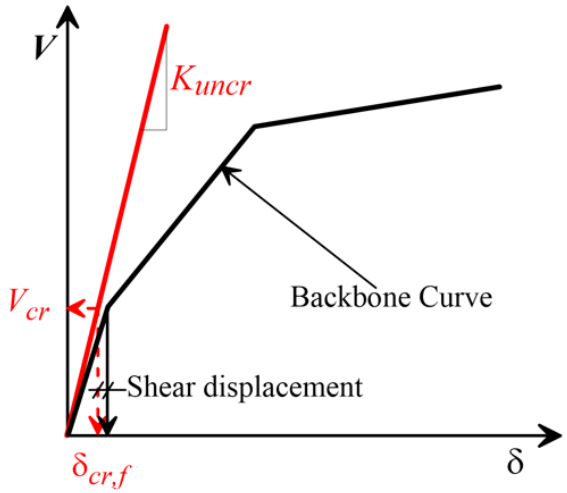

Fig. 7-3–Definition of uncracked flexural stiffness.

7.3.2. Effective "Cracked" Flexural Stiffness

The effective "cracked" stiffness (K_e) of concrete elements is typically defined as the slope of a straight line, passing through *origin* and a point on the experimental backbone curve at which first yielding of longitudinal reinforcement or the onset of concrete nonlinearity (i.e., maximum extreme fiber concrete compressive strain of 0.002) occurs, whichever is reached first. This is consistent with the definition of wall effective flexural stiffness given in ACI 369-17. However, as noted earlier, UCLA-RCWalls database contains total displacement and base shear at *general yield* ($\delta_{y,g}$, $V_{y,g}$), which is defined as the point where the hysteretic loops (or the response curve in case of monotonic loading) begin to abruptly lose stiffness, as shown in Fig. 7-3. Therefore, the *general yield* does not correspond to first yielding of longitudinal bars, but rather to yielding of most of the longitudinal bars at the boundary region in tension. Furthermore, the *general yield* displacement includes shear deformation. To account for these limitations, the following two simplifications were made:

1) The shear deformation ($\delta_{y,s}$) corresponding to the base shear at general yield are subtracted from the total deformation at general yield ($\delta_{y,g}$) using **Eq. 7-6** to obtain the flexural deformations ($\delta_{y,f}$) (curvature and bar slip/extension deformations):

$$\delta_{y,f} = \delta_{y,g} - \delta_{y,s} \quad \text{(Eq. 7-6)}$$

   Where $\delta_{y,s}$ is analytically approximated using **Eq. 7-7**, with an effective shear modulus of $G_g/3$ for all tests. This value was selected based on test results of 64 flexure-controlled walls for which the base shear-shear displacement backbones were available in the database. This 64-wall dataset was used to develop an effective shear modulus of $G_g/3$ for shear-cracked flexure-controlled walls, as discussed later.

$$\delta_{y,s} = \frac{V_{y,g} h_w f}{A_{cv}\left(G_g / 3\right)} \qquad \text{(Eq. 7-7)}$$

Fig. 7-4 shows the contribution of shear deformation to total deformation at general yield against normalized shear stress at general yield and test shear span ration (M/Vl_w), which indicates that shear displacement increases with increase in shear stress and with decrease in shear span ratio. This figure also shows that shear displacement contribution to total yield displacement ranges from 4% to 25% on average, which is reasonable for flexure-controlled walls.

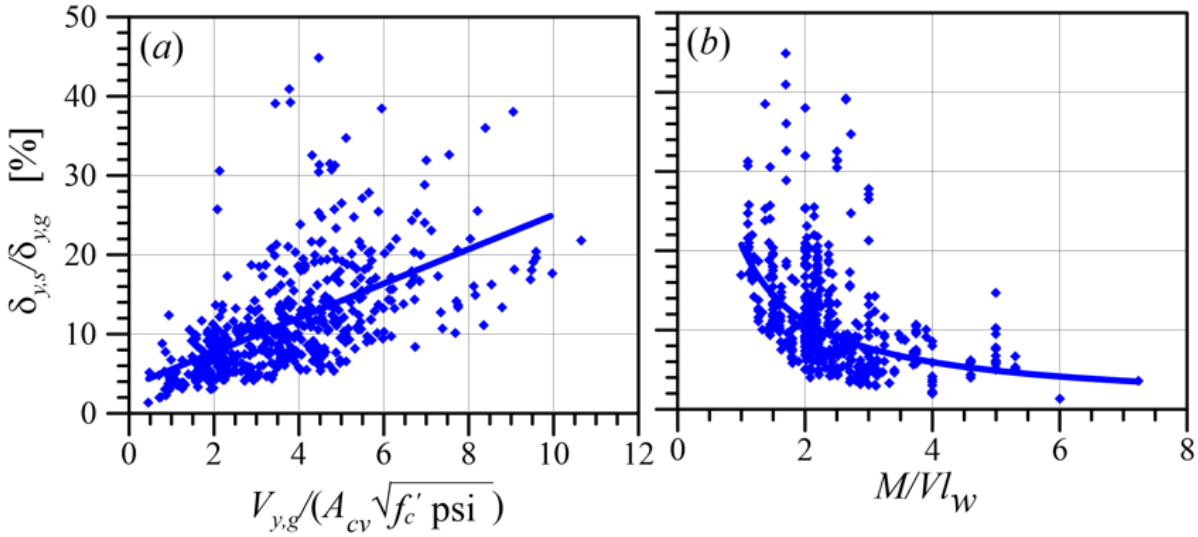

Fig. 7-4–Contribution of shear deformation to total deformation at general yield.

2) The flexural displacements at general yield ($\delta_{y,f}$) are reduced by 30% to approximately obtain effective stiffness (K_e) corresponding to first yield, as illustrated in Fig. 7-5. This approximation was verified against a subset of 20 wall tests for which the load and deformation

at first yield of longitudinal reinforcement was available (i.e., first yield identified from strain gage readings installed on longitudinal bars). Sensitivity of the results to higher and lower reduction factors was considered and found to be limited, as discussed later. Therefore, the effective flexural stiffness (E_cI_{eff}) is computed as follows for cantilever walls (**Eq. 7-8**), as an example:

$$E_c I_{eff} = \frac{V_{y,g} h_w^3}{3\left(0.7\delta_{y,f}\right)} \quad \text{(Eq. 7-8)}$$

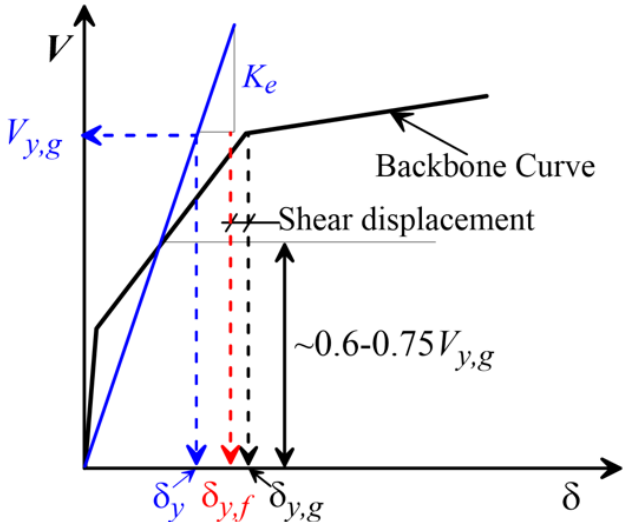

Fig. 7-5–Definition of effective first yield flexural stiffness.

The above approach to obtain E_cI_{eff} is similar to approaches used by other researchers for walls and other concrete elements (e.g., Elwood and Eberhard, 2009; Fenwick and Bull, 2000; Paulay and Priestley, 1992; Adebar et al., 2007) and ASCE/SEI 41-17, where effective stiffness is defined as a the slope of a line from *origin* passing through a point on the response curve corresponding to 0.6 to 0.75 $V_{y,g}$.

7.4. Parameters Influencing Wall Flexural Stiffness

7.4.1. Uncracked Flexural Stiffness

To identify parameters that likely have a significant influence on E_cI_{uncr}, review of available literature and a series of linear regression analyses were conducted. It was found that the most influential parameter is axial load ratio, $P/(A_g f'_c)$, with a correlation coefficient (R) of 0.58, as shown in Fig. 7-6(***a***). This is because presence of axial load leads to increase in cracking moment capacity, while cracking curvature is not influenced by axial load. It can be seen from Fig. 7-6(***a***) that uncracked flexural stiffness ranges (on average) from 0.50 to 1.40 of the gross section stiffness (E_cI_g) as $P/(A_g f'_c)$ increases from 0 to 0.60. The low values, which are mostly for walls with low to moderate $P/(A_g f'_c)$, might be due to the influence of microcracks and shrinkage. The values of $E_cI_{uncr}/E_cI_g > 1.0$ might be due to presence of longitudinal reinforcement in the cross-section that is ignored in computing I_g.

Concrete compressive strength (f'_c) has some influence on E_cI_{uncr} because of its influence on tension stiffening, elastic modulus, and modulus of rupture. However, the influence, with an R of 0.23, is not significant (Fig. 7-6(***b***)) and is already included in the $P/(A_g f'_c)$ parameter.

Fig. 7-6(***c***) indicates that M/Vl_w has a significant influence on E_cI_{uncr}; however, this is not a causal relationship. This is due to the fact that most slender walls (with high M/Vl_w) have moderate to high axial loads, as indicated by Fig. 7-6(***c***). Therefore, the parameter that drives the trend in Fig. 7-6(***c***) is $P/(A_g f'_c)$, not M/Vl_w.

It should be noted that for most walls in the dataset, cracking deformation is very small (ranging from <1 to 2.5 mm), and that accurate measurement of such small displacements is difficult.

Additionally, this damage state in the database is based on visual observation of first flexural cracks reported by the authors who conducted the tests, which might include some subjectivity. These two factors, among others, might contribute to the significant dispersion of the data.

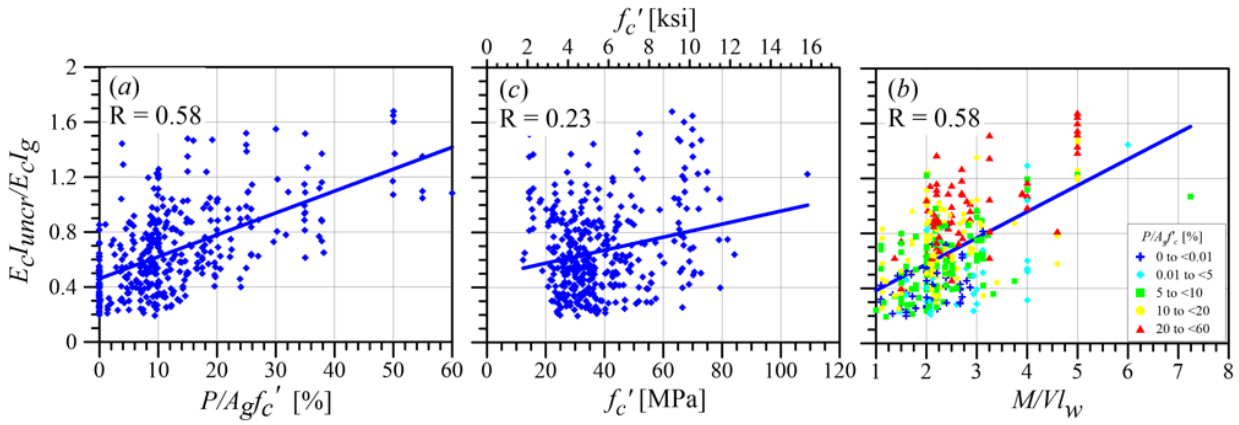

Fig. 7-6–Influence of parameters on E_cI_{uncr}. (Note: R=correlation coefficient)

7.4.2. Effective "Cracked" Flexural Stiffness

Parameters that were found to produce low to significant influence on E_cI_{eff} are $P/(A_gf'_c)$, yield strength and quantity of longitudinal reinforcement in the boundary region (f_y and $\rho_{l,BE}$), and f'_c, as shown in **Fig. 7**. The influence of axial load on stiffness of concrete members is widely recognized in many research studies and design codes/guidelines (e.g., Elwood and Eberhard, 2009; Khuntia and Ghosh, 2004a; Fenwick and Bull, 2000; Adebar et al., 2007; NZS 3101: Part 2:2006; ACI 318-14 Table 6.6.3.1.1*b*). As shown in Fig. 7-7(***a***), $P/(A_gf'_c)$ has the strongest correlation with E_cI_{eff}, with an R of 0.82. The trend shown in Fig. 7-7(***a***) is similar to that observed by Elwood and Eberhard (2009) for columns.

Increase in longitudinal reinforcement ratio in the tension zone ($\rho_{l,BE}$) results in spread of yielding and development of secondary cracks over a larger height of the wall as opposed to a one or two major cracks at or near the critical section. Furthermore, doubling $\rho_{l,BE}$, assuming everything else is constant, would be expected to have little influence on yield curvature (ϕ_y) since ϕ_y is primarily a function of wall length and reinforcement yield strain, i.e., $\phi_y \approx 2f_y/l_wE_s$ or $\phi_y \approx$ (0.0025 to 0.0035)/l_w (Thomson and Wallace 2004), but would theoretically be expected to approximately double the yield flexural strength and thereby increase E_cI_{eff} by the same amount (ATC-72, 2010). It is this reasoning that gives rise to the concept of "stiffness is proportional to strength" (Priestley and Kowalsky, 1998; Priestley et al., 2007; Paulay, 2002). However, the trend in Fig. 7-7(***b***) does not show that big of an influence as the above concept suggests, even for slender walls. This is likely due to: 1) the influence of other parameters (e.g., axial load) which cause large dispersion in the data, and 2) with increase in $\rho_{l,BE}$, the wall flexural strength increases, which results in flexural cracking spreading over a larger zone along the wall height from the foundation support. This stiffness loss reduces the stiffness gain due to large $\rho_{l,BE}$ in the lower portions of the wall. Fig. 7-7(***c***) shows that the influence of $\rho_{l,BE}$ on E_cI_{eff} is more pronounced for walls subjected to low-to-moderate $P/(A_gf'_c)$.

Yield strength of longitudinal reinforcement (f_y) has a limited influence on E_cI_{eff} since f_y is one of the factors affecting both first yield moment and curvature (i.e., $\phi_y \approx 2f_y/l_wE_s$). Walls with high yield strength reinforcement have higher yield moment and higher yield curvature (due to higher yield strain) and, consequently, the value of E_cI_{eff} is insensitive to changes in f_y, as shown in Fig. 7-7(***d***).

Use of high strength concrete modestly increases E_c, tension stiffening, tensile strength, and wall flexural strength. However, the impact of f'_c on E_cI_{eff}/E_cI_g is statistically insignificant, as shown in Fig. 7-7(***e***)**.** The influence of f'_c is more noticeable on E_cI_{uncr} than E_cI_{eff}.

Fig. 7-7(***f***) shows the combined influence of f'_c, f_y, and $\rho_{l,BE}$ on E_cI_{eff}, with an R of 0.29, which does not improve the correlation compared to the influence of $\rho_{l,BE}$ alone in Fig. 7-7(***b***).

Fig. 7-8 presents sensitivity of E_cI_{eff} to the reduction factor used in **Eq. 7-8** to convert secant stiffness corresponding to general yield to effective stiffness corresponding to first yield. Given the dispersion in the data and other uncertainties (i.e., modeling and loading), change in this reduction factor does not produce significant changes. Therefore, the 0.7 reduction factor was adopted in this study to compute E_cI_{eff}, which was backed by some limited experimental data, as noted earlier.

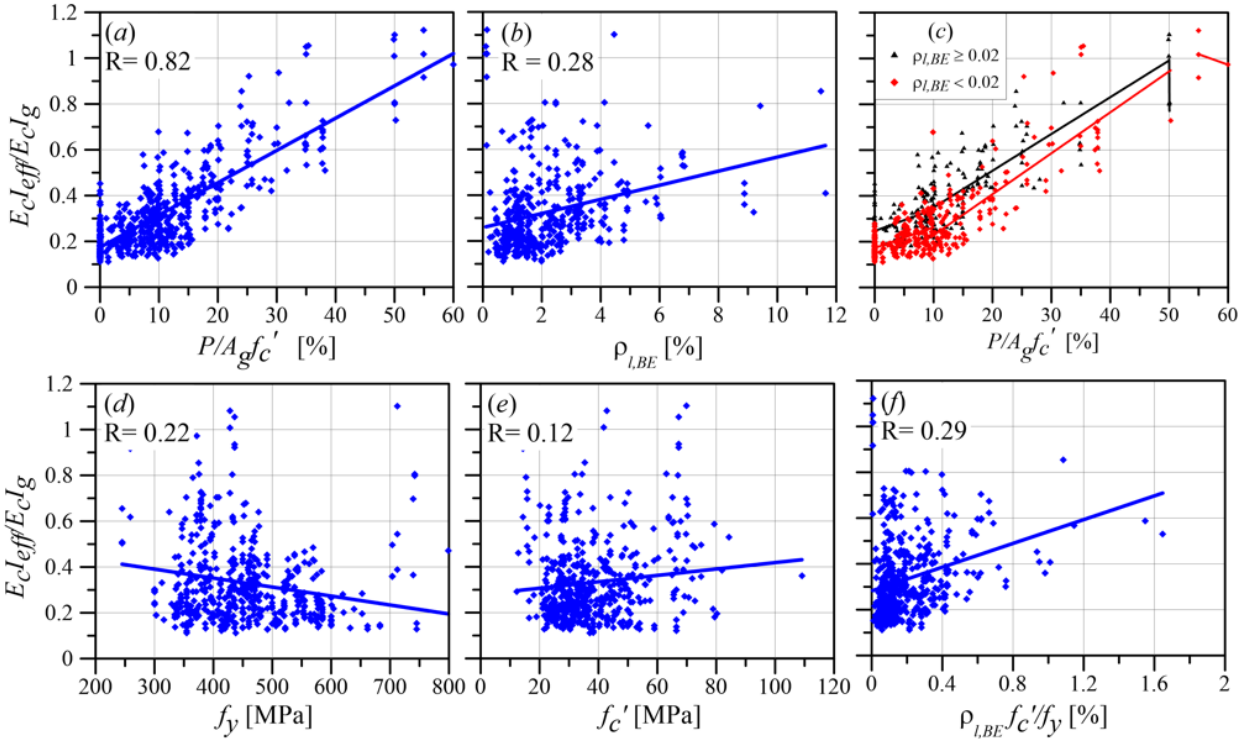

Fig. 7-7–Influence of key parameters on E_cI_{eff}. (Note: R=correlation coefficient)

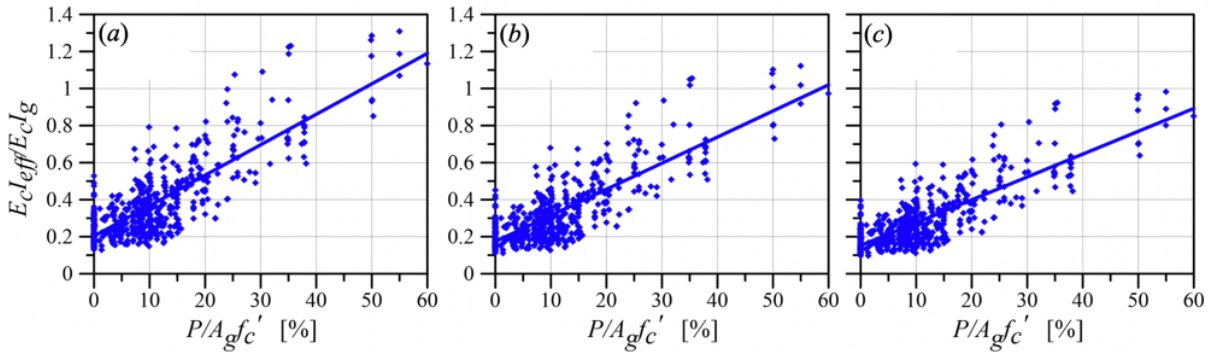

Fig. 7-8–Sensitivity of E_cI_{eff} to the reduction factor used in **Eq. 7-8**: a) 0.6, b) 0.7, and c) 0.8.

7.5. Provisions and Commentary of ACI 369-17

As noted earlier, ACI 369-17 §7.2.2 Table 5 allows wall $E_{cE}I_{eff}$ to be calculated as 35% of the gross flexural stiffness (**Eq. 7-9**):

$$E_{cE}I_{eff} = 0.35\ E_{cE}I_g \quad \text{(Eq. 7-9)}$$

Where E_{cE} is modulus of elasticity of concrete evaluated using expected material properties and I_g is the moment of inertia of gross concrete section about centroidal axis, neglecting reinforcement.

Three alternative approaches to compute $E_{cE}I_{eff}$ are given in the commentary of the standard (C7.2.2). For flexural deformations without the effect of bond slip, $E_{cE}I_{eff}$ can be calculated in accordance with **Eq. 7-10** (ACI 369-17 Eq. C5):

$$E_c I_{eff} = \frac{M_{yE}}{\phi_{yE}} \quad \text{(Eq. 7-10)}$$

Where M_{yE} is the yield moment strength evaluated per ACI 318-14 using expected material properties and applied sustained gravity axial load ($\boldsymbol{N_{UG}}$), and ϕ_{yE} is the curvature associated with M_{yE} and can be approximated as $\phi_{yE} = 2f_{ylE}/l_w E_s$ for planar walls with $N_{UG}/(A_g f'_{cE}) \leq 0.15$ and $\rho_l \leq 0.01$, where f_{ylE} and E_s are the expected yield strength and Young's modulus of the longitudinal reinforcement, respectively. Alternatively, $E_{cE}I_{eff}$ can be computed from analytical moment-curvature analysis of the cross-section using **Eq. 7-11** (ACI 369-17 Eq. C6).

$$E_c I_{eff} = \frac{M_{fyE}}{\phi_{fyE}} \quad \text{(Eq. 7-11)}$$

Where M_{fyE} and ϕ_{fyE} are respectively the moment and curvature at first yield, defined when the yield strain of the reinforcing steel is first reached in tension, or a concrete strain of 0.002 is reached in compression and evaluated using expected material properties and $\boldsymbol{N_{UG}}$.

For continuous walls, ACI 369-17 C7.2.2 provides an approach for capturing the effects of bond slip, where a reduction factor is used to modify $E_{cE}I_{eff}$ of the wall in the story directly above the wall-foundation interface (hinge region) as follows:

$$E_c I_{eff} = \frac{M_{fyE}}{\phi_{fyE}} \left(\frac{h_1}{h_1 + l_{sp}} \right) \quad \text{(Eq. 7-12)}$$

Where h_1 is the first-floor height and l_{sp} is the strain penetration depth, which is intended to approximate the length over which longitudinal reinforcement strains penetrate into the foundation system and is approximated as (**Eq. 7-13**):

$$l_{sp} = \frac{1}{48} \frac{f_{ylE}}{\sqrt{f'_{cE}}} d_b \quad \text{(Eq. 7-13)}$$

ACI 369-17 C7.2.2 provides lower and upper bounds on $E_{cE}I_{eff}$ obtained from **Eq. 7-9** through **Eq. 7-12**, which are $0.15E_{cE}I_g$ and $0.5E_{cE}I_g$, respectively.

Finally, ACI 369-17 §7.2.2 Table 5 allows wall shear stiffness to be calculated as "uncracked" gross shear stiffness (**Eq. 7-14**):

$$G_{eff}A_w = G_g A_w = 0.4\ E_c A_w \quad \text{(Eq. 7-14)}$$

Where G_g is concrete gross shear modulus taken as $0.4E_{cE}$, and A_w is area of the wall web cross section.

7.6. Evaluation of Provisions and Commentary of ACI 369-17

The effective flexural stiffness values (E_cI_{eff}) of the 527-wall dataset, as defined in Fig. 7-5, are used to evaluate the ACI 369-17 stiffness provisions and recommendations summarized in the

preceding section. Table 7-1 presents the statistics of the predicted (calculated) E_cI_{eff} values from **Eq. 7-9** through **Eq. 7-12**, normalized by the E_cI_{eff} values from the 527-wall dataset (ratios of calculated-to-experimental E_cI_{eff} values). Fig. 7-9 through Fig. 7-12 present comparison of the calculated and the experimental E_cI_{eff} results. Discussion of the results are given below.

Fig. 7-9(***a***) shows that Fig. 7-9 significantly overestimates E_cI_{eff} at low axial loads ($P/(A_g f'_c) < 0.05$) and significantly underestimates E_cI_{eff} at high axial loads ($P/(A_g f'_c) > 0.20$), with significant dispersion (Table 7-1) because taking E_cI_{eff} as a constant fraction of E_cI_g ignores the influence of key parameters highlighted earlier.

Table 7-1–Statistics of the ratios of predicted-to-experimental E_cI_{eff}/E_cI_g values.

Equation	**Eq. 7-9**	**Eq. 7-10**	**Eq. 7-11**[(1)]	**Eq. 7-12**	
				(a)[(2)]	**(b)**[(3)]
Mean	1.33	1.16	1.12	0.93	1.02
STDV	0.59	0.39	0.35	0.28	0.31
COV	0.44	0.34	0.31	0.31	0.30
Max	3.15	2.74	2.32	1.98	2.13
Min	0.31	0.32	0.28	0.25	0.27
Median	1.26	1.09	1.08	0.9	0.97

[(1)] ϕ_{yE} is computed as $2f_{ylE}/l_wE_s$
[(2)] l_{sp} calculated from **Eq. 7-13** multiplied by 2.0 to account for the influence of reduced scale.
[(3)] l_{sp} calculated from **Eq. 7-13** multiplied by 1.0 to account for the influence of reduced scale.

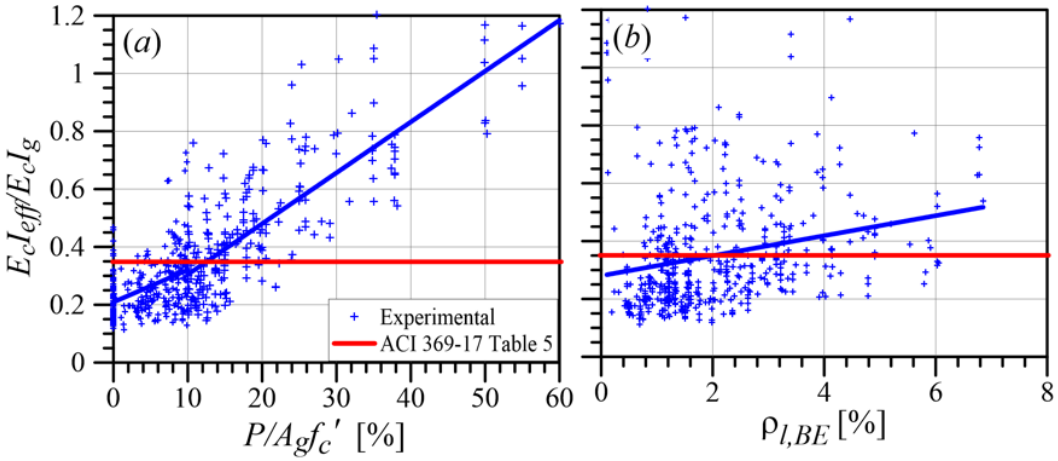

Fig. 7-9–Comparison of calculated (**Eq. 7-9**) and experimental E_cI_{eff}.

Fig. 7-10(***a***) indicates that for walls with $P/(A_gf'_c) < 0.15$, use of **Eq. 7-10** results in moderate overestimation of E_cI_{eff}, with high dispersion. This is attributed to the fact that with decrease in $P/(A_gf'_c)$, depth of neutral axis reduces and, consequently, the stress in the tension reinforcement increases, which results in larger lateral displacement contributed by bar slip/extension from the foundation that is not captured by moment-curvature analysis of the cross-section. Motter et al. (2018) observed 15 to 35% reduction in E_cI_{eff} as a result of slip/extension of longitudinal reinforcement from the foundation block for walls subjected to $P/(A_gf'_c) < 0.05$. For higher $P/(A_gf'_c)$ values, the contribution of slip/extension from the foundation could approach zero (e.g., see Elwood and Eberhard, 2009 for columns), and the wall might locate above the balance point on the P-M interaction diagram, which would result in a reduction in nominal moment capacity. Another factor is that the concrete stress-strain model used to compute nominal moment capacity does not incorporate the influence of concrete confinement. Given that most walls with high $P/(A_gf'_c)$ are likely to have some level of confinement, computing nominal moment capacity without the influence of confinement might slightly underestimate the nominal moment capacity and, thus, result in underestimation of effective stiffness.

Additionally, Fig. 7-10(***b***) indicates that use of **Eq. 7-10** for walls with high $\rho_{l,BE}$ (i.e., > 0.02) results in a slight overestimation of E_cI_{eff}. This could be attributed to the fact that increase in $\rho_{l,BE}$ helps spread of yielding not just over a larger height of the wall but also into the foundation support, which means more contribution from bar slip deformation to yield displacement.

Eq. 7-11, which is based on analytical moment and curvature corresponding to first yield, produces similar results as **Eq. 7-10**, as seen in Fig. 7-11 and Table 7-1, with slightly less overestimation and dispersion at $P/(A_g f'_c) < 0.15$. This is because the results indicate that the ratios M_{yE} to M_{fyE} (nominal/first yield) and ϕ_{yE} to ϕ_{fyE} are approximately the same (i.e., ≈1.24). The factors leading to the offsets between the calculated and experimental results are discussed in the preceding paragraphs for results from **Eq. 7-10**.

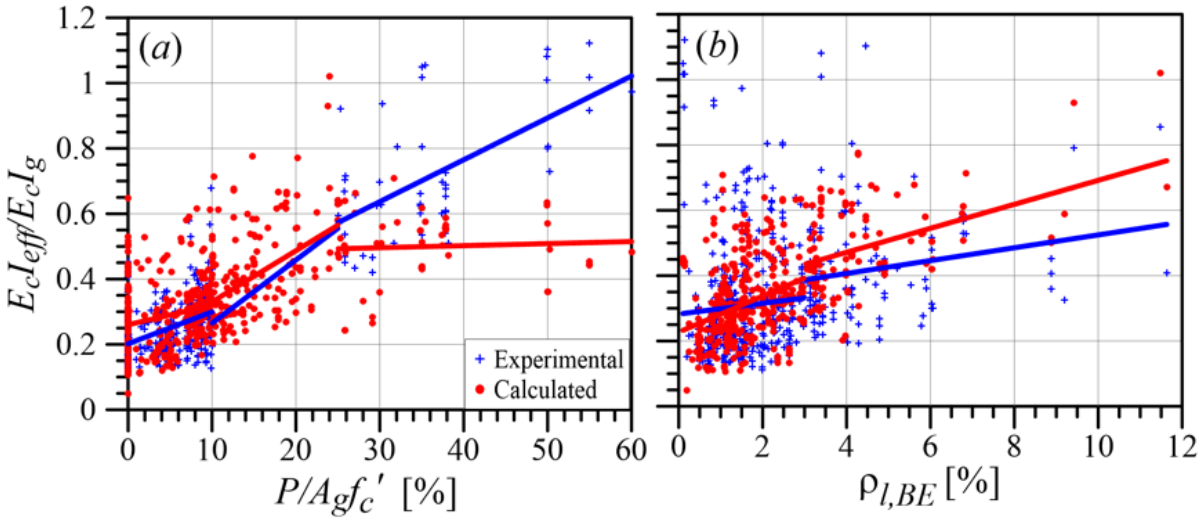

Fig. 7-10– Comparison of experimental and calculated (**Eq. 7-10**) E_cI_{eff}.

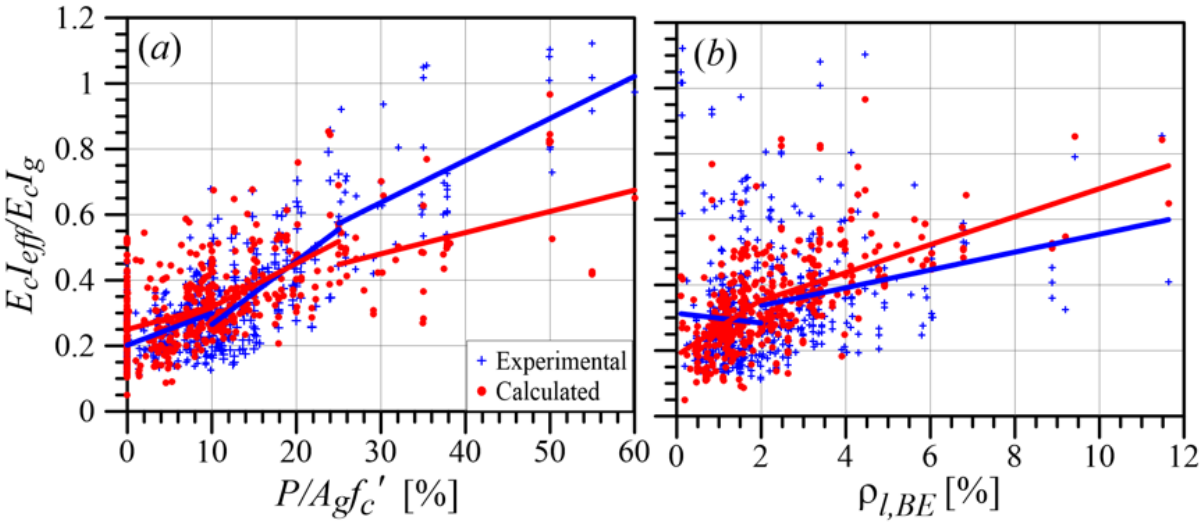

Fig. 7-11– Comparison of experimental and calculated (**Eq. 7-11**) E_cI_{eff}.

It may not be appropriate to evaluate **Eq. 7-12**, which includes a reduction factor to account for the influence of bond slip on effective stiffness, using results from the dataset described here because: 1) the reduction factor includes h_1 (first story height), while most tests in the dataset do not have a prototype wall and the database does not include story heights, 2) walls are typically tested in laboratories at reduced scales, where in addition to geometry, bar sizes are scaled down, which influences the contribution of slip/extension deformation to yield deformation and, consequently, the l_{sp} (strain penetration depth) calculated from **Eq. 7-13**. To account for these limitations, two assumptions were made: 1) h_1 is taken as 7 ft, which, assuming a one half-scale for all wall tests results in h_1 =14 ft for a full-scale prototype wall, 2) the l_{sp} calculated from **Eq. 7-13** is multiplied by a factor of 2.0, assuming again a one-half scale for the walls, to account for the reduced scale of the bars. Furthermore, the l_{sp} calculated from **Eq. 7-13** multiplied by a factor of 1.0 was also considered to highlight the sensitivity of the results to l_{sp}.

The results are presented in Table 7-1 and Fig. 7-12. Considering the assumptions made, it can be seen that **Eq. 7-12** produces results that are in good agreement with the experimental results at $P/(A_g f'_c) < 0.15$ or 0.20. For walls with high $P/(A_g f'_c)$, applying this reduction factor leads to further underestimation of $E_c I_{eff}$ relative to **Eq. 7-10** and **Eq. 7-11** because, as noted previously, these walls likely experience no or little bar slip/extension. Therefore, no reduction factor should be considered for such walls. Furthermore, Fig. 7-12 reveals that the results are only slightly sensitive to the strain penetration depth (l_{sp}).

To conclude, **Eq. 7-9** through **Eq. 7-11** overestimate $E_c I_{eff}$ by 12% to 33%, with moderate dispersions. **Eq. 7-12** produces results whose median values better match the experimental results and whose dispersion is comparable to **Eq. 7-10** and **Eq. 7-11**; however, these equations require a fair amount of calculations to compute $E_c I_{eff}$. Therefore, simplified $E_c I_{eff}$ values are proposed in the subsequent sections.

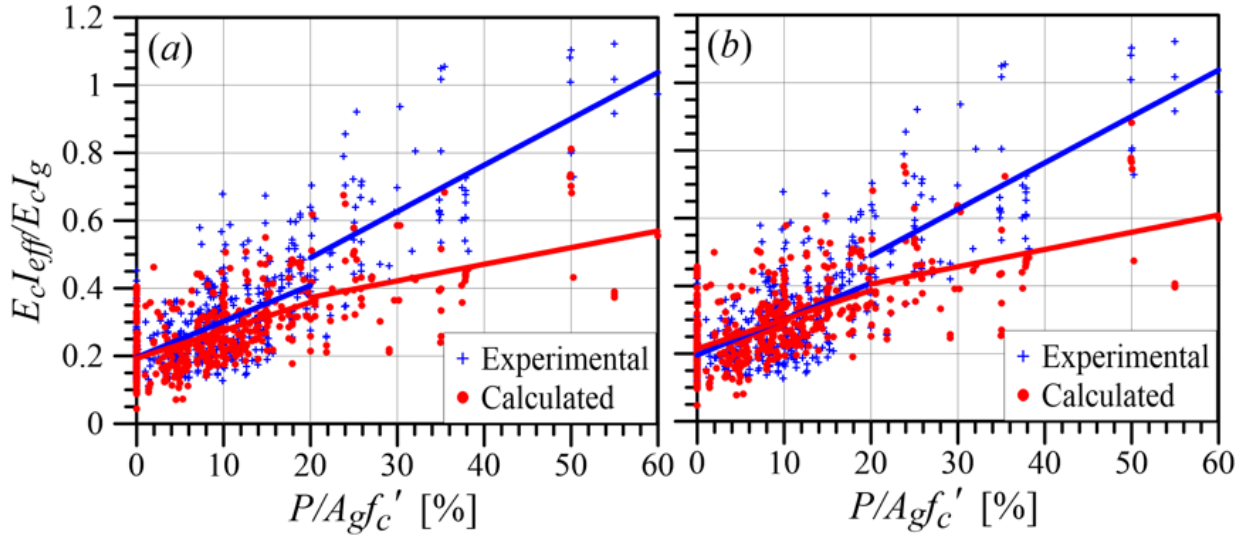

Fig. 7-12– Comparison of experimental and calculated (**Eq. 7-12**) $E_c I_{eff}$ considering an h_1 of 7 ft for one-half scale (14 ft for full scale) where l_{sp} calculated from **Eq. 7-13** and multiplied by: (***a***) 2.0, (***b***) 1.0.

7.7. Proposed Models for Flexural and Shear Stiffnesses

7.7.1. Uncracked Flexural Stiffness, E_cI_{uncr}

Flexural cracking occurs where the moment demand exceeds the cracking moment strength calculated using the modulus of rupture provided in ACI 318-14 and the expected material properties.

Based on the results presented earlier, the model shown in Fig. 7-12 (black line) is proposed, for which E_cI_{uncr}/E_cI_g ranges on average from 0.50 to 1.00 for $P/(A_gf'_c)$ increasing from 0 to 0.30. This model results in a mean and COV of 1.12 and 0.42, respectively. The results of Fig. 7-13 are presented in a tabulated format in Table 7-2. If the walls with no axial load are excluded, the blue trend line will move closer to the model (black line).

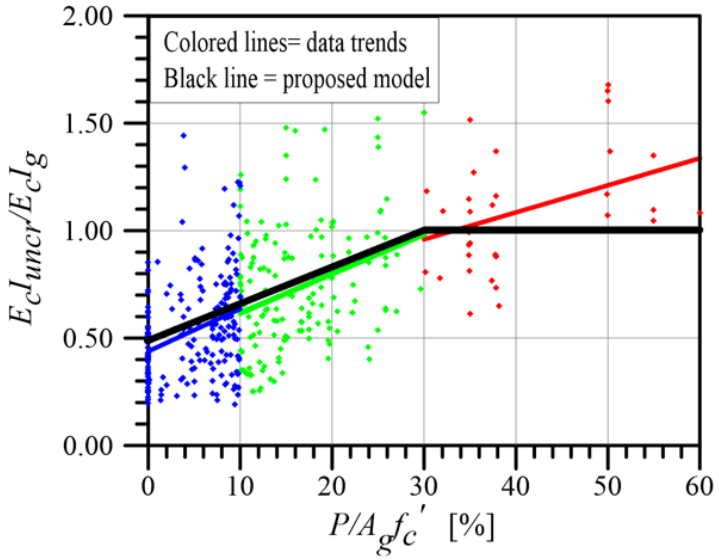

Fig. 7-13– Linear regression lines to the data and the proposed model for E_cI_{uncr}. (black line = model).

Table 7-2–Proposed values for uncracked wall flexural stiffness (E_cI_{uncr})

$\frac{P}{A_g f'_c}$	$\frac{E_C I_{uncr}}{E_C I_g}$ *
≤ 0.00	0.50
≥ 0.30	1.00

* Values between those listed should be determined by linear interpolation

As noted earlier, ACI 369-17 currently does not provide provisions to estimate wall flexural stiffness for cases where little to no cracking is expected to occur. Such provisions, however, can be found in other codes and documents (i.e., ACI 318-14 Table 6.6.3.1.1a; CSA A23.3-14; FEMA 356 Table 6-5; NZS 3101: Part 2:2006; Eurocode 8-2004). For comparison with the proposed model, these existing models were reviewed and evaluated using the dataset (Table 7-3).

Table 7-3–Existing models for uncracked or minorly cracked wall flexural stiffness

Model	ACI 318-14-Table 6.6.3.1.1a CSA A23.3-14	FEMA 356 Table 6-5	NZS 3101: Part 2:2006 Serviceability limit (μ=1.25)	NZS 3101: Part 2:2006* Serviceability limit (μ=3)	Eurocode 8-2004	PEER/TBI-10* LATBSDC-14 (Service level)	Proposed Model
$\frac{E_c I_{uncr}}{E_c I_g} =$	0.7	0.8	1.0	$0.7 \geq \left(0.5 + \frac{P}{A_g f'_c}\right) \geq 0.5$	0.5	0.75	$1.0 \geq \left(0.5 + \frac{P}{A_g f'_c}\right) \geq 0.5$
Mean	1.32	1.51	1.89	1.11	0.95	1.42	1.12
STDV	0.65	0.75	0.93	0.49	0.47	0.70	0.38
COV	0.49	0.49	0.49	0.44	0.49	0.49	0.42
MAX	3.65	4.17	5.21	3.09	2.60	3.91	3.42
MIN	0.42	0.48	0.60	0.37	0.30	0.45	0.39
Median	1.17	1.33	1.66	1.01	0.83	1.25	1.07

* A minor level of cracking is expected.

7.7.2. Effective "Cracked" Flexural Stiffness, E_cI_{eff}

As noted previously, $P/(A_g f'_c)$ is the most influential parameter on wall E_cI_{eff}. Therefore, a model, which takes the form of a piece-wise line, seems to fit the regression lines well, as shown in Fig. 7-14, where the colored lines are regression lines of the data and the black line is the simple model. The model is also shown in a tabulated format in Table 7-4.

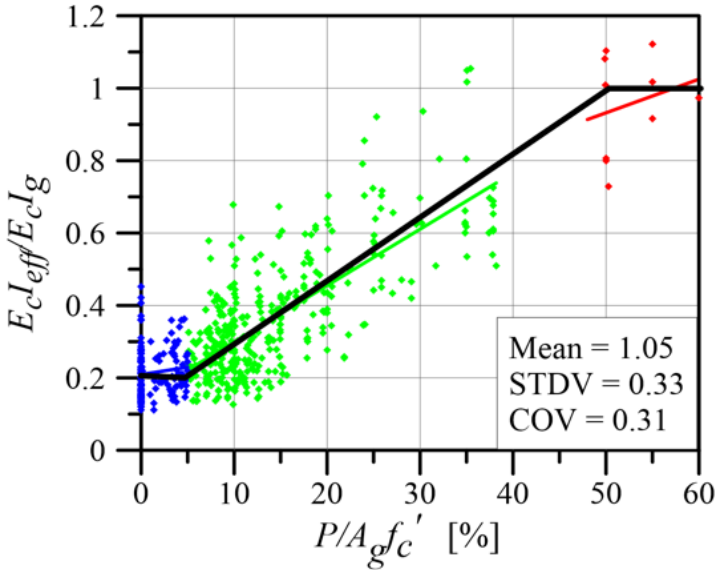

Fig. 7-14–Linear regression lines to the data and the proposed model for E_cI_{eff}. (black line = model).

Table 7-4–Proposed values for effective flexural stiffness (E_cI_{eff})

$\frac{P}{A_g f'_c}$	$\frac{E_c I_{eff}}{E_c I_g}^*$
≤ 0.05	0.20
≥ 0.50	1.00

* Values between those listed should be determined by linear interpolation

A more detailed model that includes the $\rho_{l,BE}$ as a secondary parameter in addition to axial load is presented in **Eq. 7-17** and Table 3-1. Using this refined model is slightly more accurate, especially for walls with low to moderate axial loads. As seen in Fig. 7-15(***b***), the mean E_cI_{eff} for walls with $P/(A_g f'_c) \leq 0.20$ increases by factors of about 1.5 to 2 when $\rho_{l,BE}$ increases from 0.01 to 0.03.

$$\frac{E_c I_{eff}}{E_c I_g} = 0.1 + 1.5\frac{P}{A_g f_c^{'}} + 3.5\rho_{l,BE} \leq 1.0 \qquad \text{(Eq. 7-17)}$$

Comparison of predicted (**Eq. 7-17**) and experimentally obtained E_cI_{eff}, along with the statistics, are presented in Fig. 7-16. The comparison indicates that the detailed model only modestly reduces the prediction error compared to the simplified model (Fig. 7-14).

Table 7-5–Proposed values for E_cI_{eff} as a function of $P/(A_g f'_c)$ and $\rho_{l,BE}$

$\frac{P}{A_g f'_c}$	$\rho_{l,BE}$	$\frac{E_c I_{eff}}{E_c I_g}^{*}$
≤ 0.05	≥ 0.01	0.20
	≤ 0.03	0.30
≥ 0.50	≥ 0.01	0.90
	≤ 0.03	1.00

* Values between those listed should be determined by linear interpolation

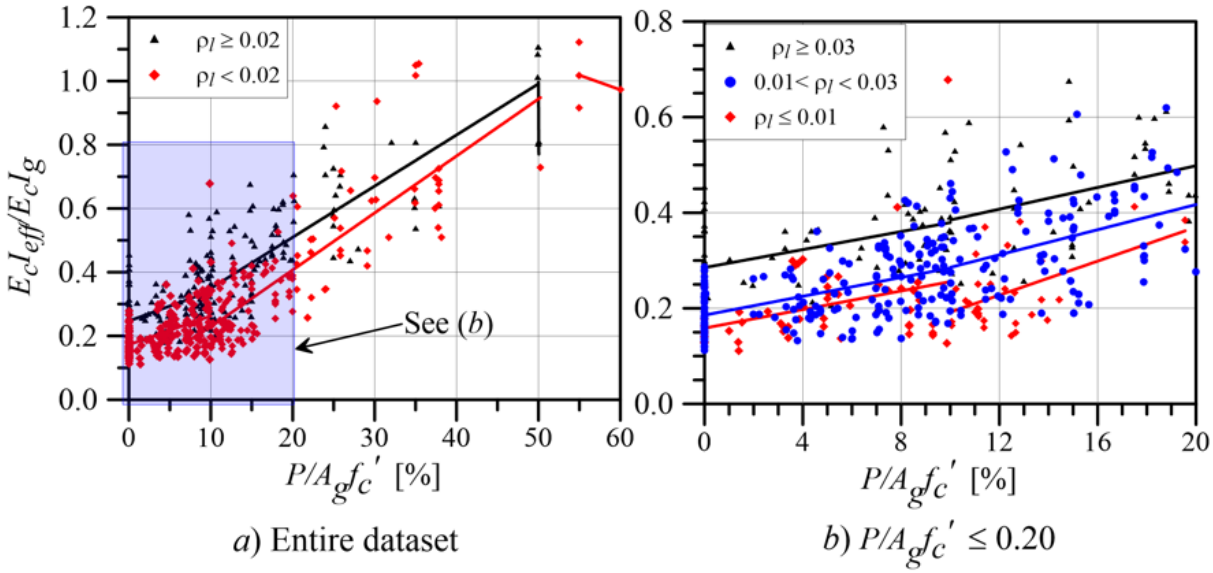

Fig. 7-15–Influence of longitudinal reinforcement ratio ($\rho_{l,BE}$) on E_cI_{eff}.

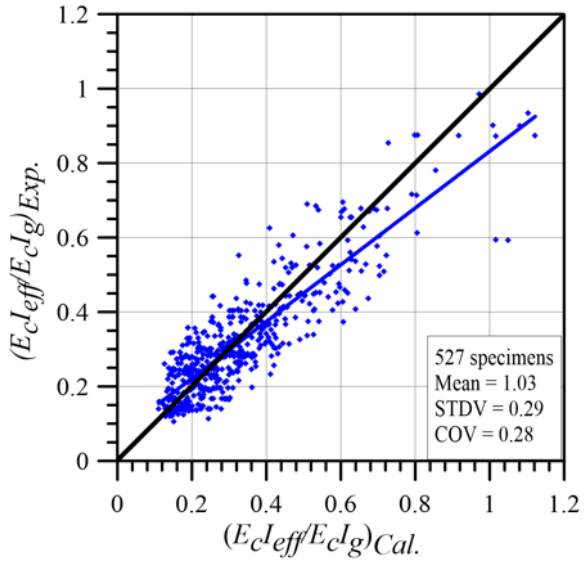

Fig. 7-16–Comparison of experimental and calculated E_cI_{eff} from **Eq. 7-17**.

7.7.3. Uncracked Shear Stiffness

Shear cracking is assumed to occur where the wall shear stress demand exceeds $2\sqrt{f_c'\,(\text{psi})}$. For upper stories of a flexure controlled wall where shear demands are < $2\sqrt{f_c'\,(\text{psi})}$, it is proposed that the shear response of the wall be modeled using the gross shear modulus (G_g) taken as $0.4E_{cE}$.

7.7.4. Cracked Shear Stiffness

The dataset of flexure-controlled wall tests described earlier was filtered to identify walls whose base shear-shear deformation backbones were available. A reduced dataset of 64 wall tests was obtained. For the reduced dataset, the effective shear modulus (G_{eff}) was computed using **Eq. 7-18**:

$$G_{eff} = \frac{V_{y,g} h_w f}{A_{cv} \delta_{y,s}} \qquad \text{(Eq. 7-18)}$$

Where $V_{y,g}$ and $\delta_{y,s}$ are the experimental base shear at general yield and the corresponding shear displacement, respectively.

Fig. 7-17 shows G_{eff} of the dataset normalized by the gross shear modulus (G_g) taken as $0.4E_c$. Note that shear stress at general yield for all walls exceeded the cracking shear strength of concrete [$V_c = 2\sqrt{f'_c}$ (psi)]. Based on the results of Fig. 7-17, a constant G_{eff} of $G_g/3$ is proposed to be used to model shear response of flexure-controlled walls.

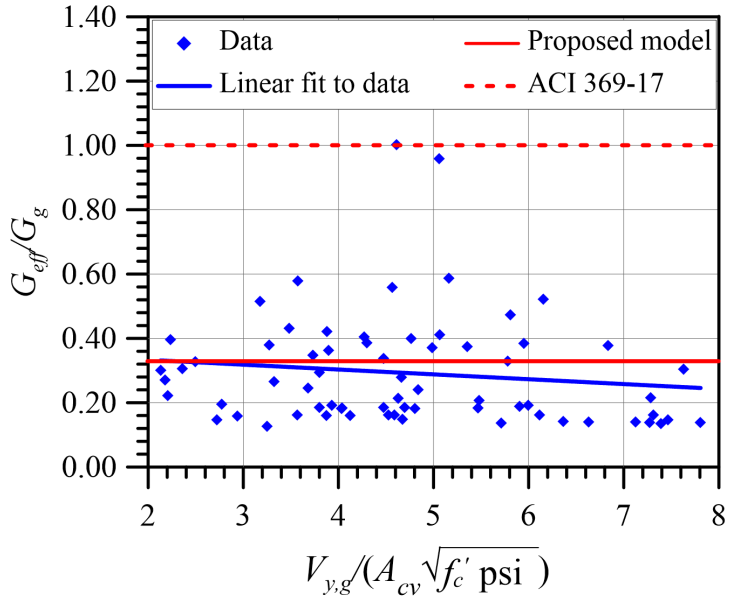

Fig. 7-17–Effective shear modulus results from 64 wall tests.

7.8. Summary and Conclusions

This study involves utilizing available experimental data on RC structural walls to develop updated stiffness provisions for seismic evaluation and retrofit of flexure-controlled reinforced concrete structural walls in ACI 369 and ASCE 41 standards. To accomplish these objectives, a subset of 527 test of flexure-controlled walls was filtered from UCLA-RCWalls database. The datasets were first used to evaluate the current stiffness provisions of ASCE 41-17 (ACI 369-17), and the results revealed that 1) use of a constant value of "cracked" effective flexural stiffness (i.e, $E_{cE}I_{eff} = 0.35E_{cE}I_g$) does not adequately consider variables that influence wall effective flexural stiffness and 2) use of 100% of the gross "uncracked" shear stiffness ($0.4E_{cE}A_w$) to model shear response in flexure-controlled walls overly estimates shear stiffness. Subsequently, the dataset was studies to identify parameters that significantly influence uncracked and cracked effective flexural and shear stiffnesses. It was found that axial load has the greatest impact on wall flexural stiffness (uncracked and cracked), and that longitudinal reinforcement ratio produced significant impact on cracked

effective flexural stiffness at low axial load ratios (i.e., <0.10 $A_g f'_c$). Based on these results, wall flexural stiffness values (cracked and uncracked) are proposed. Based on results from a subset of 64 wall tests whose base shear-shear deformation backbones were available in the database a constant effective shear modulus of one-third of gross shear modulus (i.e., $G_{eff} = G_g/3$) is proposed to be used to model shear response of shear-cracked flexure-controlled walls.

7.9. Acknowledgements

Funding for this study was provided, in part, by ATC 140 Project, and the University of California, Los Angeles. The authors would also like to thank the other member of Working Group 3 (WG3) of ATC 140 Project, which include Wassim Ghannoum, Garrett Hagen, Mohamed Talaat, Laura Lowes, and Afshar Jalalian for providing thoughtful comments on the work presented. Any opinions, findings, and conclusions or recommendations expressed in this paper are those of the authors and do not necessarily reflect the views of others mentioned here.

7.10. References

Abdullah S. A., and Wallace J. W., 2018a. UCLA-RCWalls: A database for reinforced concrete structural wall tests, *Earthquake Spectra*, submitted for review and possible publication, Oct 26, 2018, 23pp.

Abdullah, S. A., and Wallace, J. W., 2018b "UCLA-RCWalls database for reinforced concrete structural walls," *Proceedings, 11th National Conference in Earthquake Engineering*, Earthquake Engineering Research Institute, Los Angeles, CA.

ACI Committee 318. (2014). Building Code Requirements for Structural Concrete (ACI 318-14) and Commentary (ACI 318R-14), American Concrete Institute, Farmington Hills, MI. 524 pp.

ACI Committee 363. (2010). Report on high strength concrete (Report ACI 363R-10), American Concrete Institute, Farmington Hills, MI, 75 pp.

ACI CT, 2013. ACI Concrete Terminology–an ACI Standard. American Concrete Institute, Farmington Hills, MI, 65 pp.

Adebar, P., Ibrahim, A.M.M., and Bryson, M., 2007 "Test of high-rise core wall: Effective stiffness for seismic analysis", *ACI Structural Journal*, vol. 104, pp. 549-559.

ASCE/SEI Standard 41-13, Seismic Rehabilitation of Existing Buildings. American Society of Civil Engineers, Reston, VA. 518 pp.

ATC, *Modeling and Acceptance Criteria for Seismic Design and Analysis of Tall Buildings*, *ATC-72*, Applied Technology Council, Berkeley, California, 2010.

CEN, *Eurocode 8: "Design of Structures for Earthquake Resistance, Part 1: General Rules, Seismic Actions and Rules for Buildings*, *ENV 1998-1:2003"*, Comité Européen de Normalisation, Brussels, Belgium, 2004.

CSA Committee, "*Design of Concrete Structures*, *CSA A23.3-14*", Canadian Standards Association, Mississauga, Canada, 2014.

Elwood, K.J., and M.O. Eberhard (2009). "Effectiveness of Reinforced Concrete Columns" ACI Structural Journal 106 (4): 476–484.

Federal Emergency Management Agency (FEMA), *NEHRP Guidelines for the seismic rehabilitation of buildings, FEMA 356*, Washington, U.S., 2000.

Fenwick, R., and Bull, D., 2000. What is the Stiffness of Reinforced Concrete Walls, SESOC Journal, Vol. 13, No. 2.

Khuntia, M., and Ghosh, S. K., 2004, "Flexural stiffness of reinforced concrete columns and beams: Experimental Verification", *ACI Structural Journal*, vol. 101, pp. 364-374.

Mickleborough, N.C., Ning, F., Chan C.M., 1999, "Prediction of the stiffness of reinforced concrete shear walls under service loads," *ACI Structural Journal*, 96(6), pp. 1018–1026.

Motter, C.J., Abdullah, S.A., and Wallace, J.W., 2017, "Reinforced Concrete Structural Walls without Special Boundary Elements," *ACI Structural Journal*, (submitted for publication).

Paulay, T., and Priestley, M. J. N., 1992, *Seismic Design of Reinforced Concrete and Masonry Buildings*, John Wiley & Sons Inc., New York.

Priestley, M., Calvi, G., and Kowalsky, M., 2007, "*Displacement-based seismic design of structures*", IUSS Press, Pavia, Italy.

CHAPTER 8. Nonlinear Modeling Parameters for Flexure-Controlled RC Structural Walls

8.1. Abstract

The ASCE/SEI 41 standard (and other similar recommendations or guidelines, e.g., ACI Committee 369) represents a major advance in structural and earthquake engineering to address the seismic hazards posed by existing buildings and mitigate those hazards through retrofit. For nonlinear seismic evaluation of existing buildings, these standards provide modeling parameters (e.g., effective stiffness values, deformation capacities, and strengths) to construct backbone relations, as well as acceptance criteria to determine the adequacy. The modeling parameters and acceptance criteria for structural concrete walls were developed based on limited experimental data and knowledge available in the late 1990s (FEMA 273/274-1997), with minor revisions since. As a result, the wall provisions tend to be, in many cases, inaccurate and conservative, and thus can produce uneconomical retrofit schemes. This study involves utilizing available experimental data and new information on performance of structural walls to develop modeling parameters and acceptance criteria for flexure-controlled walls that will produce improved seismic assessments of wall buildings. To accomplish these objectives, a recently developed comprehensive wall database, known as UCLA-RCWalls, was utilized, which currently contains detailed information and test results from more than 1100 wall tests surveyed from more than 260 programs reported in literature. The proposed provisions include cracked and uncracked flexural and shear stiffness and updated modeling parameters and acceptance criteria for flexure-controlled walls with conforming and non-conforming detailing. The updates are expected to be significant contributions to the practice of seismic evaluation and retrofit of wall buildings.

8.2. Experimental RC Wall Database

8.2.1. Overview

The database, called the UCLA-RCWalls database (Abdullah and Wallace, 2018a), compiles detailed data on more than 1000 RC wall tests reported in the literature. The database includes three major clusters of data: 1) information about the test specimen, tests setup, and axial and lateral loading protocols, 2) test results, e.g., backbone relations and failure modes; and 3) analytically computed data, e.g., moment-curvature relationships (c, M_n, M_y, ϕ_n, ϕ_y) and wall shear strengths according to ACI 318-14. Fig. 8-1 shows a typical backbone curve for base shear versus total top displacement (curvature, shear, and bar slip/extension) from a wall test. Table 8-1 provides the definition of each response point in Fig. 8-1 and the approach used to derive these points from the experimental load-deformation relationships.

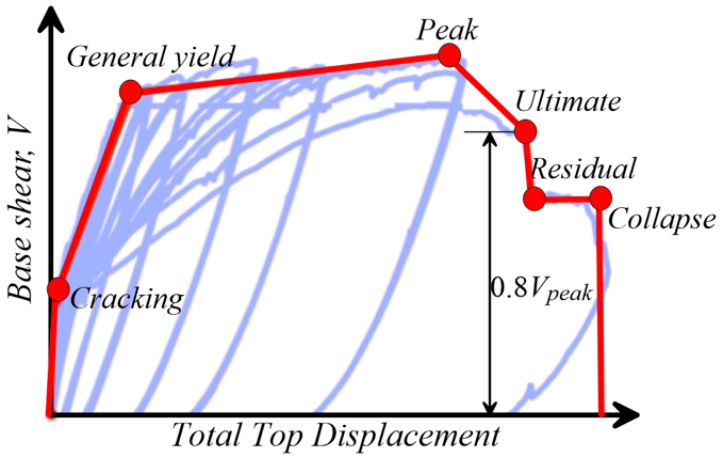

Fig. 8-1–Typical wall backbone curve contained in UCLA-RCWalls database.

Table 8-1–Definition of backbone response points

Response Point	Definition	Data Used to Define the Point
Cracking	Represents the state at which horizontal flexural cracks are first observed in the test.	The cracking load and displacement is reported for the majority of the tests in the database based on information reported by the authors who performed the tests. However, in cases where this information is not reported, attempts were made to visually identify the cracking point on the load-displacement curve (i.e., the point at which a significant change in stiffness is observed). If this was not possible, the cracking information was not reported in the database.
General yield	Represents yielding of most of the boundary longitudinal reinforcement or the onset of concrete nonlinearity in compression-controlled walls.	This point is visually identified as the point where the hysteretic loops (or the response curve in case of monotonic loading) begin to abruptly lose stiffness, which ca easily be identified for tension-yielded walls (yielding of longitudinal reinforcement), as shown in Fig. 8-1**.** For compression-yielded walls (i.e., walls tested under significant axial loads or walls with T- or L-shaped cross-section loaded with the flange in tension), stiffness degradation generally takes place in a gradual manner. It should be noted that this point does not necessarily correspond to first yielding of longitudinal bars, but rather is associated with yielding of most of the longitudinal bars in a wall.
Peak	Represents maximum lateral strength	This point is taken as the maximum lateral strength observed on the backbone.
Ultimate	Represents a significant loss in lateral strength (i.e., lateral failure)	This point is identified as the point at which lateral strength degrades by 20% in the first cycle from peak, which is widely accepted among researchers.
Residual	Represents the residual lateral strength	This point is also visually identified as the state at which the wall reaches its residual lateral strength (residual strength plateau, e.g., Fig. 8-2), if any. Many wall tests, especially earlier tests (prior to 2000s), do not have Residual point due to termination of the test before reaching residual strength.
Collapse	Represents the loss of axial-load-carrying capacity	The Collapse point was identified based on either reported axial collapse from the tests (e.g., Fig. 8-2 and Fig. 8-3) or observed concrete crushing along the entire length of the wall or out-of-plane instability such that no portion of the wall is left intact or stable to carry the applied axial load (e.g., Fig. 8-3). If axial collapse occurred at deformations smaller than the maximum deformation reached prior to axial collapse, then the maximum deformation reached is reported as the deformation for axial collapse (e.g., Fig. 8-3 (***c***)) Similar to Residual point, many wall tests, especially earlier tests (prior to 2000s) due to termination of the test before reaching residual strength.

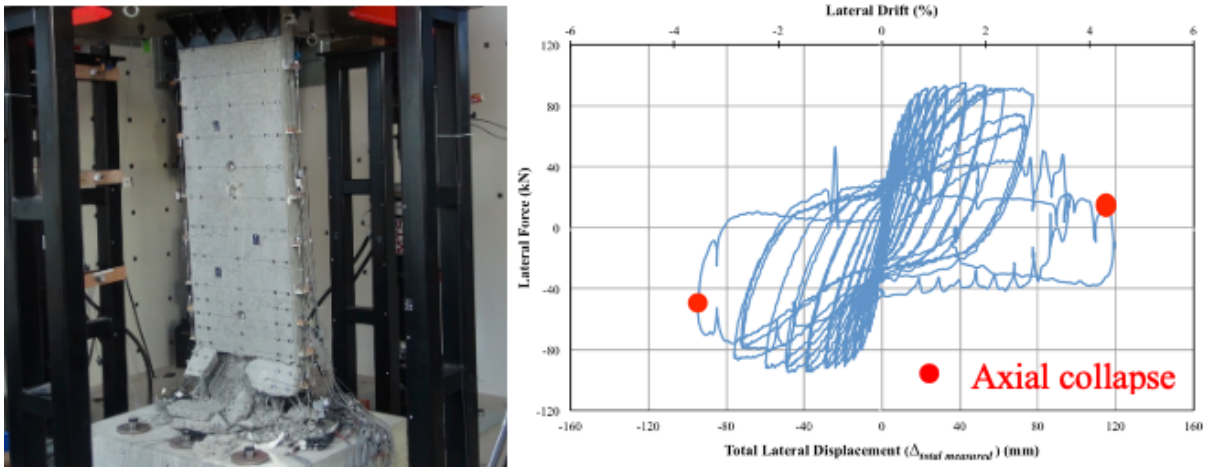

Fig. 8-2–Reported axial collapse of a wall test reported by Altheeb (2016).

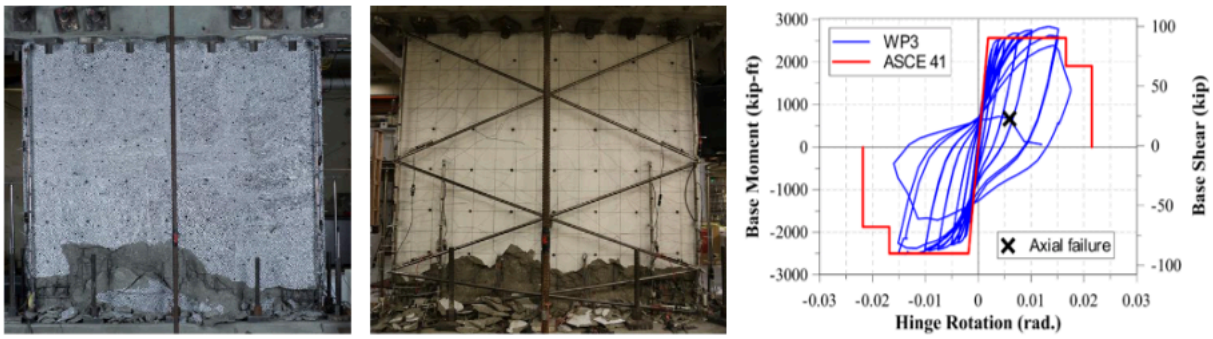

(*a*) South view (*b*) North view (*c*) Load-displacement response

Fig. 8-3–Reported axial collapse of a wall test reported by Segura and Wallace (2018a).

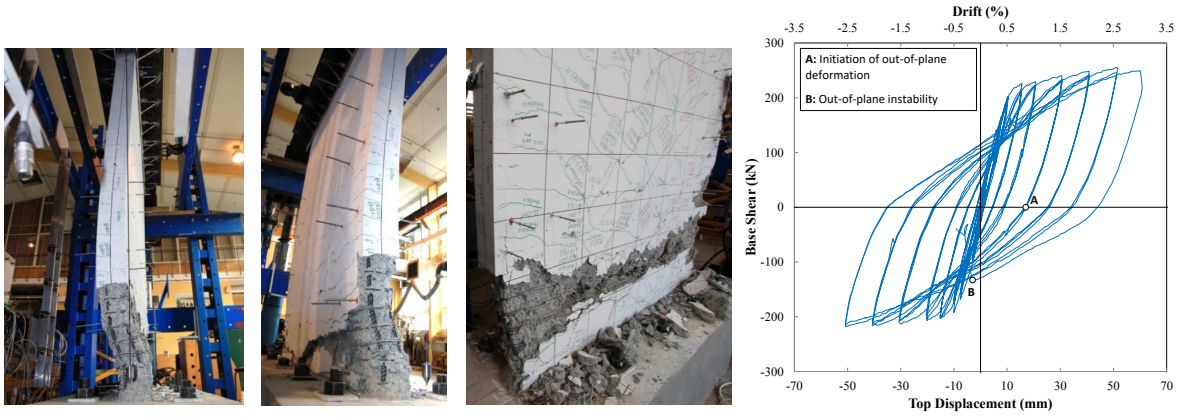

Fig. 8-4–Out-of-plane instability and concrete crushing of a wall test reported by Dashti et. (2018).

The following two datasets were filtered from the UCLA-RCWalls database and are later used to propose the updated Modeling parameters:

8.2.2. Conforming Wall Dataset

Design of RC structural walls is currently governed by the requirements of ASCE 7-16 and ACI 318-14, which includes provision for special structural walls with well-detailed special boundary elements (SBE) according ACI 318-14 §18.10.6.4 for buildings assigned to Seismic Design Category D, E, and F. Detailing requirements for SBEs have changed over the years and are likely to keep change in the future; therefore, the UCLA-RCWalls database was filtered to obtain a dataset of "Conforming Walls" using criteria that are less restrictive than the detailing requirements of ACI 318-14 §18.10.6.4. Both (a) general and (b) detailing criteria were used:

a) General criteria:
   i. Flexure-controlled walls, i.e., $V_{yE} / V_{@MyE} \geq 1.15$,
   ii. Walls with different cross-sections were included (i.e., rectangular, barbell, H-shaped, T-shaped, L-Shaped, or half-bar bell),
   iii. Walls tested under quasi-static, reversed cyclic loading,
   iv. Tests were excluded if noticeable lateral strength loss was not observed or if walls failed due to inadequate lap-slices.
   v. Walls with measured concrete compressive strength, $f_c^{'} \geq 3$ ksi,
   vi. Walls with ratio of measured tensile-to-yield strength for boundary longitudinal reinforcement, $f_u / f_y \geq 1.2$, and
   vii. Wall with web thickness, $t_w \geq 3.5$ in.,
b) Detailing criteria:

i. A minimum of two curtains of web vertical and horizontal reinforcement,

ii. Boundary longitudinal reinforcement ratio, $\rho_{Long,BE} \geq 6\sqrt{f_c^{'}(\text{psi})}/f_y$,

iii. Min ratio of provided-to-required (per ACI 318-14 §18.10.6.4) area of boundary transverse reinforcement, $A_{sh,provided}/A_{sh,required} \geq 0.7$,

iv. Ratio of vertical spacing of boundary transverse reinforcement to minimum diameter of longitudinal boundary reinforcement, $s/d_b < 8.0$, and

v. Centerline distance between laterally supported boundary longitudinal bars, h_x, between 1.0 in. and 9.0 in.

Based on the above selected filters, a total of 188 wall tests were identified that included information on lateral strength loss (i.e., 20% lateral strength loss from peak strength) and 101 of these tests had reported information on axial collapse. Histograms for various dataset parameters for the 188 tests are shown in Fig. 8-5, where $P/\left(A_g f_c^{'}\right)$ is the compressive axial load normalized by the measured concrete compressive strength $\left(f_c^{'}\right)$ and gross concrete area $\left(A_g\right)$, and M/Vl_w is the ratio of base moment-to-base shear normalized by wall length $\left(l_w\right)$. A limit of 3 ksi was specified on $f_c^{'}$ in accordance with requirements of ACI 318-14 §18.2.5 for conforming seismic systems. At least two curtains of web reinforcement were specified to be consistent with ACI 318-14 §18.10.2.2. Walls with t_w less than 3.5 in. were not included because use of two curtains of web reinforcement along with realistic concrete cover is not practical in such thin walls. The limit on ratio f_u/f_y is slightly less restrictive than the limit

of 1.25 specified in ACI 318-14 §20.2.2.5. The specified limits on $s/d_b \leq 8.0$ and $A_{sh,provided}/A_{sh,required} \geq 0.7$ are slightly less restrictive than the current limits in ACI 318-14 §18.10.6.4 of 6.0 and 1.0, respectively. The limit on $\rho_{long,BE}$ was included to avoid brittle tension failures (Lu et al., 2016), based on what was adopted in ACI 318-19 §18.10.2. ACI 318-14 §18.10.6.4e requires $h_{x,max}$ not exceeding the lesser of 14 in. or 2*b*/3; however, most of the tests in the database were conducted at less than full scale (typically 25 to 50%). Therefore, $h_{x,max}$ for the wall tests should generally be between 3.5 to 7.0 in. for the 14 in. limit. Based on the range of h_x used to filter the data, 95% of the specimens have $h_x \leq 6$ in., which is reasonable, whereas the histogram for h_x/b presented in Fig. 8-5(***f***) indicates that a majority of the tests have $h_x/b < 3/4$, which is only slightly higher than the current limit of $h_x/b < 2/3$.

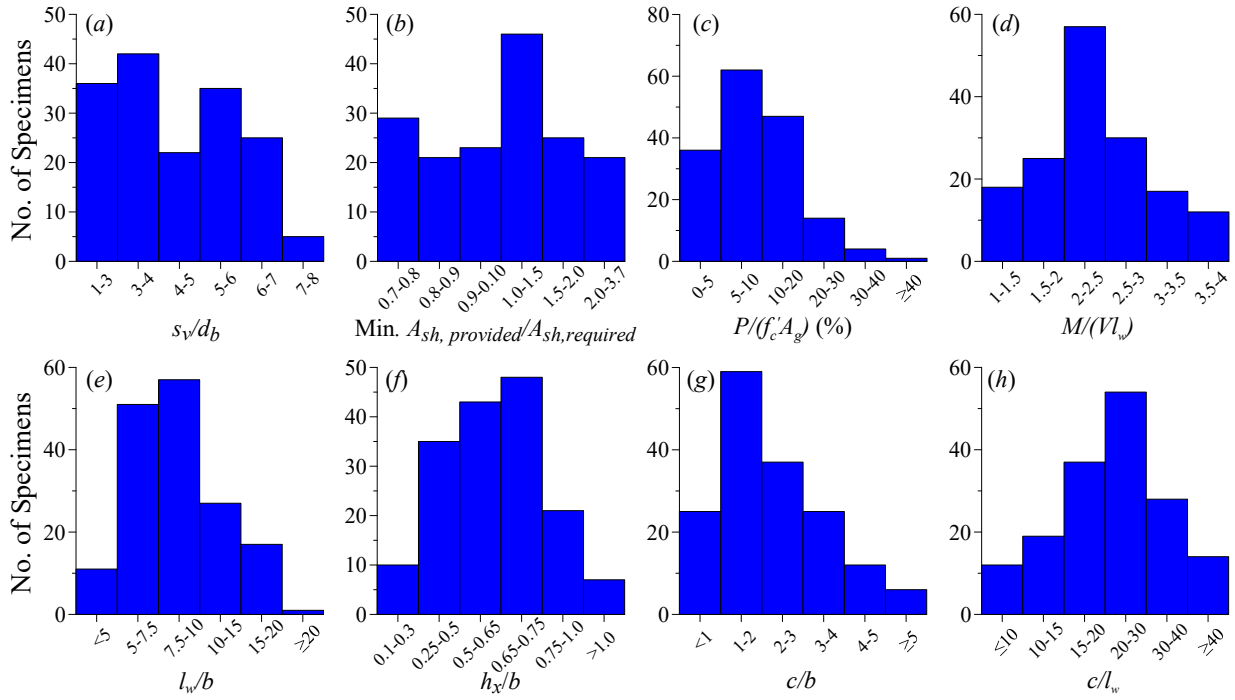

Fig. 8-5–Histograms of the first dataset (188 tests) for walls with conforming detailing.

8.2.3. Non-Conforming Wall Dataset

Walls with detailing not conforming to special structural wall provisions are common in older construction designed prior to the establishment of detailing requirements for structural walls (which were introduced in ACI 318-77 and were updated significantly in ACI 318-83 and 318-99). Additionally, the special detailing requirements of ACI 318 are relaxed where wall displacement or force demands are low; however, if the boundary longitudinal reinforcement ratio exceeds $400/f_y$, modest detailing is required by ACI 318-14 §18.10.6.5 (introduced in ACI 318-99 in §21.6.6.5) to prevent bar buckling at smaller deformation demands. These walls are sometimes referred to as walls with Ordinary Boundary Elements, or OBEs (e.g., see NIST 2011). Based on these considerations, the following (a) general and (b) detailing criteria were used to obtain a dataset of "Non-Conforming Walls":

(a) General criteria:

i. Flexure-controlled walls, i.e., $V_{yE} / V_{@MyE} \geq 1.15$,

ii. Walls with different cross-sections were included (i.e., rectangular, barbell, I-shaped, T-shaped, L-Shaped, or half-bar bell),

iii. Quasi-static, reversed cyclic loading, and

iv. Tests were excluded if noticeable lateral strength loss was not observed, or if walls failed due to inadequate lap-slices.

(b) Detailing criteria:

i. Walls with one or more curtains of web vertical and horizontal reinforcement,

ii. Min ratio of provided-to-required (per ACI 318-14 §18.10.6.4) area of boundary transverse reinforcement $A_{sh,provided} / A_{sh,required} < 0.7$, **and**/**or** ratio of vertical spacing of boundary transverse reinforcement to minimum diameter of longitudinal boundary reinforcement, $s/d_b \geq 8.0$.

Based on the above selected filters, a total of 256 wall tests were identified that included information on lateral strength loss and 118 of these tests had reported information on axial collapse. Histograms for various dataset parameters for those 256 tests are shown in Fig. 8-6.

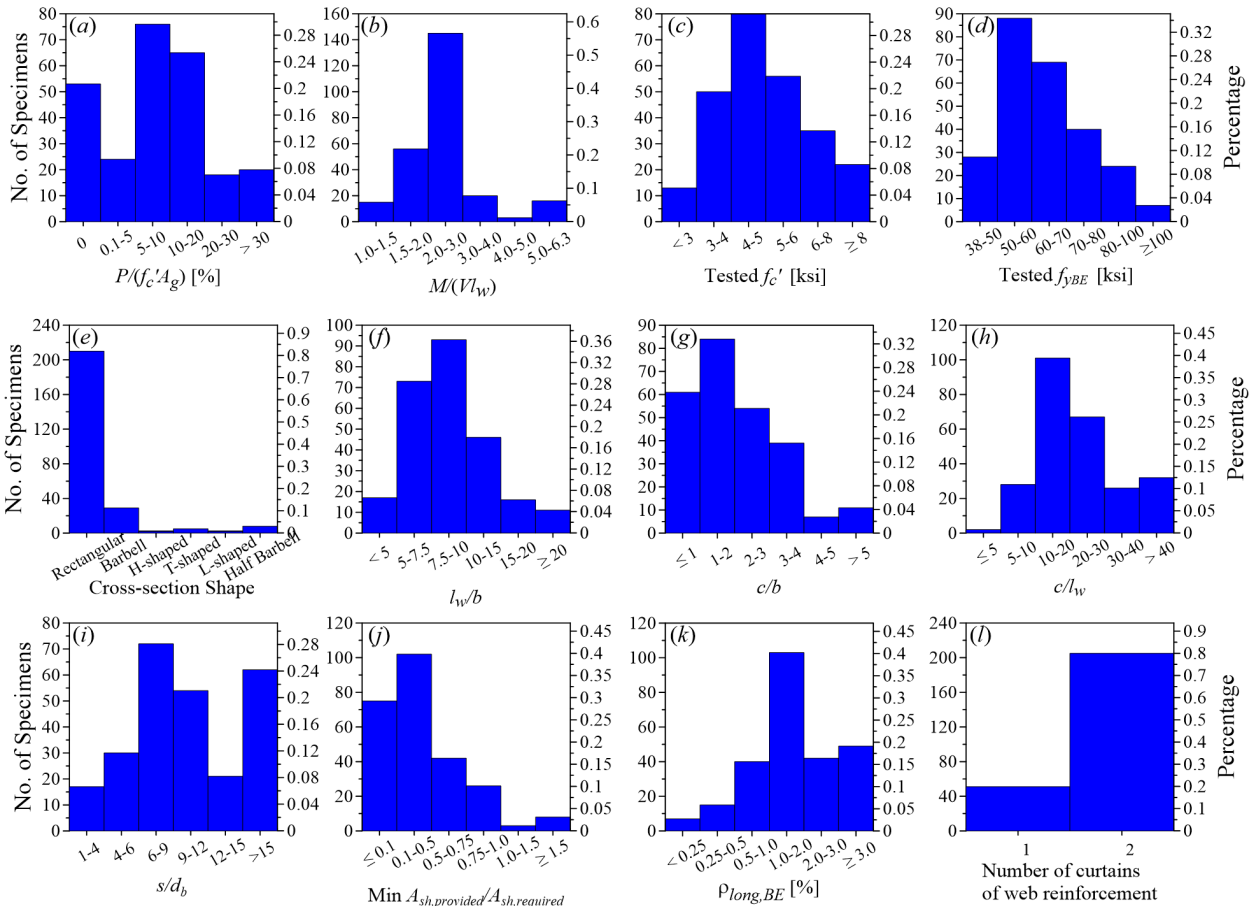

Fig. 8-6–Histograms of the second dataset (256 tests) for walls with non-conforming detailing.

8.3. Use of Total Hinge Rotation Versus Plastic Rotation

Currently, the ASCE 41-17 nonlinear deformation-based modeling parameters (i.e., Parameters *a* and *b*) are given as plastic hinge rotations. Where a lumped plasticity model is used, the hinge region, which is typically at or near the base of a wall, is modeled as a near-rigid spring with effectively no elastic deformation. However, in this study, the deformation-based modeling parameters are given as total hinge rotation capacities (Fig. 8-7), which include both the elastic and plastic deformations of the hinge region. This approach is proposed because, by using total hinge rotation capacities: 1) Modeling parameters are not sensitive to approaches (or assumptions) used to calculate yield rotation, θ_y, 2) Modeling parameters are consistent with the total drift ratio or chord rotation used to define modeling parameters for shear-controlled walls and coupling beams, respectively, and 3) Modeling parameters can be converted to strain limits by dividing by an assumed hinge length, which is convenient where fiber models are used, which is becoming increasingly popular in engineering practice.

It should also be noted that, for the proposed backbone relation shown in Fig. 8-7, two new Modeling parameters are introduced, Parameters c' and d', to represent the ratio of ultimate strength to yield strength ($V_{@Mult}/V_{@MyE}$) and the total hinge rotation capacity once the lateral residual strength is reached. Additionally, for Point C, an approximation is made such that this point has an ordinate and abscissa that are respectively equal to the ultimate (peak) lateral strength ($V_{@Mult}$) normalized by $V_{@MyE}$ (i.e., Parameter c') and the total hinge rotation capacity at 20% lateral strength loss from $V@_{Mult}$ (i.e., Parameter d). Based on this assumption, the value for peak strength is defined at the hinge rotation capacity associated with 20% loss in lateral strength.

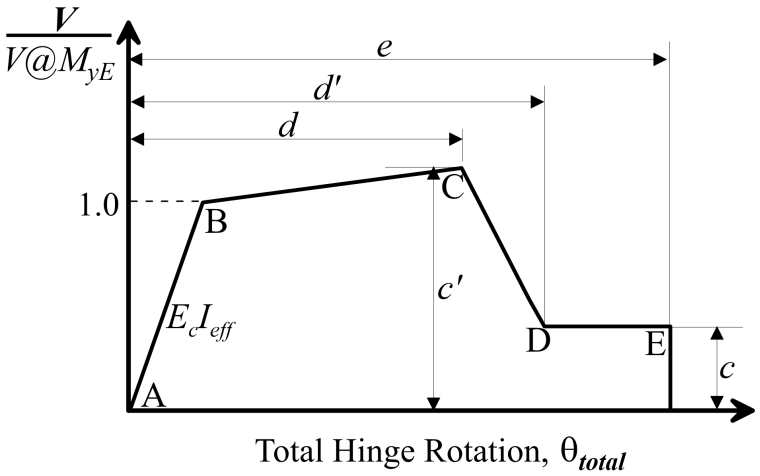

Fig. 8-7–The proposed idealized backbone relation to model hinge region of flexure-controlled walls.

The following approach was used to obtain the total hinge rotation capacities from the experimental backbone relations. The steps are given for a typical cantilever wall test (Fig. 8-8(***a***)), and a similar approach was used for panel or partial height walls. For cases where only the hinge region of the wall was tested, or hinge rotations were measured in the tests, the approach outlined below was not required:

a) Rotation capacity at Point C (i.e., at 20% lateral strength loss from peak strength)

   i. A plastic hinge length (l_p) of half the wall length (l_w/2) was assumed for all walls in the dataset (Fig. 8-8(***a***)).

   ii. The plastic displacement, δ_p, (Fig. 8-8(***c***)) is obtained by subtracting the elastic first yield displacement, δ_e, (Fig. 8-8(***d***)) from the total displacement, δ_t, (Fig. 8-8(***b***)). The plastic rotation capacity, θ_p, is calculated as δ_p divided by the wall height between the center of the hinge (located at l_w/4 from the base) and top of the wall.

iii. The elastic flexural rotation contributed by the hinge region, $\theta_{h,f}$, (Fig. 8-8(***e***)) is calculated analytically using **Eq. 8-1**. Fig. 8-9(***a***) shows the contribution of the elastic hinge rotation to the total wall elastic rotation for the conforming wall dataset. The high values (>60%) are for panel or partial height wall tests where only the bottom portion of the wall was tested. The figure also shows that a significant part of the total elastic rotation is contributed by the hinge region, which makes sense because the elastic curvature profile has a triangular shape with the highest values at the hinge region.

$$\theta_{h,f} = \frac{M_{h,ave}}{E_c I_{eff}} l_p \qquad \text{(Eq. 8-1)}$$

Where $M_{h,ave}$ is the average moment over the hinge region, and E_cI_{eff} is the effective flexural stiffness in accordance with Chapter 7 (taken as 0.20 E_cI_g and 0.50 E_cI_g for $P \Big/ \left(A_g f_c^{'} \right) \leq$ 0.05 and $\geq$ 0.50, respectively, and linear interpolation is applied for 0.05 < $P \Big/ \left(A_g f_c^{'} \right)$ < 0.50)

iv. The total hinge rotation capacity is calculated as the sum of θ_p (item *ii* above and Fig. 8-8(***c***)) and $\theta_{h,f}$ (item *iii* above and Fig. 8-8(***e***)). Fig. 8-9(***b***) shows the contribution of the hinge elastic flexural rotation to the total hinge rotation capacity $\left(\theta_{h,f} / \theta_t \right)$ for the conforming wall dataset. Examination of Fig. 8-9(***b***) reveals that for the majority of the walls in the dataset, hinge elastic rotation contributes less than 10% of the total hinge rotation capacity.

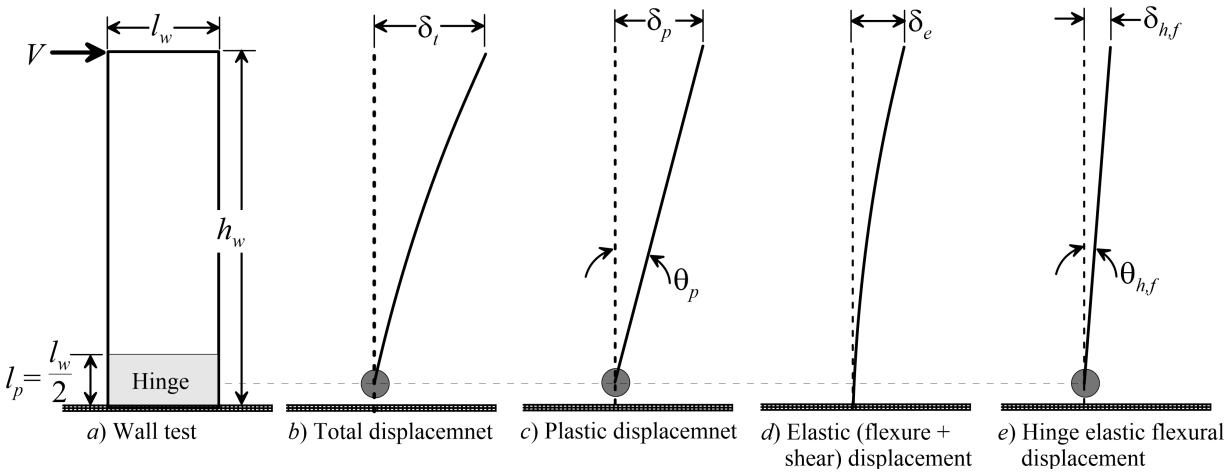

Fig. 8-8–Displacement profiles of flexure-controlled walls.

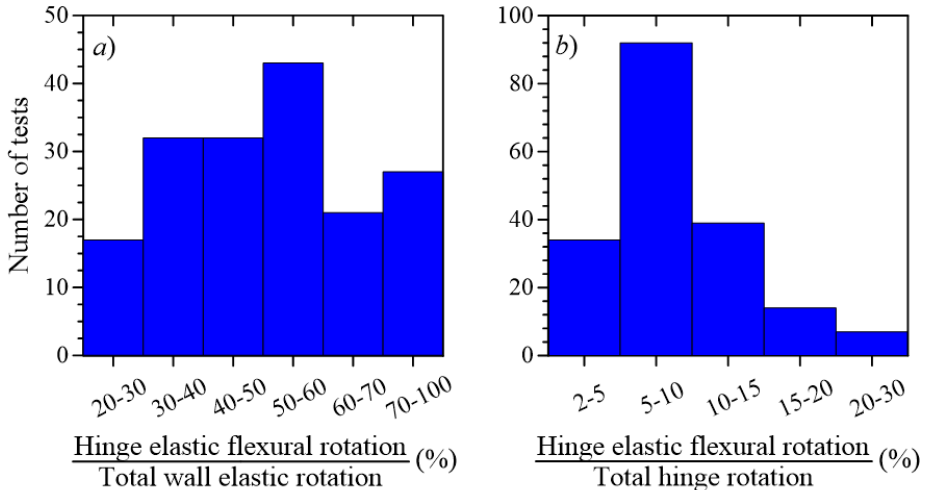

Fig. 8-9–Histograms of the contribution of computed hinge elastic flexural rotation to a) the wall total elastic rotation, and b) the total hinge rotation capacity.

b) Rotation capacity at Point D and E (i.e., at residual strength and axial collapse)

At these two points, the total hinge rotation capacity was calculated as the total wall displacement (Fig. 8-8(***b***)) divided by the wall height between the center of the hinge and the top of the wall, assuming a plastic hinge length of $l_w/2$ from the base of the wall. That is, for the Point D and E, the elastic deformation contributed by the wall above the hinge is not subtracted as was done for Point C, that is, all wall deformation is assumed to be associated with plastic rotation concentrated

in the hinge region. Shear displacements at this stage are expected to be very small and thus ignored (i.e., not subtracted from total displacement).

8.4. Evaluation of Current ASCE 41-17 Nonlinear Modeling Parameters

In this section, the Parameter ***a*** (i.e., plastic hinge rotation capacity at strength loss) of walls with "Confined Boundaries" is evaluated using results of the conforming wall dataset to highlight the conservatism associated with the current structural wall modeling parameters of ASCE 41. ASCE 41-17 Table 10-19 (ACI 369-17 Table 19), which gives modeling parameters for flexure-controlled RC structural walls, is partially shown in Table 8-2.

For the walls in the conforming dataset, which satisfy the criteria for "Confined Boundary" in Table 8-2, the plastic rotation capacities at strength loss are computed. The results, along with the plastic hinge rotation capacities from Table 8-2 (i.e., the first four rows), are presented in Fig. 8-10. Two primary observations result from a review of Fig. 8-10: 1) the current modeling parameters for walls with "confined boundaries" constitute a conservative lower-bound estimate of wall deformation capacities, and 2) the predictor variable given in the first column of the Table 8-2 (i.e., $\left[\left(A_s - A'_s\right) f_{yE} + P\right] \Big/ A_g f'_{cE}$ does not correlate well with parameter *a* and thus produces large dispersions.

Table 8-2–Partial view of ASCE 41-17 Table 10-19

Conditions			Plastic Hinge Rotation (radians)		Residual Strength Ratio
			a	*b*	*c*
i. Structural walls and wall segments					
$\frac{(A_s - A'_s)f_{yE} + P}{t_w l_w f'_{cE}}$	$\frac{V}{t_w l_w \sqrt{f'_{cE}}}$	Confined Boundary[b]			
≤0.1	≤4	Yes	0.015	0.020	0.75
≤0.1	≥6	Yes	0.010	0.015	0.40
≥0.25	≤4	Yes	0.009	0.012	0.60
≥0.25	≥6	Yes	0.005	0.010	0.30
≤0.1	≤4	No	0.008	0.015	0.60
≤0.1	≥6	No	0.006	0.010	0.30
≥0.25	≤4	No	0.003	0.005	0.25
≥0.25	≥6	No	0.002	0.004	0.20

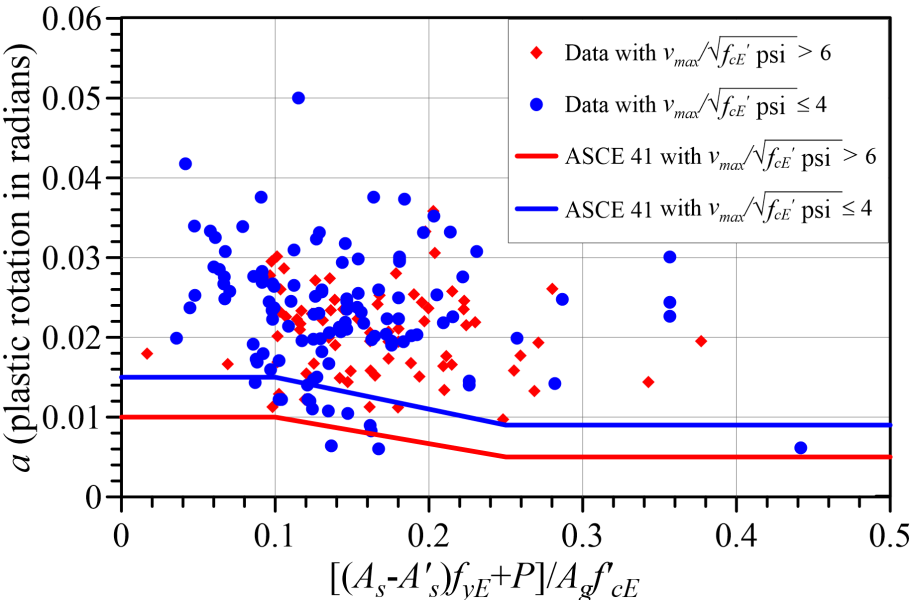

Fig. 8-10–Evaluation of Parameter ***a*** given in ASCE 41-17 for walls with "confined boundaries".

The $\left[\left(A_s - A'_s\right)f_{yE} + P\right]\Big/ A_g f'_{cE}$ parameter considers the impact of axial load ratio $\left(P\Big/ A_g f'_{cE}\right)$ and longitudinal reinforcement ratio and yield strength $\left(\left(A_s - A'_s\right)f_{yE}\Big/ A_g f'_{cE}\right)$. Fig. 8-11(***a***) shows that there is no significant trend between $\left(P\Big/ A_g f'_{cE}\right)$ (ranging from 0.0 to 0.35) and wall plastic rotation capacity at strength loss. This observation relates to the fact that $P / A_g f'_c$ alone does not indicate much about the stability of the compression zone, and its influence on deformation capacity is best accounted for through neutral axis depth of a wall section, as will be shown later. The impact of $\left(\left(A_s - A'_s\right)f_{yE}\Big/ A_g f'_{cE}\right)$ is shown in Fig. 8-11(***b***), which interestingly shows that an increase in this parameter results in increase of plastic rotation capacity for walls subjected to low values of shear stress $\left(v_{max} / \sqrt{f'_{cE}(psi)} \le 4\right)$. This is because the value of $\left(\left(A_s - A'_s\right)f_{yE}\Big/ A_g f'_{cE}\right)$ is the largest for walls with small depth of neutral axis (more reinforcement are in tension), and deformation capacity if such walls are typically limited by bar fracture of tension reinforcement and tend to have large deformation capacities (Segura and Wallace, 2018b) . Fig. 8-11(***b***) also shows no clear trend between $\left(\left(A_s - A'_s\right)f_{yE}\Big/ A_g f'_{cE}\right)$ and plastic rotation capacity for walls with high shear stresses.

Fig. 8-12 also shows that there is only a moderate trend of Parameter *a* as a function of $\left(P\Big/ A_g f'_{cE}\right)$ for walls subjected to low shear stresses, and no clear trend for walls subjected to high shear stresses for walls in the second dataset (i.e., No Confined Boundaries).

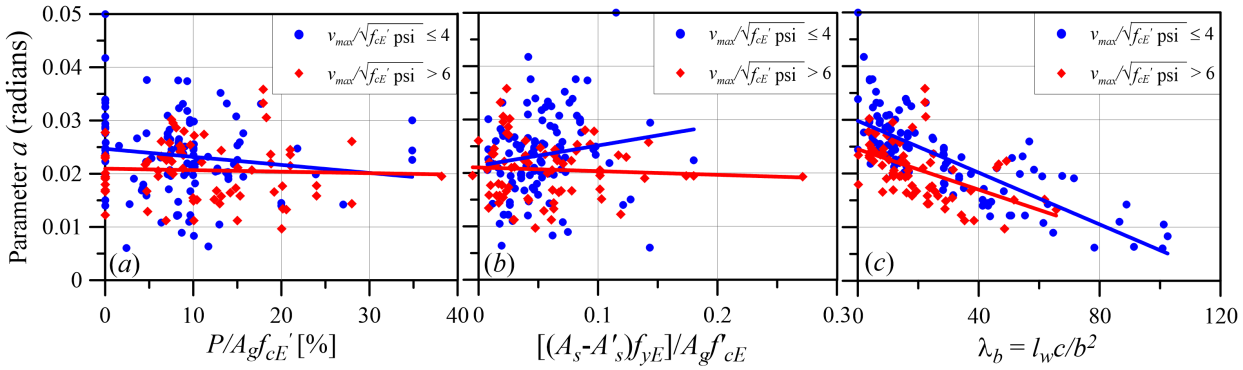

Fig. 8-11– Impact of axial load ratio, longitudinal reinforcement, and slenderness parameter ($l_w c/b^2$) on plastic rotation capacity (at strength loss) for walls with conforming detailing.

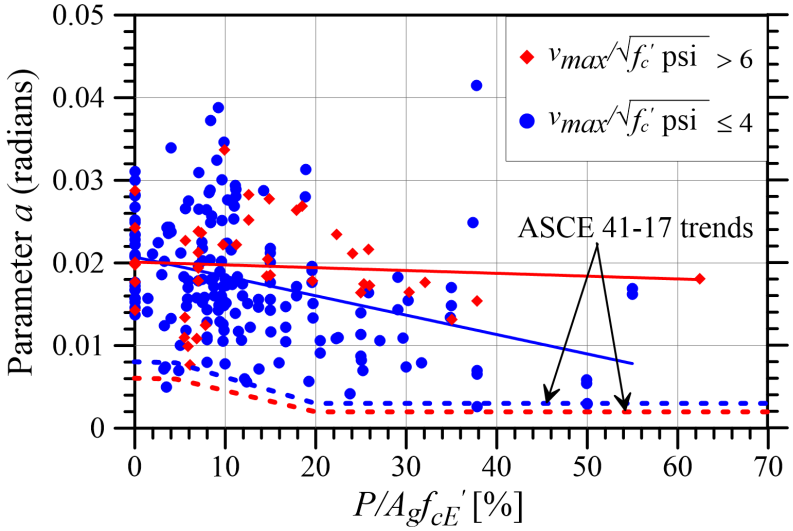

Fig. 8-12– Impact of axial load ratio on plastic rotation capacity at strength loss (Parameter a) for walls with No Confined Boundaries (note: the break points for the ASCE 41-17 trends are approximate since x-axis does not include $(A_s\text{-}A'_s)f_{yE}/(A_g f'_{cE})$).

8.5. Modeling Parameters for Conforming Walls

The idealized backbone relation proposed to model the hinge region ($l_p = l_w/2$) of flexure-controlled walls is presented in Fig. 8-7. The coordinates (strength ratios and total hinge rotation capacities) of each point on the backbone are developed in the following sections using the experimental results from the conforming wall dataset:

8.5.1. Point B (E_cI_{eff} and M_{yE})

This point corresponds to member general yield strength and requires the yield strength (M_{yE}) and the effective flexural stiffness (E_cI_{eff}) of the hinge region. The effective flexural stiffness values are given in Chapter 7 and depend on the magnitude of the sustained gravity load. The calculated yield moment strength, $M_{yE,cal}$, is evaluated as defined in ACI 369.1-17 and ASCE 41-17 based on the ACI 318-14 approach but using expected material properties. Fig. 8-13 presents the ratio of the calculated yield moment strength ($M_{yE,cal}$) to the experimental (observed) yield moment strength ($M_{yE,exp}$). It can be seen that the calculated $M_{yE,cal}$ accurately captures the strength at general yield ($M_{yE,exp}$) with a mean and coefficient of variation (COV) of 1.01 and 0.12, respectively.

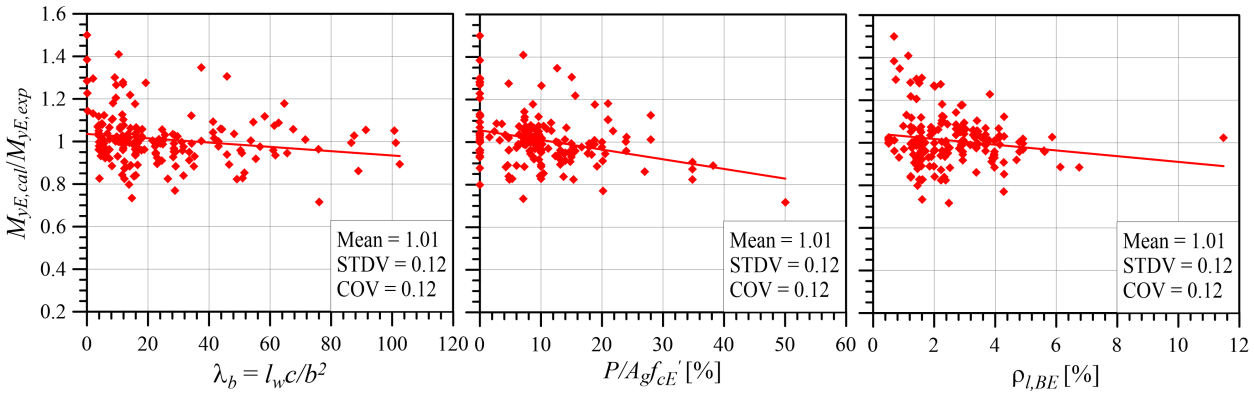

Fig. 8-13–Ratio of calculated-to- experimental yield moment strength ($M_{yE,cal}/M_{yE,exp}$) for the conforming wall dataset.

8.5.2. Point C (Parameter *c′* and Parameter *d*)

As noted previously, this point has an ordinate and abscissa that are equal to the ultimate (peak) lateral strength ($V_{@Mult}$) normalized by $V_{@MyE}$ (i.e., Parameter *c′*) and the total hinge rotation

capacity at 20% lateral strength loss from $V@_{Mult}$ (i.e., Parameter *d*), respectively. Details Parameter *c′* and Parameter *d* are presented below:

a) Parameter *c′* (i.e., $V_{@Mult}/V_{@MyE}$):

Fig. 8-14 shows the ratio of the wall ultimate moment strength obtained during the test ($M_{ult,exp}$) to the calculated $M_{yE,cal}$, and indicates that, on average, $M_{ult,exp}$ is 14% higher than $M_{yE,cal}$. Therefore, Parameter *c′* is taken as 1.15 (i.e., M_{ult} =1.15 M_{yE}) for simplicity and to be consistent with Parameter *c′* for non-conforming walls, as discussed later.

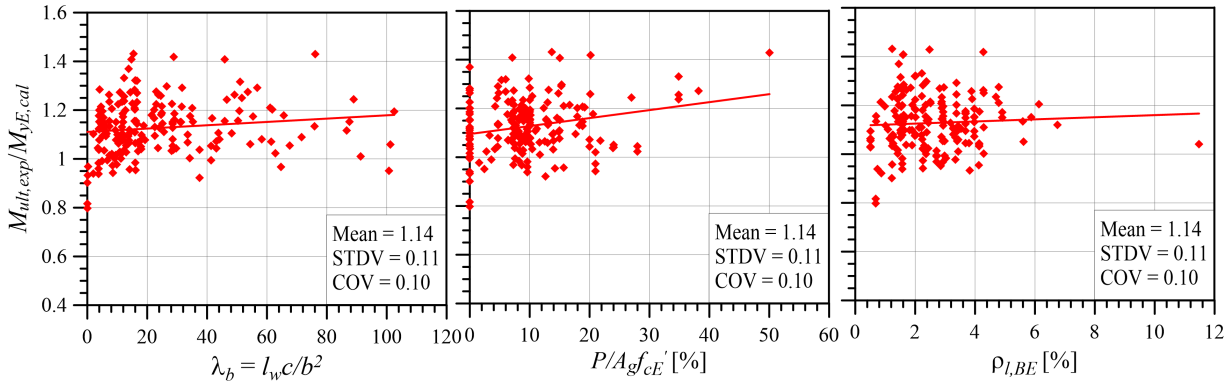

Fig. 8-14–Ratio of experimental ultimate to yield moment strength ($M_{ult,exp}/M_{yE,cal}$) for the conforming wall dataset.

b) Parameter *d* (i.e., total hinge rotation capacity at strength loss)

Abdullah and Wallace (2019) analyzed the Conforming Wall dataset and found that the following parameters had a significant impact on lateral drift capacity: (1) ratio of wall neutral axis depth-to-width of compression zone (slenderness of the compression zone), $\boldsymbol{c/b}$, (2) ratio of wall length-to-width of compression zone (slenderness of the cross-section), $\boldsymbol{l_w/b}$, (3) ratio of maximum wall shear stress to the square root of concrete compressive strength, $\boldsymbol{v_{max}/\sqrt{f_c'}}$, and (4) configuration of the boundary transverse reinforcement used, i.e., use of overlapping hoops (Fig. 8-15(***i***)) versus

a single perimeter hoop with intermediate legs of crossties (Fig. 8-15(***ii***)). They also concluded that use of a combined cross-sectional slenderness parameter $\lambda_b = l_w c / b^2$ provided an efficient means to account for slenderness of the cross section $\left(l_w / b\right)$ and the slenderness of the compression zone on the cross section $\left(c / b\right)$. Parameter $\lambda_b = l_w c / b^2$ considers the impact of concrete and reinforcement material properties, axial load, wall cross-section geometry, and quantities and distributions of longitudinal reinforcement at the boundary and in the web.

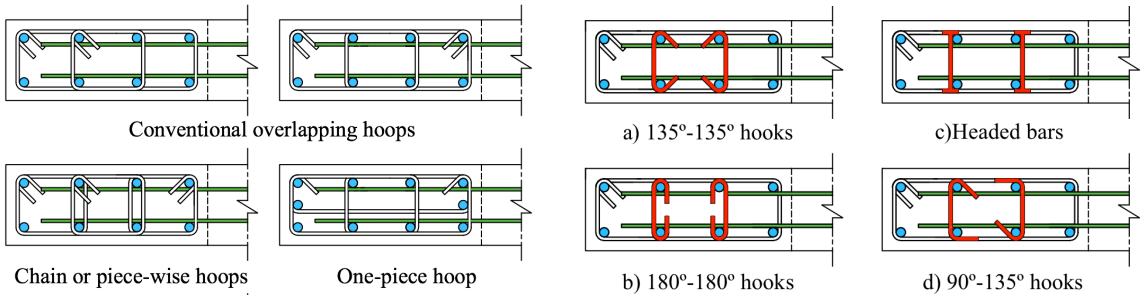

i) Overlapping hoops *ii*) Perimeter hoop with crossties

Fig. 8-15–Examples of boundary transverse reinforcement configurations.

Furthermore, Abdullah and Wallace (2019) also investigated other parameters such as the: (1) area ratio of provided-to-required (per ACI 318-14 §18.10.6.4) boundary transverse reinforcement, $A_{sh,provided} / A_{sh,required}$, (2) ratio of vertical spacing of boundary transverse reinforcement to the diameter of the smallest longitudinal reinforcement, s / d_b, (3) distance between laterally supported boundary longitudinal reinforcement, h_x, normalized by $h_{x,max}$ or width of compression zone, b, and (4) degree of lateral support provided (support for all boundary longitudinal bars versus every other bar). It was concluded that these detailing parameters did not significantly impact wall lateral drift capacity (Fig. 8-16) for walls with well-detailed boundary elements. More in-depth discussion of these parameters can be found in Abdullah and Wallace (2019).

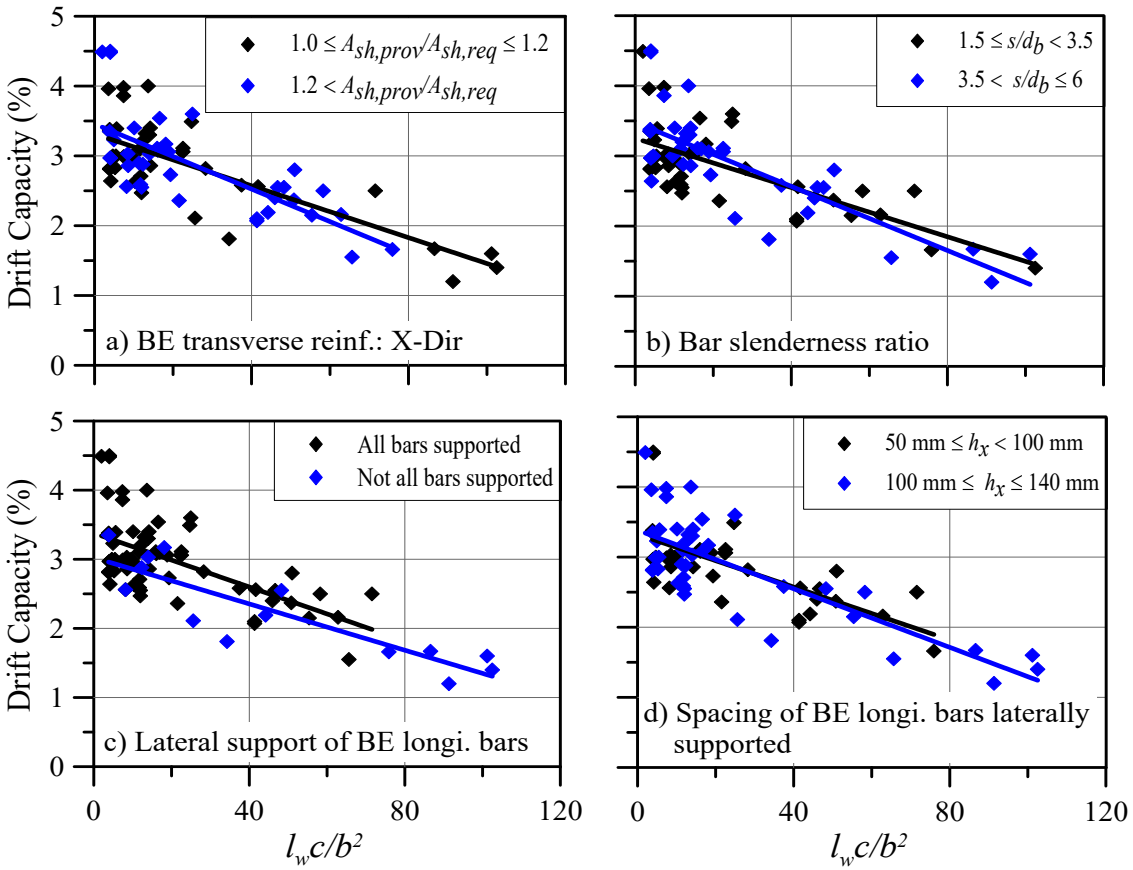

Fig. 8-16–Impact of some boundary element details on drift capacity of walls with special boundary elements.

Fig. 8-17 shows variation of Parameter *d* of the conforming dataset as a function of the aforementioned four significant parameters (i.e., $\lambda_b = l_w c / b^2$, $v_{max} / \sqrt{f'_c}$, and overlapping hoops), with piecewise best-linear fits of the data (proposed models) to derive the updated Parameter *d* values. Fig. 8-17(***a***) reveals that use of overlapping hoops for values of $\lambda_b > 40$ (i.e., walls with slender cross-sections and large compression depths) results in a significant increase in rotation capacity, because the behavior of walls with small compression zones ($c / b < 1$) tends to be controlled by bar fracture rather than flexural compression failure. It is noted that for walls with

overlapping hoops and high shear stresses, only three tests exist for $\lambda_b > 40$ (Fig. 8-17(*b*)). A detailed discussion on the impact of overlapping hoops on wall deformation capacity can be found in Abdullah and Wallace (2019) and Segura and Wallace (2018a).

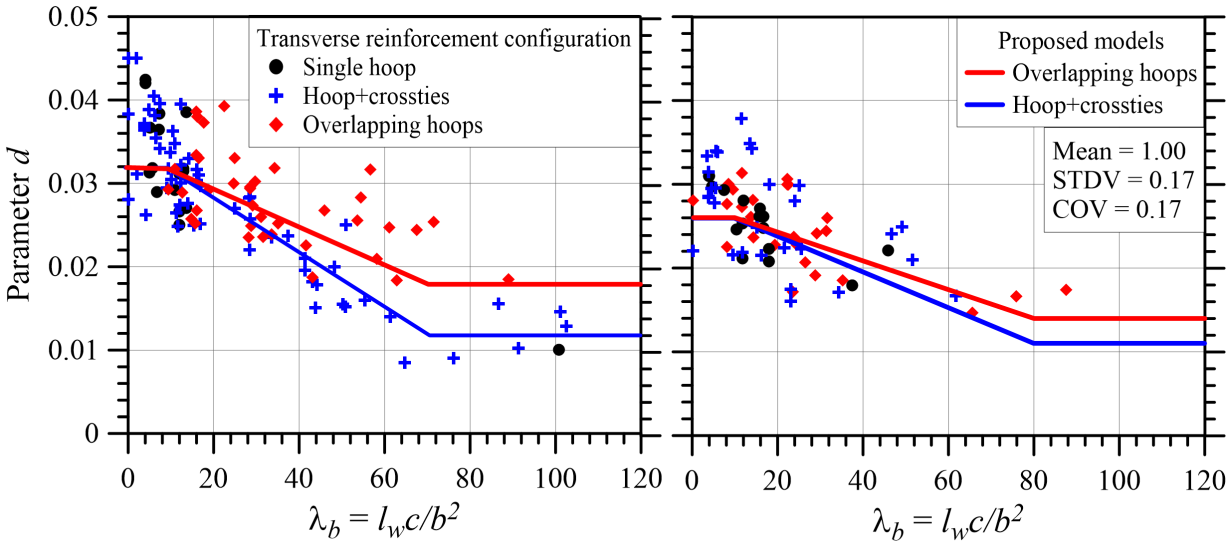

(*a*) $v_{max}/\sqrt{f_c'}$ psi≤ 4 (≤ 0.33 in MPa) (*a*) $v_{max}/\sqrt{f_c'}$ psi> 6 (≤ 0.50 in MPa)

Fig. 8-17–Proposed models for Parameter d for conforming flexure-controlled walls (Note: the statistics shown are for the ratios of predicted-to-experimental values for the entire dataset).

8.5.3. Point D (Parameter *c* and *d'*)

As shown in Fig. 8-7, this point defines the slope of the strength degrading branch of the backbone relations and has an ordinate and abscissa that are equal to the wall residual lateral strength ratio (Parameter *c*) and the rotation capacity corresponding to reaching the residual strength (Parameter *d'*), respectively. The reduced subset of 101 walls that included information on axial collapse was studied to identify parameters that influence residual strength ratio (Parameter *c*) and rotation capacity (Parameter *d'*) at Point D, as discussed below:

a) Parameter *c*

Fig. 8-18 shows the residual moment strength, $M_{residual}$, of the dataset normalized by the yield moment strength, M_{yE}, (i.e., Parameter *c*). It is clear that residual strength does not correlate well with the parameters such as λ_b and $P / A_g f'_c$, which significantly impact Parameter *d'*, as is shown next. However, from Fig. 8-18(***a***), it can be seen that the walls with $P/A_g f'_c \geq 0.2$ (~ 20 walls) have little or no residual strength, and that walls with $\lambda_b > 70$ have no residual strength regardless of the level of axial load or shear stress (i.e., no or little post-peak deformation capacity). Additional study may provide improved relations; however, the models shown in Fig. 8-18(***a***) are proposed to derive Parameter *c* for conforming walls.

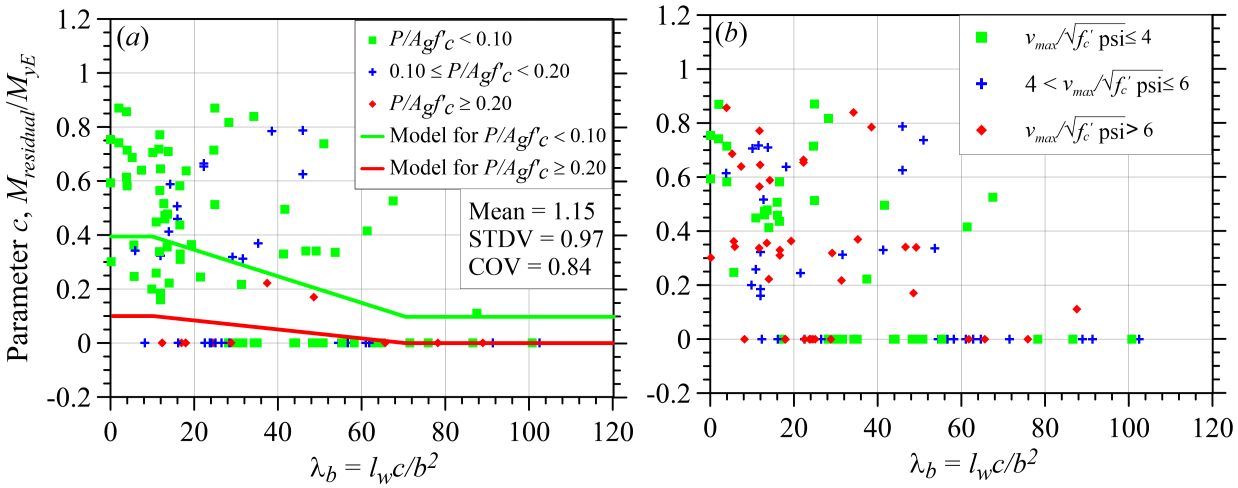

Fig. 8-18–Proposed models for Parameter c for conforming flexure-controlled walls.

b) Parameter *d'*

Fig. 8-19 shows that, in addition to $\lambda_b = l_w c / b^2$, $P / A_g f'_c$ produces a significant influence on Parameter *d'*. This is because, once strength degradation starts, the level of axial load accelerates

the rate of deterioration such that walls with high $P / A_g f_c'$ have a steep post-peak slope on the backbone relation, where no or little additional deformation capacity beyond Point C is achieved prior to axial collapse (i.e., no residual strength plateau, Fig. 8-7). Insufficient data existed to evaluate if the use of overlapping hoops in the boundary elements would influence Parameter *d'*. Therefore, λ_b and $P / A_g f_c'$ are used as predictor variables to select Parameter *d'* based on the piecewise best-linear fits (models) shown on Fig. 8-19.

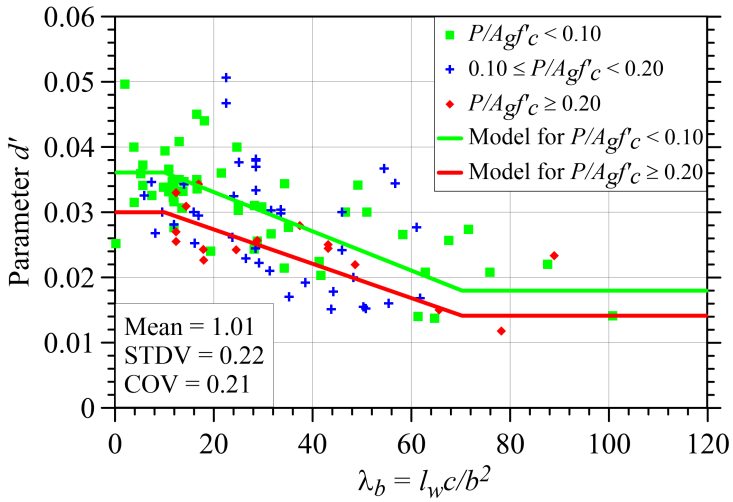

Fig. 8-19–Proposed models for *Parameter d'* for conforming flexure-controlled walls (Note: the statistics shown are for the ratios of predicted-to-experimental values).

8.5.4. Point E (Axial Collapse)

As shown in Fig. 8-7, this point is assumed to have an ordinate that is equal to the wall residual lateral strength ratio (Parameter *c*), whereas the abscissa is equal to the rotation capacity corresponding to the onset of axial collapse (Parameter *d*).

The reduced subset of 101 walls with reported information on axial collapse was studied to identify parameters that influence rotation capacity (Parameter *d'*) at Point E. Similar to Parameter *d'*, $\lambda_b = l_w c / b^2$ and $P / A_g f_c'$ significantly influence Parameter *e*. Data and the proposed models are

presented in Fig. 8-20. Segura and Wallace (2018a) reported that providing lateral restraint in the form of crossties for the web longitudinal reinforcement increased the rotation capacity at axial collapse; however, tests on walls with crossties in the web region are rare and would not allow statistical analysis.

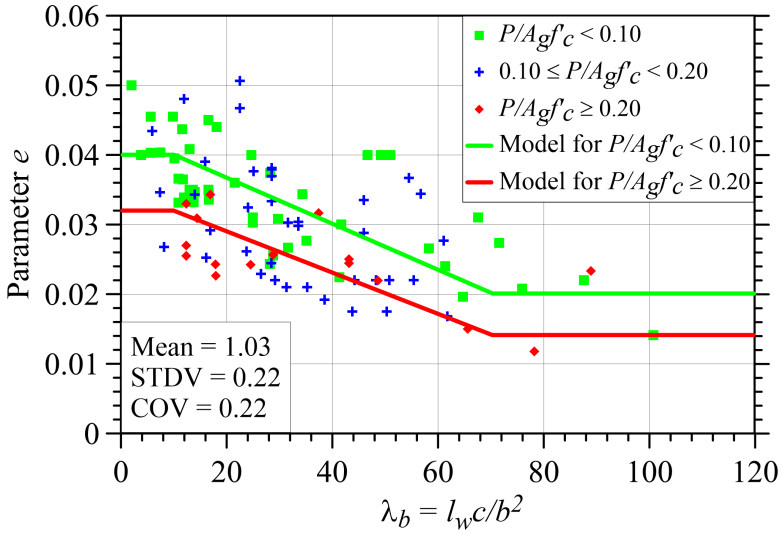

Fig. 8-20–Proposed models for Parameter e for conforming flexure-controlled walls (Note: the statistics shown are for the ratios of predicted-to-experimental values).

8.6. Proposed Modeling Parameters for Conforming Flexure-Controlled Walls

Based on results presented in the preceding sections, updated modeling parameters for conforming walls controlled by flexure are presented in Table 8-3. The statistics of each parameter are presented in Table 8-4. These statistics allow users to select appropriate modeling rules and acceptance criteria other than those recommended later in section 8.10.

Table 8-3–Modeling parameters for conforming RC structural walls controlled by flexure

Conditions			d
$\frac{l_w c_E}{b^2}$	$\frac{w_v V_{@Mult}}{A_{cv}\sqrt{f'_{cE}}}$	Overlapping hoops used?	
≤ 10	≤ 4	YES	0.032
≤ 10	≥ 6	YES	0.026
≥ 70	≤ 4	YES	0.018
≥ 70	≥ 6	YES	0.014
≤ 10	≤ 4	NO	0.032
≤ 10	≥ 6	NO	0.026
≥ 70	≤ 4	NO	0.012
≥ 70	≥ 6	NO	0.011

Conditions		C	c'	d'	e
$\frac{l_w c_E}{b^2}$	$\frac{P}{A_g f'_{cE}}$				
≤ 10	≤ 0.10	0.5	1.15	0.036	0.040
≤ 10	≥ 0.20	0.1		0.030	0.032
≥ 70	≤ 0.10	0.0		0.018	0.020
≥ 70	≥ 0.20	0.0		0.014	0.014

Notes: See Section 8.6.1

Table 8-4–Statistics of the modeling parameters given in Table 8-3*

Parameter	Mean	Median	Standard Deviation	Coefficient of Variation, COV
$M_{yE,cal}/M_{yE}$	1.01	1.00	0.12	0.12
c'	1.03	1.02	0.10	0.10
c	1.15	0.84	0.97	0.84
d	0.98	0.95	0.17	0.17
d'	1.01	1.01	0.22	0.21
e	1.03	1.01	0.22	0.21

**The statistics are for the ratios of predicted-to-experimental values.*

8.6.1. Notes on Table 8-3 (Most will apply to Table 8-5 for non-conforming walls)

1. Walls should be considered conforming when they comply with the following requirements:
   a) A minimum of two curtains of web vertical and horizontal reinforcement,
   b) Boundary longitudinal reinforcement ratio (calculated per ACI 318-14 R18.10.6.5), $\rho \geq 6\sqrt{f_c'(psi)}\Big/ f_y$,
   c) Min area ratio of provided-to-required (per ACI 318-14 §18.10.6.4) boundary transverse reinforcement, $A_{sh,provided}\Big/ A_{sh,required} \geq 0.7$,
   d) ratio of vertical spacing of boundary transverse reinforcement to the diameter of the smallest longitudinal reinforcement, $s\Big/ d_b \leq 8.0$,
   e) Adequate lap-splice of longitudinal reinforcement.
2. New and modified notations:
   a) The current tables of ASCE 41-17 use $l_w \times t_w$ for gross area (A_g) in the tables. This implies that the tables are only applicable to planar walls. Therefore, the following two notations are added:
      i. A_g = gross area of wall
      ii. A_{cv} = gross area of concrete section bounded by web thickness and length of section in the direction of shear force (= $l_w \times t_w$).
   b) Since c is defined as the residual strength ratio, use of c_E is recommended for depth of neutral axis at M_{yE} using expected material properties and axial load due to gravity loads and earthquake effects (worst case scenario).
   c) The notation b in the parameter $\lambda_b = l_w c/b^2$ is defined as width of flexural compression zone in ACI 318. In ACI 369, it is given for section width. For a simple planar wall, b is the

same as t_w; however, the tables proposed are intended to apply to walls with rectangular, flanged, and barbell cross sectional shapes (Fig. 4-8***a*** through ***f***). For cases with a large ***b***, e.g., where the barbell or flange of the wall is in compression (Fig. 4-8***a*** through ***h***), deformation capacity is likely to be relatively large (low λ_b); however, for cases with a barbell or flange in tension, and a thin wall web in compression (Fig. 4-8***b*** and ***e*** through ***h***), relatively large values of c/b and λ_b are likely, and higher shear demands are also likely; therefore, lower drift capacities are likely. For cases where ***b*** varies over ***c***, or where ***c*** varies over ***b***, a representative (e.g., weighted average) value of ***b*** or ***c*** should be used, as shown in Fig. 4-8(***c***), (***d***), (**e**) and (***h***).

3. The maximum shear demand, $V_{@Mult}$, is amplified to account for the higher mode responses using the following simplified dynamic shear amplification factor, ω_v, (ACI 318-19 §18.10.3):

$$\omega_v = 0.9 + \frac{n_s}{10} \quad for\ n_s \leq 6$$

$$\omega_v = 1.3 + \frac{n_s}{30} \quad for\ n_s > 6$$

Where n_s is the number of stories above the critical section and should not be taken less than 0.007 times the wall height above the critical section (h_{wcs}) measured in inches. This limit is imposed on n_s to account for buildings with large story heights (i.e., >12 ft. (144 in.)).

4. For overlapping hoops, the definition that has been approved for ACI 318-19 or a slightly more relaxed definition could be adopted.
5. In ASCE 41-17 §10.7.1.1, if axial load on a wall exceeded $0.35A_g f'_c$, the lateral strength and stiffness of the wall cannot be considered. It is recommended that this limit be removed because

the two datasets used to develop the new modeling parameters include walls with axial loads up to $0.6A_g f'_c$. The influence of axial load is accounted for with the $l_w c/b^2$ term.

6. For asymmetric walls (e.g., T-shaped, L-shaped, or half barbell walls, or walls with different quantities of reinforcement or different configuration of transverse reinforcement boundary elements), the user should produce backbones for both directions of loading (asymmetric backbone). However, for axial collapse, T-shaped and L-shaped walls are unlikely to lose axial load carrying capacities because tests observations have shown that the flange remains mostly intact unless it is subjected to bi-directional loading. Similarly, for wing walls (walls with a column at or near the center of the wall, if the column is well confined (spirally reinforced columns), they might not lose axial load carrying capacity. Such walls might be common in old construction (pre1980s).
7. Since different conditions are used for Parameter *d* and Parameters *d'* and *e*, Parameter *d'* and *e* should not be taken greater than Parameter *d*. In rare cases, this might happen.

8.7. Modeling Parameters for Non-Conforming Walls

Similar to conforming walls, the coordinates (strength ratios and total hinge rotation capacities) of each response point on the idealized backbone relation (Fig. 8-7) are developed in the following sections using the experimental results from the non-conforming wall dataset:

8.7.1. Point B ($E_c I_{eff}$ and M_{yE})

This point corresponds to member general yield strength and requires the yield strength (M_{yE}) and the effective flexural stiffness ($E_c I_{eff}$) of the hinge region. The effective flexural stiffness values are given in Chapter 7 and depend on the magnitude of the sustained gravity load. The calculated

yield moment strength, $M_{yE,cal}$, is evaluated as defined in ACI 369.1-17 and ASCE 41-17 based on the ACI 318-14 approach but using expected material properties.

Fig. 8-21 presents the ratio the calculated yield moment strength ($M_{yE,cal}$) to the experimental (observed) yield moment strength ($M_{yE,exp}$) for the non-conforming dataset. It can be seen that the calculated M_{yE} on average only slightly underpredicts the yield moment strength ($M_{yE,exp}$), except for walls with $P / A_g f_c' > 0.40$. Given that non-conforming walls encountered in practice typically have axial loads below $0.2A_g f'_c$, taking strength at Point B as $M_{yE,cal}$ is proposed, similar to conforming walls.

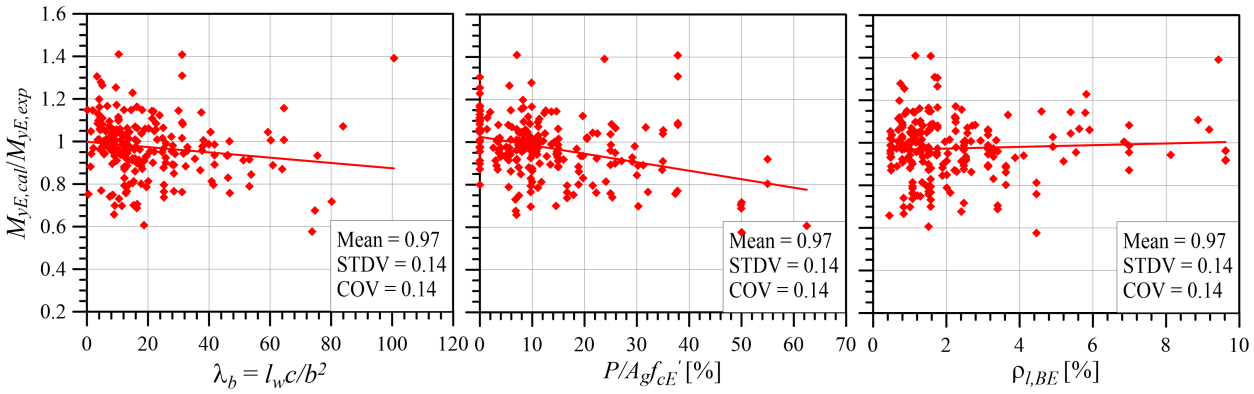

Fig. 8-21–Ratio of calculated-to- experimental yield moment strength ($M_{yE,cal}/M_{yE,exp}$) for the non-conforming wall dataset.

8.7.2. Point C (Parameter *c'* and Parameter *d*)

a) Parameter c' (i.e., $V_{@Mult}/V_{@MyE}$):

Fig. 8-22 presents the ratio of the ultimate moment strength obtained during the test ($M_{ult,exp}$) to the calculated $M_{yE,cal}$ for the non-conforming dataset, which shows that, on average, $M_{ult,exp}$ is 18%

higher than $M_{yE,cal}$. This value is slightly larger than that of conforming walls. Based on these results and results of the conforming wall dataset, Parameter c' is taken as 1.15 (M_{ult} =1.15 M_{yE}).

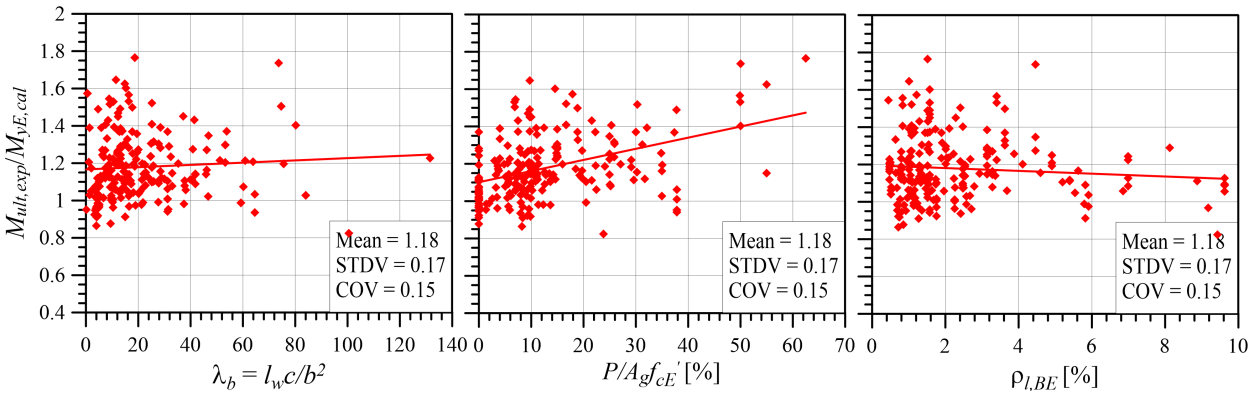

Fig. 8-22– Ratio of experimental ultimate-to-yield moment strength ($M_{ult,exp}/M_{yE,cal}$) for the non-conforming wall dataset.

b) Parameter *d* (i.e., total hinge rotation capacity at strength loss):

The non-conforming wall dataset was studied to highlight parameters that influence Parameter *d*. Fig. 8-23 shows variation of Parameter *d* against $\lambda_b = l_w c / b^2$ for three levels $P / A_g f_c'$. and wall shear stress ratio ($v_{max} / \sqrt{f_c'}$). It is clear that, similar to conforming walls, Parameter *d* is highly influenced by $\lambda_b = l_w c / b^2$, but the influence of $P / A_g f_c'$ and $v_{max} / \sqrt{f_c'}$ is not clear. As noted previously, $P / A_g f'_c$ does not correlate well with wall lateral deformation capacity at 20% lateral strength loss (Fig. 8-23(***a***)). Fig. 8-23(***b***) shows that the impact of $v_{max} / \sqrt{f_c'}$ is not as apparent as it was for walls in the conforming wall dataset, which might suggest that walls with non-conforming detailing might fail due to lack of proper detailing before the negative impact of shear

stress takes effect. It is also noted that there are relatively few walls in the dataset with high shear stresses ($v_{max} / \sqrt{f'_c} > 6$) at $\lambda_b = l_w c / b^2 > 20$ (Fig. 8-23(***b***)).

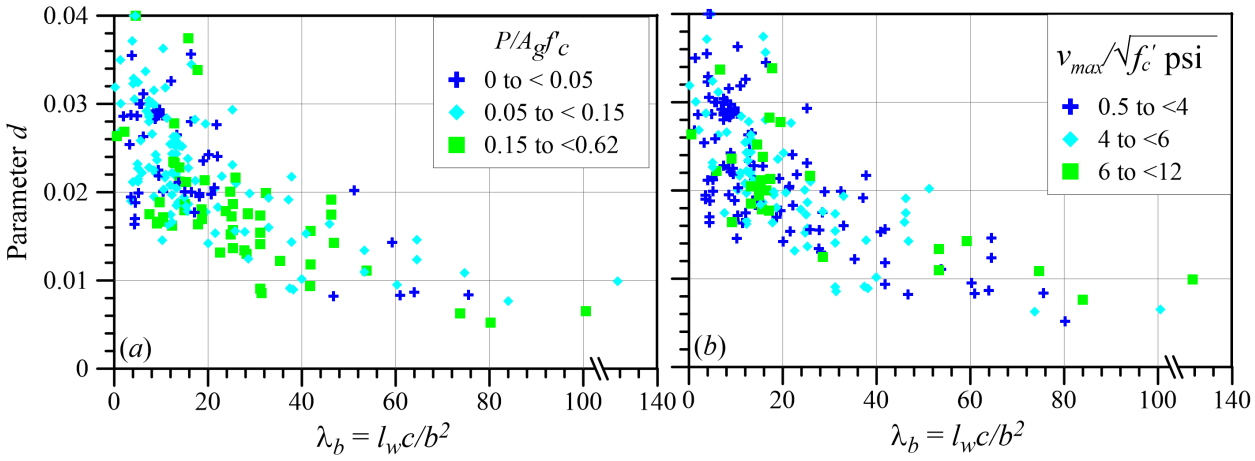

Fig. 8-23–Impact of $\lambda_b = l_w c / b^2$, $P / A_g f'_c$, and $v_{max} / \sqrt{f'_c}$ on Parameter d for walls with non-conforming detailing.

Additionally, performing a series of linear regression analyses were conducted on the non-conforming dataset and revealed that detailing parameters such as provided A_{sh}, s/d_b, and $\rho_{long,BE}$ play an important role in Parameter *d*, as shown in Fig. 8-24. It is noted that $\rho_{long,BE}$ is computed in accordance with ACI 318-14 R18.10.6.5, and the dataset includes walls with $\rho_{long,BE} \geq 0.004$ (see Fig. 8-21 and Fig. 8-22). Walls with very low $\rho_{long,BE}$ and low $P / A_g f'_c$ could have significantly less deformation capacity because such walls may develop one or two major cracks at or near the base with little or no secondary cracks, which leads to strain concentration at the major cracks and eventual bar fracture.

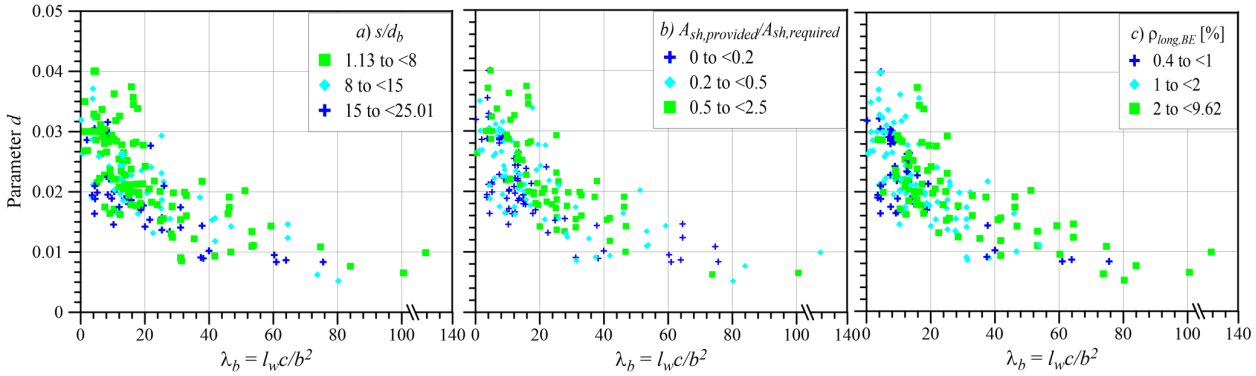

Fig. 8-24–Impact detailing parameters on Parameter d of non-conforming walls.

Fig. 8-25 shows the combined impact of A_{sh} and s/d_b along with the proposed models for Parameter d. It can be seen that the dispersion of the data at $\lambda_b < 20$ is significant. In this region, walls tend to have different flexure-failure modes. For example, walls with slender cross-sections ($l_w/b > 12$) and small compression zones ($c/b < 1.5$) tend to be limited by tensile strains that develop in the boundary longitudinal reinforcement (e.g., T-shaped wall loaded with the flange in compression), where providing additional transverse reinfrcement does not result in increased deformation capacity. These walls typically have rotation capacities larger than 0.02 unless they are reinforced with brittle (non-ductile) longitudinal reinforcement, or their longitudinal reinforcement ratio in the boundary region is small (i.e., < 0.0025). On the other hand, for walls that have squat cross-sections ($l_w/b < 8$) and moderate compression demands ($c/b > 2$), which most of the non-confroming walls fall into this category (Fig. 8-6), the deformation capacity tends to be limited by flexure compression failures, for which increased transverse reinforcement and bar restraint would likely lead to increased deformation capacity by providing improved lateral restraint against rebar buckling. Walls with $\lambda_b > 60$, which are characterized with slender cross-sections and high compression demands (i.e., thin walls), are typically controlled by brittle compression failures and/or out-of-plane instability.

Fig. 8-25 also shows walls with one curtain of web reinforcement, which, except for seven walls, all had no transverse reinofrcenent within the boundary region. Fig. 8-25 reveals that walls with one curtain of web reinforcement have rotation capacities comparable to those with two curtains of web reinforcement. Therefore, it is proposed that walls with one curtain of web reinfrocement be treated similar to walls with two curtains of web reinfrocement.

8.7.3. Point D (Parameter *c* and *d′*)

Fig. 8-26 shows the residual moment strength of the dataset normalized by M_{yE} (i.e., Parameter *c*), and reveals that, similar to conforming walls, Parameter *c* does not correlate well with the parameters that significantly impact Parameter *d′* (as shown next) such as λ_b and $P / A_g f_c'$. In the absence of additional studies, the piecewise best-linear fits (models) shown in Fig. 8-26 are proposed to derive Parameter *c* for non-conforming walls.

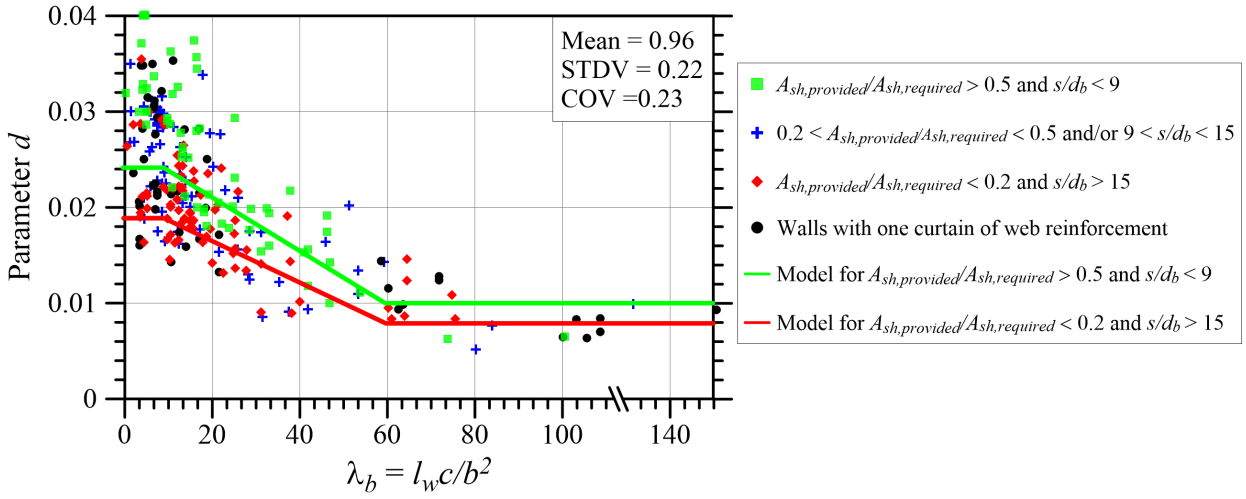

Fig. 8-25–Proposed models for Parameter *d* for non-conforming walls as a function of A_{sh} ratio and s/d_b.

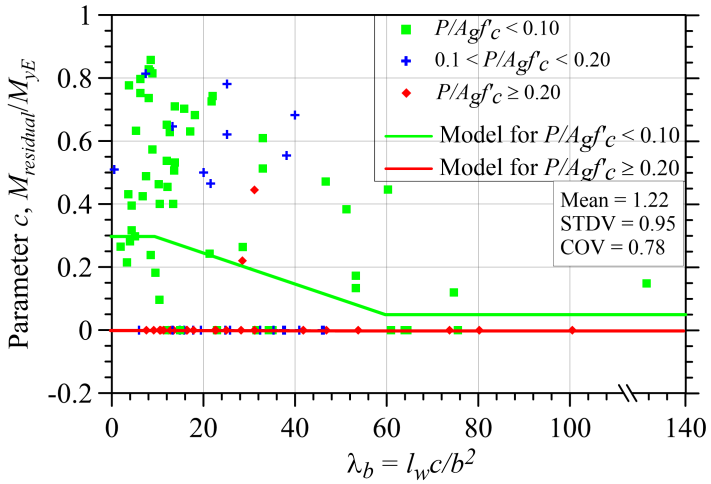

Fig. 8-26–Proposed models for Parameter c for non-conforming flexure-controlled walls.

Additionally, similar to conforming walls, $\lambda_b = l_w c / b^2$, $P / A_g f'_c$ were found to have a significant influence on Parameter *d'*, as shown in Fig. 8-27. Therefore, these two parameters are used as predictors for selecting Parameter *d'* based on the models shown in Fig. 8-27.

8.7.4. Point E (Axial Collapse)

Similar to Parameter *d'*, $\lambda_b = l_w c / b^2$ and $P / A_g f'_c$ significantly influence Parameter *e*. The results of the dataset, along with the proposed models, are presented in Fig. 8-28.

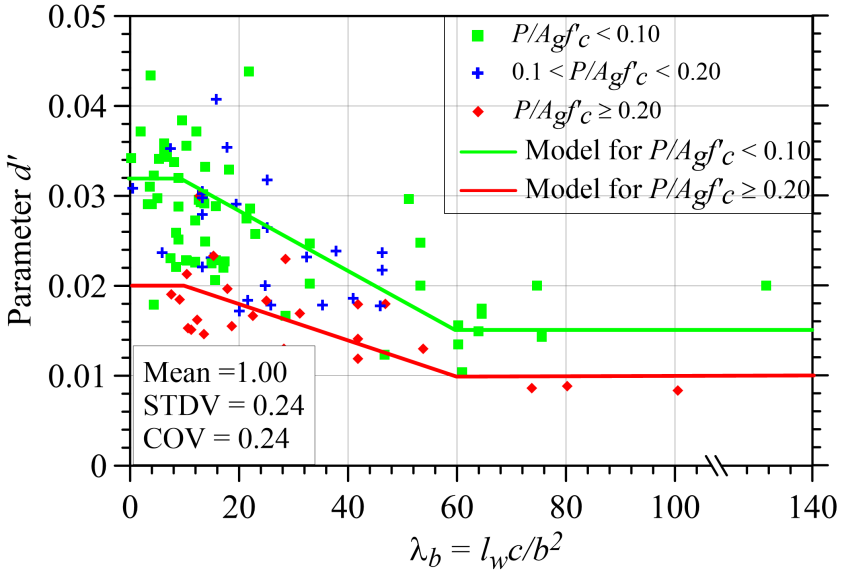

Fig. 8-27–Proposed models for Parameter d' for non-conforming flexure-controlled walls.

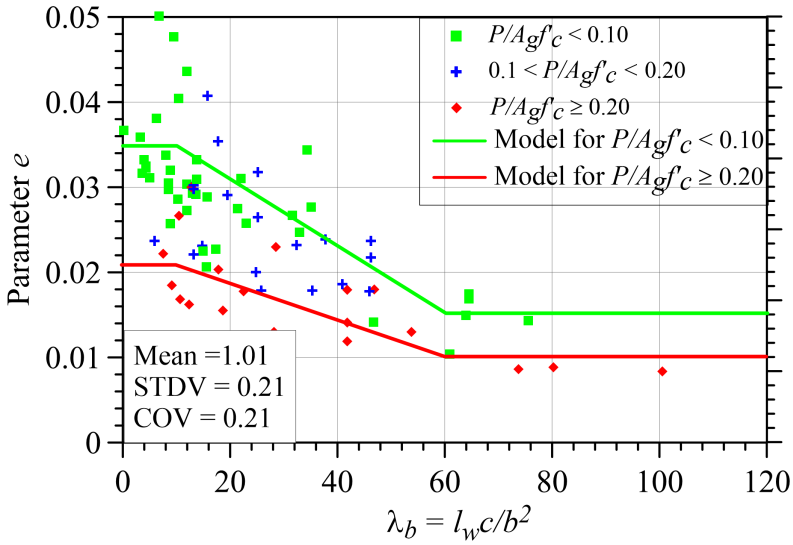

Fig. 8-28–Proposed models for Parameter e for conforming flexure-controlled walls.

8.8. Wall with Low Longitudinal Reinforcement Ratios

As noted previously, the non-conforming dataset contains walls with longitudinal reinforcement ratios in the boundary region ($\rho_{l,BE}$) equal to, or greater than, 0.0025 (minimum web longitudinal

reinforcement ratio of ACI 318-14). However, walls with distributed longitudinal reinforcement ratios < 0.0025 are found in buildings constructed prior 1970s (i.e., prior to establishment of modern seismic building codes). Furthermore, walls with longitudinal reinforcement ratios < 0.0015 are currently treated as force-controlled components/actions (ASCE 41-17 §10.7.2.3), which makes it virtually impossible to meet the strictly defined performance objectives at the BSE-2E hazard level when no ductility capacity is permitted, especially in wall buildings since the strength limit is reached at exceptionally low drift demands.

To address this issue, the database was filtered to identify walls with distributed longitudinal reinforcement ratios (ratio of area of total longitudinal reinforcement to gross concrete area perpendicular to the reinforcement), ρ_{lw}, < 0.0025, where ρ_{lw} is ratio of area of total longitudinal reinforcement to gross concrete area perpendicular to that reinforcement in a wall or wall segment)and a subset of 11 walls were identified with 0.001< ρ_{lw} < 0.0025. For those 11 wall tests, only data up lateral strength loss is available (i.e., Parameter *d*). The limited data are presented in Fig. 8-29 along with the models of Fig. 8-25 (non-conforming walls with longitudinal reinforcement ratio ≥ 0.0025). This figure suggests that non-conforming walls with such low longitudinal reinforcement ratios can perform significantly worse than those with higher reinforcement ratios when subjected to relatively low compression demands (i.e., $l_w c / b^2 < 10$), for which the failure mode is typically more tension-fracture of longitudinal bars due to the significant tensile strains expected to be developed in the extreme tension bars. This figure also reveals that walls with ρ_{lw} < 0.0025 and moderate-to-high compression demands perform similar to the data presented in Fig. 8-25 (i.e., walls with $\rho_{lw} \geq 0.0025$) because the deformation capacity of such walls is not particularly limited by tension-fracture of longitudinal bars, but rather by

concrete crushing and bar buckling. Therefore, the following is proposed until further data and information on walls with $\rho_{lw} < 0.0025$ become available.

The models presented in Fig. 8-25, Fig. 8-27, and Fig. 8-28 do not apply to walls with $\rho_{lw} < 0.001$ and a reduction factor should be applied for ρ_{lw} between 0.001 and 0.0025 and for low values of the parameter $l_w c / b^2$. A reduction factor of 0.4 for $\rho_{lw} = 0.001$ and $l_w c / b^2 \leq 10$ and 1.0 for $\rho_{lw} = 0.0025$ and $l_w c / b^2 \geq 20$ should be applied to the hinge rotation capacity values obtained from models shown in Fig. 8-25, Fig. 8-27, and Fig. 8-28. Linear interpolation of the reduction factor with respect to ρ_{lw} and $l_w c / b^2$ should be permitted for intermediate values. This proposed approach is shown in Fig. 8-29 (broken red line) with the limited test data and models of Fig. 8-25.

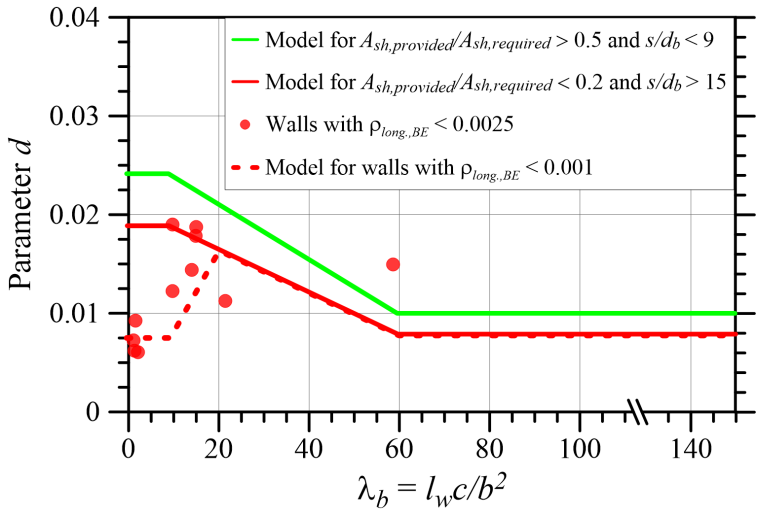

Fig. 8-29–Proposed model for Parameter d of flexure-controlled walls with $\rho_{lw} < 0.0025$.

8.9. Proposed Modeling Parameters for Non-Conforming Flexure-Controlled Walls

Based on results presented in the preceding sections, updated modeling parameters for non-conforming walls controlled by flexure are given in Table 8-5. The statistics of the parameters are

given in Table 8-6. These statistics allow users to select appropriate modeling rules and acceptance criteria other than those recommended later in section 8.10.

Table 8-5–Modeling parameters for non-conforming RC structural walls controlled by flexure

Conditions		d
$\frac{l_w c_E}{b^2}$	Detailing	
≤ 10	$\frac{A_{sh,provided}}{A_{sh,required}} \geq 0.5$ and $\frac{s}{d_b} \leq 9$	0.034
≤ 10	$\frac{A_{sh,provided}}{A_{sh,required}} < 0.2$ and $\frac{s}{d_b} > 15$	0.019
≥ 60	$\frac{A_{sh,provided}}{A_{sh,required}} \geq 0.5$ and $\frac{s}{d_b} \leq 9$	0.010
≥ 60	$\frac{A_{sh,provided}}{A_{sh,required}} < 0.2$ and $\frac{s}{d_b} > 15$	0.008

Conditions		c	c'	d'	e
$\frac{l_w c_E}{b^2}$	$\frac{P}{A_g f'_{cE}}$				
≤ 10	≤ 0.10	0.4	1.15	0.032	0.035
≤ 10	≥ 0.20	0.1		0.020	0.021
≥ 60	≤ 0.10	0.0		0.015	0.015
≥ 60	≥ 0.20	0.0		0.010	0.010

Notes: See section 8.9.1

Table 8-6–Statistics of the modeling parameters given in Table 8-5*

Parameter	Mean	Median	Standard Deviation	Coefficient of Variation
$M_{yE,cal}/M_{yE}$	0.97	0.97	0.14	0.14
c'	1.03	0.97	0.15	0.15
c	1.22	1.00	0.95	0.78
d	0.95	0.93	0.22	0.23
d'	1.01	0.97	0.24	0.24
e	1.01	1.02	0.21	0.21

**The statistics are for the ratios of predicted-to-experimental values.*

8.9.1. Notes on Table 8-5 (in addition to the applicable notes on Table 8-3)

1. Walls should be considered non-conforming when they do not satisfy all the requirements of conforming walls.
2. If values of both $A_{sh,provided}/A_{sh,required}$ and s/d_b fall between or outside the limits given in the table, linear interpolation should independently be performed for both $A_{sh,provided}/A_{sh,required}$ and s/d_b, and the lower resulting value of Parameter d should be taken.
3. Values of $A_{sh,provided}/A_{sh,required}$ and s/d_b should be provided over a horizontal distance that extends from extreme compression fiber at least $c_E/2$.
4. The d, d', and e parameters in this table do not apply to walls with ρ_{lw} lower than 0.001 and a reduction factor should be applied for ρ_{lw} between 0.001 and 0.0025 (ρ_{lw} = ratio of area of total longitudinal reinforcement to gross concrete area perpendicular to that reinforcement in a wall or wall segment) and for low values of parameter $l_w c / b^2$. A reduction factor of 0.4 for ρ_{lw} = 0.001 and $l_w c / b^2 \leq 10$ and 1.0 for ρ_{lw} = 0.0025 and $l_w c / b^2 \geq 20$ should be

applied to the hinge rotation capacity values obtained from this table. Linear interpolation of the reduction factor with respect to ρ_{lw} and $l_w c / b^2$ should be permitted for intermediate values.

5. Interpolation between table of conforming and non-conforming walls is not allowed.
6. This table applies to walls with either one or multiple curtains of web reinforcement.
7. Since different conditions are used for Parameter *d* and Parameters *d′* and *e*, Parameter *d′* and *e* should not be taken greater than Parameter *d*. In rare cases, this might happen.

8.10. Acceptance Criteria for Non-linear and Linear Procedures

8.10.1. General

Acceptance criteria are limiting values of deformation demands for deformation-controlled actions and strength demands for force-controlled actions, which are used to determine the conformance of a structure with the design requirements or performance objectives. ASCE 41-17 § 7.5.1 requires that prior to selecting component acceptance criteria (AC) for acceptability of force and deformation actions, each component that affects the lateral stiffness or distribution of lateral forces in the building, or are loaded as a result of lateral deformation of the building should be classified as primary or secondary, and each action should be classified as deformation-controlled (ductile) or force-controlled (nonductile). In general, a structural component that is required to resist seismic forces and accommodate the associated seismic deformations for the structure to achieve the selected performance level are classified as primary (e.g., the lateral force resisting system of the building), whereas a structural component that only needs to accommodate seismic deformations and is not required to resist seismic forces for the structure to achieve the selected performance level is permitted to be classified as secondary (the gravity system of the building).

In all cases, the engineer needs to verify that gravity load-carrying capacity of the structural system is not compromised, regardless of the designation of primary and secondary components. Currently, there is no AC for walls as secondary components in ASCE 41-17. This could be because walls typically provide add considerably or reliably to the lateral resistance of the building against seismic induced demands.

ASCE 41-17 §7.5.1.2 gives guidance on classifying actions as either deformation controlled or force controlled. In general, deformation-controlled actions are those for which the component can undergo measurable inelastic deformations without compromising the ability to maintain its load-carrying capacity, whereas force-controlled actions are those for which the component loses its load-carrying capacity once the elastic limit (yield strength) is exceeded (no ductility). In ASCE 41-17, actions are defined as deformation-controlled by the standard if linear and nonlinear AC are designated to them. In cases, where linear and nonlinear AC are not specified in the standard, actions should be classified as force controlled, unless component testing is performed to demonstrate otherwise. Currently, both shear and flexure actions in RC structural walls are treated as deformation-controlled actions, with AC specified for linear approaches in the form of deformation-based *m*-factors and for nonlinear approaches in the form of plastic hinge rotations. Other actions, such as axial, based shear sliding, as well as shear in walls with a transverse reinforcement ratio < 0.0015 (ASCE 41-17 § 10.7.2.3) and flexure in walls where the cracking moment strength exceeds the yield strength (ASCE 41-17 § 10.7.2.3), are currently treated as force-controlled actions, unless component testing is performed to demonstrate otherwise. The AC proposed herein in do not result in changes to the designation of force and deformation-controlled actions.

8.10.2. Distribution of Data for Parameters *d* and *e*

Fig. 8-30 presents the distributed of the data for the ratios of experimental-to-predicted *d* and *e*, along with normal and lognormal distributions associated with the means and standard deviations of the data. It can be seen that the data are better fit using a lognormal distribution. The data for Parameter *e* is not as well-fit using a lognormal distribution as Parameter *d,* and using normal distribution is not much better, either. This could be a limitation of the data set size (smaller) and the selected bin widths. For both distributions, the lower tail is more important, since this is the side of the distribution that affects the AC. For Parameter *d*, the lognormal distribution does a better job capturing that lower tail than the normal distribution. Furthermore, to be consistent with distributions used for other component in the standard and to avoid negative values of AC, lognormal distribution is assumed for deriving the AC, as shown below.

8.10.3. Proposed Acceptance Criteria (AC) for Nonlinear Procedures

The ASCE 41-17 §7.6.3 standard provides a procedure for defining AC based on experimental data. For both primary and secondary components, the standard defines AC for the Immediate Occupancy (IO) performance objective as the deformation at which permanent, visible damage occurred in the experiments (acceptable damage), but not greater than 2/3 of the deformation limit (AC) for Life Safety (LS). For both secondary and primary members, ASCE 41-17 §7.6.3 defines AC as 75% of Parameter *e* for LS and 100% of Parameter *e* for collapse prevention (CP). It is important to note that the current modeling parameters in the standard were selected very conservatively, as shown before; therefore, by taking AC as fractions of Parameter *e* or *d*, the standard in essence aims at deformation limits smaller than values at which lateral strength loss or axial failure occurs. Therefore, for more severe performance objectives (i.e., LS and CP), for which structural stability and safety are of significant concern, ensuring a fixed probability of exceeding

the deformation corresponding to the onset of lateral-strength degradation (Parameter *d*) or the onset of axial failure (Parameter *e*) is more appropriate and is consistent with performance objective of columns in ACI 369-17 (Ghannoum and Matamoros, 2014). As a result, the following acceptance criteria for nonlinear procedures are recommended for RC structural walls:

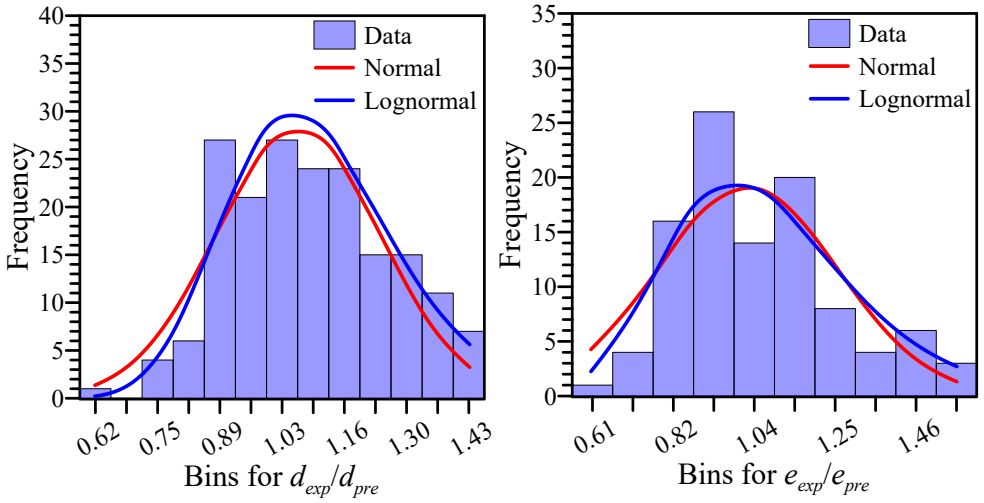

(*a*) Conforming Walls

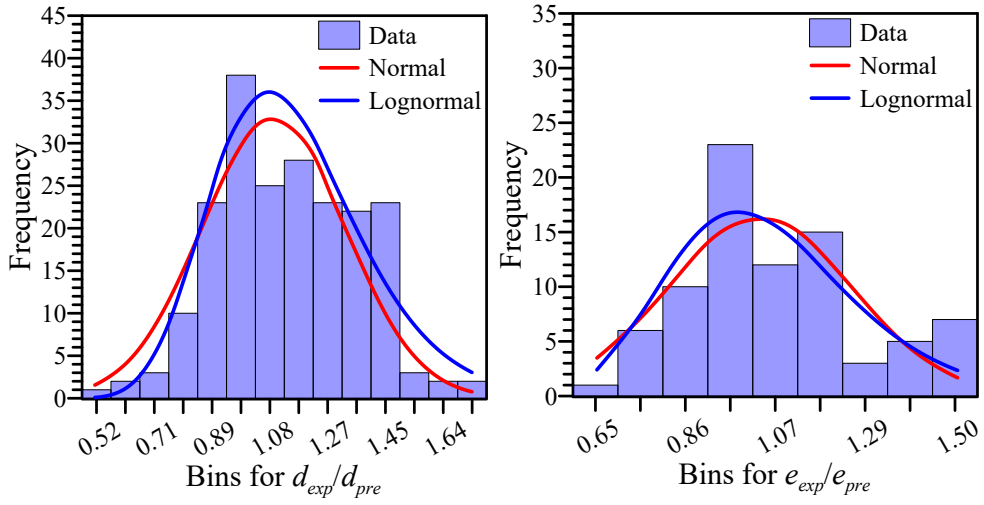

(*b*) Non-Conforming Walls

Fig. 8-30–Distribution of ratios of experimental-to-predicted *d* and *e*, along with normal and lognormal distributions associated with the means and standard deviations of the data

1. It is proposed here that AC for IO be based on a percentage of the plastic hinge rotation value (d - θ_y) plus the yield rotation. A conservative value of θ_y + 0.10 (d - θ_y) is selected as the limiting deformation at which a reinforced concrete wall is deemed to need repair and no longer satisfy the IO performance objective.
2. For LS of primary members, it is proposed that total hinge rotations should not exceed the 20th percentile of Parameter *d.* For a member critical to the stability of a structure, satisfying the AC for LS would indicate an 80% level of confidence that the member under consideration has not initiated lateral strength degradation.
3. For CP of primary members, it is proposed that total hinge rotations should not exceed the 35th percentile of Parameter *d.*
4. For LS of secondary members, it is proposed that total hinge rotations should not exceed the 10th percentile of Parameter *e* nor be less than AC for LS of primary members. Due to the more critical nature of the behavioral milestone identified by Parameter *e*, a lower percentile was selected for this AC than for primary members.
5. For CP of secondary members, total hinge rotations should not exceed the 25th percentile of Parameter *e* nor be less than AC for CP of primary members.
6. In all case, the AC for primary members should not be larger than those for secondary members.

Based on the above approach and assuming lognormal distribution for Parameters *d* and *e*, Table 8-7 and Table 8-8 present AC for conforming walls, where Table 8-7 uses the actual medians of the data for Parameters *d* and *e* (biased models), and Table 8-8 uses the medians rounded to 1.0

(unbiased models). Similarly, the results for non-conforming walls are presented in Table 8-9 and Table 8-10.

Table 8-7–Acceptance criteria for conforming structural walls: biased models are used

Performance Level	Component Type	Percentile	Percentage	Acceptance Criteria
IO	Primary	-	-	$\theta_y+0.1(d - \theta_y)$
	Secondary	-	-	$\theta_y+0.1(d - \theta_y)$
LS	Primary	20th of d	91%	$0.91d$
	Secondary	10th of e	74%	$0.74e \geq 0.91d$
CP	Primary	35th of d	98%	$0.98d$
	Secondary	25th of e	85%	$0.85e \geq 0.98d$

Table 8-8–Acceptance criteria for conforming structural walls: unbiased models are used

Performance Level	Component Type	Percentile	Percentage	Acceptance Criteria
IO	Primary	-	-	$\theta_y+0.1(d - \theta_y)$
	Secondary	-	-	$\theta_y+0.1(d - \theta_y)$
LS	Primary	20th of d	86.7%	$0.87d$
	Secondary	10th of e	74%	$0.74e \geq 0.87d$
CP	Primary	35th of d	93.6%	$0.94d$
	Secondary	25th of e	85.9%	$0.86e \geq 0.94d$

Table 8-9–Acceptance criteria for non-conforming structural walls: biased models are used

Performance Level	Component Type	Percentile	Percentage	Acceptance Criteria
IO	Primary	-	-	$\theta_y+0.1(d - \theta_y)$
	Secondary	-	-	$\theta_y+0.1(d - \theta_y)$
LS	Primary	20th of d	90.5%	$0.91d$
	Secondary	10th of e	74.9%	$0.75e \geq 0.91d$
CP	Primary	35th of d	99.6%	$1.00d$
	Secondary	25th of e	85.10%	$0.85e \geq 1.00d$

Table 8-10–Acceptance criteria for non-conforming structural walls: unbiased models are used

Performance Level	Component Type	Percentile	Percentage	Acceptance Criteria
IO	Primary	-	-	θ_y+0.1(d - θ_y)
	Secondary	-	-	θ_y+0.1(d - θ_y)
LS	Primary	20th of d	84.3%	0.84d
	Secondary	10th of e	76.4%	0.76$e \geq$ 0.84d
CP	Primary	35th of d	92.2%	0.92d
	Secondary	25th of e	86.8%	0.87$e \geq$ 0.92d

The impact of ignoring possible bias in the models for Parameter d on the AC results in lower (conservative) allowable rotation values for the AC. This may be conservative. The difference is about 4% for the conforming walls and about 7% for the non-conforming walls. The impact of ignoring possible bias in the models for Parameter e on the AC results in about the same allowable rotation values for the AC (≈1% difference). Since the medians and dispersions of Parameter d and e are close for conforming and non-conforming walls, a single set of AC for both conforming and non-conforming walls might be appropriate. Table 8-11 presents a recommended set of AC for both conforming and non-conforming walls. Approximate location of AC on the backbone relation is shown in Fig. 8-31.

Table 8-11–Recommended acceptance criteria for conforming and non-conforming flexure-controlled concrete structural walls.

Performance Level	Component Type	Acceptance Criteria
IO	Primary and Secondary	θ_y+0.1(d - θ_y)
LS	Primary	0.90d
	Secondary	0.75$e \geq$ 0.90d
CP	Primary	1.00d
	Secondary	0.85$e \geq$ 1.00d

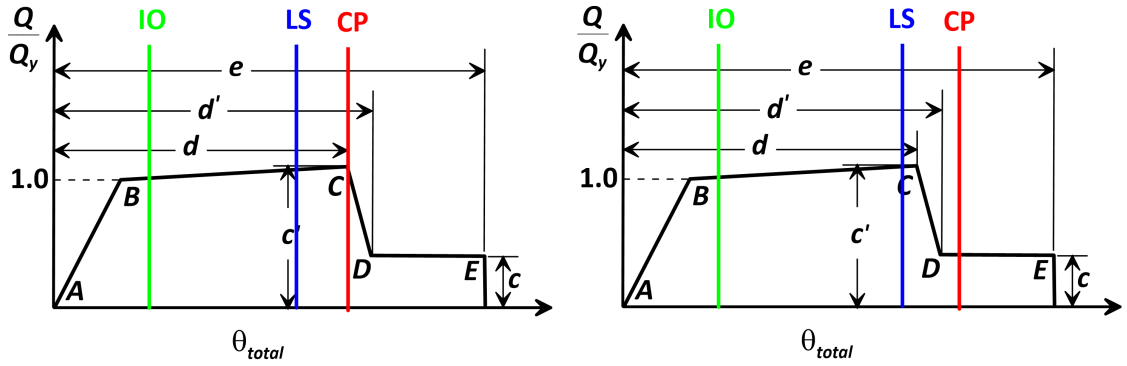

(*a*) Primary components (*b*) Secondary components

Fig. 8-31–Approximate location of AC on backbone relation.

8.10.4. Proposed Acceptance Criteria (AC) for Linear Procedures– *m*-factors

As noted in the previous section, for AC in nonlinear procedures, deformation limits are used. However, for the AC in the linear procedures, these deformation limits are converted to *m*-factors, defined as component capacity modification factors to account for the expected ductility associated with the action at the selected performance level. Since drift and deformation demands are not explicitly evaluated for ASCE 41 linear procedures, the *m*-factors are used as a proxy for limiting allowable drifts and deformations.

Provisions ASCE 41-17 §7.6.3 stipulate that *m*-factors be selected based on the nonlinear modeling parameters *d* and *e* from experimental data according to the relationships shown in Table 8-12. Because these *m*-factors are defined in terms of nonlinear modeling parameters *d* and *e*, the relationships in Table 8-12 are applicable to all types of walls, regardless of level of detailing.

Table 8-12–m-factors for reinforced concrete walls based on provisions of ASCE 41-17 §7.6.3

Component Type	Performance Level		
	IO	LS	CP
Primary	$\frac{3}{8}\left(\frac{d_{nl}}{\theta_y}\right)$	$\frac{9}{16}\left(\frac{d_{nl}}{\theta_y}\right)$	$\frac{9}{16}\left(\frac{e_{nl}}{\theta_y}\right)$
Secondary	$\frac{3}{8}\left(\frac{e_{nl}}{\theta_y}\right)$	$\frac{9}{16}\left(\frac{e_{nl}}{\theta_y}\right)$	$\frac{3}{4}\left(\frac{e_{nl}}{\theta_y}\right)$

The yield rotation (θ_y) in Table 8-12 is the average hinge rotation corresponding to the first yield of longitudinal reinforcement and is computed from sectional analysis of the wall as yield curvature (ϕ_y) times the hinge length (l_p). Fig. 8-32 presents variation of yield curvature computed from sectional analysis for a dataset of 978 walls versus wall length (l_w). A best fit model in the form of $\phi_y = 0.00375/ l_w$ results in a mean of 1.02 and a coefficient of variation of 0.21. The upper- and lower-bounds shown in Fig. 8-32 represent roughly the mean plus and minus two standard deviations, respectively. Assuming an l_p of $l_w/2$ and uniform distribution of curvature over l_p, a mean value of hinge yield rotation (θ_y) of 0.188% can be obtained. For the purpose of obtaining *m*-factors, it might be more appropriate to use the upper-bound yield curvature, which results in a θ_y of 0.25%, producing conservative values of *m*-factors. It is noted that these yield rotation values do not take into account the increase in yield rotation (flexibility) as a result of bar slip/extension into the foundation, which could increase θ_y by another 5% to 20% for walls with low-to-moderate axial loads (more axial load results in less bar slip/extension).

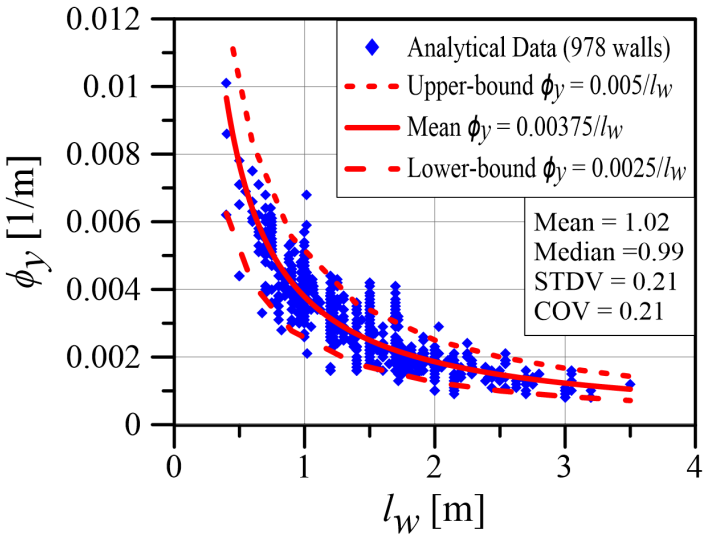

Fig. 8-32–Yield curvature (ϕ_y) computed from sectional analysis as a function of wall length (l_w).

8.11. Summary and Conclusions

This study involves utilizing the available experimental data and new information on performance of structural walls to develop updated modeling parameters and acceptance criteria for seismic evaluation and retrofit of flexure-controlled reinforced concrete structural walls. The current ASCE 41-17 nonlinear deformation-based modeling parameters (i.e., Parameters *a* and *b*) are given as plastic hinge rotations. Where a lumped plasticity model is used, the hinge region, which is typically at or near the base of a wall, is modeled as a near-rigid spring with effectively no elastic deformation. However, in this study, the deformation-based modeling parameters are given as total hinge rotation capacities, which include both the elastic and plastic deformations of the hinge region ($l_w/2$). This approach is proposed because, by using total hinge rotation capacities: 1) Modeling parameters are not sensitive to approaches (or assumptions) used to calculate yield rotation, θ_y, 2) Modeling parameters are consistent with the total drift ratio or chord rotation used to define modeling parameters for shear-controlled walls and coupling beams, respectively, and 3)

Modeling parameters can be converted to strain limits by dividing by an assumed hinge length, which is convenient where fiber models are used, which is becoming increasingly popular in engineering practice.

To accomplish these objectives, two subsets of data were filtered from UCLA-RCWalls database, one for walls with conforming "or special" detailing and the other for walls with non-conforming "or ordinary" detailing. The datasets were first used to evaluate the current modeling parameters of ASCE 41-17 (ACI 369-17), and the results revealed that the current modeling parameters for walls constitute a conservative lower-bound estimate of wall deformation capacities, and that the predictor variable $\left[\left(A_s - A'_s\right) f_{yE} + P\right] \Big/ A_g f'_{cE}$ used to select modeling parameters does not correlate well with the modeling parameters and thus produces large dispersions. Subsequently, the two datasets were studies extensively to identify parameters that have moderate to significant influence on each modeling parameter on the backbone relation. Based on the results, two sets of modeling parameters are proposed, one for walls with conforming "or special" detailing and the other for walls with non-conforming "or ordinary" detailing. The proposed modeling parameters produce dispersions are that very low (coefficient of variation ranging from 0.18 to 0.25). The updates are expected to be significant contributions to the practice of seismic evaluation and retrofit of wall buildings.

8.12. Acknowledgements

Funding for this study was provided, in part, by ATC 140 Project, and the University of California, Los Angeles. The authors would also like to thank the other member of Working Group 3 (WG3) of ATC 140 Project, which include Wassim Ghannoum, Garrett Hagen, Mohamed Talaat, Laura

Lowes, and Afshar Jalalian for providing thoughtful comments on the work presented. Any opinions, findings, and conclusions or recommendations expressed in this paper are those of the authors and do not necessarily reflect the views of others mentioned here.

8.13. References

Abdullah, S. A., and Wallace, J. W., 2018a "UCLA-RCWalls database for reinforced concrete structural walls," *Proceedings, 11th National Conference in Earthquake Engineering*, Earthquake Engineering Research Institute, Los Angeles, CA.

Abdullah, S. A., and Wallace, J. W., 2018b, "A Reliability-Based Deformation Capacity Model for ACI 318 Compliant Special Structural Walls," *Proceedings, 2018 Structural Engineers Association of California (SEAOC) Convention*, Palm Springs, CA.

Abdullah S. A., Wallace J. W., 2019, "Drift capacity of RC structural walls with special boundary elements," *ACI Structural Journal*, Vol. 116, No. 1, pp. 183–194.

ACI Committee 318. (2014). Building Code Requirements for Structural Concrete and Commentary (ACI 318), American Concrete Institute, Farmington Hills, MI. 524 pp.

ASCE Standards ASCE/SEI 41-17 "Seismic Evaluation and Retrofit of Existing Buildings (ASCE/SEI 41-17)," American Society of Civil Engineers, Reston, VA, 576 pp.

ASCE/SEI Standards, 2016, "Minimum Design Loads for Buildings and Other Structures (ASCE/SEI 7-16)," American Society for Civil Engineers, Reston, VA, 690 pp.

Birely, A., Lowes, L., and Lehman, D., 2014, "Evaluation of ASCE 41 Modeling Parameters for Slender Reinforced Concrete Structural Walls," ACI Special Publication (SP-297–4).

FEMA 273, 1997, *Guidelines to the Seismic Rehabilitation of Existing Buildings*, Federal Emergency Management Agency, Washington, D.C.

Ghannoum W.M., Matamoros A.B., 2014, "Nonlinear modeling parameters and acceptance criteria for concrete columns," *ACI Special Publication*, 297, pp. 1-24.

Lu, Y., Gultom, R., Henry, R. S., Ma, Q. T., 2016 “Testing of RC walls to investigate proposed minimum vertical reinforcement limits in NZS 3101:2006 (A3)”, Proceedings of the 2016 NZSEE Annual Conference, Christchurch, April 1-3.

NIST, 2011. *Seismic Design of Cast-in-Place Concrete Special Structural Walls and Coupling Beams: A Guide for Practicing Engineers*, *NIST GCR 11-917-11 REV-1*, NEHRP Consultants Joint Venture, National Institute of Standards and Technology, Gaithersburg, Maryland

Segura, C. L., and Wallace, W. J., 2018a, “Seismic performance limitations and detailing of slender reinforced concrete walls,” *ACI Structural Journal*, V. 115, No. 3, pp. 849-860.

Segura, C. L., and Wallace, W. J., 2018b, “Impact of geometry and detailing on drift capacity of slender walls,” *ACI Structural Journal*, V. 115, No. 3, pp. 885–896.

Tran, T. A. (2012). “Experimental and analytical studies of moderate aspect ratio reinforced concrete structural walls.” Ph.D. dissertation, Dept. of Civil and Environmental Engineering, Univ. of California, Los Angeles.

Wallace, J. W., “Slender Wall Behavior and Modeling,” PEER/EERI Technical Seminar Series, New Information on the Seismic Performance of Existing Concrete Buildings, 2006. see www.eeri.org/

CHAPTER 9. Conclusions and Recommendations

The main body of this dissertation consists of seven distinct and yet closely related chapters. Detailed conclusions and recommendations are outlined in each chapter; however, the key conclusions and recommendations are summarized below:

1. A comprehensive and large relational database of RC wall tests known as UCLA-RCWalls was developed that currently contains detailed and parameterized information and test results of over 1100 wall tests surveyed from more than 260 experimental programs reported in the literature around the world. The database can serve as a valuable resource for the structural/earthquake engineering community to assess behavior of RC walls against a wide range of design parameters, develop empirical models that capture data trends, validate analytical studies, and identify gaps in the available experimental data and guide future test programs on RC structural walls.

2. Displacement capacity of ACI 31-14 code-compliant walls is primarily a function of parameters that are not adequately addressed in ACI 318-14 code, such as wall cross-section geometry $\left(l_w/b\right)$, neutral axis depth $\left(c/b\right)$, wall shear stress demand $\left(v_{max}/\sqrt{f_c'}\right)$, as well as the configuration of the boundary transverse reinforcement (use of overlapping hoops versus a single perimeter hoop with supplemental crosstie legs). Based on these variables, drift capacity of walls with special boundary elements (SBEs) varies roughly by a factor of 3, ranging from approximately 0.012 to 0.035. In general, lower drift capacities result for walls with $l_w/b \geq 15$, $c/b \geq 3.0$, and wall shear stress levels approaching the ACI 318-14 limit of $10\sqrt{f_c'}$ psi $\left(0.83\sqrt{f_c'}\text{ MPa}\right)$ for an individual wall.

3. The underlying premise of the ASCE 7-10 and ACI 318-14 provisions is that special structural walls satisfying the provisions of ACI 318-14 §18.10.6.2 through §18.10.6.4 possess adequate drift capacity to exceed the expected drift demand determined from ASCE 7-10 analysis procedures. However, results presented in this study show that this assumption is not always correct, and that, in some case, the intended performance objectives may not be achieved. To address this deficiency, a new reliability-based design methodology is proposed where a drift demand-capacity ratio (DDCR) check is performed to provide a low probability (i.e., 10% or lower) that roof drift demands exceed roof drift capacity at strength loss for the **DE** level shaking. In general, walls with slender cross sections $\left(l_w/b>15\right)$, large neutral axis depth relative to width of flexural compression zone $\left(c/b>3\right)$, shear stresses approaching the ACI 318 §18.10.4.4 limit $\left(10\sqrt{f_c^{'}}\right)$, and roof drift demands approaching the maximum story drift allowed by ASCE 7-10 are screened out for redesign.

4. Drift capacity of flexure-controlled structural walls asscoiated with axial failure is strongly impacted by $\lambda_b = l_w c / b^2$ and $P / A_g f_c^{'}$. This is because, once strength degradation initiates, the level of axial load accelerates the rate of deterioration such that walls with high $P / A_g f_c^{\prime}$ have a steep post-peak slope on the backbone relation, where little to no additional deformation capacity beyond the deformation at initiation of lateral strength loss is achieved prior to axial failure (i.e., no residual strength plateau). For shear-controlled walls, a shear friction model is calibrated and validated to predict drift capacity at axial failure, and a simplified model that is only based on axial load ratio is also provided.

5. Analysis of reported failure modes of about 1000 wall tests indicated that the flexure- and shear-controlled walls have a shear-to-flexure strength ratio ($V_n/V_{@Mn}$) > 1.0 and < 1.0, respectively, whereas walls with failure modes reported as flexure-shear are mainly scattered between $0.7 < V_n/V_{@Mn} < 1.3$.

6. Axial load has the greatest impact on wall flexural stiffness (uncracked and cracked), and that longitudinal reinforcement ratio produced significant impact on cracked effective flexural stiffness at low axial load ratios (i.e., < $0.10A_g f'_c$). For axial loads ranging from 0.05 to $0.50A_g f'_c$, cracked effective stiffness ($E_c I_{eff}$) increases from 0.20 to 1.0 of the gross section stiffness ($E_c I_g$). Uncracked flexural stiffness ($E_c I_{uncr}$) varies from 0.50 to 1.0 $E_c I_g$ for axial load increasing from zero to $0.30A_g f'_c$. Furthermore, based on results from a subset of 64 wall tests, a constant effective shear modulus of one-third of gross shear modulus (i.e., $G_{eff} = G_g/3$) is proposed for use to model shear response of shear-cracked flexure-controlled walls.

7. The results presented herein revealed that the current modeling parameters of ASCE 41-17 (ACI 369-17) for flexure-controlled structural walls constitute a conservative lower-bound estimate of wall deformation capacities, and the predictor variable $\left[\left(A_s - A'_s\right) f_{yE} + P\right] \Big/ A_g f'_{cE}$ used to select modeling parameters does not correlate well with the modeling parameters. Based on the results of large datasets for flexure-controlled walls, two sets of modeling parameters are proposed, one for walls with conforming "or special" detailing and the other for walls with non-conforming "or ordinary" detailing. The proposed modeling parameters, except for Parameter *c*, produce dispersions are that very low (coefficient of variation ranging from 0.18 to 0.25). The updated deformation-based modeling

parameters are given as total hinge rotations over a plastic hinge length of half the wall length ($l_w/2$).

APPENDIX A – References of Data in UCLA-RCWalls Database

This appendix presents all the references where information on the wall tests in UCLA-RCWalls database are reported and that were available to the author:

Program	References
Abdulridha and Palermo 2014	Abdulridha, A., and Palermo D., 2014, "Response of a hybrid-SMA reinforced concrete shear wall," Proceedings of 10th U.S. National Conference on Earthquake Engineering, July 21-25, Anchorage, Alaska.
	Abdulridha, A., and Palermo D., 2017, "Behavior and modelling of hybrid SMA-steel reinforced concrete slender shear wall," Engineering Structures, Vol. 147, pp. 77–89.
	Maciel, M., Palermo, D., Abdulridha, A., 2016, "Seismic Response of SMA Reinforced Shear Walls," Special Topics in Structural Dynamics, Volume 6, Conference Proceedings of the Society for Experimental Mechanics Series, DOI 10.1007/978-3-319-29910-5_19
Adajar et al., 1995	Adajar, J.C., Yamaguchi, T., and Imai, H.,1995, "Seismic Behavior of Precast Shear Wall with Bar Splices Confine to Spiral Steel," Proceedings of the Japan Concrete Institute, Vol. 17, No. 2, pp. 285-290.
	Adajar, J.C., Yamaguchi,1996, "New Connection Method for Precast Shear Wall," Proceedings of 11th World Conference on Earthquake Engineering, June 23-28, Acapulco, Mexico, Paper No. 590.
Adebar	Adebar, P., Ibrahim, A. M. M., and Bryson, M., 2007, "Test of High-Rise Core Wall: Effective Stiffness for Seismic Analysis," ACI Structural Journal, Vol. 104, No. 2, pp. 549-559.
Alarcon 2013	Alarcon, C., Hube, M.A., and De la Llera, J.C., 2014, "Effect of axial loads in the seismic behavior of reinforced concrete walls with unconfined wall boundaries," Engineering Structures, Vol. 73, pp. 13–23.
	Alarcon, C., and Hube, 2013, "Influence of Axial Load in the Seismic Behavior of Reinforce Concrete Walls with Non-seismic Detailing," PhD Dissertation, Pontifical Catholic University of Chile, Santiago, Chile.
Ali and WIght 1990	Ali, A., and Wight, J.K., 1990, "Reinforced Concrete Structural Walls with Staggered Opening Configurations under Reversed Cyclic Loading," Report No. UMCE 90-05, University of Michigan, Ana Arbor, Michigan.
	Ali, A., and Wight, J.K., 1991, "RC Structural Walls with Staggered Door Openings," Journal of Structural Engineering, Vol. 117, No. 5, pp. 1514-1531.
Almeida et al 2014	Almeida, J., Prodan, O., Rosso, and A., Beyer, K., 2017, "Tests on Thin Reinforced Concrete Walls Subjected to In-Plane and Out-of-Plane Cyclic Loading," Earthquake Spectra, Vol. 33, No. 1, pp. 323-345.
	Almeida, J., and Beyer, K., 2014, "Seismic Behavior of Existing Reinforced Concrete Buildings with Thin Walls," Final Report for Stiftung zur Förderung der Denkmalpflege, École Polytechnique Fédérale de Lausanne, Lausanne.
	Rosso, A., Almeida, J., and Beyer, K., 2015, "Stability of thin reinforced concrete walls under cyclic loads: state-of-the art and new experimental findings," Bulletin of Earthquake Engineering, Vol. 14, No. 2, pp. 455-484.
	Almeida, J., Rosso, A., Beyer, K., and Sritharan, S., 2014, "New experimental findings on the stability of thin reinforced concrete walls," 5th Portuguese Conference on Structural Engineering, Nov. 26-28, Lisbon, Portugal.

	Almeida J., Prodan, O., Rosso, A., and Beyer, K., 2017, "Tests on Thin Reinforced Concrete Walls Subjected to In-plane and Out-of-plane Cyclic Loading," Earthquake Spectra, Vol. 33, No. 1, pp. 323-345.
Albidah 2016	Albidah, A., 2016, "Vulnerability and Risks of Collapse of Structural Concrete Walls in Regions of Low to Moderate Seismicity," PhD Dissertation, The University of Melbourne, Melbourne, Australia.
Altheeb 2016	Altheeb, H., 2016, "Seismic Drift Capacity of Lightly Reinforced Concrete Shear Walls," PhD Dissertation, The University of Melbourne, Melbourne, Australia.
Altin et al., 2013	Altin, S., Kopraman, Y., and Baran, M., 2013, "Strengthening of RC walls using externally bonding of steel strips," Engineering Structures, Vol. 49, pp. 686-695.
	Altin, S., Anil, O., Kopraman, Y., and Kara, M., 2013, "Hysteretic behavior of RC shear walls strengthened with CFRP strips," Elsevier, Composites: Part B, Vol. 44, pp. 321-329.
Ichinose 2014	Anoda, J., 2014, "Effect of Construction Joint and Arrangement of Vertical Bars on Slip Behavior of Shear Walls," Master's Thesis, Nagoya Institute of Technology, Nagoya, Japan. (in Japanese)
	Matsuba, M., Hosona, J., Anoda, E., Takahashi, S., and Ichinose, T., 2015, "An Experimental Study on the Effect of Construction Joint and Bar Arrangement on the Slip Behavior of RC Shear Walls: Part 1 Outline of Experiment and Load-Displacement Relationship," Architectural Institute of Japan, Vol. 218, No.53, pp. 157-160. (in Japanese)
	Hosona, J., Anoda, E., Takahashi, S., and Ichinose, T., 2015, "The Effect of Construction Joint and Arrangement of Bars on the Slip Behavior of Shear Walls," Proceedings of the Japan Concrete Institute, Vol. 36, No. 2, pp. 355-360. (in Japanese)
Athanasopoulou 2010	Athanasopoulou, A., 2010, "Shear Strength and Drift Capacity of Reinforced Concrete and High-Performance Fiber Reinforced Concrete Low-Rise Walls Subjected to Displacement Reversals," PhD Dissertation, The University of Michigan, Ana Arbore, Michigan.
	Athanasopoulou, A., and Parra-Montesinos, G., 2013, "Experimental Study on the Seismic Behavior of High-Performance Fiber-Reinforced Concrete Low-Rise Walls," ACI Structural Journal, Vol.110, No. 5, pp. 767-777
Bae et al., 2010	Bae, Y., Tanizawa, K., Yun, K., and Kabeyasawa, S., 2010, "Experimental study on structural characteristics of columns with sleeve walls," Proceedings of the Japan Concrete Institute, Vol. 32, No. 2, pp.115-120. (in Japanese)
Baek and Park 2015	Baek, J., and Park, H., 2015, "Shear-Friction Strength of RC Walls with 550 MPa Bars," Proceedings of the Tenth Pacific Conference on Earthquake Engineering, Nov. 6-8, Sydney, Australia, Paper No. 180.
Baek et al., 2014	Baek, J., Park, H., and Yim, S., 2014, "Applicability of Grade 550 MPa Shear Bars in RC Walls with Aspect Ratio of 2.0," Proceedings of the 2nd International Conference on Advances in Civil, Structural, and Environmental Engineering (ACSEE), Oct. 25-26, Zurich, Switzerland, pp. 135-139.
Baek et al., 2015	Baek, J., Park, H., and Yim, S., 2014, "Behavior of RC Walls with Different Steel Grades and Aspect Ratio of 2.0," Proceedings of the 2015 World Congress on Advances in Structural Engineering and Mechanics, August 25-29, Incheon, Korea.
Baek et al., 2017	Baek, J., Park, H., and Yim, S., 2017, "Cyclic Loading Test for Walls of Aspect Ratio 1.0 and 0.5 with Grade 550 MPa (80 ksi) Shear Reinforcing Bars," ACI Structural Journal, Vol. 114, No. 4, pp. 969-982.

Baek et al., 2018	Baek, J., Park, H., Choi, K., Seo, M., and Chung, L.., 2018, "Minimum Shear Reinforcement of Slender Walls with Grade 500 MPa (72.5 ksi) Reinforcing Bars," ACI Structural Journal, Vol. 115, No. 3, pp. 761-774.
Barda 1972	Barda, F., 1972, " Shear Strength of Low-Rise Walls with Boundary Elements," PhD Dissertation, Lehigh University Bethlehem, Pennsylvania.
Barda et al., 1977	Barda, F., Hanson, J., and Corley, W., 1977, "Shear Strength of Low-Rise Walls with Boundary Elements," ACI Special Publication, SP 53-8, pp. 149-202.
Bertero et al., 1973	Bertero, V.V., Popov, E.P., Wang, T.Y., and Vallenas, J., 1977, "Seismic Design Implication of Hysteretic Behavior of Reinforced Concrete Structural Walls," Proceedings of the 6th World Conference on Earthquake Engineering, January 10-14, New Delhi, India, pp. 1898-1904.
	Wang, T. Y., Bertero, V. V., and Popov, E. P., 1975, "Hysteric Behavior of Reinforced Concrete Framed Walls," Report No. EERC 75-23, Earthquake Engineering Research Center, University of California Berkeley, Berkeley, CA.
	Wang, T. Y., Bertero, V. V., and Popov, E. P., 1975, "Hysteric Behavior of Reinforced Concrete Framed Walls," Report No. EERC 75-23, Earthquake Engineering Research Center, University of California Berkeley, Berkeley, CA.
	Iliya, R., and Bertero, V. V., 1980, "Effects of Amount and Arrangement of Wall- Panel Reinforcement on Hysteretic Behavior of Reinforced Concrete Walls," Report No. UCB/EERC- 80/04, University of California Berkeley, Berkeley, CA.
	Vallenas, J. M., Bertero, V. V., and Popov, E.P., 1979, "Hysteretic Behavior of reinforced Concrete Structural Walls," Report No. UCB/EERC-79/20, University of california Berkeley, Berkeley, CA.
Bimschas 2010	Bimschas, M., 2010, "Displacement Based Seismic Assessment of Existing Bridges in Regions of Moderate Seismicity," PhD Dissertation, Institute of Structural Engineering Swiss Federal Institute of Technology Zurich, Zurich, Switzerland.
	Bimschas, M., and Dazio, A., 2008, "Large Scale Quasi-Static Cyclic Test of Existing Bridge Piers," Proceedings of the 14th World Conference on Earthquake Engineering, Oct. 12-17, Beijing, China.
Birely	Lowes, L., Lehman, D., and Birely, A., 2011, "Behavior, Analysis, and Design of Complex Wall Systems: Planar Wall Testing Program Summary Document," University of Washington, Seattle and University of Illinois, Urbana-Champaign, Illinois.
	Birely, A., 2011, "Seismic Performance of Slender Reinforced Concrete Structural Walls," A Proposal to PhD Dissertation, University of Washington, Seattle, WA.
	Birely, A. C., 2012, "Seismic Performance of Slender Reinforced Concrete Structural Walls," PhD Dissertation, University of Washington, Seattle, WA.
	Birely, A., Lehman, D., Lowes, L., Kuchma, D., Hart, C., and Marley, K., 2008, "Investigation of the Seismic Behavior and Analysis of Reinforced Concrete Structural Walls," Proceedings of the 14th World Conference on Earthquake Engineering, Oct. 12-17, Beijing, China.
	Brown, P., Ji, J., Oyen, P., Sterns, A., Lehman, D., Lowes, N., Kuchma, and D., Zhang, J., 2006, "Investigation of the Seismic Behavior and Analysis of Reinforced Concrete Structural Walls," Proceedings of the 8th U.S. National Conference on Earthquake Engineering, April 18-22, San Francisco, California, USA, Paper No. 532.

	Brown, P., Ji, J., Oyen, P., Sterns, A., Lehman, D., Lowes, N., Kuchma, and D., Zhang, J., 2012, "Earthquake response of slender planar concrete walls with modern detailing," Engineering Structures, Vol. 43, pp 31-47.
	Lehman, D., Lowes, L., Birely, A., Kuchma, D., Hart, C., and Marley, K., 2009, "Investigation of the Seismic Response of Slender Concrete Walls," Presentation.
Bouchon et al., 2004	Lafolie F., and Bouchon M.,1992, "Behavior of reinforced concrete walls subjected to alternating dynamic loads," Proceedings of the 10th World Conference on Earthquake Engineering, July 19-24, 1992, Madrid, Spain.
	Bouchon, M., Orbovic, N., and Foure, B., 2004, "Tests on Reinforced Concrete Low-Rise Shear Walls Under Static Cyclic Loading", Proceedings of 13th World Conference on Earthquake Engineering, August 1-6, Vancouver, B.C., Canada, Paper No. 257.
	Gantenbein, F., Queval, J. C., Epstein, A., Dalbera, J., and Duretz, C., 1991, "Experimental Study on Concrete shear Wall Behavior under Seismic Loading," Proceedings of the International Association for Structural Mechanics in Reactor Technology (IASMiRT), Aug. 18, Tokyo, Japan, pp 315-320.
	Gantenbein, F., Queval, J.C., and Epstein, A., 1991, "Experimental Study on Concrete Shear Wall Behavior Under Seismic Loading," Proceedings of the 11th Internal Conference on Structural Mechanics in Reactor Technology, Aug. 18-23, Tokyo, Japan.
Brueggen 2009	Brueggen, B. L., 2009, “Performance of T-shaped Reinforced Concrete Structural Walls under Multi-Directional Loading,” PhD Dissertation, University of Minnesota, Minneapolis, MN.
	Aaleti, S., Brueggen, B.L., Johnson, B., French, C.E., and Sritharan, S., 2013, " Cyclic Response of Reinforced Concrete Walls with Different Anchorage Details: Experimental Investigation," Journal of Structural Engineering, Vol. 139, No. 7, pp. 1181-1191.
Burgueno et al., 2010	Liu, X., Burgueño, R., Egleston, and Hines, E.M., 2009, “Inelastic Web Crushing Performance Limits of High-Strength-Concrete Structural Walls," Research Report CEE-RR – 2009/03, Department of Civil and Environmental Engineering, Michigan State University, East Lansing, Michigan.
	Liu, X., 2010, "Inelastic Web Crushing Performance Limits of High-Strength-Concrete Structural Walls," PhD Dissertation, Michigan State University, East Lansing, Michigan.
	Brugueno, R., Liu, X., and Hines, E., 2010, "Inelastic Web Crushing Performance Limits of High-Strength-Concrete-Structural Walls," Research Report No. CEE-RR-2010/11, Michigan State University, East Lansing, Michigan.
	Brugueno, R., Liu, X., and Hines, E., 2014, "Web Crushing Capacity of High-Strength Concrete Structural Walls: Experimental Study," ACI Structural Journal, Vol 111, No.4, pp 235-246.
Cao et al., 2002	Cao, W., Xue, S., and Zhang, J., 2002, "Seismic Performance of RC Shear Walls with Concealed Bracing," Advances in Structural Engineering, Vol. 6, No. 1, pp. 1-13.
Cao et al., 2008	Cao, W., Wang, M., Wang, S., Zhang, J., and Zeng, B., 2008, "Aseismic research of composite shear wall and core walls with rectangular concrete filled steel tube columns," Engineering Mechanics, Vol 25, Sup. 1, pp. 58-70. (in Chinese)

	Cao, W., Wang, M., Zeng, B., Zhang, J., 2011, "Seismic Experimental Research of Concrete Filled Steel Tube Columns-Concrete Composite Shear Wall," *Research Report funded by National Natural Science Foundation of China,* College of Architecture and Civil Engineering , Beijing University of Technology, Beijing, China. (in Chinese)
Cao et al., and Cao et al, 2009	Cao, W., Zhang, Y., Zhang J., Wang, M., and Chang, W., 2008, "Study on Seismic Performance of Shear Walls with Concealed Steel Truss," Beijing University of Technology, Beijing, China. (in Chinese)
	Cao, W., Zhang, J., Zhang, J., and Wang, M., 2009, "Experimental study on seismic behavior of mid-rise RC shear wall with concealed truss," Frontiers of Architecture and Civil Engineering in China, Vol 3, No. 4, pp. 370-377.
	Zhang, J., Cao, W., Wang, Z., and Yang, Y., 2008, " Study on seismic behavior of mid-rise RC composite shear walls with concealed truss under high axial compression," Engineering Mechanics, Vol. 25, Sup. 2, pp. 158-163. (In Chinese)
Cao et al., 2010	Li, L., Xue, S., and Cao, W., 2010, "Experimental study on seismic behavior of high strength RC shear wall incorporated with formed steel," Journal of Beijing University of Technology, Vol. 36, No. 7, pp. 920-927.
Cardenas et al., 1972	Cardenas, A., and Magura, D., 1972, "Strength of High-Rise Shear Walls-Rectangular Cross Section," ACI Special Publication, SP 36-7, pp. 119-150.
	Cardenas, A., Hanson, J., Corley, W., and Hognestad, E., 1973, "Design Provisions for Shear Walls," ACI Journal, Title No. 7-23, pp. 221-230.
	Wood, S., 1989, "Minimum Tensile Reinforcement Requirements in Walls," ACI Structural Journal, Vol. 86, No. 4, pp. 582-591.
Carrillo and Alococer 2013	Correal, J., Harran, C., Carrilo, J., Reyes, J., and Hermida, G., 2018, "Performance of hybrid fiber-reinforced concrete for low-rise housing with thin walls," Construction and Building Materials, Vol. 185, pp. 519-529.
	Miguel, F., 2008, "Seismic Behavior of Concrete Walls Rehabilitated with Glass and Resin Fiber," Master's Thesis, The National Polytechnic Institute of Mexico. (in Spanish)
Carvajal and Poller 1983	Carvajal, O. and Pollner, E., 1983, “Reinforced concrete walls with minimal reinforcement (Muros de Concreto Reforzados con Armadura Minima),” Boletin Tecnico, Universidad Central de Venezuela, Facultad de Ingenieria, Ano 21 (72-73), Enero-Diciembre, pp. 5-36 (in Spanish)
Chen	Chen, X. Y., 2005, “Effect of Confinement on the Response of Ductile Shear Walls,” Master’s Thesis, McGill University, Montreal, Canada.
Chen and Qian	Chen, Q., 2002, "Elastoplastic analysis of reinforced concrete double-limb shear wall," PhD Dissertation, Tsinghua University, Beijing, China. (In Chinese)
	Chen, Q., Qian, J., and Li, G., 2004, "Static elastic-plastic analysis of shear walls with macro-model," China Civil Engineering Journal, Vol. 37, No. 3, pp. 35-46. (In Chinese)
	Lin, Q., 2013, "A tall building based on OpenSees Earthquake catastrophe analysis," Department of Civil Engineering, Tsinghua University, Beijing, China. (In Chinese)
	Yong, W., and Jiaru Q., 2005,"Nonlinear time-history analysis of shear wall using SAP2000 program," Journal of Tsinghua University (Natural Science Edition), Vol. 45, No. 6, pp. 740 -744 (in Chinese)
	Qin, C., Jiaru, Q., 2002, "Static inelastic analysis of RC shear walls," Earthquake Engineering and Engineering Vibration, Vol. 1, No.1, pp. 94-99.

Cheng et al., 2016	Cheng, M., Hung, S., Lequesne, R., and Lepage, A., "Earthquake-Resistant Squat Walls Reinforced with High- Strength Steel," ACI Structural Journal, Vol 113, No. 5, pp. 1065-1076
Chiou et al., 2003	Chiou, Y.J., Mo, Y.L., Hsiao, F.P., Liou, Y.W., and Sheu, M.S., 2003, "Experimental and Analytical Studies on Large-Scale Reinforced Concrete Framed Shear Walls," ACI Special Publication, SP 211–10, pp. 201-221.
	Chiou, Y.J., Mo, Y.L., Hsiao, F.P., Liou, Y.W., and Sheu, M.S., 2003, "Experimental and Analytical Studies on Large-Scale Reinforced Concrete Framed Shear Walls," Proceedings of the 13th World Conference on Earthquake Engineering, August 1-6, Vancouver, B.C., Canada.
Choi et al., 2008	Choi, Y.C., Choi, H.K., and Choi, C.S., 2008, "A Study on Retrofit Method of Shear Wall by New Openings," Journal of the Architectural Institute of Korea Structure & Construction, Vol. 24, No. 1, pp. 71-78. (in Korean)
	Bae, B., Choi, Y. C., Choi, C.S, and Choi, H. K., 2010, "Shear Strength Reduction Ratio of Reinforced Concrete Shear Walls with Openings," Journal of the Korea Concrete Institute, Vol. 22, No. 4, pp. 451-460. (in Korean)
	Bae, B., Choi, H.K., and Choi C.S., 2010, "Evaluation of Shear Strength Reduction Ratio of Reinforced Concrete Shear walls with Openings," Proceedings of International Conference on Sustainable Building Asia (SB10 Seoul), Feb. 24-26, Seoul, Korea.
Choi et al., 2017	Choi, H., K., 2017, "Experimental Study on Shear Wall with Slab and Openings," International Journal of Civil Engineering, Vol. 15, pp. 451-471.
Cong et al.,2017	Chong, X., Xie, L., Ye, Jiang, Q., and Wang, D., 2017, "Experimental Study on the Seismic Performance of Superimposed RC Shear Walls with Enhanced Horizontal Joints," Journal of Earthquake Engineering, Vol, 23, NO. 1, pp. 1-17.
Choun and Park 2015	Choun, Y., S., 2013, "Evaluation of Shear Resisting Capacity of a Conventional Reinforced Concrete Wall with Steel or Polyamide Fiber Reinforcement," Journal of the Korean Society of Hazard Mitigation, Vol. 13, No. 3, pp. 001-007. (in Korean)
	Choun, Y., S., and Park, J., 2015, "Evaluation of Seismic Shear Capacity of Prestressed Concrete Containment Vessels with Fiber Reinforcement," Nuclear Engineering and Technology, Vol 47, pp. 756-765.
Christidis et al., 2010	Christidis, K.I., and Trezos, K., G., 2017, "Experimental investigation of existing non-conforming RC shear walls," Engineering Structures, Vol. 140, pp. 26-38.
	Christidis, K., Trezos, K., G., and Vougioukas, E., 2013, "Seismic assessment of existing RC shear walls non-compliant with current code provisions," Magazine of Concrete Research, Vol. 65, No. 18, pp. 1059-1072.
	Christidis, K., Vougioukas, E., and Trezos, K., 2014, "Deformation Capacity of Older Shear Walls: Experimental Assessment and Comparison with Eurocode 8-Part 3 Provisions," Proceedings of the 2nd European Conference on Earthquake Engineering and Seismology, Aug. 24-29, Istanbul, Turkey.
	Christidis, K.I., Anagnostopoulou, V.V., Trezos, K.G., and Zeris, C.A., 2015, "Deformation Capacity of Non-Conforming RC Shear Walls: Analytical and Numerical Estimation- Test Verification," Proceedings of the 5th International Conference on Computational Methods in Structural Dynamics and Earthquake Engineering, May 25-27, Crete Island, Greece.
	Papaionnoud, D. S., 2013, "Experimental investigation of the behavior of inadequately reinforced concrete walls," Master's Thesis, National Technical University of Athens, Athens, Greece, 135 pp.

Chu et al., 2011, 2013, 2017	Chu, M., Liu, J., and Sun, Z., 2017, "Experimental study on mechanical behaviors of new shear walls built with precast concrete hollow molds," European Journal of Environmental and Civil Engineering, https://doi.org/10.1080/19648189.2017.1349692.
	Sun, Z., Mao, Y., Liu, J., Zhao, Q., and Chu, M., 2014, "Experimental Study on Assembled Monolithic Concrete Shear Walls Built with Precast Two-Way Hollow Slabs," The Open Civil Engineering Journal, Vol. 8, pp. 161-165.
	Chu, M. J., Liu, J. L., Cui, H. C., Hou J. Q., and Zhou Y. L., & Zhang Z. Y., 2013, "Experimental study on shear behavior of assembled monolithic concrete shear walls built with precast two-way hollow slabs," Engineering Mechanics, Vol. 30, No. 7, pp. 219–228.
	Sun, Z.S., Liu, J., and Chu, M., 2013, "Experimental Study on Behaviors of Adaptive-slit Shear Walls," The Open Civil Engineering Journal, Vol. 7, pp. 189-195.
	Chu, M.J., Fend, P., Ye, L.P., and Hou, J.Q., 2011, "Experimental Study on Shear Behaviors of Cold-Formed Thin-Walled Steel Reinforced Concrete Shear Walls with Different Details," Engineering Mechanics, Vol. 28, No. 8, pp. 45-55.
Chun et al., 2011	Chun, Y., S., 2012, "Seismic Evaluation of RC Special Shear Wall with Improved Reinforcement Details in Boundary Elements," Land and Housing Institute Journal, Vol., No. 2, pp. 195-202.
	Chun, Y. S., Kim, S. Y., and Lee, 2011, "Detailed development of quasi-special shear wall to alleviate structural system height limitation," Research Report 2011-56, Korea Institute of Land and Housing, 270 pp.
	Chun, Y., S., Lee, K., H., Lee, H., W., Park, Y., E., and Song, J., K., 2013, "Seismic Performance of Special Shear Wall Structural System with Effectively Reduced Reinforcement Detail," Journal of Korea Concrete Institute, Vol 25, No. 3, pp. 271-281
Chun 2013	Chun, Y., S., 2015, "Seismic Performance of Special Shear Wall with the Different Hoop Reinforcement Detail and Spacing in the Boundary Element," Land and Housing Institute Journal, Vol 6, No. 6, pp. 11-19.
	Chun, Y. S., 2013, "Experimental Study to Revise Reinforcement Details of Special Reinforced Concrete Structural Walls," Research Report 2013, Korea Institute of Land and Housing, 248 pp.
Chun et al., 2015	Chun, Y., S., and Park, J., Y., 2016, "Seismic Performance of Special Shear Wall with Modified Details in Boundary Element Depending on Axial Load Ratio," Land and Housing Institute Journal, Vol 7, No. 1, pp. 31-41.
	Chun, Y. S., Park, J. Y., and Lee, S. W., 2015, "Development of Nonlinear Hysteresis by Member for Introducing Performance-Based Design Method (1) Focusing on Shear Wall and Shear Wall Connection Beam," Research Report 2015-63, Korea Institute of Land and Housing, 116 pp.
Correal et al., 2017	Rosso, A., Almeida, J., and Beyer, K., 2015, "Stability of thin reinforced concrete walls under cyclic loads: state-of-the art and new experimental findings," Bulletin of Earthquake Engineering, Vol 14, No. 2, pp. 455-484.
Cortes-Puentes 2017	Cortés-Puentes, W. L., and Palermo, D., 2017, "SMA tension brace for retrofitting concrete shear walls," Engineering Structures, Vol. 140, pp. 177–188.
	Cortes Puentes, W.L., 2017, "Seismic Retrofit of Squat Reinforced Concrete Shear Walls Using Shape Memory Alloys," PhD Dissertation, University of Ottawa, Ottawa, Canada.

	Cortes-Puentes, W.L., and Palmero, D., 2018, "Seismic Retrofit of Concrete Shear Walls with SMA Tension Braces," Journal of Structural Engineering, Vol. 144, No. 2, 04017200.
	Cortes-Puentes, W.L., and Palmero, D., 2018, "Performance of pre-1970s Squat Reinforced Concrete Shear Walls," Canadian Journal of Civil Engineering, Vol. 45, No. 11, pp. 922-935.
Dabbagh 2005	Dabbagh, H., "Strength and Ductility of High-Strength Concrete Shear Walls Under Reversed Cyclic Loading," PhD Dissertation, The University of New South Wales, Sydney, Australia.
Dan et al., 2011	Fabian, A., Stoian, V., and Dan, D., 2010 "Composite Steel- Concrete Shear Walls with Steel Encased Profiles. Numerical Analysis," Annals of the University of Oradea, Constructions and Hydroedility Facilities, Romania, pp. 107-112
	Dan, D., Fabian, A., and Stoian, V., 2011, "Theoretical and experimental study on composite steel–concrete shear walls with vertical steel encased profiles," Journal of Construction Steel Research, Vol. 67, pp. 800-813.
	Dan, D., Fabian, A., and Stoian, V., 2012, "Experimental study on composite steel-concrete shear walls with vertical steel encased profiles," Proceedings of the Behavior of Steel Structures in Seismic Areas (STESSA), Jan. 9-11, Santiago, Chile, pp. 639-644.
	Boita, I.E., Dan, D., and Stoian, V., 2017, "Seismic Behavior of Composite Steel Fibre Reinforced Concrete Shear Walls," Proceedings of IOP Conference Series: Materials Science and Engineering, 245. doi:10.1088/1757-899X/245/2/022006
	Dan, D., Nagy-Gyorgy, T., Stoian, V., Fabian, A., and Demeter, I., 2012, "FRP Composites for Seismic Retrofitting of Steel-Concrete Shear Walls with Steel Encased Profiles," Proceedings of the Behavior of Steel Structures in Seismic Areas (STESSA), Jan. 9-11, Santiago, Chile.
Dashti et al., 2017	Dashti, F., Dhakal, R.P., and Pampanin, S., 2018, "Inelastic Strain Gradients in Reinforced Concrete Structural Walls," Proceedings of the 16th European Conference on Earthquake Engineering, June 18-21, Thessaloniki, Greece.
	Dasti, F., Dhakal, R.P., and Pampanin, S., 2015, "Development of out-of-plane instability in rectangular RC structural walls," New Zealand Society for Earthquake Engineering (NZSEE) Conference, April 10-12, Rotorua, New Zealand.
	Dasti, F., Dhakal, R.P., Pampanin, S., 2017, "An Experimental Study on Out-of-Plane Deformations of Rectangular Structural Walls Subject to In-Plane Loading," Proceedings of the 16th World Conference on Earthquake, Jan. 9-13, Santiago, Chile.
	Dashti, F., Dhakal, R.P., Pampanin, S., 2017, "Tests on Slender Ductile Structural Walls Designed According to New Zealand Standard," Bulletin of the New Zealand Society for Earthquake Engineering, Vol. 50, No. 4, pp. 504-516.
Dazio et al., 1999	Belmouden, y., Lestuzzi, P., 2007, "Analytical model for predicting nonlinear reversed cyclic behavior of reinforced concrete structural walls," Engineering Structures, Vol. 29, pp. 1263-1276.
	Dazio, A., Wenk, T., and Bachmann, H., 1999 "Tests on RC walls under cyclic-static action," Report No. 239, Institute of Structural Engineering, Swiss Federal Institute of Technology Zurich, 157 pp.
	Dazio, A., Beyer, K., Bachmann, H., 2009, "Quasi-static cyclic tests and plastic hinge analysis of RC structural walls," Engineering Structures, Vol. 31, pp. 1556-1571.

Deng et al., 2013	Lu, Y., and Huang, L., 2015, "Influence of Confining Stirrups on Deformation Capacity of RC Concrete Walls with Flexure Failure." Engineering Mechanics. DOI: 10.6052/j.issn.1000-4750.2013.10.0961
	Deng, K., Pan, P., Shi, Y., Miao, Q., Li, W., Wang, T., 2012, "Quasi-Static Test of Reinforced Concrete Shear Wall with Low Concrete Strength and Reinforcement Ratio." China Civil Engineering Journal, Vol. 45, pp. 213-217.
	Pan, P., Deng, K., Shi, Y., Miao, Q., Li, W., Wang, T., 2013, "Experimental Study on Single Side Strengthening of Low-Reinforced Shear Wall," Earthquake Resistant Engineering and Retrofitting, Vol. 35, No. 2, pp. 68- 74.
	Pan, P., Deng, K., Shi, Y., Miao, Q., Li, W., Wang, T., 2013, "Experimental Study on Single Side Strengthening of Low-Reinforced Shear Wall." Earthquake Resistant Engineering and Retrofitting, Vol. 35, No. 5, pp. 55- 60.
Deng et al., 2017	Deng, K., Pan, P., Wang, H., Shen, S., 2017, "Experimental study on slotted RC wall with steel energy dissipation links for seismic protection of buildings," Engineering Structures, Vol 145, pp. 1-11
Deng et al., 2008	Deng, M., Liang, X., and Yang, K., 2008, "Experimental study on seismic behavior of high-performance concrete shear wall with new strategy of transverse confining stirrups," Proceedings, 14th World Conference on Earthquake Engineering, Oct. 12-17, Beijing, China.
	Kou, J.L., Lian, X., Qian, L., Deng, M., 2013, "Nonlinear Analysis and Study on Allowable Value for Seismic Behavior of High-Strength Concrete Shear Walls," Engineering Mechanics, vol. 30, No. 2, pp. 232-239.
El-Azizy	El-Azizy, O., Shedid, M., El-Dakhakhni, W., and Drysdale, R., 2015, "Experimental evaluation of the seismic performance of reinforced concrete structural walls with different end configurations," Journal of Engineering Structures, Vol. 101, pp. 246–263.
	El-Azizy, O., Shedid, M., El-Dakhakhni, W., and Drysdale, R., 2012, "Proposed Experimental Study to Compare the Seismic Performance of reinforced Concrete and Reinforced Masonry Structural Walls," 15th International Brick and Block Masonry Conference, Florianopolis, Brazil.
Effendy et al., 2006	Effendy, E., Liao, W.I., Song, G., Mo, Y.L., Loh, C.H., 2006, "Seismic Behavior of Low-Rise Shear Walls With SMA Bars," 10th Biennial International Conference on Engineering, Construction, and Operations in Challenging Environments and Second NASA/ARO/ASCE Workshop on Granular Materials in Lunar and Martian Exploration.
Elnady 2008	Elnady, M.M.E., 2008, "Seismic Rehabilitation of RC Structural Walls," PhD Dissertation, McMaster University, Canada.
El-Sokkary and Galal 2012	El-Sokkary, H., Galal, K., 2013, "Seismic Behavior of RC Shear Walls Strengthened with Fiber-Reinforced Polymer," Journal of Composites for Construction, Vol. 15, No. 5, pp. 603-613.
	El-Sokkary, H., Galal, K., 2012, "Cyclic Tests on FRP-Retrofitted RC Shear Wall Panels," Proceedings of 15th World Conference on Earthquake Engineering, Sept. 24-28, Lisbon, Portugal.
	El-Sokkary, H., 2012, "Seismic Retrofit of Reinforced Concrete Shear Walls using Fiber Reinforced Polymer Composites," PhD Dissertation, Concordia University.
Fang et al., 2011	Fang, X., Li, Z., Wei, H., Jiang, Y., 2011, " Experimental Study on Seismic Behavior of High-Performance Concrete Shear Wall with High Reinforcement Ratio Boundary Elements," Journal of Building Structures, Vol. 32, No. 12, pp. 145-153.

Farvashany et al., 2008	Frvashany, F.E., Foster S.J., Rangan, B. V., 2008, " Strength and Deformation of High-Strength Concrete Shear walls," ACI Structural Journal, Vol. 105, No. 1, pp. 21-29.
Furukawa et al., 2003	Furukawa, J., Arakawa, G., Ogawa, M., Ichikawa, M., Kakeo, T., 2003, " Experimental Study on Bending Structural Performance of Reinforced Concrete Shear Walls: Part 1 Test Plan and Outline of Results," Summaries of technical papers of Annual Meeting Architectural Institute of Japan. C-2, Structures IV, pp. 317-318. (in Japanese)
	Arakawa, G., Furukawa, J., Ichikawa, M., Ogawa, M., Kakeo, T., 2003, "Experimental Study on Flexural Behavior Of Reinforced Concrete Shear Walls. Part 2: Discussion of Test Results," Summaries of technical papers of Annual Meeting Architectural Institute of Japan. C-2, Structures IV, pp. 319-320. (in Japanese)
Ghorbani-Renani et al. 2009	Ghorbani-Renani, I., Velev, N., Tremblay, R., Palermo, D., Massicotte, B., and Leger, P., 2009, “Modeling and testing influence of scaling effects on inelastic response of shear walls,” ACI Structural Journal, Vol. 106, No. 3, pp. 358–367.
	Ghorbanirenani, I., 2010, "Experimental and numerical Investigations of Higher Mode Effects of Seismic Inelastic Response of Reinforced Concrete Shear Walls," PhD Dissertation, Écpele Polytechnique De Montreal.
Goodsir 1985	Paulay, T., Goodsir, W.J., 1985, "The Ductility of Structural Walls," Bulletin of The New Zealand National Society for Earthquake Engineering, Vol 18, No. 3, pp. 250-269.
	Goodsir, W.J., 1985, "The Design of Coupled Frame-Wall Structures for Seismic Actions," PhD Dissertation, University of Canterbury, Christchurch, New Zealand.
	Paulay, T., Priestley, J.N., 1993, "Stability of Ductile Structural Walls," ACI Journal, Vol. 90, No. 4, pp. 385-392.
Greifenhagen 2006	Greifenhagen, C., 2006, "Seismic Behavior of Lightly Reinforced Concrete Squat Shear Walls,"PhD Dissertation, École Polytechnique Federale De Lausanne.
	Greifenhagen, C., Lestuzzi, P., 2005, "Static cyclic tests on lightly reinforced concrete shear walls," Engineering Structures, Vol. 27, pp. 1703-1712.
Gupta and Rangan 1998	Gupta, A., Rangan, B.V., 1998, "High-Strength Concrete Structural Walls," ACI Structural Journal, Vol. 95, No. 2, pp. 194-203.
Ha et la., 2001	Ha, S. S., Yun, H. D., Choi, C. S., Oh, Y. H., Yi, L. H., and Lee, L. H, 2011, “Experimental study of structural capacity evaluation of RC t-shape walls with the confinement effect,” Journal of the Korea Concrete Institute, Vol. 2001, No.11, pp. 191–196. (in Korean)
	Choi, C., Ha, S., Lee, L., Oh, Y., Yun, H., 2004, "Evaluation of Deformation Capacity for RC T-Shaped Cantilever Walls," Journal of Earthquake Engineering, Vol. 8, No. 3, pp. 397–414
Habibi et al., 2018	Habibi, F., Seikh, S.A., Orbovic, N., Panesar, D.K., Vecchio, F.J., 2015, "Alkali Aggregate Reaction in Nuclear Concrete Structures: Part3: Structural Shear Wall Elements," 23rd Conference on Structural Mechanics in Reactor Technology, Manchester, United Kingdom, Division I.
	Habibi, F., Sheikh, S.A., Becchio, F., Panesar, D.K., 2018, "Effects of Alkali-Silica Reaction on Concrete Squat Shear Walls," ACI Structural Journal, V. 115, No. 5, pp. 1329-1339.

Han et al., 2008	Chen, X.W., Han, X.I., 2011, "Research and Development of the Shear Wall Nonlinear Macro-Element," Engineering Mechanics, Vol. 28, No. 5, pp. 111-123.
	Han, X., Chen, X., Jack, C., Mao, G., Wu, P., 2008, "Numerical Analysis of Cyclic Loading Test of Shear Walls based on OpenSEES," The 14th World Conference on Earthquake Engineering, Beijing, China.
	Chen, X., Han, X., 2011, "Research on Deformation Limit State of Components of Shear-Wall Structure and Development of the Computing Platform," PhD Dissertation, South China University of Technology, Guangzhou, China.
Hannewald et al., 2013	Hannewald, P., Bimschas, M., Dazio, A., 2013, "Quasi-static cyclic tests on RC bridge piers with detailing deficiencies," IBK Report No. 352. Institut für Baustatik und Konstruktion, ETH Zürich.
	Hannewald, P., Beyer, K., 2013, "Plastic hinge models for the displacement-based assessment of wall-type bridge piers with poor detailing," Vienna Congress on Recent Advances in Earthquake Engineering and Structural Dynamics.
	Hannewald, P., Beyer, K., 2012, "Plastic hinge models for the seismic assessment of reinforced concrete wall-type piers with detailing deficiencies," Proceedings of 15th World Conference on Earthquake Engineering, Sept. 24-28, Lisbon, Portugal.
Hidalgo et al., 1999	Hidalgo, P.A., Jordan, R.M., Martinez, M.P., 2000, "Development and use of an Analytical Model to Predict the Inelastic Seismic Behavior of Shear Wall, Reinforced Concrete Buildings," Proceedings of 12th WCEE, New Zealand.
	Hidalgo, P.A., Ledezma, C.A., Jordan, M., 2002, "Seismic Behavior of Squat Reinforced Concrete Shear Walls," Earthquake Spectra, Volume 18, No. 2, pp. 287–308.
	Larenas, J. L., 1994, "Seismic Behavior of Reinforced Concrete Walls Failing in Shear (Comportamiento Sísmico de Muros de Hormigón Armado que Fallan por Esfuerzos de Corte),"Master's Thesis, Pontifical Catholic University of Chile, Santiago, Chile, 163 pp. (in Spanish)
	Ledezma, C., 1999, "Shear strength of reinforced concrete shear walls (Resistencia al esfuerzo de corte de muros de hormigón armado),"Master's Thesis, Pontifical Catholic University of Chile, Santiago, Chile, 135 pp. (in Spanish)
Hines et al., 2002	Hines, E. M., Seible, F., and Priestley, M. J. N., 2002, “Seismic Performance of Hollow Rectangular Reinforced Concrete Piers with Highly Confined Corner Elements–Phase I: Flexural Tests, and Phase II: Shear Tests,” Structural Systems Research Project 99/15, University of California, San Diego, CA, 266 pp.
	Hines, E.M., Seible, F., 2004, "Web Crushing Capacity of Hollow Rectangular Bridge Piers," ACI Structural Journal, Vol. 101, No. 4, pp, 569-579.
	Hines, E.M., Seible, F., Priestly, M.J.N., 2002, "Seismic Performance of Hollow Rectangular Reinforced Concrete Piers with Highly-Confined Boundary Elements Phase I: Flexural Tests, Phase II: Shear Tests," Structural Systems Research Project, Report No. SSRP- 99/15, UCSD.
	Hines, E.M., Dazio, A., Seible, F., 2002, "Seismic Performance of Hollow Rectangular Reinforced Concrete Piers with Highly-Confined Boundary Elements Phase III: Web Crushing Tests," Structural Systems Research Project, Report No. SSRP-2001/27.

Hiotakis 2004	Hiotakis, S., 2004, "Repair and Strengthening of Reinforced Concrete Shear Walls for Earthquake Resistance Using Externally Bonded Carbon Fibre Sheets and a Novel Anchor System," Master of Applied Science, Carleton University, Ottawa, Ontariom Canada
	Cruz-Noguez, C.A., Hassan, A., Lau, D.T., Woods, J., Shaheen, I., 2014, "Seismic Retrofit of Deficient RC Shear Walls with FRP Tow Sheets," Proceedings of the 10th U.S. National Conference on Earthquake Engineering, July 21-25, Anchorage, Alaska.
	Lau, D.T., Cruzo-Noguez, C.A., 2013, "Developments on Seismic Retrofit of RC Shear Walls with FRP," 5th International Conference on Advances in Experimental Structural Engineering, Taipei, Taiwan.
Hiraishi et al. 1984	Hirashi, H., Tosai, H., Kawashima, S., Inoue, Y., 1989, "Experimental study on toughness after bending yielding of multi-story shear walls with flat incidental columns," Architectural Institute of japan Structural Papers, Vol 395, pp 48-59.
	Hirashi, H., Shiohara, H., Kawashima, T., Tomatsuri, H., Kurosawa, A., Budo, Y., 1988, "Experimental Study on Seismic Performance of Multistory Shear Walls with Flanged Cross Section," Proceedings of 9th World Conference on Earthquake Engineering, Aug. 2-6, Tokyo-Kyoto, Japan.
Hiraishi et al., 1988	Minami, N., Nakachi, T., 2008, "Three-Dimensional Nonlinear Finite Element Analysis on Reinforced Concrete Walls Enhanced by Transverse Confining Steel," The 14th World Conference on Earthquake Engineering, Beijing, China.
	Hiraishi, H., Teshigawara, M., Kawashima, T., Nakachi, T., Tubosaki, H., Oguma, M., 1988, " Experimental Study on Deformation Capacity of Wall Columns After Flexural Yielding," Proceedings of 9th World Conference on Earthquake Engineering, Aug. 2-6, Tokyo-Kyoto, Japan.
	Hiraishi, H., Inai, E., Nakachi, T., Kawashima, T., Teshigawara, M., 1990, "Experimental Study on Deformation Capacity Beyond Flexural Yielding of Wall Columns," Architecture Institute of Japan's Journal of Structural and Construction Engineering, , Report No. 410, pp. 41-52. (in Japanese)
Hiraishi et al, 1983	Hiraishi, H., Yoshimura, M., Isoishi. H., Nakata, S., 1983, "Planar Tests on Reinforced Concrete Shear Wall Assemblies," Building Research Institute, Ministry of Construction, Paper No. 98.
Hirosawa 1975	Hirosawa, M., 1975, "Past Experimental Results on Reinforced Concrete Shear Walls and Analysis on them," Report No. 6, Building Research Institute, Ministry of Construction, Japan, 279 pp. (in Japanese)
Ho 2006 and Ho and Kuang 2006	Kuang, J.S., Ho, Y., 2013, "Inherent Ductility of Non-seismically Designed and Detailed Reinforced Concrete Shear Walls," HKIE Transactions, Vol. 14, No.1, pp. 7-12.
	Kuang, J.S., Ho, Y.B., 2007, "Enhancing ductility of non-seismically designed RC shear walls," Proceedings of the Institution of Civil Engineers Structures and Buildings 160, Issue SB3, pp. 139-149.
	Kuang, J.S., Ho, Y.B., 2008, "Seismic Behavior and Ductility of Squat Reinforced Concrete Shear Walls with Non-Seismic Detailing," ACI Structural Journal, Vol. 105, No. 2 pp. 225-231.
	Ho, Y.B., 2006, "Enhancing the Ductility of Non-Seismically Designed Reinforced Concrete Shear Walls," Master's Thesis, The Hong Kong University of Science and Technology, Hong Kong.
Holden 2001	Holden, T.J., 2001, "A Comparison of the Seismic Performance of Precast Wall Construction: Emulation and Hybrid Approaches," M.Eng. Report, University of Canterbury Christchurch, New Zealand.

	Holden, T., Restrepo, J., Mander, J.B., 2003, "Seismic Performance of Precast Reinforced and Prestressed Concrete Walls," Journal of Structural Engineering, Vol 129, No. 3, pp. 286-296.
Hosoya 2007	Hosoya, H., 2007, "Structural performance of RC rectangular section core walls," Proceedings of the Japan Concrete Institute, Vol. 29, No. 3, pp. 313–318. (in Japanese)
	Hosoya, H., and Oka, Y., 2006, "Study on Structural Performance of R/C Rectangular Section Core Walls: Part 1: Experiment on Variables in a Confined Area," Summaries of Technical Papers of Annual Meeting, Architecture Institute of Japan, Vol. C-2, pp. 169-170. (in Japanese)
	Kishimoto, T., Hosoya, H., Oka, Y., 2008, "Study on structural performance of R/C rectangular section core walls (Part 3 and 4)," Summaries of Technical Papers of Annual Meeting, Architecture Institute of Japan, Vol. C-2, 355-358. (in Japanese)
Hou et al., 2016	Hou, H., Ma, T., Qu, Z., Cui, S., Shi, L., Fu, W., Cheng, J., Zhu, W., 2016, "Quasi-Static Experimental Study on Prefabricated Superimposed Ribbed Reinforced Integral Shear Wall," Building Structure, Vol. 46, No. 10, pp. 14-19.
Hsiao et al.,	Hsio, F.P., Wang, J.C., Chiou, Y.J., 2008, "Shear Strengthening of Reinforced Concrete Framed Shear Walls Using CFRP Strips," The 14th World Conference on Earthquake Engineering, Beijing, China.
Hu 2004	Hu, G., 2004, "Experimental study on seismic behavior of short-limb shear wall structures with conversion layer," Master's Thesis, Tongji University. (in Chinese)
	La, H., Li, S., Jin, G., Hu, G., Huang, D., 2005, "Tests and finite element analysis of earthquake resistant capability of shallow-section shear walls on transfer floor of a tall building," Earthquake Engineering and Engineering Vibration, Vol 25, No. 2, pp. 77-81.
	Zhou, Y., and Lu, X., 2008, "SLDRCE database on static tests of structural members and joint assemblies," State key laboratory of disaster reduction in civil engineering. Shanghai, China: Tongji University; 2008. (in Chinese)
Huq 2017	Huq, M.S., Weber-Kamin, A.S., Lequesne, R.D., Lepage, A., 2017, "High-Strength Steel Bars in Reinforced Concrete Walls: Influence of Steel Mechanical Properties on Deformation Capacity," Conference: 16th World Conference on Earthquake Engineering, 16WCEE 2017, At Chile.
	Huq, M.S., Lepage, A., Lequesne, R.D., Weber-Kamin, A.S., Ameen, S., 2017, "Influence of Mechanical Properties of High Strength Steel on Deformation Capacity of Reinforced Concrete Walls," 16th World Conference on Earthquake Engineering, Santiago Chile.
Idosaka et al., 2017	Idosako, Y., Sakashita, M., Tani, M., Nishiyama, M., 2017, "Bi-Directional Lateral Loading Tests on RC Shear-Dominant Walls," Journal of Structural and Construction Engineering, AIJ, Vol 82, No. 735, pp. 683-692.
	Sakashita, M, 2008, "Study on Lateral Load Resisting Mechanism of Reinforced Concrete Shear-dominant Walls Subjected to Bi-directional Loading," Report, National Research Institute of Building and Entrepreneurship.
Imanishi 1996	Imanishi, T., 1996, "Post-Yield Behaviors of Multi-Story Reinforced Concrete Shear Walls Subjected to bilateral Deformations Under Axial Loading," 11th World Conference on Earthquake Engineering, Paper No. 404.

	Imanishi T., Nishinaga, M., Itakura, Y., and Morita, S., 1996, "An experimental study on the bending failure behavior of reinforced concrete shear walls subjected to horizontal loads in two directions," Proceedings of the Japan Concrete Institute, Vol. 18, No., 2, pp. 1055-1060.
Ireland, 2007	Ireland, M., 2007, "Development of a Selective Weakening Approach for the Seismic Retrofit of Reinforced Concrete Structural Walls," Master's Thesis, University of Canterbury Christchurch, New Zealand.
Ibrahim	Ibrahim, A. M. M., 2000, "Linear and Nonlinear Flexural Stiffness Models for Concrete Walls in High Rise Buildings," PhD Dissertation, The University of British Columbia.
	Ireland, M.G., Pampanin, S., and Bull, D.K., 2007, "Experimental Investigations of a Selective Weakening Approach for the Seismic Retrofit of R.C. Walls," Proceedings of New Zealand Society for Earthquake Engineering (NZSEE) Conference, pp. 1-8
Islam and Saito 2015	Islam, Md. S., Saito, T., 2015, "Displacement Based Evaluation for Confinement Requirement of Boundary Elements of Shear Wall and Retrofit Design Using Carbon Fiber Sheet (CFS)," International Institute of Seismology and Earthquake Engineering, Building Research Institute, Vol. 49, pp. 21-38.
Jeon and Park 2016	Jeon, S.H., Park, J.H., 2016 "Experimental Assessment of Numerical Models for reinforced Concrete Shear Walls with Deficient Details," Journal of the Earthquake Engineering Society of Korea, Vol. 20, No. 4, pp. 211-222. (in Korean)
Ji 2002	Ji, S., 2002, "Elastoplastic time-history response analysis of high-rise reinforced concrete frame-shear structure under earthquake action," Master's Thesis, Tongji University. (in Chinese)
	Zhou, Y., and Lu, X., 2008, "SLDRCE database on static tests of structural members and joint assemblies," State key laboratory of disaster reduction in civil engineering. Shanghai, China: Tongji University; 2008. (in Chinese)
Ji et al., 2012	Ji, X.D., Qian, J.R., 2015, "Study of Earthquake-Resilient Coupled Shear Walls", Engineering Mechanics,
	Qian, J., Ziang, Z., Ji, X., 2012, "Behavior of steel tube-reinforced concrete composite walls subjected to high axial force and cyclic loading," Engineering Structures, Vol 36, pp. 173-184.
Ji et al., 2015	Ji, X., Qian, Y., Lu, X., 2015, "Seismic behavior and modeling of steel reinforced concrete (SRC) walls," Earthquake Engineering & Structural Dynamics, Vol. 44, pp. 955–972.
Jiang 1999	Ji, S., 2002, "Elastoplastic time-history response analysis of high-rise reinforced concrete frame-shear structure under earthquake action," Master's Thesis, Tongji University.
Jiang et al., 2011	Jiang, H., Ying, Y., Wang, B., 2011, "Experimental Investigation on Damage Behavior of RC Shear Walls," Advanced Materials Research, Vols 250-253, pp. 2407-2411
	Jiang, h., Wang, B., Lu, X., 2013, "Experimental Study on Damage Behavior of Reinforced Concrete Shear Walls Subjected to Cyclic Loads," Journal of Earthquake Engineering, Vol 17, No.7, pp. 958-971,
Johnson 2007	Aaleti, S., 2009, "Behavior of rectangular concrete walls subjected to simulated seismic loading," PhD Dissertation, Iowa State University, Ames, Iowa.

	Aaleti, S., Brueggen, B.L., Johnson, B., French, C.E., and Sritharan, S., 2013, " Cyclic Response of Reinforced Concrete Walls with Different Anchorage Details: Experimental Investigation," Journal of Structural Engineering, Vol. 139, No. 7, pp. 1181-1191.
	Waugh, J., Aaleti, S., Sritharan, S., and Zhao, J., 2008, "Nonlinear Analysis of Rectangular and T-Shaped Concrete Walls," ISU- ERI-Ames Report ERI-09327 Submitted to the National Science Foundation, Iowa State University, Ames, Iowa.
	Johnson, B., 2010, “Anchorage detailing effects on lateral deformation components of R/C shear walls,” Master Thesis, University of Minnesota, Minneapolis, Minnesota.
Kabeyasawa and Matsumoto 1992	Kabeyasawa, T., Hiraishi, H., 1998, "Tests and Analyses of high-Strength Reinforced Concrete Shear Walls in Japan," ACI Special Publication, SP 176-13, pp. 281-310.
	Kabeyasawa, T., and Matsumoto, K., 1994, "Experimental Study on Strength and Deformability of High Strength Reinforced Concrete Shear Walls," Report, 253 pp.
	Kabeyasawa, T., and Matsumoto, K., 1992 "Tests and analyses of ultra- high strength reinforced concrete shear walls," Proceedings of the 10th World Conference on Earthquake Engineering, July 19-24, Madrid, Spain, 3291-3296.
	Matsumoto, K., and Kabeyasawa, T., 1990, "Experimental Study on Strength and Deformability of High Strength Reinforced Concrete Shear Walls," Proceedings of the Japan Concrete Institute, Vol. 12, No. 2, pp. 545-550. (in Japanese)
Kabeyasawa et al, 1996	Milev, J.I., 1996, "Two-Dimensional Analytical Model of Reinforced Concrete Shear Walls," Proceedings of the11th World Conference on Earthquake Engineering, June 23-28, Acapulco, Mexico, Paper No. 320.
	Chen, S., Kabeyasawa, T., 200, "Modelling of Reinforced Concrete Shear Wall for Nonlinear Analysis," 12th WCEE, Auckland, New Zealand.
	Kabeyasawa, T., Ohkubo, T., Nakamura, Y., 1996, "Tests and Analysis of Hybrid Wall Systems," Proceedings of the 11th World Conference on Earthquake Engineering, June 23-28, Acapulco, Mexico
Kabeyasawa et al., 2007	Kabeyasawa, T., Kabeyasawa, T., Kabeyasawa, T., Kim, Y., Tojo, Y., 2007, "Experimental study on shape and reinforcing of RC walls: Part1: Effect of boundary," Summaries of technical papers of Annual Meeting Architectural Institute of Japan. C-2, Structures IV, pp. 461-462. (in Japanese)
	Kabeyasawa, T., Tojo, Y., Kim, Y., Kabeyasawa, T., Igarashi, S., 2016, "Tests of Reinforced Concrete Shear Walls Strengthened Using Polyester Sheet," Proceedings of 8th Pacific Conference on Earthquake Engineering, December 5-7, Singapore, Paper Number 182.
Kabeyasawa et al., 2008	Kabeyasawa, T., Kabeyasawa, T., Tojo, Y., and Kabeyasawa, T., 2008, "Experimental study on columns with wing walls failing in shear," Proceedings of the Japan Concrete Institute, Vol. 30, No. 3, pp. 115-120. (in Japanese)
	Kabeyasawa, T., Kabeyasawa, T., Kim, Y., Kabeyasawa, T., bae, K., 2009, "Test on Reinforced Concrete Columns with Wing Walls for Hyper-Earthquake Resistant System," Proceedings of 3rd International Conference on Advances in Experimental Structural Engineering, Oct, San Francisco.
Kabeyasawa et al., 2012	Sato, M., Kabeyasawa, T., Kim, Y., and Fukuyama, H., 2012, "Experimental study on RC shear walls subjected to bi-directional loading," Proceedings of the Japan Concrete Institute, Vol. 34, No. 2, pp.115-120. (in Japanese)

	Kabeyasawa, T., Kato, S., Sato, m., Kabeyasawa, T., Fukuayana, H., Tani, M., Kim, Y., Hosokawa, Y., 2014, "Effects of Bi-Direction Lateral Loading on the Strength and Deformability of Reinforced Concrete Walls with/ without Boundary Columns," Proceedings of the 10th U.S. National Conference on Earthquake Engineering, July 21-25, Anchorage, Alaska.
Kang et al., 2013	Kang, S.M., Kim, O.K., Parl, H.G., 2013, "Cyclic Loading test for emulative precast concrete walls with partially reduced rebar section," Engineering Structures, Vol. 56, pp. 1645-1657.
Khalil 2005	Ghobarah, A., Khalil, A.A., 2004, "Seismic Rehabilitation of Reinforced Concrete Walls Using Fibre Composites," Proceedings of the 13th World Conference on Earthquake Engineering, August 1-6, Vancouver, B.C., Canada.
	Khalil, A.A., 2005, "REhabilitation of Reinforced Concrete Structural Wall Using Fibre Composites," PhD Dissertation, McMaster University.
	Khalil, A., Ghobarah, A., 2003, "Behavior of Rehabilitated Structural Walls," Journal of Earthquake Engineering, Vol. 9, No. 3, pp. 371-391.
Kimura and Ishikawa 2006	Kimura, H., and Ishikawa, Y., 2006, "Study on structural performance of rectangular cross section R/C walls," Proceedings of the Japan Concrete Institute, Vol. 28, No. 2, pp. 469-474. (in Japanese)
Kimaru and Sugano 1996	Kimaru, H., Sugano, S., 1996, "Seismic Behavior of high Strength Concrete Slender Wall Under High Axial Load," Proceedings of 11th World Conference on Earthquake Engineering, June 23-28, Acapulco, Mexico, Paper No. 653.
Kimura et al. 1996	Kimaru, H., Yasuo, E., Kawai, T., Sumi, A., Matsumoto, T., 1996, "23256 Bending Shear Test of Multi-story Shear Wall Using High Strength Concrete under High Axial Force: Part 1: Outline of Experiment," Architectural Institute of Japan, pp. 511-512.
Kono et al., 2012	Kono, S., Sakamoto, K., Sakashita, M., Mukai, T., Tani, M., Fukuyama, H., 2012, "Effects of boundary columns on the seismic behavior of cantilever structural walls," 15th WCEE, Lisboa.
	Sokamoto, K., Sakashita, M., Kono, S., Tani, M., 2012, "Influence of frame column and end restraint reinforcement on ultimate deformation performance of shear wall," Concrete Engineering Annual Proceedings, Vol 34, No. 2, pp. 379-384.
	Kono, S., Taleb, R., Sakashita, M., Tani, M., Mukai, T., Fukuyama, H., 2013, "Effect of Boundary Area Confinement on the Ultimate Flexural Drift Capacity of Cantilever Structural Walls," Proceeding the 6th Civil Engineering Conference in Asia Region: Embracing the Future through Sustainability.
	Taleb, R., Kono, S., Sakashita, M., Tani, M., 2014, "Effects of Boundary Regions Confinement on the Seismic PErformance of Flexural RC Structural Walls," Proceedings of the 2nd European Conference on Earthquake Engineering and Seismology, Aug. 24-29, Istanbul, Turkey.
Kono et al., 2014	Taleb, R., Kono, S., Tani, M., Sakashita, M., 2014, "Effects of End Region Confinement on Seismic Performance of RC Cantilever Walls," Proceedings of the 10th U.S. National Conference on Earthquake Engineering, July 21-25, Anchorage, Alaska.
	Kono, S., Tani, M., Mukai, T., Fukuyama, H., Taleb, R., Sakashita, M., 2014, "Seismic Behavior of Reinforced Concrete Walls for a Performance Based Design," Proceedings of the 2nd European Conference on Earthquake Engineering and Seismology, Aug. 24-29, Istanbul, Turkey.

Kotsovos et al., 2011	Zygouris, N., Kotsovos, G.M., Cotsovos, D.M., Kotsovos, M.D., 2015, "Design for earthquake-resistant reinforced concrete structural walls," Meccanica, Col 50, No. 2, pp. 295-309.
	Kotsovos, G.M., Kotsovos, M.D., Cotsovos, D.M., Kounadis, A.N., 2011, "Seismic behavior of RC walls: an attempt to reduce reinforcement congestion," Magazine of Concrete Research, Vol. 63, Issue 4, pp. 235–246
Kumagai et al., 1990	Hitoshi, K., Inada, Y., Sakaguchi, N., Yamanobe, K., Koda, S., 1990, "Structural behavior of high strength concrete shear walls," Summaries of technical papers of Annual Meeting Architectural Institute of Japan. Structures II, pp. 611-612.
Layssi 2013	Layssi, H., 2013, "Seismic Retrofit of Deficient Reinforced Concrete Shear Walls," PhD Dissertation, McGill University, Montreal, Canada.
	Layssi, H., Mitchell, D., 2002,"Experiments on Seismic Retrofit and Repair of Reinforced Concrete Shear Walls," Proceedings of 6th International Conference on FRP Composites in Civil Engineering, CICE 2012.
	Layssi, H., Cook, W.D., Mitchell, D., 2012, "Seismic Response and CFRP Retrofit of Poorly Detailed Shear Walls," Journal of Composites for Construction, Vol 16, No, 3, pp. 332-339.
Lefas and Kotsovos 1990 and Lefas et al., 1990a	Lefas, L.D., Kotsovos, M.D., 1990, "Strength and Deformation Characteristics of Reinforced Concrete Walls under Load Reversals," ACI Structural Journal, Vol. 87, No. 6, pp. 716-726.
	Lefas, L.D., Kotsovos, M.D., Ambraseys, N.N., 1990, "Behavior of Reinforced Concrete Structural Walls: Strength, Deformation Characteristics, and Failure Mechanism," ACI Structural Journal, Vol 87, No. 1, pp. 23-31.
Li and Li 2002	Li, H., Li, B., 2002, "Experimental study on Seismic Restoring Performance of Reinforced Concrete Shear Walls," Journal of Building Structures, Vol. 32, No. 5, pp. 728-732.
	Li, H.N., Li, B., 2004, "Experimental Study on Seismic Reporting Performance of Reinforced Concrete Shear Walls," 13th World Conference on Earthquake Engineering, August 1-6, Vancouver, B.C., Canada.
	Li,B., Li,H., 2010, "Research on Quasi-Static Test of Reinforced Concrete Shear Walls with Different Shear-Span Ratio," Industrial Construction, Vol. 40, No. 9, pp. 32-36.
Li et al., 2015	Li, B., Zhao, Y., Pan, Z., 2015, "Seismic behavior of lightly reinforced concrete structural walls with openings," Magazine of Concrete Research, Vol 67, No. 14, pp. 843-854.
Li et al., 2017	Li, J., Wung, L., Lu, Z., Wang, Y., 2017, "Experimental study of L-shaped precast RC shear walls with middle cast-in-situ joint," Structural Design Tall Special Buildings, Vol 27, No. 1, e1457, DOI: 10.1002/tal.1457
Li et al., 2011	Huang, C.L., 2011, "Studies on the Seismic Behaviors of Reinforced Concrete Structural Walls," PhD. Dissertation, National Taipei University of Technology.
	Li, Y.F., Huang, C.L., Lin, C.T., Hsu, T.H., 2011, "A Study on the High Seismic Performance of RC Structural Walls under Reversed Cyclic Loading," Advances in Structural Engineering, Vol 15, No. 7, pp. 1239-1252.
Lian et al., 2009	Yang, L.P., Yu, S.L., Zhang, Q.L., Cui, J.C., 2016, "Aseismic Behavior of Superimposed Shear Walls under Different Axial Load Ratios," Journal of Vibration and Shock, Vol 35, No. 9, pp. 227-239.
	Jiang, Q., Ye, X., Lian, X., Chang, L., Wang, D., 2010, "Analysis on Energy Dissipation of Superimposed Slab Shear Walls," Journal of Jiangsu University, Vol. 31, No. 4, pp. 483-487.

	Lian,X., Ye,X., Jiang, Q., Wang, D., 2010, "A New Green Resident Structure System: The Superimposed Slab Shear Walls System," Industrial Construction, Vol. 40, No. 6, pp. 79-92.
Liang et al., 2013	Liang, X., Che, J., Yang, P., Deng, M., 2013, "Seismic Behavior of High-Strength Concrete Structural Walls with Edge Columns," ACI Structural Journal, Vol, 110, No. 6, pp. 953-964.
	Cui, X., Liang, X., Yang, P., 2013, "Seismic Behavior of High-Performance Concrete Shear Wall with End Columns," Industrial Construction, Vol. 443, No., 2, pp. 1-8.
	Liang, X., Yang, P., Cui, X., Deng, M., Zhang, X., 2010, "Experimental Studies on Seismic behavior of High Strength Concrete Shear Wall with Boundary Columns," Journal of Building Structures, Vol. 31., No.1, pp. 23-32.
Liu et al., 2010	Liu, G.R., Song, Y.P., Qu, F.I., 2010, "Post-fire cyclic behavior of reinforced concrete shear walls," J. Cent. South Univ. Technol., Vol 17, pp. 1103-1108.
	Lui. G., Song, Y., Qu, F., 2011, "Experimental study on seismic behavior of reinforced concrete shear walls after fire," Journal of Dalian University of Technology, Vol. 51, No. 4, pp. 555-560.
Liu et al., 2013	Liu, J., Chen, Y., Guo, Z., Zhang, J., 2013, "Test on Seismic Performance of Precast Concrete Shear Wall with U-shaped closed Reinforcements Connected in horizontal Joints," Journal of Southeast University, Vol. 43, No. 3, pp. 565-570.
	Chen, Y., Liu, J., Guo, Z., Zhang, J., 2013, "Test on Seismic Performance of Precast Shear Wall with Reinforcements Grouted in holes and Spliced Indirectly in Horizontal Connections," Journal of Harbin Institute of Technology, Vol. 45, No. 6, pp. 83-89.
Lombard 1999	Lombard, J.C., 1997, "Seismic Strengthening and Repair of Reinforced Concrete Shear walls using Externally Bonded Carbon Fiber Tow Sheets," Master's Thesis, Carleton University, Ottawa, Canada.
	Lombard, J., Lau, D.T., Humar, J.L., Foo, S., Ceung, M.S., 2000, "Seismic Strengthening and Repair of Reinforced Concrete Shear Walls," 12th WCEE Auckland, New Zealand.
	Lau, D.T., Cruz-Noguez, C.A., 2013, "Development on Seismic Retrofit of RC Shear Walls with FRP," 5th International Conference on Advances in Experimental Structural Engineering, Taipei, Taiwan.
	Cruz-Noguez, C.A., Hassan, A., Lau, D.T., Woods, J., Shaheen, I., "Seismic Retrofit of Deficient RC Shear Walls with FRP Tow Sheets," Proceedings of the 10th U.S. National Conference on Earthquake Engineering, July 21-25, Anchorage, Alaska.
Looi and Su 2017	Loo, T., Wee, D., 2017, "Seismic Axial Collapse of Short Shear Span Reinforced Concrete Shear Walls," PhD. Dissertation, University of Hong Kong.
	Looi, D.T.W., Su, R.K.L., 2017, "Predictive Seismic Shear Capacity Model of Rectangular Squat Shear Walls in Flexural and Shear Zones," Proceedings of the 16th World Conference on Earthquake Engineering, January 9-13, Santiago, Chile.
	Looi, D.T.W., Su, R.K.L., 2018, "Seismic axial collapse of short shear span RC shear walls above transfer structure," Proceedings of 14th International Conference on Concrete Engineering and Technology, Aug. 8-9, Kuala Lumpur, Malaysia.

	Looi, D.T.W., Su, R.K.L., 2018, "Seismic Axial collapse of short shear Damaged Heavily Reinforced Shear Walls Experiencing Cyclic Tension-Compression Excursions: A Modified Mohr's Axial Capacity Model," Journal of Earthquake Engineering.
	Looi, D.T.W., Su, R.K.L., Cheng, B., Tsang, H.H., 2017, "Effects of axial load on seismic performance of reinforced concrete walls with short shear span," Engineering Structures, Vol. 151, pp. 312-326.
Lopes 2000	Lopes, M.S., 2001, "Experimental Shear-Dominated Response of RC Walls Part I: Objectives, methodology and results," Engineering Structures, Vol. 23, pp. 229-239.
	Lopes, M.S., 2001, "Experimental Shear-Dominated Response of RC Walls Part II: Discussion of Results and Design Implications," Engineering Structures, Vol. 23, pp. 564-574.
	Lopes, M.S., and Elnashai, A.S., 1992, "A New Experimental set-up for high shear loading of reinforced concrete walls," Proceedings of the 10th World Conference on Earthquake Engineering, July 19-24, Madrid, Spain.
	Lu, H., 2004, "Effect of Concrete Strength on the Response of Ductile Shear Walls," Master's Thesis, McGill University, Montreal, Canada.
	Lu, X., and Wu, H., 2017, "Study on seismic performance of prestressed precast concrete walls through cyclic lateral loading test," Magazine of Concrete Research, Vol. 69, No. 17, pp. 878–891.
Lu and Mao 2014 and Lu et al., 2014 and 2016	Lu, X., Jiang, H., 2016, "Recent Study on Seismic Performance and Response Control of Tall Buildings," Proceedings of the International Association for Bridge and Structural Engineering (IABSE) Congress.
	Lu, X., Wu, H., 2017, "Study on seismic performance of prestressed precast concrete walls through cyclic lateral loading test," Magazine of Concrete Research, Vol. 16, No. 17, pp. 1-14.
	Dang, X., Lu, X., Zhou, Y., 2014, "Experimental Study and Numerical Simulation of Self-Centering Shear Walls with Horizontal Bottom Slit," Earthquake Engineering and Engineering Dynamics, Vol 34, No 4, pp.154-161.
	Lu, X., Dang, X., Quin, j., Zhou, Y., Jiang, H., "Experimental Study of Self-Centering Shear Walls with Horizontal Bottom Slits," Journal of Structural Engineering, Vol. 143, Issue 3.
	Wu, H., Jiang, H., Shi, W., Li, J., 2016, "Experimental Study on Seismic Performance of Prestressed Precast Concrete Shear Walls," Journal of Building Structures, Vol 37, No. 5, pp. 208-217.
	Mao, Y., Lu, X., 2014, "Quasi-Static Cyclic Test of RC Shear Wall with Replaceable foot Parts," Journal of Central South University (Science and Technology), Vol. 45, No 6, pp. 2029-2040.
	Lu, X., Mao, Y., Chen, Y., Zhao, Y., 2014, "Earthquake Resilience of Tall Buildings Using Replaceable Energy Dissipation Members," Proceedings of the 10th U.S. National Conference on Earthquake Engineering, July 21-25, Anchorage, Alaska.
	Wu, Hao, Lu, X., Zhang, Q., 2015, "Experimental Behavior of Unbonded Post-tensioned Precast Concrete Shear Walls for Seismic Regions," Proceedings of the 5th Structural Engineers World Congress, At Singapore.
Lu et al., 2017	Henry, R.S., Lu, Y., Seifi, P., Ingham, J.M., 2015, "Recent Research to Improve the Seismic Performance of Lightly Reinforced and Precast Concrete Walls," Proceedings of the Tenth Pacific Conference on Earthquake Engineering Building an Earthquake-Resilient Pacific, Sydney, Australia.

	Lu, Y., 2017, "Seismic Design of Lightly Reinforced Concrete Walls," PhD. Dissertation, The University of Auckland.
	Lu, Y., Henry, R.S., Ma, Q.T., 2014, "Numerical Modelling and Testing of Concrete Walls with Minimum Vertical Reinforcement," Proceedings of New Zealand Society for Earthquake Engineering (NZSEE) Conference, March 21-23, Auckland, New Zealand.
	Lu, Y., Henry, R.S., Ma, Q.T., 2014, "Modelling and Experimental Plan of Reinforced Concrete Walls with Minimum Vertical Reinforcement," Proceedings of the 10th U.S. National Conference on Earthquake Engineering Frontiers of Earthquake Engineering, July 21-25, Anchorage, Alaska.
	Lu, Y., Henry, R.S., Gultom, R., Ma, Q.T., 2015, "Experimental testing and modelling of reinforced concrete walls with minimum vertical reinforcement," New Zealand Society for Earthquake Engineering (NZSEE) Conference, April 10-12, Rotorua, New Zealand.
	Lu, Y., Henry, R.S., Gultom, R., Ma, Q.T., 2017, "Cyclic Testing of Reinforced Concrete Walls with Distributed Minimum Vertical Reinforcement," Journal of Structural Engineering, Vol 143, No. 5.
Luna 2015	Rocks, J.F., 2012, "large Scale Testing of Low Aspect Ratio Reinforced Concrete Walls," Master's Thesis, University of Buffalo, State University of New York.
	Luna, B.N., 2015, "Seismic Response of Low Aspect Ratio Reinforced Concrete Walls for Building and Safety-Related Nuclear Application," PhD Dissertation, University of Buffalo, State University of New York.
	Luna, B.N., Rivera, J.P., Rocks, J.F., Goksu, C., Whittaker, A.S., 2013, "Seismic Performance of Low Aspect Ratio Reinforced Concrete Shear Walls," SMiRT-22, San Francisco, California.
	Lu.N., Rivera, J.P, Whittaker, A.S., 2015, "Seismic Behavior of Low-Aspect-Ratio Reinforced Concrete Shear Walls," ACI Structural Journal, Vol. 112, No. 5, pp. 593-604.
	Rivera, J.P., Luna, B.N., Whittaker, A.S., 2018, "Seismic Damage Assessment of Low Aspect Ratio Reinforced Concrete Shear Walls," Technical Report MCEER-18-0003.
Ma 2015	Ma, G., 2015, "Seismic performance tests and calculation theory for recycled aggregate thermal insulation concrete (RATIC) shear wall" PhD Dissertation, Taiyuan University of Technology, Taiyuan, China, 137 pp. (in Chinese)
	Ma, G., Liu, Y., Zhang, Y., and Li, Z. 2015, "Seismic behavior of recycled aggregate thermal insulation concrete shear walls," Magazine of Concrete Research, Vol. 67, No. 3, pp. 145-162.
Ma et al., 2013	Ma, H., Zhang, H.M., and Zhai, Y.Q. 2013, "Experimental Study on Seismic Performance of RC Shear Wall and High-strength Rebars," *Journal from of International Efforts in Lifeline Earthquake Engineering*, pp. 505-512.
	Li, Z., Song, Y., Zhang, H., Xie, Y., and Ma, H. 2014, "Study of Seismic Performance of RC Shear Wall With 1000 MPa High-Strength Rebars," *Journal of Industrial Construction*, Vol. 44, No. 12, pp. 57-62.
Maeda et al., 1986 (Kabeyasawa)	Kabeyasawa, T., and Hiraishi, H. 1998, "Test Analyses of High-Strength Reinforced Concrete Shear Walls in Japan," ACI Structural Journal, Vol. 176, No. 13, pp. 281-310.
Maeda et al., 2017	Maeda et al., "Examination of the effect of prior damage on ultimate strength by seismic wall test," Report, Tohoku University, Japan, 48 pp. (in Japanese) https://www.nsr.go.jp/data/000215343.pdf

	Maeda, M., Koike, T., Hosoya, N., Susuki, Y., Tsurugar, K., and Nimura, A. 2017, "Damage and Residual Seismic Performance Evaluation Of Reinforced Concrete Shear Walls," Proceedings, 16th World Conference on Earthquake, Santiago, Chile, 9-13 January, No. 1971.
	Maeda, M., Hosoya, N., Koiike, T., Hanzawa, M., Ogata, Y., and Jin, K. 2017, "Static Loading Test On Seismic Capacity Of Reinforced Concrete Shear Walls In Nuclear Power Plant Part 2 Evaluation Of Damage And Residual Capacity," Proceedings, SMiRT-24 BEXCO, Busan, Korea, 20-25 August.
Marihuen 2014	Hube, M.A., Marihuen, A., De la Liera, J.C., and Stojadinovic, B. 2014, "Experimental Campaign of Reinforced Concrete Walls with Non-Seismic Detailing," Proceedings, 10th U.S. National Conference on Earthquake Engineering, July 21-25, Anchorage, Alaska.
	Hube, M.A., Marihuen, A., De la Liera, J.C., and Stojadinovic, B. 2014, "Seismic behavior of slender reinforced concrete walls," *Proceedings*, *ELSEVIER Journal of Engineering Structures*, Vol. 80, pp. 377-388.
	Marihuén, A, 2014, "Seismic behavior of slender reinforced concrete walls," Master's Thesis, Pontificia Universad Católica de Chile, Chile, 133 pp. (in Spanish)
Marius 2012	Nagy-Gyorgy, T., Mosoarca, M., Solan, V., Gergely, H., and Dan, D. 2005, "Retrofit of reinforced concrete shear walls with cfrp composites," Article from Symposium 'Keep Concrete Attractive, Budapest, pp. 1-6.
	Mosoarca, M., and Stolan, V. 2012, "Seismic Energy Dissipation In Structural Reinforced Concrete Walls With Staggered Openings," Journal of Applied Engineering Sciences, Vol. 2, No. 15, pp. 71-78.
	Marius, M. 2013, "Seismic behavior of reinforced concrete shear walls with regular and staggered openings after the strong earthquakes between 2009 and 2011," *ELSEVIER Journal of Engineering Failure Analysis*, Vol. 34, pp. 537-565.
	Mosoarca, M. 2014, "Failure analysis of RC shear walls with staggered openings under seismic loads," *ELSEVIER Journal of Engineering Failure Analysis*, Vol. 41, pp. 48-64.
	Mosoarca, M. 2014, "Bearing Structures in Architecture," *PhD Dissertation*, The Polytechnic University of Timisoara, Timișoara, Romania, pp. 1-159.
Massone 2006	Orakcal, K., Massone, L.M., and Wallace, J.W. 2009, "Shear Strength of Lightly Reinforced Wall Piers and Spandrels," ACI Structural Journal, Vol. 106, No. 43, pp. 455-465.
	Sanchez, L. 2006, "RC Wall Shear- Flexure Interaction: Analytical and Experimental Responses," *PhD Dissertation*, University of California, Los Angeles, United States, pp. 1-398.
	Massone, L. 2009, "Strength prediction of squat structural walls via calibration of a shear-flexure interaction model," *ELSEVIER Journal of Engineering Structures*, Vol. 32, pp. 922-932.
Matsubara et al., 2012	Matsubara, S., Sanada, Y., Takahashi, S., and Ichinose, T., 2012, "Experimental study on the effect of structural details of the compression zone on the deformation performance of a bending fracture bearing wall," Proceedings of the Japan Concrete Institute, Vol. 34, No. 2, pp. 361-366. (in Japanese)
	Kono, S., Kabeyasawa, T., Sanada, Y., Sakashita, M., Nishiyama, M., Ichinose, T., Takahashi, S., Tani, M., and Fukuyama, H. 2012 "Seismic Behavior of Reinforced Concrete Structural Walls based on the Japanese Domestic Research Efforts," Research Report, pp. 1-11.

	Matsubara, S., Sanada, Y., Tani, M., Takahashi, S., Ichinose, T., and Fukuyama, H., 2013, "Structural parameters of confined area affect flexural deformation capacity of shear walls that fail in bending with concrete crushing," Journal of Structural and Construction Engineering, Vol. 78, No. 691, pp. 1593–1602. (in Japanese)
	Yamamoto, N., Sanada, Y., ad Matsubara, S. 2014, "Tests and Analyses for Seismic Performance Evaluation Of R/C Shear Walls Fail in Bending with Concrete Crushing," Proceedings of the10th US National Conference on Earthquake Engineering, July 21-25, Anchorage, Alaska.
Matsui et al., 2014	Matsui, T., Saito, T., and Reyna, R. 2014, "Basic Study on Reinforced Concrete Shear Walls Without Boundary Columns Retrofitted by Carbon Fiber Sheets," *Journal of Disaster Research*, Vol. 9, No. 6, pp. 1008-1014.
Matsui et al., 2017	Matsui, T., Saito, T., and Reyna, R. 2017, "Structural Performance of Rectangular Reinforced Concrete Walls Retrofitted by Carbon Fiber Sheets," Proceedings of the 16th World Conference on Earthquake, Santiago, Chile, 9-13 January 2017.
Mehmood et al., 2015	Mehmood, T., Warnitchai, P., and Hssain, K. 2015, "Seismic evaluation of flexural-shear dominated RC walls in moderate seismic regions," Magazine of Concrete Research, Vol. 67, No. 18, pp. 1003-1015.
Mestyanek 1986	Mestyanek, J.M. 1986, "The Earthquake Resistance of Reinforced Concrete Structural Walls of Limited Ductility," *Master Dissertation*, University of Canterbury, Christchurch, New Zealand, pp. 1-239.
Mickleborough et al., 1999	Mickleborough, N.C., Ning, F., and Chan C.M. 1999, "Prediction of Stiffness of Reinforced Concrete Shear Walls under Service Loads," ACI Structural Journal, Vol. 96, No. 113, pp. 1018-1026.
	Ning, Feng., Mickleborough, N.C., and Chan, C.M. 2001, "Service load response prediction of reinforced concrete flexural members," *Journal of Structural Engineering and Mechanics,* Vol. 12, No. 1, pp. 1-16.
Mitchell and Chen 2005 & Mitchell and Liu 2004	Chen, C.Y. 2005, "Effect of Confinement on the Response of Ductile Shear Walls," *PhD Dissertation*, McGill University, Montreal, Canada, pp. 1-116.
	Liu, H. 2004, "Effect of Concrete Strength on the Response of Ductile Shear Walls," *PhD Dissertation*, McGill University, Montreal, Canada, pp. 1-101.
Mobeen 2002	Mobeen, S., 2002, "Cyclic Tests of Shear Walls Confined with Double Head Studs," Master's Thesis, University of Alberta, Edmoton, AB, Canada.
	Mobeen, S.S., Elwi, A.E., and Ghali, A. 2005, "Double-Headed Studs in Shear walls," *Concrete International Journal*, Vol. 27, No. 3, pp. 59-63.
Mohamed 2013	Mohamed, N.A.A.R. 2013, "Strength and Drift Capacity of GFRP-Reinforced Concrete Shear Walls," PhD Dissertation, University of Sherbrooke, Quebec, Canada, pp. 1-155.
	Mohamed, N., Farghaly, A.S., Benmokrane, B., Neale, K.W. 2012, "Cyclic Load Behavior of GFRP Reinforced Concrete Shear Wall: Experimental Approach," Proceedings of the 6th International Conference on Advanced Composite Materials in Bridges and Structures, Ontario Canada, 22-25 May 2012, pp. 1-8.
	Mohamed, N., Farghaly, A.S., Benmokrane, B., and Neale, K.W. 2014, "Experimental Investigation of Concrete Shear Walls Reinforced with Glass Fiber–Reinforced Bars under Lateral Cyclic Loading," *Journal of Composites for Construction*, Vol. 18, No. 3, pp. A40140011-A401400111.

Mohammadi-Doostdar 1994	Mohammadi-Doostdar, H. 1994, "Behavior and Design of Earthquake Resistant Low-Rise Shear Walls," PhD Dissertation, University of Ottawa, Ottawa, Canada, pp. 1-250.
Morgan et al., 1986	Morgan, B J., Hiraishi, H., and Corley W. G., 1986, "US-Japan quasi-static test of isolated wall planar reinforced concrete structure," Report to National Science Foundation, submitted by Construction Technology Laboratories, Portland Cement Association, Skokie, IL.
Motter 2017	Motter, C. 2014, "Large-Scale Testing of Steel-Reinforced Concrete (SRC) Coupling Beams Embedded into Reinforced Concrete Structural Walls," PhD Dissertation, University of California, Los Angeles, California, pp. 1-344.
	Motter, C., Abdullah, S.A., and Wallace, J.W. 2018, "Reinforced Concrete Structural Walls without Special Boundary Elements," ACI Structural Journal, Vol. 115, No. 55, pp. 723-733.
Mun et al., 2016	Mun, J. H., Yang, K. H., and Lee, Y., 2016, "Seismic tests on heavyweight concrete shear walls with wire ropes as lateral reinforcement," ACI Structural Journal, Vol. 113, No. 4, pp. 665–675.
	Mun, J.H., Yang, K.H., and Song, J.K. 2017, "Shear Behavior of Squat Heavyweight Concrete Shear Walls with Construction Joints," *ACI Structural Journal*, Vol. 114, No. 83, pp. 1019-1029.
Murakami and Ikawa 2010	Murakami, H., and Ikawa, N., 2010, "Development of RC Multi-story Shear Wall Structure-Part1 Experimental Study on Structural Performance" Konoike Group Technical Research Report, pp. 27-38. (in Japanese)
Nagae et al., 2011	Nagae, T., Tahara, K., Matsumori, T., Shiohara, H., Kabeyasawa, T., Kono, S., Nishiyama, M., Wallace, J., Ghannoum, W., Moehle, J., Sause, R., Keller, W., and Tuna, Z. 2011, "Design and Instrumentation of the 2010 E-Defense Four-Story Reinforced Concrete and Post-Tensioned Concrete Buildings," *Pacific Earthquake Engineering Research Center*, pp. 1-234.
	Nagae, T., Matsumori, T., Shiohara, H., Kaheyasawa, T., Kono, S., Nishiyama, M., Moehle, J., Wallace, J., Sause, R., and Ghannouum, W. 2010, "The 2010 E-Defense Shaking Table Test On Four-Story Reinforced Concrete And Post-Tensioned Concrete Buildings," Proceedings of the10th U.S. National Conference on Earthquake Engineering, July 21-25, Anchorage, Alaska.
	Nagae, T., Ghannoum, W.M., Kwon, J., Tahara, K., Fukuyama, K., Matsumori, T., Shiohara, H., Kabeyasawa, T., Kono, S., Nishiyama, M., Sause, R., Wallace, J.W., and Moehle, J.P. 2015, "Design Implications of Large-Scale Shake-Table Test on Four-Story Reinforced Concrete Building," ACI Structural Journal, Vol. 112, No. 12, pp. 135-146.
	Tuna, Z., Gavridou, S., Wallace, J.W., Nagae, T., and Matsumori, T. 2012, "2010 E-Defense Four-Story Reinforced Concrete and Post-Tensioned Buildings – Preliminary Comparative Study of Experimental and Analytical Results," Proceedings of the 15th World Conference on Earthquake Engineering, Sept. 24-28, Lisbon, Portugal.
	Tuna, Z., Wallace, J.W., Gavridou, S., Nagae, T., and Matsumori, T. 2014, "2010 E-Defense Four-Story RC And Pt Buildings - Comparative Study of Experimental and Analytical Results," Proceedings of the 10th US National Conference on Earthquake Engineering, July 21-25, Anchorage, Alaska, pp. 1-21.
Nagashima et al., 1993	Nagashima, T., et al., 'Seismic behavior of reinforced concrete shear walls using high strength concrete (in Japanese),' Proceedings of the Japan Concrete Institute, Vol. 15, No. 2, 1155- 1160(1993).

Nakachi et al., 1990	Minami, N., and Nakachi, T. 2008, "Three-Dimensional Nonlinear Finite Element Analysis on Reinforced Concrete Walls Enhanced by Transverse Confining Steel," Proceedings of the 14th World Conference on Earthquake Engineering, October 12-17, 2008, Beijing, China.
	Minami, N., and Nakachi, T. 2008, "Finite Element Analysis on Reinforced Concrete Wall Columns Enhanced by Transverse Confining Steel," Fukui University of Technology, Fukui, Japan, pp. 179-184.
	Makita, T., Nakachi, T., hayakawa, Y., and Toda, T., 1990, "Experimental Study on Flexural Type RC Shear Walls in High-Rise Construction," Proceedings of the Japan Concrete Institute, Vol. 12, No. 2, pp. 551-556. (in Japanese)
	Nakachi, T., Toda, T., and Makita, T. 1992, "Experimental study on deformation capacity of reinforced concrete shear walls after flexural yielding," Proceedings of the 10th World Conference on Earthquake Engineering, July 19-24, Madrid, Spain, pp. 3231-3236.
Nakamura et al., 2009	Kanechika, M., Kobayashi, A., Kato, M., Sakanishi, M., Suzuki, N., et al, 1989, "Application Of high strength rebar for RC shear wall part-1," Summaries of technical papers of annual meeting of AIJ. Structures II, pp. 567–568. (in Japanese).
	Nakamura, N., Tsunashima, N., Nakano, T., and Tachibana, E. 2009, "Analytical study on energy consumption and damage to cylindrical and I-shaped reinforced concrete shear walls subjected to cyclic loading," ELSEVIER Journal of Engineering Structures, Vol. 31, pp. 999-1009.
Niroomandi et al., 2018	Niroomandi, A., Pampanin, S., Dhakal, R.P., and Soleymani Ashtiani, M. 2018, "Experimental Study on Slender Rectangular RC Walls Under Bi-Directional Loading," Proceedings of the 11th U.S. National Conference on Earthquake Engineering, Los Angeles, California, June 25-29.
	Niroomandi, A., Pampanin, S., Dhakal, R.P., Soleymani Ashtiani, M., and De La Torre, C. 2018, "Rectangular RC Walls Under Bi-Directional Loading: Recent Experimental and Numerical Findings," Proceedings of New Zealand Concrete Industry Conference, October 11-13, Hamilton, New Zealand.
Oesterle et al.,	Fiorato, A.E., Oesterle, R.G., and Corley, W.G. 1983, "Behavior of Earthquake Resistant Structural Walls Before and After Repair," *ACI Structural Journal*, Vol. 80, No. 5, pp. 403-413.
	Corley, W.G., Fiorato, A.E., and Oesterle, R.G. 1981, "Structural Walls," *Research Report*, Vol. 72, No. 1, pp. 77-132.
	Fiorato, A.E., Oesterle, R.G., and Corley V.G. 1977, "Ductility of Structural Walls for Design of Earthquake Resistant Buildings," *Research Report*, Vol. 72, No. 1, pp. 2797-2802.
	Fiorato, A.E., Oesterle, R.G., and Corley, W.G. 1983, "Behavior of Earthquake Resistant Structural Walls Before and After Repair," ACI Structural Journal, Vol. 80, No. 5, pp. 403-413.
	Wood, S. 1989, "Minimum Tensile Reinforcement Requirements in Walls," *ACI Structural Journal*, Vol. 86, No. 56, pp. 582-591.
	Wood, S., 1986, "Observed Behavior of Slender Reinforced Concrete Walls Subjected to Cyclic Loading," *ACI Structural Journal*, Vol. 127, No. 11, pp. 453-477.
	Oesterle, R.G., 1986, “Inelastic Analysis for In-Plane Strength of Reinforced Concrete Shear Walls,” *PhD Dissertation*, Northwestern University, Evanston, Illinois, June 1986, 332 pp. 1-329.

	Oesterle, R. G., Fiorato, A. E., Johal, L. S., Carpenter, J. E., Russell, H. G., and Corley, W. G., 1976, "Earthquake Resistant Structural Walls–Tests of Isolated Walls," Report to National Science Foundation (GI-43880), Construction Technology Laboratories, Portland Cement Association, Skokie, IL, 315 pp. 1-232.
	Oesterle, R. G., Aristizabal-Ochoa, J. D., Fiorato, A. E., Russell, H. G., and Corley, W. G., 1979, "Earthquake Resistant Structural Walls–Phase II," Report to National Science Foundation (ENV77-15333), Construction Technology Laboratories, Portland Cement Association, Skokie, IL, 331 pp.1-207.
	Oesterle, R.G., Fiorato, A.E., Aristizabal-Ochoa, and Corley, W.G. 1980, "Hysteretic Response of Reinforced Concrete Structural Walls," ACI Structural Journal, Vol. 63, No. 11, pp. 243- 273.
	Oesterle, R.G., Fiorato, A.E., and Corley, W.G. 1980b, "Reinforcement Details for Earthquake-Resistant Structural Walls," *Concrete International Journal,* Vol. 2, No. 12, pp. 55-66.
	Oesterle, R.G., Aristizabal-Ochoa, J.D., Shiu, K.N., and Corley, W.G. 1984, "Web Crushing of Reinforced Concrete Structural Walls," *ACI Journal*, Vol. 81, No. 22, pp. 231-241.
Ogura et al. 2014	Kono, S., Obara, T., Taleb, R., and Watanabe, H. 2015, "Simulation of drift capacity of RC walls with different section configurations," Proceedings of the 10th Pacific Conference on Earthquake Engineering, Sydney, Australia, pp. 181-188.
	Yuniarsyah, E., Kono, S., Tani, M., Taleb, R., Sugimoto, K., and Mukai, T. 2016, "Damage evaluation of lightly reinforced concrete walls in moment resisting frames under seismic loading," *ELSEVIER Journal of Engineering Structures*, Vol. 132, pp. 349-371.
	Tani, M., Mukai, T., Ogura, M., Taleb, R., and Kono, S. 2014, "Full-Scale Experiment on Non-Structural RC Walls Focused on Failure of Modes and Damage Mitigation," Proceedings of the 2nd European Conference on Earthquake Engineering and Seismology, Aug. 24-29, Istanbul, Turkey, pp. 1-12.
	Yuniarsyah, E., Taleb, R., Watanabe, H., Kono, S., Tani, M., and Mukai, T. 2015, "Experimental Study On Residual Damage Of Full-Scale RC Non-Structural Wall Specimens Part 3: Experimental Program For Improved Specimens," *Proceedings,* Architectural Institute of Japan Annual Meeting, At Yokohama, Japan, pp. 129-130.
	Taleb, R., Yuniarsyah, E., Watanbe, H., Kono, S., Tani, M., and Mukai, T. 2015, "Experimental Study On Residual Damage Of Full-Scale RC Non-Structural Wall Specimens Part 4: Experimental Results For Improved Specimens," *Proceedings*, Architectural Institute of Japan Annual Meeting, At Yokohama, Japan, pp. 131-132.
	Yuniarsyah, E., Kono, S., Tani, M., Taleb, R., Watanabe, H., Obara, T., and Mukai, T. 2017, "Experimental study of lightly reinforced concrete walls upgraded with various schemes under seismic loading," *ELSEVIER Journal of Engineering Structures*, Vol. 138, pp. 1-15.
Oh 1998	Oh, Y. H., 1998, "Evaluation of the response modification factor for shear walls in apartment buildings," PhD Dissertation, Hanyang University, 289 pp. (in Korean).

	Han, S. W., Oh, Y.-H., and Lee, L.-H, 1999, "Evaluation of Deformation Capacity According to the Lateral Reinforcement of Wall Ends," Journal of the Korean Concrete Institute, Vol. 11, No. 6, pp. 101-112. (in Korean)
	Oh, Y.H., Han, S.W., and Lee, L.H. 2002, "Effect of boundary element details on the seismic deformation capacity of structural walls," *Article in Earthquake Engineering and Structural Dynamics*, Vol. 31, pp. 1583-1602.
	Han, S.W., Oh, Y.H., and Lee, L.H. 2002, "Seismic behavior of structural walls with specific details," *Magazine of Concrete Research*, Vol. 54, No. 5, pp. 333-345.
	Oh, Y.H., Han, S.W., and Choi, Y.S. 2006, "Evaluation and Improvement of Deformation Capacities of Shear Walls Using Displacement-Based Seismic Design," *International Journal of Concrete Structures and Materials*, Vol. 18, No. 1, pp. 55-61.
Okamoto et al., 1990	Ishimura. K., Odajima, M., Irino, K., and Hashiba, T. 1991, "Study on Reactor Building Structure Using Ultrahigh Strength Materials, Part 1: Summary of Research," *ELSEVIER Journal on Nuclear Engineering and Design*, Vol. H, No. 1, pp. 359-364.
	Kabeyasawa, T., and Hiraishi, H. 1998, "Test Analyses of High-Strength Reinforced Concrete Shear Walls In Japan," *ACI Structural Journal*, Vol. 176, No. 13, pp. 281-310.
	Okamoto, S., et al., 'Study on reactor building structure using ultrahigh strength materials: Part 1. Bending shear test of RC shear wall - Outline (in Japanese),' Summaries of technical papers of annual meeting, Architectural Institute of Japan, Cll, 1469- 1470(1990).
	Uchiyama, T., Ishimura, K., Takahashi, T., and Hirade, T. 1991, "Study on Reatcor Building Structure Using Ultrahigh Strength Materials Part 4 Bending Shear Tests of RC Shear Walls," *Research Report*, Vol. H, No. 1, pp. 377-382.
	Iwashita, K., Ishimura, K., Kurihara, K., and Imai, M. 1991, "Study on Reactor Building Structure Using Ultrahigh Strength Materials Part 5 Nonlinear Analysis of RC Shear Wall," *Research Report*, Vol. H, No. 1, pp. 383-388.
Oyarzo 2006	Leiva, G. 2004, "Experimental Evaluation of Damage of Reinforced Concrete Structural Walls Subjected to High Levels of Cyclic Actions," Proceedings of the 13th World Conference on Earthquake Engineering, August 1-6, Vancouver, B.C., Canada.
	Oyarzo Vera, C. 2006, "Damage Evaluation in R/C Shear Walls Using the Damage Index of Park & Ang," Proceedings of the 1st European Conference on Earthquake Engineering and Seismology, Sept. 3-8, Geneva, Switzerland.
	Oyarzo, C. (2003), Evaluación Del Daño En Muros De Hormigón Armado Sometidos a Altas Demandas De Ductilidad. Memoria para optar al título de Ingeniero Civil, UTFSM, Valparaíso, Chile.
Palermo and Vecchio 2002	Vecchio, F., Haro de la Pena, O., Bucci, F., and Palermo, D. 2002, "Behavior of Repaired Cyclically Loaded Shear Walls," *ACI Structural Journal*, Vol. 99, No. 34, pp. 327-334.
	Palermo, D., and Vecchio, F. 2002, "Behavior and Analysis of Reinforced Concrete Walls Subjected to Reversed Cyclic Loading," *Research Report*, May 2002, pp. 1-351.
	Palermo, D., and Vecchio, F. 2002, "Behavior of Three-Dimensional Reinforced Concrete Shear Walls," *ACI Structural Journal*, Vol. 99, No. 9, pp. 81-89.

Park et al., 2013	Park, H., Lee, J., Shin, H., and Baek, J. 2013, "Cyclic Loading Test for Shear Strength of Low-rise RC Walls with Grade 550 MPa Bars," *Journal of the Korea Concrete Institute*, Vol. 25, No. 6, pp. 601~612.
	Park, H., Lee, J., Shin, H., and Baek, J. 2014, "Shear Strength of Low-rise RC Walls with Grade 550 MPa Bars," *Proceedings,* 2014 International Conference on Geological and Civil Engineering, Vol. 62, No. 7, pp. 34-39.
	Park, H., Baek, J., Lee, J., and Shin, H. 2013, "Cyclic Loading Tests for Shear Strength of Low-Rise Reinforced Concrete Walls with Grade 550 MPa Bars," *ACI Structural Journal*, Vol. 112, No. 24, pp. 299-310.
Paterson 2001	Paterson, J. 2001, "Seismic Retrofit of Reinforced Concrete Shear walls," *Master Dissertation*, McGill University, Montreal, Canada. pp. 1-123.
	Paterson, J., and Mitchell, D. 2003, "Seismic Retrofit of Shear Walls with Headed Bars and Carbon Fiber Wrap," *ASCE Journal of Structural Engineering,* Vol. 129, No. 5, pp. 606-614.
Peng 2014	Peng, Y., 2014, "Strength and deformation capacity of squat recycled concrete walls under cyclic loading," PhD Dissertation, China University of Mining and Technology, Xuzhou, China, 109 pp. (in Chinese)
	Peng, Y., Wu, H., and Zhuge, Y. 2015, "Strength and drift capacity of squat recycled concrete shear walls under cyclic loading," *ELSEVIER Journal on Engineering Structures*, Vol. 100, pp. 356-369.
Peng and Wong 2011	Peng, X. 2011, "Study of Torsional Behavior of Reinforced Concrete Walls," *PhD Dissertation*, The Hong Kong Polytechnic University, pp. 1-189.
	Peng, X., and Wong, Y. 2016, "Experimental study on reinforced concrete walls under combined flexure, shear and torsion," *Magazine of Concrete Research*, Vol. 63, No. 6, pp. 459-471.
Peng et al., 2015	Peng, Y., 2010, "Experimental Study on Seismic Behavior of Pre-cast Reinforced Concrete Shear Walls," MS Thesis, Tsinghua University, Beijing, China, 137 pp. (in Chinese)
	Peng, Y.Y., Qian, J.R., and Yang, Y.H. 2015, "Cyclic performance of precast concrete shear walls with a mortar–sleeve connection for longitudinal steel bars," *Journal of Materials and Structures*, Vol. 49, No. 6, pp. 1-15.
Pilakoutas 1990	Elnashai, A., Pilakoutas, K., and Ambraseys, N. 1989, "Experimental BehaviorOf Reinforced Concrete Walls Under Earthquake Loading," Article in Earthquake Engineering and Structural Dynamics, Vol. 19, No. 1, pp. 389 407.
	Pilakoutas, K. 1990, "Earthquake Resistant Design of Reinforced Concrete Walls," *PhD Dissertation*, Imperial College of Science Technology and Medicine, University of London, South Kensington, London, pp. 1-360.
	Pilakoutas, K., and Elnashai, A. 1995, "Cyclic Behavior of Reinforced Concrete Cantilever Walls, Part 1: Experimental Results," *ACI Structural Journal*, Vol. 92, No. 25, pp. 271-281.
	Pilakoutas, K., and Elnashai, A. 1995, "Cyclic Behavior of Reinforced Concrete Cantilever Walls, Part II: Discussions and Theoretical Comparisons," *ACI Structural Journal,* Vol. 92, No. 41, pp. 425-433.
Pilette 1988	Pilette, C.F. 1988, "Behavior of Earthquake Resistant Squat Shear Walls," *Master Dissertation*, University of Ottawa, Ottawa, Canada, pp. 1-130.
Pollalis 2018	???

Puranam and Pujol 2017	Puranam, A., and Pujol, S. 2017, "Minimum Flexural Reinforcement In Reinforced Concrete Walls," *Proceedings,* 16th World Conference on Earthquake Engineering, Santiago, Chile, Vol. 2017, No. 1059, pp. 1-9.
Qazi 2013	Nguyen, K., Brun, M., Limam, A., Ferrier, E., and Michel, L. 2013, "Local and Non-Local Approaches for simulating CFRP-reinforced concrete shear walls under monotonic loads," Proceedings of the 5th ECCOMAS Thematic Conference on Computational Methods in Structural Dynamics and Earthquake Engineering, Kos Island, Greece, 12–14 June 2013.
	Nguyen, K., Brun, M., Limam, A., Ferrier, E., and Michel, L. 2013, "Pushover experiment and numerical analyses on CFRP-retrofit concrete shear walls with different aspect ratios," *ELSVIER Journal of Composite Structures*, Vol. 113, No. 1, pp. 403-418.
	Qazi, S., 2014, "Mechanical behavior of RC walls under seismic activity strengthened with CFRP," European Journal of Environmental and Civil Engineering, Vol. 17, No. 6, pp. 1-191.
	Qazi, S., Michel, L., and Ferrier, E. 2013, "Mechanical behavior of RC walls under seismic activity strengthened with CFRP," European Journal of Environmental and Civil Engineering, Vol. 17, No. 6, pp. 1-191.
Qian et al., 2011	Qian, J., Yang, X., Qin, H., Peng, Y., Zhang, J., and Li, J. 2011, "Tests on seismic behavior of pre-cast shear walls with various methods of vertical reinforcement splicing," *Journal of Building Structures*, Vol. 32, No. 6, pp. 51-59.
	Qian, J., Yang, X., Qin, H., Peng, Y., Zhang, J., and Li, J. 2011, "Tests on seismic behavior of pre-cast shear walls with various methods of vertical reinforcement splicing," Journal of Building Structures, Vol. 32, No. 6, pp. 51-59.
Rama Rao et al., 2014	Parulekar, Y., Rastogi, R., Reddy, G., Bhasin, V., and Vaze, K.K. 2012, "Assessing Safety of Shear Walls: An Experimental, Analytical and Probabilistic Study," *Article in Industrial Safety and Lifecycle Engineering*, pp. 589-610.
	Parulekar, T.m., Reddy, G.R., Singh, R.K., Gopalkrishnan, N., and Ramarao, G.V. 2016, "Seismic performance evaluation of mid-rise shear walls: experiments and analysis," *Journal of Structural Engineering and Mechanics*, Vol. 59, No. 2, pp. 291-312.
	Ramarao, G.V., Gopalakrishnan, N., Jaya, K., Muthumani, K., Reddy G.R., and Parulekar, Y.M. 2015, "Studies on Nonlinear Behavior of Shear Walls of Medium Aspect Ratio under Monotonic and Cyclic Loading," *ASCE Journal of Performance of Constructed Facilities*, Vol. 30, No. 1, pp. 040142011-0401420114.
	Rama Rao, G.V., Gopalakrishnan, N., Jaya, K.P., and Dhaduk, R. 2016, "Studies on ductility of shear walls," *Journal of Structural Engineering*, Vol. 42, No. 6, pp. 540-549.
	Reddy, A., Charles, S., Priya, C., Rama Rao, G.V., Gopalakrishnan, N., and Rao, A. 2013, "Damage Detection of Cyclically Loaded Concrete Shear Wall using EMI Technique," *Journal of Structural Durability and Health Monitoring,* Vol. 9, No. 4, pp. 325-347.
Ramarozatovo et al., 2016	Ramarozatovo, R., Hosono, J., Kawai, T., Takahashi, S., and Ichinose, T. " Effects of construction joints and axial loads on slip behavior of RC shear walls-Chapter 2 Outline of Experiment," Nagoya Institute of Technology Nagoya, Japan. (in Japanese)

	Ramarozatovo, R., Hosono, J., Kawai, T., Takahashi, S., and Ichinose, T. " Effects of construction joints and axial loads on slip behavior of RC shear walls-Chapter 3 Experimental Results," Nagoya Institute of Technology Nagoya, Japan. (in Japanese)
	Ramarozatovo, R., Hosono, J., Kawai, T., Takahashi, S., and Ichinose, T. 2016, "Effects of construction joints and axial loads on slip behavior of RC shear walls," Proceedings, The 5th International Congress on Engineering and Information, Kyoto, Japan, pp. 1-12.
	Ramarozatovo, R., Hosono, J., Kawai, T., Takahashi, S., and Ichinose, T. 2016a, "Effects of construction joints and axial loads on slip behavior of RC shear walls," *International Journal of Civil, Structural, Environmental and Infrastructure Engineering*, Vol. 6, No. 4, pp. 1-10.
Raongjant 2007	Raongjant, W., 2007, "Seismic Behavior of Lightweight Reinforced Concrete Shear Walls," PhD Dissertation, Leibniz University Hannover, Germany, 138 pp.
	Raongjant, W., and Jing, M. 2009, "Analysis Modelling of Seismic Behavior of Lightweight Concrete Shear Walls," Proceedings, 2009 International Multi Conference of Engineers and Computer Scientists, Vol. 2, No. 1, pp. 1-6.
Riva and Franchi 2001	Riva, P., and Franchi, A. 2001, "Behavior of Reinforced Concrete Walls with Welded Wire Mesh Subjected to Cyclic Loading," *ACI Structural Journal*, Vol. 98, No. 31, pp. 324-334.
Saito et al., 1989	Saito, H., Kikuchi, R., Kanechika, M., and Okamoto, K. 1989, "Experimental Study of the Effect of Concrete Strength of Shear Wall Behavior," *Article from NC State University*, Raleigh, North Carolina, pp. 227-232.
Saitoh et al., 1990	Kabeyasawa, T., and Kiraishi, H. 1998, "Tests and Analyses of High-Strength Reinforced Concrete Shear Walls in Japan," *ACI Structural Journal*, Vol. 176, No. 13, pp. 281-310.
	Saitoh, F., Kuramoto, H. and Minami, K., 'Shear behavior of shear walls using high strength concrete (in Japanese),' Summaries of technical papers of annual meeting, Architectural Institute of Japan, Cll, 605-606(1990).
Salonikios 1998	Salonikios T. N., 1998, "Experimental investigation of the behavior of R/C walls with aspect ratio 1, 1.5 reinforced by conventional and non-conventional type of reinforcement, under seismic loading," PhD Dissertation, Aristotle University of Thessaloniki, Greece, 297 pp. (in Greek)
	Salonikios, T. 2002, "Shear strength and deformation patterns of R/C walls with aspect ratio 1.0 and 1.5 designed to Eurocode 8 (EC8)," ELSEVIER Journal of Engineering Structures, Vol. 24, No. 1, pp. 39-49.
	Salonikios, T. 2007, "Analytical Prediction of the Inelastic Response of RC Walls with Low Aspect Ratio," ASCE Journal of Structural Engineering, Vol. 133, No. 6, pp. 844-854.
	Salonikios, T., Tegos, I., Kappos, A., and Penelis G. 1996, "Squat RC Walls Under Inelastic Reversals," *Proceedings*, 11th World Conference on Earthquake Engineering, June 23-28, Acapulco, Mexico, pp. 1-8.
	Salonikios, T., Kappos, A., Tegos, I., and Penelis, G. 1999, "Cyclic Load Behavior of Low-Slenderness Reinforced Concrete Walls: Design Basis and Test Results," *ACI Structural Journal,* Vol. 96, No. 73, pp. 649-660.
	Salonikios, T., Kappos, A., Tegos, I., and Penelis, G. 2000, "Cyclic Load Behavior of Low-Slenderness Reinforced Concrete Walls: Failure Modes, Strength and Deformation Analysis, and Design Implications," *ACI Structural Journal*, Vol. 97, No. 15, pp. 132-142.

Sanada and Kabeyasawa 2006	Murase, M., Kaburiyazawa, T., Sanada, A., and Igarashi, S., 2005, "Study on seismic reinforcement of reinforced concrete walls using polyester fiber sheet," Proceedings of the Japan Concrete Institute, Vol. 27, No. 2, pp. 1075-1080. (in Japanese)
	Sanada, T., and Kabeyasawa, T. 2006, "Local Force Characteristics of Reinforced Concrete Shear Wall," *Proceedings*, 8th U.S. National Conference on Earthquake Engineering, Vol. 2006, No. 324, pp. 1-10.
Sanada et al., 2012	Sanada, Y., Takahashi, H., and Toyama, H. 2012, "Seismic Strengthening of Boundary Columns in R/C Shear Walls," *Proceedings*, 15th World Conference on Earthquake Engineering, Sept. 24-28, Lisbon, Portugal, pp. 1-10.
Sato et al., 1989	Sato, s., Ogata, T., Yoshizaki, S., Kanata, K., Yamaguchi, T., Nakayama, T., Inada, T., and Kadoriku J. 1989, "Behavior of Shear Wall Using Various Yield Strength of Rebar Part 1: An Experimental Study," *Article from NC State University*, Raleigh, North Carolina, pp. 233-238.
Segura 2017	Segura, C. L., 2017, "Seismic Performance Limitations and Reinforcement Detailing of Slender RC Structural Walls," PhD Dissertation, University of California, Los Angeles, Los Angeles, CA, 238 pp.
	Segura, C. L., and Wallace, W. J., 2018a, "Seismic performance limitations and detailing of slender RC walls," ACI Structural Journal, Vol. 115, No. 03, pp. 849-860.
	Segura, C. L., and Wallace, W. J., 2018b, "Impact of geometry and detailing on drift capacity of slender walls," ACI Structural Journal, Vol. 115, No. 03, pp. 885-896.
	Segura, C. L., and Wallace, W. J., 2015, "Experimental study on the seismic performance of thin reinforced concrete structural walls" Structural Engineering Frontier Conference, March 18-19, Tokyo Institute of Technology, Yokohama, Japan.
	Segura, C. L., Wallace, W. J., Arteta, C.A., and Moehle, J. P., 2016, "Deformation capacity of thin reinforced concrete shear walls," New Zealand Society for Earthquake Engineering Annual Technical Conference, April 1-3, Christchurch, NZ.
Seo et al., 2007	Seo et al., "Hysteretic Behavior of Recycle R/C Shear Wall with Various Transverse Reinforce in Boundary Element," Report. (in Korean)
	Seo, S., Yoon, S., and Cho, Y. 2007, "Strength and Hysteretic Characteristics of RC Shear Wall with Boundary Elements," Proceedings of the Korea Concrete Institute Conference, pp. 69-73. (in Korean)
	Seo, S., Oh, T.G., Kim, K.T., and Yoon, S.J. 2010, "Hysteretic Behavior of RC Shear Wall with Various Lateral Reinforcements in Boundary Columns for Cyclic Lateral Load, " *Jornal of the Korea Concrete Institute*, Vol. 22, No. 2, pp. 357-366.
Shaingchin et al., 2006	Shaingchin, S., Lukkunaprasit, P., and Wood, S. 2006, "Influence of diagonal web reinforcement on cyclic behavior of structural walls," *ELSEVIER Journal of Engineering Structures*, Vol. 29, No. 4, pp. 498-510.
Shegay 2017	Shegay, A., Motter, C., Henry, R., and Elwood, K. 2018, "Impact of Axial Load and Detailing on the Seismic Response of Rectangular Walls," *ASCE Journal of Structural Engineering*, Vol. 144, No. 8, pp. 1-110.
	Sheygay, A., Motter, C., Henry, R., and Eldwood, K. 2006, "Large Scale Testing Of A Reinforced Concrete Wall Designed To The Amended Version Of Nzs3101," The New Zealand Concrete Industry Conference 2016, Auckland, New Zealand, pp. 1-9.

	Sheygay, A., Motter, C., Henry, R., and Eldwood, K. 2017, "Modeling of RC Walls with Ductile Detailing Subjected to High Axial Loads," *Proceedings*, 16th World Conference on Earthquake, Santiago Chile, pp. 1-11.
	Shegay, A., Motter, C., Henry, R., amd E;dwppd L. 2017, "Experimental Study on Reinforced Concrete Walls with High Axial Loads," *Proceedings*, 2017 New Zealand Society for Earthquake Engineering Conference, Auckland, New Zealand, pp. 1-9.
	Shegay, A., Motter, C., Eldwood, K., Henry, R., Lehman, D., and Lowes, L. 2018, "Impact of Axial Load on the Seismic Response of Rectangular Walls," *ASCE Journal of Structural Engineering*, Vol. 144, No. 8, pp. 040181241-0401812414.
Shen et al., 2017	Shen, D., Yang, Q., Jiao, Y., Cui, Z., and Zhang, J. 2016, "Experimental investigations on reinforced concrete shear walls strengthened with basalt fiber-reinforced polymers under cyclic load," *ELSEVIER Article on Construction and Building Materials*, Vol. 136, pp. 217-229.
Shimazaki 2008	Shimazaki, K. 2009, "Damage-Free Reinforced Concrete Buildings with Good Repairability," *Article of Dept. of Architecture and Building Engineering,* Kanagawa University, Japan, pp. 1-6.
	Shimazaki, K., 2008, "Reinforced concrete shear walls with de-bonded diagonal reinforcements for the damage-less reinforced concrete building," Proceedings, 14th World Conference on Earthquake Engineering, Oct. 12-17, Beijing, China.
	Hirata, N., and Shimizaki, K. 2009, "An Experimental Study on Damage-Free Reinforced Concrete Shear Walls with De-Bonded Diagonal Reinforcements," *Structural Engineering Article*, Vol. 55, No. 1, pp. 1-8.
Shui et al, 1981	Daniel, J., Shiu, K., and Corley, W. 1986, "Openings in Earthquake-Resistant Structural Walls," *ASCE Library*, Vol. 112, No. 7, pp. 1660-1676.
	Shiu, K. N., Daniel, J. I., Aristizabal-Ochoa, J. D., Fiorato, A. E., and Corley, W. G., 1981, "Earthquake Resistant Structural Walls–Tests of Walls with and Without Openings," Report to National Science Foundation (R/D 1679), Construction Technology Laboratories, Portland Cement Association. Skokie, IL.
Sittipunt and Wood 2000	Sittipunt, C., and Wood, C. 2000, "Development of Reinforcement Details to Improve the Cyclic Response of Slender Structural Walls," Proceedings, 12th World Conference on Earthquake Engineering, Auckland, New Zealand, pp. 1-6.
	Sittipunt, C., Wood, S., Lukkunaprasit, P., and Pattararattanakul, P. 2001, "Cyclic Behavior of Reinforced Concrete Structural Walls with Diagonal Web Reinforcement," *ACI Structural Journal*, Vol. 98, No. 4, pp. 554-562.
Solak et al., 2015	Solak, A., Tama, Y., Yilmaz, S., Kaplan, H. 2015, "Experimental study on behavior of anchored external shear wall panel connections," *Article in Bulletin Of Earthquake Engineering*, Vol. 13, No. 10, pp. 3065–3081.
Sosa et al., 2017	Sosa, D., Arévalo, D., Mora, E., Correa, M., Albuja, D., and Gómez, C. 2017, "Experimental and Analytical Study of Slender Reinforced Concrete Shear Wall under Cyclic In-Plane Lateral Load," Hindawi Journal of Mathematical Problems in Engineering, Vol. 2017, No. 4020563, pp. 1-14.
Sun et al., 2015	Sun, J., Qiu, H., Yang, Y., and Lu, B. 2015, "Experimental and analytical studies on the deformability of a precast RC shear wall involving bolted connections," *Science China Article on Technological Sciences*, Vol .58, No. 8, pp. 1439–1448.

	Sun, Jian., Qiu, H., and Lu, Y. 2016, "Experimental study and associated numerical simulation of horizontally connected precast shear wall assembly," *Article on The Structural Design of Tall And Special Buildings*, Vol. 25, No. 13, pp. 659-678.
	Sun, J., Qiu, H., Tan, Z., and Yang, Y. 2016b, "Experimental Study on Mechanical Behaviorof Rectangular Precast Reinforced Concrete Shear Wall Utilizing Bolted Connections," Journal of Building Structures, Vol. 37, No. 3, pp. 67-75.
	Sun, J., Qiu, H., and Lu, Y. 2016c, "Experimental study and associated numerical simulation of horizontally-connected precast shear wall assembly" *Article on The Structural Design of Tall And Special Buildings,* Vol. 25, No. 13, pp. 659-678.
Synge and Paulay 1980	Synge, A.J., Paulay, T., and Priestley, M.J.N. 1980, "Ductility of Squat Shear Walls," *Research Report,* University of Canterbury*,* Christchurch, New Zealand, pp. 1-142.
	Paulay, T., Priestley, M.J.N., and Paulay, T. 1982, "Ductility in Earthquake Resisting Squat Shear walls," *ACI Structural Journal,* Vol. 79, No. 4, pp. 257-269.
Tabata et al., 2003	Tabata, T., et al. (2003). Experimental study on structural performance of R/C walls under high flexural stress. Proceedings of the Japan Concrete Institute. 25:2, 625-630. (in Japanese)
Tabata et al., 2004	Toshio MATSUMOTO, Hiroshi NISHIHARA and Taku TABATA, 2004, "Development of Slab Type High-Rise Residential Building- Part 3 Bending shear loading test on bearing walls with precast concrete boundary columns". vol. 10.
Taghdi 1998	Taghdi, M., Bruneau, M., and Saatcioglu, M. 1998, "Seismic retrofit of non-ductile concrete and masonry walls by steel-strips bracing," *Proceedings,* 11th European Conference on Earthquake Engineering, Paris, France, pp. 1-11.
	Taghdi, M. 1998, "Seismic Retrofit of Low-Rise Masonry and Concrete Walls by Steel Strips," *PhD Dissertation*, University of Ottawa, Ottawa, Canada, pp. 1-214.
	Taghdi, M., Bruneau, M., and Saatcioglu, M. 2000, "Seismic retrofit of non-ductile concrete and masonry walls by steel-strips bracing," *ASCE Journal of Structural Engineering*, Vol. 126, No. 9, pp. 1-9.
Takahashi et al., 2011	Yoshida, K., Takahashi, Y., Sanada, E., and Ichinose, T. 2010, "Flexural deformation performance of RC shear wall with one side column," *Proceedings of the Japan Concrete Institute,* Vol. 32, No. 2, pp. 421-426.
	Yoshida, K. 2009, "Flexural Deformation Capacity of RC Wall with One Side Column," *Master Dissertation*, Nagoya Institute of Technology Graduate School, Nagoya, Japan.
	Takahashi, Y., Yoshida, K., Ichinose, T., Sanada, E., and Matsumoto, K. 2011, "Flexural deformation capacity of RC shear walls without column on compressive side," *Proceedings of the Japan Concrete Institute*, Vol. 76, No. 660, pp. 371-377.
	Takahashi, Y., 2011, "Conditions for omitting frame columns of reinforced concrete shear walls," *PhD Dissertation*, Nagoya Institute of Technology, Nagoya, Japan, pp. 1-116.

	Takahashi, S., Ichinose, T., Izumi, N., Sanada, Y., Matsubara, S., Fukuyama, H., and Suwada, H. 2012, "Experimental Verification on Flexural Drift Capacity of Reinforced Concrete Wall with Limited Confinement," *Proceedings,* 15th World Conference on Earthquake Engineering, Sept. 24-28, Lisbon, Portugal, pp. 1-10.
	Takahashi, S., Yoshida, K., Ichinose, T., Sanada, Y., Matsumoto, K., Fukuyama, H., and Suwada H. 2013, "Flexural Drift Capacity of Reinforced Concrete Wall with Limited Confinement,"*ACI Structural Journal*, Vol. 110, No. 1, pp. 95-104.
	Matsubara, S., Sanada, Y., Tani, M., Takahashi, S., Ichinose, T., and Fukuyama, H. 2013, "Structural Parameters of Confined Area Affect Flexural Deformation Capacity of Shear Walls that Fail in Bending with Concrete Crushing," *Article in Journal of Structural and Construction Engineering,* Vol. 78, No. 691, pp. 1593-1602.
Takara et al., 2008	Takara, S., Yamakawa, T., and Yamashiro, K. 2008, "Experimental and Analytical Investigation of Seismic Retrofit For RC Framed Shear Walls," *Proceedings,* The 14th World Conference on Earthquake Engineering, Beijing, China, pp. 1-8.
Takeda et al., 1999	Takeda, T., Yamanaka, H., Yamada, T., Tano, K., and Yabuuchi, K. 1999, "Experimental study on the bending properties of high-strength reinforced concrete shear walls," *Article from Japanese Society of Architecture Society Academic Lectures*, No. 23186, pp. 371-372.
	Tano, K., Yamanaka, H., Yamada, T., Yabuuchi, K., and Takeda, T. 1999, "Experimental study on the bending properties of Takayumi steel rebar reinforced concrete shear walls," *Article from Japanese Society of Architecture Society Academic Lectures*, No. 23187, pp. 373-374.
Takenaka et al., 2012	Takenaka, H., Hamada, S., Kikuta, S., and Ishioka, T., 2012, “experimental study of l-shaped three-dimensional shear walls for high-rise reinforced concrete buildings” Proceedings of the Japan Concrete Institute, Vol. 34, No. 2, pp. 391–396. (in Japanese)
	Takenaka, H., Hamada, S., Kikuta, S., Watabe, T., Ishioka, T., Oota, Y., and Denno, S. 2012, "Experimental Study on Seismic Performance of Reinforced Concrete L-Shaped Core Structural Wall Using Super High-rise Buildings," *Toda Corporation Technical Research Report,* Vol. 38, pp. 1-7.
Tanabe et al., 2011	Tanabe, Y., Ishikawa, Y., Iida, M., and Hassan, U. 2011, "Experimental study on solid core wall using high-strength concrete," *Research Report*, Vol. 33, No. 2, pp. 385-390.
Tani 2012	Kono, S., Tani, M., Mukai, T., Fukuyama, H., Taleb, R., and Sakashita, M., 2014, "Seismic Behavior of Reinforced Concrete Walls for a Performance Based Design," Proceedings, Second European Conference on Earthquake Engineering and Seismology, Aug. 24-29, Istanbul, Turkey, pp. 1-10.
	Tani, M. 2013, "Fundamental Study on Sliding Shear Failure of Reinforced Concrete Bearing Walls," MAKENHI Journal, No. 24760464, pp. 1-4. (in Japanese)
	Tani, M. 2013, "Fundamental Study on Sliding Shear Failure of Reinforced Concrete Bearing Walls," Article from International Institute of Seismology and Earthquake Engineering, pp. 45-46. (in Japanese)
Tasnimi 2000	Tasnimi, A. A., 2000, "Strength and deformation of mid-rise shear walls under load reversal," *ELSEVIER Journal of Engineering Structures,* Vol. 22, No. 4, pp. 311-322.

Teng and Chandra 2016	Teng, S., and Chandra, J. 2016, "Cyclic Shear Behavior of High-Strength Concrete Structural Walls," *ACI Structural Journal*, Vol. 113, No. 6, pp. 1335-1345.
Terzioglu 2011	Gutiérrez, S., 2012, " Study of the behavior of short concrete walls with axial load using a shear-flexure interaction model," PhD Dissertation, University of Chile, Santiago, Chile, 110 pp.
	Terzioglu, T., 2008, "Experimental evaluation of the lateral load behavior of squat structural walls," Master Dissertation, Boğaziçi University, Istanbul, Turkey, pp. 1-155.
	Terzioglu, T., Orakcal, K., and Massone, L., 2018, "Cyclic lateral load behavior of squat reinforced concrete walls," *ELSEVIER Journal of Engineering Structures*, Vol. 160, No. 1, pp. 147-160.
Thomsen and Wallace 1995	Thomsen, J. H. IV, and Wallace, J. W., 1995, "Displacement-based design of reinforced concrete structural walls: an experimental investigation of walls with rectangular and T-shaped cross-sections," Report of Research Sponsored by NSF, University of California, Berkeley, California, United States, pp. 1-353.
	Thomsen, J. H. IV, and Wallace, J. W., 2004, "Displacement-based design of slender reinforced concrete structural walls—experimental verification," Journal of Structural Engineering, Vol. 130, No. 4, pp. 618–630.
	Wallace, J.W., and Orakcal, K. 1995, "Slender Wall Behavior & Modeling," *Presentation on Structural Engineering*, University of California, Los Angeles, California, United States, pp. 1-58.
	Orakcal, K., Massone, L., and Wallace, J.W. 2006, "Analytical Modeling of Reinforced Concrete Walls for Predicting Flexural and Coupled–Shear-Flexural Responses," *Article of Pacific Earthquake Engineering Center*, University of California, Los Angeles, California, United States, pp. 1-213.
Tomazevic et al., 1995	Tomazevic, M., Capuder, F., Lutman, M., and Petkovic, L. 1995, "Influence of Distribution of Reinforcement on Seismic Behavior of RC Shear Walls," *Proceedings*, 7th Canadian Conference on Earthquake Engineering, Montreal, Canada, pp. 689-696.
	Tomazevic, M., Capuder, F., Lutman, M., and Petkovic, L. 1996, "Seismic behavior of RC shear-walls: an experimental study," Proceedings of the 11th World Conference on Earthquake Engineering, June 23-28, Acapulco, Mexico, pp. 1-8.
Tran 2012	Tran, T. 2012, "Experimental and Analytical Studies of Moderate Aspect Ratio Reinforced Concrete Structural Walls," *PhD Dissertation,* University of California, Los Angeles, California, United States, pp. 1-300.
	Tran, T. A., and Wallace, J. W., 2012, "Experimental Study of Nonlinear Flexural and Shear Deformations of Reinforced Concrete Structural Walls," *ACI Structural Journal*, Vol. 112, No. 6, pp. 196-206.
	Tran, T. A., and Wallace, J. W., 2012b, "Experimental study of the lateral load response of moderate aspect ratio reinforced concrete structural walls," Report 2012/12, UCLA Structural & Geotechnical Engineering Laboratory (UCLA-SGEL), University of California, Los Angeles, CA.
	Tran, T. A., and Wallace, J. W., 2014, "Cyclic behavior of special reinforced concrete shear walls," Proceedings of the 10th U.S. National Conference on Earthquake Engineering, July 21-25, Anchorage, Alaska, pp. 1-12.
	Tran, T. A., and Wallace, J. W., 2015, "Cyclic Testing of Moderate-Aspect-Ratio Reinforced Concrete Structural Walls," ACI Structural Journal, Vol. 112, No. 6, pp. 653-665.

	Tran, T., Motter, C., Segura, C., and Wallace, J. 2017, "Strength and deformation capacity of shear walls," *Proceedings,* 16th World Conference on Earthquake Engineering, January 09-13, Santiago Chile, pp. 2-10.
Tupper 1999	Cho, S., Lee, L., Tupper, B., and Mitchell, D. 2000, "Ductile concrete walls with steel ends," Proceedings, 12th World Conference on Earthquake Engineering, Auckland, New Zealand, pp. 1-8.
	Cho, S., Tupper, B., Cook, W., and Mitchell, D. 2004, "Structural Steel Boundary Elements for Ductile Concrete Walls," *ASCE Journal of Structural Engineering*, Vol. 130, No. 5, pp. 1-7.
	Tupper, B. 1999, "Seismic Response of Reinforced Concrete Walls with Steel Boundary Elements," Master Thesis, McGill University, Montreal, Canada, 95 pp.
Villalobos 2014	Escolano-Margarit, D., Klenke, A., Pujol, S., and Benavent-Climent, A., 2012, "Failure Mechanism of Reinforced Concrete Structural Walls with and without Confinement," *Proceedings*, 15th World Conference on Earthquake Engineering, Sept. 24-28, Lisbon, Portugal, pp. 1-9
	Fernandez, E. 2014, "Seismic Response of Structural Walls with Geometric and Reinforcement Discontinuities," *PhD Dissertation*, Purdue University, West Lafayette, Indiana, pp. 1-306.
	Villalobos, E., and Pujol, S. 2014, "Seismic Response of Reinforced Concrete Walls with Lap Splices," Proceedings of the 10th U.S. National Conference on Earthquake Engineering, July 21-25, Anchorage, Alaska, pp. 1-11.
Wang et al., 2011	Wang, Z., Liu, W., Lu, J., and Wei, W. 2011, "Test of Composite Reinforced Concrete Shear Walls Without Opening Under Cyclic Loading," Journal of Nanjing University of Technology, Nanjing, China, pp. 6-11.
Wang et al., 2012	Wang, R., Shen, X., Zhang, W., and Ma, W. 2012, "Experimental Study on Force Transmission Properties of the Horizontal and Vertical Connections of Superimposed Wall Panels," *Industrial Construction Journal*, Vol. 42, No. 4, pp. 51-55. (in Chinese)
Wang et al., 2013	Wang, M., Song, X., and Wang, Z. 2013, "Experimental study on seismic performance of high damping concrete shear wall with concealed bracings," *Journal of Earthquake Engineering and Engineering Vibration*, Vol. 33, No. 5, 154-161. (in Chinese)
Wang et al., 2015	Wang, Z., Liu, W., Zhai, W., Li, X., Xu, Q., and Wang, Y, "Experimental study on seismic behavior of new type reinforced concrete composite shear wall,"*Journal of Central South University,* Vol. 46, No. 4, pp. 1410-1419. (in Chinese)
Wasiewicz 1988	Wasiewicz, Z. 1988, "Sliding Shear in Low Rise Shear Walls under Lateral Load Reversals," *Master Dissertation*, University of Ottawa, Canada, pp. 1-127.
Wiradinata 1985	Wiradinata, S. 1985, "Behavior of Squat Walls Subjected to Load Reversals," *Master Dissertation*, University of Toronto, Toronto, Canada, pp. 1-171.
Wong 2005	Wong, S. 2005, "Seismic performance of reinforced concrete wall structures under high axial load with particular application to low-to moderate seismic regions," Master Dissertation, University of Hong Kong, Pok Fu Lam, Hong Kong, pp. 1-249.
	Su, R., and Wong, S. 2006, "Seismic behavior of slender reinforced concrete shear walls under high axial load ratio," *ELSEVIER Journal of Engineering Structures,* Vol. 29, No. 8, pp. 1957-1965.

Woods et al., 2016 and 2017	Woods, J. 2014, "Seismic Retrofit of Deficient Reinforced Concrete Shear Walls using Fibre-reinforced Polymer Sheets: Experimental Study and Anchor Design," *Master Dissertation*, Ottawa-Carleton Institute of Civil and Environmental Engineering, Ottawa, ON, pp. 1-134.
	Woods, J., Lau, D., Cruz-Noguez, C. 2016, "In-Plane Seismic Strengthening of Nonductile Reinforced Concrete Shear Walls Using Externally Bonded CFRP Sheets," ASCE Journal of Composites for Construction, Vol. 20, No. 6, pp. 1943-1953.
	Woods, J., Lau, D., Cruz-Noguez, C. 2016, "In-Plane Seismic Strengthening of Nonductile Reinforced Concrete Shear Walls Using Externally Bonded CFRP Sheets," *ASCE Journal of Composites for Construction*, Vol. 20, No. 6, pp. 1943-1953.
Wu et al., 2015	He, J., Zhu, Z., and Dong, J. 2017, "Research on seismic performance of precast concrete shear wall structure," J*ournal of Harbin Institute of Technology*, Vol. 39, No. 4, pp. 124-130. (in Chinese)
	Wu, D., Liang, S., Guo, Z., and Xiao, Q. 2015, "Bending bearing capacity calculation of the improved steel grouted connecting precast wall," *Journal of Harbin Institute of Technology*, Vol. 47, No. 12, pp. 112-116. (in Chinese)
	Wu, D., Liang, S., Guo, Z., Zhu, X., and Fu, Q., 2016b, "Flexural Capacity Calculation Approach for Precast Grouted Shear Wall Influenced by Joint Interface Displacements," *Hindawi Journal on Advances in Materials Science and Engineering,* Vol. 2015, No. 120759, pp. 1-11.
	Wu, D., Liang, S., Guo, Z., Zhu, X., and Fu, Q., 2016, "The development and experimental test of a new pore-forming grouted precast shear wall connector," KSCE Journal of Civil Engineering, Vol. 20, No. 4, pp.1462–1472.
Xiang 2009	Li, B., and Lim, C. 2010, "Tests on Seismically Damaged Reinforced Concrete Structural Walls Repaired Using Fiber-Reinforced Polymers," *ASCE Journal of Composites for Structures*, Vol. 14, No. 5, pp. 597-608.
	Li, Bing., Pan, Z., and Xiang, W. 2016, "Experimental Evaluation of Seismic Performance of Squat RC Structural Walls with Limited Ductility Reinforcing Details," *Journal of Earthquake Engineering*, Vol. 19, No. 2, pp. 313-331.
	Xiang, W. 2009,"Seismic Performance of RC Structural Squat Walls with Limited Transverse Reinforcement," *PhD Dissertation*, Nanyang Technological University, Singapore, pp. 1-281.
Xiao 2005	Xiao, S., 2005, "Experimental report on seismic behavior of shear wall with inclined steel reinforced concrete (steel column)" Dalian University of Technology, China, 77 pp. (in Chinese)
	Xiao, S., Li, H., and Zhang, H. 2006, "Experimental Study on Aseismic Characteristics of RC Shear Walls with Diagonal Profile-Steel Bracings," *Proceedings*, 10th Biennial International Conference on Engineering, Construction, and Operations in Challenging Environments and Second NASA/ARO/ASCE Workshop on Granular Materials in Lunar and Martian Explorati, Texas, United States, pp. 170-176.
	Xiao, S., Li, H., Zhao, Y., and Zhang, J. 2007, "Seismic Damage Characteristics of RC Shear Wall with Diagonal Profile Steel Braces by Experiment," *Key Engineering Materials Journal*, Vol. 340-341, No. 2, pp. 1115-1120.
Xiao and Guo 2014	Xiao, Q., and Guo, Z. 2014, "Quasi-static test for double-wall precast concrete short-leg shear walls," *Journal of Harbin Institute of Technology*, Vol. 46, No. 12, pp. 84-88. (in Chinese)

	Xiao, Q., and Guo, Z., 2014a, "Low-cyclic reversed loading test for double-wall precast concrete shear wall," Journal of Southeast University, Vol. 44, No. 4, pp. 826–831. (in Chinese)
Xiao et al. 2004	Xiao, Z., Li, K., and Jiang, F. 2004, "Research on the seismic behavior of HPC shear walls after fire," *Article in Materials and Structures,* Vol. 37, No. 1, pp. 506-512.
Xiao et al., 2009	Chen, T., Xiao, C., Tian, C., and Xu, P. 2009, "Experimental study on Press-bending behavior of composite shear wall with high axial compression ratio," China Civil Engineering Journal, Vol. 44, No. 6, pp. 1-8. (in Chinese)
	Xiao, C., Tian, C., Chen, T., and Jiang, D. 2012, "Compression-bending Behavior of Steel Plate Reinforced Concrete Shear Walls with High Axial Compression Ratio," *Proceedings,* 15th World Conference on Earthquake Engineering, Sept. 24-28, Lisbon, Portugal, pp. 21-30.
	Xiao, C., Jiang, D., Xu, Z., and Chen, T. 2012b, "Seismic Behavior of Steel Plate Reinforced Concrete Shear Walls," *Proceedings*, CTBUH 2012 9th World Congress, Shanghai, China, pp. 671-678.
Xiao et al., 2016	Xiao, J., Xie, Q., Li, Z., and Wang, W. 2016, "Fire Resistance and Post-fire Seismic Behavior of High Strength Concrete Shear Walls," *Article in Fire Technology*, Vol. 53, No. 1, pp. 55-86.
Yamakawa et al., 1993	Yamakawa, T., Irami, S., Tamaki, Y., Matsunaga, S., and Hamada, A. 1993, "An Experimental Study on Damage Affecting Aseismatic Behavior of Structural Walls under Chloride Attack Environment in the Semitropical Region," Bulletin of Faculty of Engineering, University of the Ryukyus, Okinawa, Japan, No. 46, pp. 114-130. (in Japanese)
Yan et al., 2008	Zhang, W., Zhang, L, and Yan, S. 2008, "Test seismic behavior of high-strength steel of high strength concrete wall," *Journal of Seh nyang Jianzhu University,* Vol. 26, No. 1, pp. 119-123. (in Japanese)
	Yan, S., Zhang, L., and Zhang, Y. 2008, "Seismic Performances of High-strength Concrete Shear Walls Reinforced with High-strength Rebars," *Proceedings,* 11th Biennial ASCE Aerospace Division International Conference on Engineering, Long Beach, California, pp. 1-8.
Yan et al., 2016	Yang, W., Zheng, S., Zhang, D., Sun, L., and Gan, C. 2016, "Seismic behaviors of squat reinforced concrete shear walls under freeze-thaw cycles: A pilot experimental study," *ELSEVIER Journal of Engineering Structures,* Vol. 124, No. 1, pp. 49-63.
Yanagisawa et al., 1992	Yanagisawa, N., Kamide, M., Kanoh, Y. et al., 'Study on high strength reinforced concrete shear walls: Part 1 Outline of tests; Part 2 Deformability and maximum strength (in Japanese),' Summaries of technical papers of annual meeting, Architectural Institute of Japan, Cll, 347-350(1992).
	Takagi, H., 2001, "Shear Reinforcement Limits for Reinforced Concrete Shear Walls made of High-Strength Materials" Concrete Research and Technology, Vol.12 No.2 May 2001, pp. 13-26.
Yanez et al., 1991	Yanez, F., Park, R., and Paulay, T. 1991, "Seismic Behavior of Reinforced Concrete Structural Walls with Regular and Irregular Openings," Proceedings, Pacific Conference on Earthquake Engineering, Auckland, New Zealand, pp. 67-78.
	Yanez, F., Park, R., and Paulay, T, 1992, "Seismic behavior of walls with irregular openings," Proceedings of the 10th World Conference on Earthquake Engineering, July 19-24, Madrid, Spain, pp. 3303-3306.

Yang and Wu 2015	Xu, G., Wang, Z., Wu, B., Bursi, O., Tan, X., Yang, Q., and Wen, L. 2017, "Seismic performance of precast shear wall with sleeves connection based on experimental and numerical studies," ELSEVIER Journal of Engineering Structures, Vol. 150, No. 1, pp. 347-358.
	Yang, Q. 2015,"Experimental study on seismic behavior of full-scale precast shear wall box module," *Master Dissertation*, Harbin Institute of Technology, Heilongjiang Sheng, China, pp. 1-83.
	Wan, L., Xu, G., Yang, Q., Wen, L., Yu, Z., Tan, X., Jia, D., and Wu, B. 2016, "Quasi-Static Test of Seismic Behavior of Shear Wall With Stirrup Bolted By Vertical Reinforcement in Vertical Connections," *China Academic Journal,* Vol. 46, No. 4, pp. 60-64.
Yang et al., 2016	Yang, W., Zheng, S., Zhang, D., Sun, L., and Gan, C. 2016, "Seismic behaviors of squat reinforced concrete shear walls under freeze-thaw cycles: A pilot experimental study," *ELSEVIER Journal of Engineering Structures*, Vol. 124, No. 1, pp. 49-63.
Yoshida et al., 1998	Yoshida N., Matsuzaki Y., Fukumaya H., and Hayashida N., 1998, "A Study on Retrofitting of Shear Wall with Continuous Fiber Sheet" Proceedings of Concrete Engineering Annual Report, Vol., 20, No. 1, pp. 485-490. (in Japanese)
	Yoshida N., Matsuzaki Y., Fukumaya H., and Hayashida N., 1998, "A Study on Retrofitting of Shear Wall with Continuous Fiber Sheet" Proceedings of Concrete Engineering Annual Report, Vol., 20, No. 1, pp. 485-490. (in Japanese)
Yu et al., 2016	Yu, Q., Xu, K., Xu, Z., Fang, Y., and Lu, X. 2016, "Seismic Behavior of Precast Shear Walls with Vertical Reinforcements Overlap Grouted in Constraint Sleeve, "Technical Journal of the Faculty of Engineering University of Zulia, Vol. 39, No. 6, pp. 207-217.
	Yu, Q., Gong, X., Fang, Y., Xu, Z., and Lu, X. 2016b, "Grouted Sleeve Lapping Connector and Component Performance Tests," Technical Journal of the Faculty of Engineering University of Zulia, Vol. 39, No. 6, pp. 136-145.
Yuksel 2014	Yuksel, S. 2014, "Experimental Behavior of Rectangular Shear Walls Subjected to Low Axial Loads," ATINER's Conference Paper Series, No: CIV2014-0965.
	Yuksel, S. 2014b, "Structural Behavior of Lightly Reinforced Shear Walls of Tunnel Form Buildings," *IACSIT International Journal of Engineering and Technology,* Vol. 6, No. 1, pp. 34-37.
Yun 1994	Yun H. D., 1994, "Seismic Performance of High Strength Reinforced Concrete Structural Walls," PhD Dissertation, Hanyang University, 365 pp. (in Korean)
	Yun, H., Choi, C., and Lee, L. 2004, "Earthquake Performance of High-Strength Concrete Structural Walls with Boundary Elements," *Proceedings,* 13th World Conference on Earthquake Engineering, August 1-6, Vancouver, Canada, pp. 1-18.
	Yun, H., Choi, C., and Lee, L. 2004b, "Behavior of high-strength concrete flexural walls," *Proceedings*, Institution of Civil Engineers, pp.37-48.
Zhang 2007	Zhou, Y., and Lu, X., 2008, "SLDRCE database on static tests of structural members and joint assemblies," State key laboratory of disaster reduction in civil engineering. Shanghai, China: Tongji University; 2008. (in Chinese)
	Zhang, H., Liu, Song., Duan, Y., and Du, Q. 2013, "Nonlinear analysis of RC shear walls by vector form intrinsic finite element method," Proceedings, The 2013 World Congress on Advances in Structural Engineering and Mechanics, Jeju, Korea, pp. 1486-1502.

	Zhang, H. 2007, "Shear wall R11," *National Key Laboratory of Civil Engineering Disaster Prevention of Tongji University*, Vol. 29, pp. 169-188.
	Zhang, S., Lu, Xilin., and Zhang, H. 2009, "Experimental and Analytical Studies on the Ultimate Displacement of RC Shear Walls," *China Civil Engineering Journal*, Vol. 42, No. 4, pp. 11-16.
	Zhang, H., Lu, X., Duan, Y., and Zhu, Y. 2014, "Experimental Study on Failure Mechanism of RC Walls with Different Boundary Elements under Vertical and Lateral Loads," *Article in Advances in Structural Engineering*, Vol. 17, No. 3, pp. 361-379.
Zhang 2015	Zhang, Z. 2015, "Seismic Behavior of Non-Rectangular RC Walls with Inferior Details Subjected to Loading from Different Direction," PhD Dissertation, Nanyang Technological University, Nanyang, China.
	Zhang, Z., and Li, B., 2014, "Evaluation of Seismic Performance of Slender L-Shaped and T-shaped RC Structural Walls," Proceedings, 2nd European Conference on Earthquake Engineering and Seismology, Aug. 24-29, Istanbul, Turkey, pp. 1-11.
	Zhang, Z., and Li, Bing. 2016, "Seismic Performance Assessment of Slender T-Shaped Reinforced Concrete Walls," Journal of Earthquake Engineering, Vol. 20, No. 8, pp. 1342-1369.
	Zhang, Z., Li, Bing., and Qian, K. 2016, "Experimental Investigations on Seismically Damaged Nonrectangular Reinforced-Concrete Structural Walls Repaired by FRPs," ASCE Journal of Composite Construction, Vol. 20, No. 1, pp. 11-14.
Zhang and Liu 2012	Zhang, H., Lu, X., Duan, Y., and Li, J. 2011, "Experimental Study and Numerical Simulation of Partially Prefabricated Laminated Composite RC Walls," Advances in Structural Engineering, Vol. 14, No. 5, pp. 967-979.
	Zhang, H., Lu, X., Duan, Y., and Li, J. 2012, "Seismic Behavior of the Partially Prefabricated Laminated RC Walls Under Different Axial Ratios," *Proceedings*, 15th World Conference on Earthquake Engineering, Sept. 24-28, Lisbon, Portugal, pp. 1-10
	Zhang, H., and Liu, S., 2012, "Seismic behavior study of the laminated RC Shear Walls under Low-reversed Cyclical Experiment," Science paper Online, pp. 1-8. (in Chinese)
	Li, J., Wang, Y., Lu, Z., and Li, J. 2017, "Experimental Study and Numerical Simulation of a Laminated Reinforced Concrete Shear Wall with a Vertical Seam," Applied Sciences, Vol. 7, No. 6, pp. 1-22.
Zhang and Wang 2000	Zhang, Y., and Wang, Z., 2000, “Seismic behavior of reinforced concrete shear walls subjected to high axial loading,” ACI Structural Journal, Vol. 97, No., 5, pp. 739–750.
Zhang et al., 2010	Zhang, H., Lu, X., and Wu, X. 2009, "Cyclic Loading Experiment and Numerical Simulation of RC Walls," *Proceedings,* 2009 World Congress on Computer Science and Information Engineering, Jan. 12-14, Shanghai, China, pp. 642-647.
	Zhang, H., Lu, X., and Wu, X., 2009, "Experimental Study and Numerical Simulation of the Reinforced Concrete Walls with Different Stirrup in the Boundary Element," Journal of Asian Architecture and Building Engineering, Vol. 9, No. 2, pp. 447-454.

	Zhang, H., Lu, X, Duan, Y., and Zhu, Y., 2014, "Experimental Study on Failure Mechanism of RC Walls with Different Boundary Elements under Vertical and Lateral Loads," Journal in Advances in Structural Engineering, Vol. 17, No. 3, pp. 361-379.
	Zhang, H., Lu, X., Liang, L., and Wenqing, C., 2007, "Influence of boundary element on seismic behavior of reinforced concrete shear walls," Journal of Earthquake Engineering and Engineering Vibration, Vol. 27, No. 1, pp. 92-98. (in Chinese)
Zhang et al., 2016	Zhang, J., Cai, C., Cao, W., Li, W., and Wu, M., 2016, "Research of Seismic Behavior of Mid-rise RC Shear Wall with Single Row of Steel Bars and Inclined Reinforcement" Journal of Beijing University of Technology, Vol. 42, No. 11, pp. 1681-1690. (in Chinese)
Zhang et al., 2016b	Zhang, Q., Bai, L., Liang, X., and Xiong, E., 2016, "Experimental study on seismic behavior of steel tube confined high-strength concrete shear walls," Journal of Vibroengineering, Vol. 18, No. 4, pp. 2263-2277.
Zhang Q2	Zhang, W., et al., "Master's Thesis Presentation–Personal Communication" Beijing University of Technology
Zhao et al., 2018	Zhao, Z., Fan, G., He, X., and Liu, X. 2018, "Seismic Performance of Steel Tube-high Strength Concrete Squat Walls," *Proceedings of IOP Conference Series: Materials Science and Engineering, pp. 1-10.*
Zheng et al., 2012	Zheng, S., Hou, P., Li, L., Wang, B., Yu, F., and Zhang, H. 2012, "Experimental study of the damage of RC shear walls under low cycle reversed loading," China Civil Engineering Journal, Vol. 45, No. 2, pp. 52-59. (in Chinese)
	Zheng, S., Hou, P., Li, L., Wang, B., Yu, F., and Zhang, H. 2012, "Experimental study of the damage of RC shear walls under low cycle reversed loading," China Civil Engineering Journal, Vol. 45, No. 2, pp. 52-59. (in Chinese)
Zheng et al., 2015	Zheng, S., Qin, Q., Yang, W., Gan, C., and Zhang, Y., and Ding S. 2015, "Experimental research on the seismic behaviors of squat RC shear walls under offshore atmospheric environment," Journal of Harbin Institute of Technology, Vol. 47, No. 12, pp. 64-69. (in Chinese)
Zhi et. al. 2015	Zhi, Q., Song, J., and Guo, Z., 2015. "Experimental study on behavior of precast shear wall using post-cast at the connection" Proceedings, 5th International Conference on Civil Engineering and Transportation (ICCET 2015), Nov. 28-29, Nanjing, China. pp. 1089-1092.
Zhong et al., 2009	Liao, W., Zhong, J., Lin, C., Mo, Y., and Loh, C. 2004, " Experimental studies of high seismic performance shear walls," *Proceedings*, 13th World Conference on Earthquake Engineering, August 1-6, Vancouver, B.C., Canada, pp. 1-13.
	Zhong, J., Mo, Y., and Liao, W. 2009, "Reversed Cyclic Behavior of Reinforced Concrete Shear Walls with Diagonal Steel Grids," ACI Special Publication, SP-265-3, pp. 47-72.
Zhou 2004	Zhou, G., Sun, H., and Zhou, D. 2010. "Experimental research on earthquake-resistant behavior of reinforced concrete shear-walls," Journal of Shandong Jianzhu University, Vol. 25, No. 1, pp. 41-45. (in Chinese)
	Zhou, Z., 2009, “Experimental study and analysis on aseismic performance of mid-rise recycled aggregate concrete shear wall," Journal of Beijing University of Technology, Vol. 26, No.2, pp. 1-81. (in Chinese)
Zhu 2009	Zhang, J., Cao, W., Zhu, H., and Dong H. 2010, "Study on seismic behavior of mid-rise recycled aggregate concrete shear wall," Journal of Beijing University of Technology and Key Laboratory of Urban Security and Disaster Engineering, Vol. 27, No. 1, pp. 270-285. (in Chinese)

	Liu, H., Tan, Z., and Yoshioka, B. 2015, "Anti-seismic Property of Recycled Concrete Middle-high-rise Shear Wall," Journal of Mechanical Engineering Research and Developments, Vol. 38, No. 1, pp. 66-73.
	Zhang, Y., and Zhang, L. 2013, "Low-Cyclic Reversed Load Test on New Precast Concrete," Journal of Shenyang Jianzhu University (Natural Science), Vol. 30, No.5, pp. 125-130. (in Chinese)
Zhu and Ghuo 2013	Tang, Lei., 2015, "Nonlinear Finite Element Analysis of New Precast Concrete Shear Wall," Proceedings, 5th International Conference on Civil Engineering and Transportation (ICCET 2015), Nanjing, China, pp. 322-324.
	Xiao, Q., and Guo, Z., 2014, "Low-cyclic reversed loading test for double-wall precast concrete shear wall," Journal of Southeast University, Vol. 44, No. 4, pp. 826–831. (in Chinese)
Zhu and Ghuo 2016	Zhi, Q., Song, J., and Guo, Z., 2016, "Experiments on Hybrid Precast Concrete Shear Walls Emulating Monolithic Construction with Different Amounts of Posttensioned Strands and Different Debond Lengths of Grouted Reinforcements," Article in Advances in Materials Science and Engineering, Vol. 2016, No. 5, pp. 11-13.
	Zhi, Q., Song, J., and Guo, Z., 2017, "Experimental Study on Emulative Hybrid Precast Concrete Shear Walls," Korean Society of Civil Engineers (KSCE) Journal of Civil Engineering, Vol. 2017, No. 1, pp. 329-338.
Zygouris et al., 2013	Zygouris, N. S., Kotsovos, M. D., and Kotsovos, G. M., 2013, "Effect of transverse reinforcement on short structural wall behavior," Magazine of Concrete Research, Vol. 65, No. 17, pp. 1034–1043.
	Zygouris, N. S., Kotsovos, M. D., and Kotsovos, G. M., 2014, "Design for earthquake-resistant reinforced concrete structural walls," Proceedings, 8th German-Greek-Polish Symposium Recent Advances in Mechanics September 09-13, Goslar, Germany.
	Zygouris, N. S., Kotsovos, M. D., and Kotsovos, G. M., 2015, "Design for earthquake-resistant short RC structural walls," Article in Earthquake and Structures, Vol. 8, No. 3, pp. 713–732.